



<https://theses.gla.ac.uk/>

Theses Digitisation:

<https://www.gla.ac.uk/myglasgow/research/enlighten/theses/digitisation/>

This is a digitised version of the original print thesis.

Copyright and moral rights for this work are retained by the author

A copy can be downloaded for personal non-commercial research or study,
without prior permission or charge

This work cannot be reproduced or quoted extensively from without first
obtaining permission in writing from the author

The content must not be changed in any way or sold commercially in any
format or medium without the formal permission of the author

When referring to this work, full bibliographic details including the author,
title, awarding institution and date of the thesis must be given

Enlighten: Theses

<https://theses.gla.ac.uk/>
research-enlighten@glasgow.ac.uk

RANDOM WAVE GENERATION

AND

ANALYSIS PROCEDURES

AUTHOR: Malcolm C.R. Sharp

Submitted for the degree 'Master of Science (M.Sc)'

Research work was conducted part-time at the
University of Glasgow, Department of Naval
Architecture and Ocean Engineering,
Hydrodynamics Laboratory

Submitted in June 1982

Amended in June 1983

ProQuest Number: 10984705

All rights reserved

INFORMATION TO ALL USERS

The quality of this reproduction is dependent upon the quality of the copy submitted.

In the unlikely event that the author did not send a complete manuscript and there are missing pages, these will be noted. Also, if material had to be removed, a note will indicate the deletion.



ProQuest 10984705

Published by ProQuest LLC (2018). Copyright of the Dissertation is held by the Author.

All rights reserved.

This work is protected against unauthorized copying under Title 17, United States Code
Microform Edition © ProQuest LLC.

ProQuest LLC.
789 East Eisenhower Parkway
P.O. Box 1346
Ann Arbor, MI 48106 – 1346

Thesis
6967
copy 1

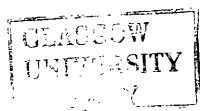


Table of Contents

Summary

List of Figures

List of Tables

List of Plates

- Chapter 1 - Introduction
- Chapter 2 - The Hydrodynamics Laboratory
- Chapter 3 - The Laboratory Computer System
- Chapter 4 - Sea Spectra
- Chapter 5 - Spectral Analysis of Time Series
- Chapter 6 - Synthesis of Irregular Seaway Time
Histories
- Chapter 7 - Wave Generation Programs
- Chapter 8 - Data Acquisition Hardware and
Programs
- Chapter 9 - Spectral Analysis Routine
- Chapter 10 - The Wave Spectrum Routines
- Chapter 11 - Derivation of the Flat-Top Window
Coefficients
- Chapter 12 - Test of Random Wave Generation and
Analysis System
- Chapter 13 - Conclusions and Possible Future
Improvements

References

Figures

Tables

Plates

SUMMARY

The thesis describes the development of the capabilities for random seaway generation and spectral analysis of signals within the Hydrodynamics Laboratory at the University of Glasgow.

In the course of developing the computer software to provide random analogue time series signals of known spectral form and subroutines to perform the analysis of the response time series signals from the test in progress, work in the following areas was done.

- (a) Representation of wave spectral formulations in a rational system of units, and coding of the resulting formulas as computer subroutines
- (b) Computer data-acquisition and storage programs
- (c) Computer coding of random data analysis routines including spectral windowing, Fast Fourier Transforms, computation of auto and cross spectra, frequency response function and coherence.
- (d) Development of a specialised spectral window formula for use in the accurate determination of the amplitude of components in harmonic signal analysis via the Fast Fourier Transform

The thesis covers a method of 'iterative refinement' of the correction to the wave drive signal to account for the non-linear transfer function characteristic of the servo-hydraulic wavemaker system used.

Results of 3 series of tests are presented. The first test defines the transfer function characteristic of the servo-hydraulic wavemaker and its operating envelope. The second test generated the required drive time series signals for a 1/100th scale Pierson-Moskowitz wave spectrum of significant wave heights 5, 10 and 15 metres. The third test series uses the drive test signals generated in the second test, in an experiment to determine the motion characteristics of a model tethered oil storage buoy. Graphs of the wave spectra and motion responses obtained are presented.

The concluding chapter covers the limitations of the system as described in the thesis and suggests improvements that might be made.

ACKNOWLEDGEMENTS

The author would like to thank the staff of the University of Glasgow Hydrodynamics Laboratory for their help during the preparation of this thesis. In particular the author would like to thank Mr. N.S. Miller, Dr. A.M. Ferguson and Dr. R.C. McGregor for their assistance and encouragement during the project and Mr. R.B. Christison, Mr. D. Sinclair and Mr. J. Aitken for their assistance in the preparation of the experimental equipment and models.

List of Figures

1. Test Tank experiment area.
2. Old wavemaker system
3. Servo-hydraulic wavemaker system
4. Distribution of energy in a seaway
5. Spectral distribution of energy in a seaway
6. Calculation of m_0 from time series records
7. Effect of windspeed on seaway spectrum
8. Aliasing of frequency values due to sampling
9. Typical sampled Time series function for D.F.T.
10. Infinite periodic continuous time series and corresponding continuous frequency spectrum
11. Infinite random time series and corresponding continuous frequency spectrum.
12. Sampled random time series and corresponding discrete frequency spectrum

13. Transfer function diagram for single input - single output system
14. Discontinuities in non-periodic components within frame
15. Comparison of window functions in frequency domain
16. Boxcar window
17. Von Hann (Hanning) window
18. Hamming window
19. Blackman 3-term window
20. Blackman-Harris 4-term window
21. Flat-top window
22. Reconstructed records from windowed data
23. Increase in frequency resolution due to the adding of zeros
24. Increase in resolution bandwidth due to frequency averaging
25. Iterative transfer function correction loop flow diagram
26. Flow diagram for program 'WAVGEN'.

27. Flow diagram for program 'WAVEM'.
28. AR11 analogue sub-system and test tank wiring layout
29. Disc data storage format for time series data
30. Flow diagram for program 'CALIBRATE'
31. Flow diagram for program 'RUNDAT'
32. Scallop loss using BOXCAR window
33. Reduced scallop loss using Flat Top window
34. Amplitude spectra of unit amplitude single frequency time series via FFT and using 'BOXCAR' window
35. Amplitude spectra of unit amplitude single frequency time series via FFT and using 'Flat Top' window
36. First test series experiment layout
37. Wavemaker calibration - frequency base
38. Wavemaker calibration - wavelength base
39. Wavemaker transfer function
40. Beach wave attenuation

41. Tank sub-beach assembly
42. Second test series experiment layout
43. Actual and Desired spectra for 1/100 scale model $H_{1/3} = 10\text{m}$
full scale
44. Actual and Desired spectra for 1/100 scale model $H_{1/3} = 5\text{m}$
full scale
45. Actual and Desired spectra for 1/100 scale model $H_{1/3} = 15\text{m}$
full scale
46. 'Scotbuoy' test arrangement
47. TEST06 mean wave power spectral density
48. TEST06 heave power spectral density
49. TEST06 pitch/roll power spectral density
50. TEST06 heave response amplitude operator spectrum
51. TEST06 pitch/roll response amplitude operator spectrum
52. TEST06 heave coherence spectrum
53. TEST06 pitch/roll coherence spectrum

- 54. TEST06 heave phase angle spectrum

- 55. TEST06 pitch/roll phase angle spectrum

- 56. TEST09 mean wave power spectral density

- 57. TEST09 heave power spectral density

- 58. TEST09 pitch/roll power spectral density

- 59. TEST09 heave response amplitude operator spectrum

- 60. TEST09 pitch/roll response amplitude operator spectrum

- 61. TEST09 heave coherence spectrum

- 62. TEST09 pitch/roll coherence spectrum

- 63. TEST09 heave phase angle spectrum

- 64. TEST09 pitch/roll phase angle spectrum

- 65. TEST10 mean wave power spectral density

- 66. TEST10 heave power spectral density

- 67. TEST10 pitch/roll power spectral density

- 68. TEST10 heave response amplitude operator spectrum

69. TEST10 pitch/roll response amplitude operator spectrum
70. TEST10 heave coherence spectrum
71. TEST10 pitch/roll coherence spectrum
72. TEST10 heave phase angle spectrum
73. TEST10 pitch/roll phase angle spectrum
74. TEST08 mean wave power spectral density
75. TEST08 heave response amplitude operator spectrum
76. TEST08 pitch/roll response amplitude operator spectrum
77. TEST06 heave response amplitude operator spectrum using SELSPOT
78. TEST06 pitch/roll response amplitude operator spectrum using SELSPOT
79. TEST08 pitch/roll response amplitude operator spectrum

Tables

1. Conversion table for different wave spectra definitions.
2. Statistical parameters and approximate sea state for Pierson-Moskowitz Spectrum.
3. Statistical Reliability table.
4. Window function coefficients and effective resolution bandwidths.
5. AR11 Analogue-to-Digital converter specifications.
6. 'Scotbuoy' Model tests 25/5/80 to 29/5/80.

CHAPTER 1

Introduction

The ability to create scale representations of real ocean seaways and to subject models of structures to them, so as to measure their responses, is of great value to Naval Architects and Ocean Engineers. The information so obtained can be used to check mathematical models, run on either Analog or Digital computers, confirming if the mathematical models, usually based on empirical fluid loading equations and interference correction factors, produce acceptable results. If this is the case the mathematical model can then be used to predict the motion responses and loads likely on the full scale structure with a greater degree of confidence than if the model tests had not been carried out. Testing of models in random seaways of different types may also highlight non-linear effects associated with the particular design that may not be represented by the (of necessity) simplified Analog or Digital mathematical representations.

Prior to the purchase of the Laboratory PDP 11/40 computer, and the adaptation of the existing test tank wavemaker to servo-hydraulic control, model response work was achieved by measuring the model motions and loads at a

number of discrete wave frequencies and heights. This procedure plus the subsequent analysis of the records by hand was a laborious and time-consuming procedure. With the digital computer and random wave capability it is now possible to determine a specific model response to a defined sea state, to an acceptable accuracy, with only one model test run and subsequent computer analysis. This represents a reduction in experimental test time of at least an order of magnitude. Such a reduction in time enables the experimenter to subject the model to a greater number of test wave conditions than hitherto possible, the additional results giving a greater insight into the models' behaviour.

Central to test methods using irregular or random seaway inputs are the techniques and procedures of Spectral Analysis. It is the use of these procedures, implemented on the Laboratory digital computer, that is the main concern of this thesis. The 'interfacing' of these computer routines to the outside 'real' world, i.e. the collection of sampled data from the model under test, and the output of the wavemaker drive signal are, however, also discussed. The interface methods used depend upon the electronic transducer system, computer and wavemaker used, and thus are not of such a general application as the Spectral Analysis procedures.

It should be stressed that the methods chosen to produce a workable random wave generation and analysis

system in this Laboratory do not represent an optimum solution to the problem. The methods used were chosen from those available within the constraints of project time, finance and Laboratory manpower available to the author. The use of existing Laboratory equipment, whenever possible, was a further constraint on the project. The methods chosen have, however, been implemented in such a manner that modifications to the present system, e.g. altering the wavemaker design or computer configuration, can be easily accommodated.

Chapters 2 and 3 give a brief description of the Laboratory tank and computer facilities. A history of the development of the present wavemaker and computer configurations are also included as these played an important part in the method chosen for the random wave generation.

Chapter 4 gives an introduction to the concepts of sea spectra and a description of the spectral formulas finally chosen for incorporation into the wave generation programs.

Chapter 5 gives an overview of the Spectral Analysis techniques incorporated into the computer programs written, and also some supporting theoretical background to the subject.

Chapter 6 describes the options available for the synthesis of random seaways and describes in detail the

method finally chosen.

Chapters 7 to 10 cover in detail the wave generation, data sampling, spectral analysis and wave spectra routines written for the computer.

Chapter 11 describes the method used to derive the Flat-top window function developed by the author.

Chapter 12 is a description of the experimental tests conducted on the final system, and includes some experimental results from a storage-buoy model to demonstrate the potential of the system.

Chapter 13 gives the authors conclusions and ideas for further improvement of the system.

CHAPTER 2

The Hydrodynamics Laboratory

The Test Tank

The test tank for which the random wave generation and analysis programs were written is the ship model test tank at Glasgow University Hydrodynamics Laboratory and has dimensions 77m. long, 2.4m. deep and 4.6m. wide. The tank was originally constructed for ship model resistance test work using a towing carriage with resistance dynamometer running over the tank on accurately aligned rails. See figure 1. In order that ship model added resistance tests could be made in regular head and following seas a simple plunger wavemaker driven by a constant speed AC motor via a variable ratio gearbox and adjustable crank was installed at one end of the tank. See figure 2. A beach type wave absorber was constructed at the opposite end of the tank to absorb the wave energy and prevent reflection of the waves back up the tank.

In order that response tests of models could be made over a wider range of input wave frequencies, the constant speed motor was replaced by a variable speed DC motor and Thyristor speed control system in 1968. A crude attempt

was made to generate random sea spectra using this wavemaker system in 1975, by the addition of a pin patchboard plus uniselector assembly to control the thyristor control reference voltage (and hence motor speed). The uniselector was stepped once for every revolution of the wavemaker crank selecting a new patch pin (and hence reference voltage) on the patchboard, the patchboard allowing selection of 1 of 25 motor speeds for each of 100 'program' steps (crank revolutions) before repeating. Initial tests with this system were disappointing, with spectra of limited frequency range being produced. This problem, in addition to the unreliability of the thyristor drive, and the inability of the system to retain the voltage control to frequency calibration, led to the abandonment of this approach.

A Hydraulic servo-system designed and supplied by Dr. H. Ratcliffe of the University of Glasgow, Department of Mechanics and Mechanisms, was installed, replacing the motor-crank drive arrangement in January 1979. The system was fully operational and calibrated by January 1980. The hydraulic system, as shown in figure 3 comprises a 1 inch diameter ram with a stroke of 400mm., a hydraulic pump, motor and reservoir assembly with associated filters and regulators delivering hydraulic fluid at pressures up to 2000 PSI, a hydraulic accumulator and a 'Dowty' electro-hydraulic shuttle valve. The electrical displacement feedback signal is taken from a 500mm. stroke LVDT displacement transducer mounted on the wavemaker

chassis and sensing the vertical motion of the plunger. The electronics, comprising the LVDT displacement amplifier, difference circuit and shuttle valve drive amplifier were built by the University of Glasgow, Department of Electrical Engineering workshop staff.

The wave absorbing beach originally installed was designed primarily to absorb the wake energy from ship model tests and from the short, small height waves generated by the original wavemaker assembly. The design was a compromise between efficient wave absorption and small size, so that it could be swung down into the tank to allow access to the dock area from the tank. For random sea work over the extended frequency range now available the beach was found to have inadequate performance (see Chapter 12) and a 'sub-beach' partially transparent to waves was designed, constructed and mounted in front of the existing beach in an effort to reduce the reflection of wave energy.

Instrumentation

In order to measure and record test parameters of interest (displacements, loads, accelerations, trim angles, wave heights etc.) the Laboratory has a comprehensive selection of electronic transducers, signal conditioning equipment and recording devices.

Transducers available include a range of LVDT

displacement and inclinometer transducers, differential inductance displacement, acceleration and pressure transducers, load cells and strain bars, 'proving' rings and miniature flush diaphragm pressure transducers. Signal conditioning is handled, in the main, by carrier amplifier-demodulators made by Messrs. RDP Electronics, capable of handling the signals from all the above devices. Sum and difference amplifiers, buffer amplifiers and electronic filter circuits constructed by the Laboratory staff are also available.

Recording devices include a 4 channel pen recorder, an X-Y/T flat bed plotter, a 12 channel UV recorder and a 4 channel FM tape cassette recorder in addition to the computer based data-logger.

Water surface elevation measurements are made using a set of wave monitors and probes based on a design by Fryer and Thomas (1), and supplied by Messrs. Churchill Electronics. These have been found to be accurate and reliable in use provided the probes are kept clean.

For non-contact displacement work a 'Selspot' optical infra-red tracking system is available. This system uses cameras equipped with semi-conductor sheet infra-red detectors and differential amplifiers to resolve the co-ordinates of the images of pulsed infra-red emitting diodes fixed to the structure under test, in the image plane of the camera. Two cameras each giving position

information about 3 diodes fixed to the structure is the minimum system that will allow the computation of all 6 degrees of freedom of the structure via a computer transform (2). Two cameras mounted orthogonally and a set of 6 strategically placed diodes on the structure allows the use of a simpler transform that can be applied by means of simple analog sum and difference circuits to the separate 'Selspot' analog outputs to yield analog voltage signals proportional to motion in any of the 6 degrees of freedom of the model.

The 6 degree of freedom computer transform for the 'Selspot' system has been written by the author. The system is, however, normally used with only one camera to resolve only the planar motion of the model under test in unidirectional waves.

CHAPTER 3

The Laboratory Computer System

Hardware history

The original Digital Equipment Corporation PDP 11T40 minicomputer system was installed in April 1976, and comprised

- 1 PDP 11/40 processor with 64 Kbytes core memory and memory management

- 2 RK05 2.4 Mbyte removable cartridge disc drives and controller

- 1 AR11 analog sub-system

- 1 DEC LA36 'Decwriter' terminal

In addition the software originally supplied included the RT11 single-user operating system, a FORTRAN IV compiler, a BASIC interpreter, and a 'Scientific Subroutines Package' SSPLIB.

A storage oscilloscope was borrowed and connected to the Digital-to-Analog outputs of the AR11 to give simple graphics output. Subsequently an A4 size flat-bed X-Y plotter was modified to operate from the same AR11 outputs to give the system a 'hard copy' graphics capability. A FORTRAN callable graphics library for these devices was written in the machine assembler code by the author (3). This subroutine package included routines for the generation of alphanumeric characters, automatic axis scaling and drawing, curve drawing etc.. Later a DEC VT55 raster graphics terminal with hard copy, ordered at the same time as the original computer system, was installed, and routines to operate the limited graphics features of this device were written (4).

From the outset it was apparent that the use of the system for stand-alone FORTRAN program development projects by final year and post-graduate students, research workers and others had been underestimated. At times there were up to 6 users competing for time on the single user system. A terminal time booking system was introduced to organise machine useage, but the use of the system for Laboratory tank data-logging work and the generally unpredictable nature of the research work being done made the booking system all but unworkable. By this time the system had been reconfigured so that the LA36 was being used solely as a printer, the VT55 was used as the background/console terminal, and an ASR33 teletype was installed in the Laboratory tank area to handle the foreground

data-collection.

A decision was made in the summer of 1977 to purchase the DEC RSX11-M multi-user multiprogramming operating system to allow access to the system by several users simultaneously. This operating system was installed, including the addition of an additional 64 Kbytes of core memory, in September 1977. The use of RSX11-M eased the organisational demands of the system but brought further problems in its wake. The most serious was the restrictions on the use of the AR11 sub-system (see Chapter 8), one of which was the inability of using the AR11 for driving plotting devices thus restricting graphics output to the VT55 terminal.

Demand for standalone FORTRAN program development was still increasing, the system now having 10 full time users. A severe shortage of on-line disc storage space for data files and programs was now apparent, due to trying to cater for all users on 4.8 Mbytes of on-line storage. Funds available in the summer of 1978 allowed the purchase of a 10 Mbyte disc drive compatible with the existing disc drive controller, a fast dot-matrix printer and a further 64 Kbytes of core memory. The purchase in November 1978 of a DZ11 terminal multiplexer and a single 'floppy disc' drive, allowed the connection of further terminals to the system and a data exchange medium with a small portable data-logging system at that time under consideration.

Finally in January 1979 funds were available to purchase a Tektronix 4010 storage graphics terminal and a compatible Tektronix 4662 A4 size flat-bed plotter enabling, at last, the production of good report quality graphics.

The present system (supporting 14 users) now comprises

- 1 PDP 11/40 with 192 Kbytes of core memory
- 1 DZ11 8 terminal multiplexer
- 2 2.4 Mbyte cartridge disc drives and controller
- 1 10 Mbyte fixed disc drive
- 1 RX01 compatible single sided, single density floppy disc drive
- 1 AR11 analog sub-system
- 1 150 characters per second dot-matrix printer
- 3 VDU terminals
- 3 Hard copy terminals
- 1 Tektronix 4010 graphics terminal

1 Tektronix 4662 flat bed plotter

Software

Under RSX11-M the language options available on the laboratory system are FORTRAN IV, PASCAL, BASIC and MACRO Assembler.

Three different text editors and a text formatter program are available for program development work and report generation.

Library packages include a recompiled version of the DEC Scientific subroutines package for RSX11-M, a subset of the Numerical Algorithms Group (NAG) Fortran subroutine library, a subset of the GHOST package written by the author for plotting on the Tektronix devices, the University of Glasgow, Department of Electrical Engineering plotting package TEKLIB and the University of Bradford SIMPLEPLOT graphics package modified by the author for use with Tektronix devices.

Program packages at present (October 1980) developed and running on the system include a two-dimensional finite element stress package, a comprehensive ship hydrostatics program, mathematical models for the motion and load responses of circular caisson and twin hull type semi-submersibles, fluid loading and frame analysis

programs for arbitrarily shaped structures comprising cylindrical members, and programs for the investigation of 'squat' phenomena with VLCC tankers and other bluff floating bodies.

In general, the only restrictions found with the use of the present minicomputer system have been the restricted memory capacity and address range for handling large data matrices, the limited amount of on-line disc storage and to a minor extent the speed of the processor in handling large computer bound mathematical model and analysis programs.

CHAPTER 4

Sea Spectra

The following is a brief introduction into the specification of unidirectional seaways by means of wave spectral formulas. The author has only considered the unidirectional case for reasons of brevity and because it is all that can be created with the present wavemaker system in the Laboratory.

A typical seaway is comprised of an infinite collection of waves, all of different sizes, lengths and directions, created usually by wind generated disturbances of different intensities, locations and directions.

In our unidirectional irregular sea the wave crests are continuous breadthwise (long-crested) and all the wave components move forward in the same direction with velocity

$$\text{velocity} = \sqrt{\frac{g\lambda}{2\pi} \tanh \frac{2\pi h}{\lambda}}$$

where g is the acceleration due to gravity

λ is the wave length

h is the water depth

As there are an infinite number of components with

non-harmonic periods and random phases there can be no unique period associated with the seaway and thus the shape or pattern of the seaway can never repeat. We can, however, define the seaway in terms of the energy it contains. The total energy must of necessity be made up of the sum of small regular waves that make up the sea. The energy of a sinusoidal water wave per unit area of water surface can be shown to be

$$\text{Energy} = \frac{\rho g A^2}{2}$$

where ρg is the weight of the fluid per unit volume
 A is the wave amplitude

and thus the total energy per unit area of the irregular seaway must be given by

$$\text{Energy} = \frac{\rho g}{2} \sum_{n=1}^{\infty} A_n^2$$

Hence we can define any particular seaway by the distribution of energy within it by means of a frequency spectrum, in which the energy contained within any given frequency band is plotted against frequency. See figure 4. As the number of frequency components is essentially infinite this will, in the limit, give rise to a smooth curve, the total area under which is the total energy in the seaway.

In practise it is common to plot the spectrum in terms of amplitude² for each wave component instead of energy. Such a spectrum is called the 'Spectral Energy Density' or 'Energy Spectrum' and is denoted by $S(f)$. See figure 5.

A drawback of the display of seaway spectra in the amplitude form is that it will suppress the effect of smaller wave components and thus make the comparison of similar spectra or the examination of small aberrations more difficult. For these purposes a display of wave component amplitudes is to be preferred. Thus

$$\text{Total Energy} = pg \int_0^{\infty} S(f) df$$

NOTE: This only applies to spectrum scaled in terms of $\frac{1}{2}A^2$. See later.

The moments of such a spectrum are defined as

$$m_j = \int_0^{\infty} f^j S(f) df \quad j = 0, 1, 2, \dots$$

The zeroth moment m_0 gives us the total energy using the relation

$$\text{Total Energy} = pgm_0$$

Instead of obtaining m_0 by integration of the spectrum we can obtain it from measurements of the water surface elevation x , about the mean surface level \bar{x} , at equal time intervals t . If N such measurements are taken as shown in figure 6 then

$$m_0 = \frac{1}{N} \sum_{i=1}^N x_i^2$$

Table 1 gives the relationship between m_0 and the spectrum area for the amplitude², height², and 2height² spectra occasionally encountered in literature (5).

Growth of Spectra

Seaway spectra build up from the high frequency end, that is for a given wind speed the first waves generated are those of short wavelength and then as the wind continues to blow longer and longer wavelength waves are generated until finally the condition known as the 'fully aroused sea' is reached. The seaway has now reached a maximum energy state and will grow no further no matter how long the wind may blow or over how much more area. As more and more energy is put into the seaway its spectrum changes and as it grows it includes more and more low frequency waves and its maximum energy value shifts toward the low frequency end. A similar process also occurs for 'fully aroused seas' if the windspeed increases. See figure 7.

Wave Height Statistics

If the spectrum is assumed to be of narrow bandwidth the distribution of wave amplitudes will follow a Rayleigh distribution. In many cases wave spectra do not appear to satisfy this narrow band criterion. However, the statistical distribution of observed wave amplitudes tends to follow the Rayleigh distribution with sufficient accuracy to justify the conclusions that follow. Thus the probability that the wave amplitude lies within the increment $(A, A+\delta A)$ is $p(A)\delta A$ where the probability density function is given by

$$p(\zeta) = \zeta \exp(-\zeta^2/2)$$

$$\text{where } \zeta = A/\sqrt{m_0}$$

Statistics for wave height $H=2A$ can be derived from the above probability density function. For instance the average wave height H is given by

$$H = 2 \int_0^{\infty} Ap(\zeta) d\zeta = 0.886 \sqrt{m_0}$$

In many cases we are interested primarily in the larger waves. The most common parameter that takes this into account is the Significant Wave Height $H_{1/3}$, defined as the average of the highest one third of all the waves.

$$H_{1/3} = \frac{2 \int_{\zeta_0}^{\infty} Ap(\zeta) d\zeta}{\int_{\zeta_0}^{\infty} p(\zeta) d\zeta}$$

where the integral lower limit ζ_0 is chosen such that

$$\int_{\zeta_0}^{\infty} p(\zeta) d\zeta = 1/3$$

In a similar manner values for $H_{1/10}$, $H_{1/100}$ and so on may be obtained.

For practical measurement the evaluation of the Significant Wave Height by this method is inadvisable as it is too dependant on the measurement bandwidth of the measurement equipment and the noise it introduces. A better practical measurement method for Significant Wave Height is directly from the zeroth moment of wave amplitude over the period of interest viz.

$$m_0 = \frac{1}{N} \sum_{i=1}^N x_i^2$$

In this case the Significant Wave Height is given by

$$H_{1/3} = 4 \sqrt{m_0}$$

as before.

Table 1 contains a list of the conversions between the most useful points on the Rayleigh distribution and the area under the most common scalings of seaway wave spectra.

Note that although the wave heights in a seaway follow a Rayleigh distribution, the actual instantaneous water surface elevation tends to follow the Gaussian distribution, although there are 2 main shortcomings:

1. Wave heights are finite because of wave-breaking truncating the distribution.
2. Finite amplitude waves tend to a trochoidal shape causing the distribution to be skewed.

Wave Spectral Formulas

In order to calculate the various parameters

associated with a particular seaway condition, or the motions or loads on vessels or structures subject to the seaway, we need to know the quantitative values of that particular wave spectra and how they are related to the environmental conditions causing them.

Several spectral formulas have been derived from observed sea wave data. It is not the purpose of this thesis to describe the methods used in deriving these formulas. The author has, however, rationalised some of the more widely used formulas, so that instead of presenting them in a form involving a wide variety of dimensional units and scalings, they are all presented in terms of SI units with the independent variable, frequency, in Hertz. All formula have been scaled to give $\frac{1}{2}$ amplitude² spectra in units of metres² per Hertz. All windspeeds have been corrected to the standard u using the DnV wind gradient formula (6).

$$u(z) = (0.93 + 0.007z)^{\frac{1}{2}}u_{10}$$

where u_{10} is the windspeed measured 10 metres above
mean sea level

The classical approach has been the one parameter formulas based upon windspeed. These formulas contend that a known steady wind will build up the sea in a consistent manner and thus one can determine all of the seaway properties from a knowledge of the windspeed alone. Needless to say these formula can only be applied to the limiting 'fully aroused sea' case as to cater for the

'partially aroused sea' case the time dependant nature of such a sea would have to be accounted for, thus adding a further parameter.

Pierson-Moskowitz Spectrum

The first successful one parameter formulation was that due to Neumann, and subsequently modified in the light some discrepancies by several other researchers.

The Pierson-Moskowitz formulation which followed has now been accepted as 'the equation' to use for fully aroused ocean wave spectra (7).

$$S(f) = \frac{\alpha g^2}{(2\pi)^4 f^5} \exp \left[-\beta \left(g / (2.065 \pi f u_{10}) \right)^4 \right]$$

$$\text{or } S(f) = \frac{\alpha g^2}{(2\pi)^4 f^5} \exp \left[-5/4 \left(f_m / f \right)^4 \right]$$

$$\text{and } H_{1/3} = \frac{2(u_{19.5})^2}{g} \left(\alpha / \beta \right)^{1/2}$$

$$H_{1/3} = \frac{2.133 (u_{10})^2}{g} \left(\alpha / \beta \right)^{1/2}$$

where

α = Philips empirical constant

= 0.0081

β = 0.74

f_m = frequency of spectrum peak

= $1.327 / u_{10}$

When f_m is in Hz and

u_{10} is in metres/sec

The Pierson-Moskowitz formula makes no allowance for situations where the effective distance over which the wind would develop waves (the fetch) is restricted. The Pierson-Moskowitz spectrum was subsequently modified by Silvester (8) to cover this 'limited fetch' case by correcting the values of α , β and f_m based on the ratio of

true fetch to that required for the fully aroused sea.

$$\begin{aligned}
 F_{FAS} &= 17500u_{10}^{1.5} && F \text{ is fetch in metres} \\
 \alpha &= 0.0081 (F/F_{FAS})^{-0.194} && F_{FAS} \text{ is fetch length} \\
 \beta &= 0.1 \exp \left[\ln(7.4) (F/F_{FAS})^{-0.284} \right] && \text{for 'fully aroused sea'} \\
 f_m &= 0.804 \exp \left[0.5 (F/F_{FAS})^{-0.284} \right] / u_{10} && \text{in metres} \\
 H_{1/3} &= \frac{2.133(u_{10})^2}{g} (\alpha/\beta)^{1/2}
 \end{aligned}$$

These figures are then used in the existing Pierson-Moskowitz formula above.

JONSWAP Spectrum

The JOint North Sea WAVE Project (JONSWAP) (9) derived a spectral formulation to cover the fetch limited case based on measurements of fetch limited North Sea waves. The JONSWAP spectrum is given by

$$S(f) = \left[\frac{\alpha g}{(2\pi)^4 f^5} \exp \left(-5/4 \left(\frac{f_m}{f} \right)^4 \right) \right] \gamma \exp \left(-\frac{(f-f_m)^2}{2\sigma^2 f_m^2} \right)$$

The formula is the basic Pierson-Moskowitz formula modified by the factor

$$\gamma \exp \left(-\frac{(f-f_m)^2}{2\sigma^2 f_m^2} \right)$$

known as the 'peak enhancement factor', in which

$$\bar{x} = Fg/u_{10}^2 \qquad H_S \approx \left(2.56 \times 10^{-6} \frac{Fu_{10}^2}{g} \right)^{1/2}$$

$$f_m = \frac{3.5g\bar{x}^{-0.33}}{u_{10}}$$

F is fetch in metres

$$\alpha = 0.076\bar{x}^{-0.22}$$

The factors σ and γ depend upon the exact North Sea location but the mean values of

$$\begin{aligned}\gamma &= 3.3 \\ \sigma &= 0.07 \text{ for } f < f_m \\ \sigma &= 0.09 \text{ for } f \geq f_m\end{aligned}$$

are often used.

Darbyshire Spectrum

Another fetch limited spectrum often used is the Darbyshire (ocean) spectrum (10) where

$$S(f) = \left\{ \begin{array}{l} 1.494 H_{1/3}^2 Y \exp - (Y^2 (f-f_m)^2 / (0.0085(Y(f-f_m) + 0.042)))^{1/2} \\ 0 \text{ for } Y(f-f_m) < -0.042 \end{array} \right\}$$

$$F^1 = 0.00054F$$

F is fetch in metres

F^1 is fetch in nautical miles

$$Y = \frac{F^{13} + 3F^{12} + 65F^1}{F^{13} + 12F^{12} + 260F^1 + 80}$$

$$f_m = Y^{-3/4} / (2.706 \sqrt{u_{10}} + 3.56 \times 10^{-6} u_{10}^4)$$

$$H_{1/3} = 0.0121Y^{1.5} u_{10}^2$$

This formulation has generally been superceded by the JONSWAP.

Two parameter Bretschneider and ISSC Spectrums

The second class of spectral formulations are those based on the actual measurement of H_s and T_{-1} the significant wave height and energy averaged period. If one can obtain data for these parameters for a particular

location and environmental condition, one can 'recreate' the spectra using one of two main formula.

The Bretschneider formula (11)

$$S(f) = \frac{0.16843H_S^2}{T_{-1}^4 f^5} \exp(-0.674/(T_{-1}^4 f^4))$$

The ISSC (International Ship Structures Congress) formula (12)

$$S(f) = \frac{0.11068H_S^2}{T_{-1}^4 f^5} \exp(-0.443/T_{-1}^4 f^5)$$

where in both cases

H_S is in metres

T_{-1} is the energy averaged period in seconds

$$T_{-1} = 2\pi \left(\frac{m_{-1}}{m_0} \right) \quad m_{-1}, m_0 \text{ are moments of the desired spectrum}$$

It should be noted that energy averaged period is a difficult quantity to measure accurately in practice, as it is affected by the bandwidth of the measurement and subsequent analysis. For instance, if a large bandwidth is used the higher frequency noise introduced will tend to lower the energy averaged period measurement, whilst too small a bandwidth may not include some higher frequency components of the wave and thus increase the measured energy averaged period.

British Towing Tank Panel Spectrum

Still occasionally used is the British Towing Tank Panel (BTTP) spectrum (13)

$$S(f) = \begin{cases} 1.344H_S^2 \exp(-(f-f_0)^2/(0.0103(f-f_0 + 0.0414)))^{1/2} \\ \text{for } -0.0414 < f-f_0 < 0.2626 \\ 0 \text{ elsewhere} \end{cases}$$

H_S is in metres

$$f_0 = \frac{0.501}{T_Z} + \frac{1.429}{T_Z^2}$$

T_Z is mean upward crossing
period in seconds

The further empirical relationships are also given

$$\frac{1}{f_0} = 0.6185H_S + 8.4823$$

For each of these spectral formulas computer subroutines were written and tested. See Chapter 10.

Table 2 gives a list of significant wave heights, periods and wavelengths for several wind speeds obtained using the Pierson-Moskowitz spectrum.

CHAPTER 5

Spectral Analysis of Time Series

Spectral Analysis has become a significant tool in the statistical analysis of time series since the late 1940's when J.W. Tukey and M.S. Bartlett proposed the technique in its' original form. Blackman and Tukey rationalised the procedures for obtaining power spectra and cross spectra via auto and cross correlations in 1957. The use of Spectral Analysis as a routine tool was accelerated with the publication of the first Fast Fourier Transform (FFT) algorithm by Cooley and Tukey in 1965. This algorithm, coupled with the use of fast digital computers, enabled the processing of time series and other data at a significantly more rapid rate than had been previously attainable.

The author has not attempted within this chapter to cover the entire range of spectral analysis techniques but merely to highlight some of the main procedures and operations considered in the development of the computer routines written for use within the Laboratory. A full derivation of the Discrete Fourier Transform (DFT) is, however, given as it is a central part of the spectral analysis procedure when applied to sampled data. For reasons of brevity the author has not covered Sampling

Theory or the Statistical background underlying random processes in any depth, but merely states the conditions that must be met for the subsequent analysis techniques to be valid. No mention is made of the auto and cross correlation or the analysis routes via them to the power spectra and transfer function. The auto and cross correlation routes have now been superceded by the use of the FFT, although auto and cross correlations themselves are still important analysis tools in other areas. References (14), (15) and (16) provide a fuller background to Spectral Analysis procedures and the underlying statistical and sampling theories.

The Sampled Time Series

The data records processed by time series methods are the time histories of processes. Because of the nature of their origin and the means we have at our disposal to record them, the data records of these time histories have three main limitations:

1. Finite length of data recorded.
2. Limit on the precision to which the data is recorded due to the digital quantisation and noise introduced by the recording medium setting a lower limit to the data values we can detect.
3. The data is recorded not as a continuous function

but as a series of samples, usually equally spaced in time.

These limitations impose further limitations on what can be observed from the data both in the time and (when Fourier transformed) frequency domains.

We can denote a time function in the following manner:

$x(t)$ where x is a continuous function of t

but when sampled we only have values for x at discrete values of t , $i\Delta t$ where Δt is the sample interval and i is an integer.

thus $x_i = x(i\Delta t)$

where x_i is the i^{th} sample of the function $x(t)$

For a finite length of data record we can only approximate to (for instance) the true mean

$$\bar{x} = \frac{1}{T} \int_0^T x(t) dt \quad \text{where } T \text{ is the length of the record}$$

by the summation

$$\hat{x} = \frac{1}{N} \sum_{i=0}^{N-1} x_i \quad \text{where } N \text{ is the number of samples in the record.}$$

Similarly for the variance

$$S_x^2 = \frac{1}{T} \int_0^T [x(t) - \bar{x}]^2 dt$$

becomes

$$S^2_x = \frac{1}{N-1} \sum_{i=0}^{N-1} [x_i - \bar{x}]^2$$

Aliasing

A further limitation arising from the sampling data is that of aliasing. If a sinusoid of frequency $\gg 1/(2\Delta t)$ Hertz is sampled at an interval of Δt seconds, then the sinusoid if 'reconstructed' from the sampled data will appear at a lower frequency in the range 0 to $1/(2\Delta t)$ Hertz. The frequency $1/(2\Delta t)$ Hertz is called the Nyquist or 'folding' frequency.

To illustrate let us define

$$x(t) = \sin 2\pi f t \quad \text{where } f = (n + p)/2\Delta t$$

where n is an integer and $0 < p < 1$ then

$$\begin{aligned} x(k\Delta t) &= \sin 2\pi \frac{n+p}{2\Delta t} k\Delta t \\ &= \sin \pi k(n+p) \\ &= \sin \pi k n \cos \pi k p + \cos \pi k n \sin \pi k p \end{aligned}$$

As k, n are integers $\sin \pi k n = 0$ for all k, n

$$x(k\Delta t) = \cos \pi k n \sin \pi k p$$

but $\cos \pi k n$ is constant for $n = 0, 2, 4, 6 \dots$

and $\sin \pi k p = \sin \pi k(-p)$

so we will obtain similar values for x for frequencies

$$f = \frac{0+p}{2\Delta t}, \frac{2-p}{2\Delta t}, \frac{2+p}{2\Delta t}, \frac{4-p}{2\Delta t}, \frac{4+p}{2\Delta t} \dots$$

Thus all frequency components present in the time history are 'folded' back into the frequency measurement band $0 - 1/(2\Delta t)$ by the sampling process as shown in Figure 8.

Filtering of Time Series data

As the Nyquist or folding frequency acts as a limit to the range of frequencies that can be analysed without aliasing we must ensure that we sample at such a rate that all the frequency components in the time series can be recorded without aliasing error. A sufficient condition for this to be true is for the sampling rate to be at least twice the frequency of the highest component present in the time series.

If the time series contains both the information we wish to analyse in addition to unwanted higher frequency signals, it is possible to sample at a rate which will include the unwanted components (without aliasing) and then apply the sampled time series data to a digital low pass filter (16)(17) to reduce the unwanted signal to negligible proportions. This method is however wasteful of both computer time and storage. Another strategy is to remove the unwanted signals by analog filtering before sampling. This is the method employed at the laboratory if unwanted signals are present within the data signal, but at a higher frequency.

It is important that the experimenter approaches the selection of sample rate and anti-alias frequency filter frequencies with an open mind at the start of his experimental work. It is preferable to start with as large a measurement bandwidth as possible and then investigate all areas of interest shown up with reduced bandwidth and hence increased frequency resolution. If the experimenter prejudices the output time series signals from the tests and selects a measurement bandwidth and anti-alias frequency to suit he may well filter out some effect of interest beyond the measurement band selected.

Before further analysis is performed on the 'raw' time series data it is useful to 'clean up' or 'pre-whiten' the data, by removal of long term trends and zero offsets. Also at this time it is important to detect and correct any erroneous data samples within the record. Care should be taken that the pre-whitening process does not remove any real observable effects actually recorded but only unwanted amplifier and transducer drift etc..

Fourier's Theorem

Fourier's theorem states that any periodic function $x(t)$ can be expressed as the sum (to an infinite number of terms, if necessary) of functions of the type

$$x(t) = A \cos(\omega_0 t + \phi)$$

where the frequencies appropriate to each term in the sum

are integral multiples $n\omega_0$ of ω_0 and the amplitudes A_n and phases ϕ_n are in general different for different values of n .

This implies that any periodic function in time can be analysed into its frequency components or, alternately, the original function can be reconstructed by summation of the frequency components. Thus in general

$$x(t) = \frac{1}{T} \sum_{n=0}^{\infty} A_n \cos(n\omega_0 t + \phi_n)$$

and using the identity

$$\cos\theta = \frac{1}{2}(e^{j\theta} + e^{-j\theta})$$

we obtain

$$x(t) = \frac{1}{2T} \sum_{n=0}^{\infty} A_n e^{jn\omega_0 t} e^{j\phi_n} + \frac{1}{2T} \sum_{n=0}^{\infty} A_n e^{-jn\omega_0 t} e^{-j\phi_n}$$

Changing the sign and the summation limits of n in the second term gives

$$x(t) = \frac{1}{2T} \sum_{n=0}^{\infty} A_n e^{jn\omega_0 t} e^{j\phi_n} + \frac{1}{2T} \sum_{n=-\infty}^0 A_n e^{jn\omega_0 t} e^{j\phi_n}$$

If we let

$$x_n = \frac{1}{2} A_n e^{j\phi_n} \text{ for } n > 0$$

$$x_n = \frac{1}{2} A_{-n} e^{-j\phi_{-n}} \text{ for } n < 0$$

we obtain

$$x(t) = \frac{1}{T} \sum_{n=-\infty}^{\infty} x_n e^{jn\omega_0 t}$$

and by multiplying both sides by $e^{-jm\omega_0 t}$ and then integrating over 1 complete cycle we obtain

$$\int_0^T x(t) e^{-jn\omega_0 t} dt = \frac{1}{T} \sum_{n=-\infty}^{\infty} X_n \int_0^T e^{-jn\omega_0 t} e^{jn\omega_0 t} dt$$

But

$$\int_0^T e^{-jn\omega_0 t} e^{jn\omega_0 t} dt = \begin{cases} 0 & \text{when } n \neq m \\ T & \text{when } n = m \end{cases}$$

thus

$$X_n = \int_0^T x(t) e^{-jn\omega_0 t} dt$$

The equations

$$x(t) = \frac{1}{T} \sum_{n=-\infty}^{\infty} X_n e^{jn\omega_0 t}$$

$$X_n = \int_0^T x(t) e^{-jn\omega_0 t} dt$$

are known as the Continuous Fourier Transform pair.

The Discrete Fourier Transform

If instead of a continuous function $x(t)$ we now have a sampled function with values $x(t_i)$ at intervals Δt apart, and the length over which the function is defined $T = N\Delta t$. See figure 9. The integral over T

$$X_n = \int_0^T x(t) e^{-jn\omega_0 t} dt$$

now becomes the summation over N

$$X_n = \sum_{i=0}^{N-1} x(t_i) e^{-jn\omega_0 (i\Delta t)} \Delta t$$

As all X must be harmonic within the buffer length

$$\omega_0 = \frac{2\pi}{T} = \frac{2\pi}{N\Delta t} \quad \text{and} \quad x(t_i) = x_i$$

$$X_n = \sum_{i=0}^{N-1} x_i e^{-j2\pi in/N} \Delta t$$

If we let

$$W^{in} = e^{-j2\pi in/N}$$

$$\frac{X_n}{\Delta t} = \sum_{i=0}^{N-1} x_i W^{in}$$

and multiplying both sides by W^{-kn} we obtain

$$\frac{X_n}{\Delta t} W^{-kn} = \sum_{n=0}^{N-1} x_i W^{in} W^{-kn} = \sum_{n=0}^{N-1} x_i \sum_{n=0}^{N-1} W^{in} \cdot W^{-kn}$$

But

$$\begin{aligned} \sum_{n=0}^{N-1} W^{in} W^{-kn} &= 0 \text{ for } i \neq k \\ &= N \text{ for } i = k \end{aligned}$$

As we only need consider cases where $i = k$

$$\frac{X_n}{\Delta t} W^{-kn} = N \sum_{n=0}^{N-1} x_n$$

$$\therefore x_i = \frac{1}{N} \sum_{n=0}^{N-1} \frac{X_n}{\Delta t} e^{-j2\pi in/N} ; x_i = \frac{1}{N\Delta t} \sum_{n=0}^{N-1} X_n e^{-j2\pi in/N}$$

$$X_i = \Delta f \sum_{n=0}^{N-1} X_n e^{-j2\pi in/N} \quad \text{where } \Delta f = 1/(N\Delta t)$$

The equations

$$X_i = \sum_{n=0}^{N-1} X_n e^{j2\pi in/N \Delta f}$$

$$X_n = \sum_{i=0}^{N-1} x_i e^{-j2\pi in/N \Delta t}$$

are known as the Discrete Fourier Transform pair.

Frequency Spectra

With the Fourier transform pairs we have a method of representing the time series data with either time or frequency as the independent variable, the Fourier equations enabling us to transform data from the time domain to the frequency domain or vice versa. The variation of the frequency components in the frequency domain is known as the frequency spectrum of the time series from which they were derived.

For a periodic time series the spectrum obtained by the use of the continuous Fourier transform is shown in

figure 10 and consists of values only at the fundamental and harmonic frequencies.

For non-periodic (random) functions the spectrum obtained by the use of the continuous Fourier transform is shown in figure 11 and is a continuous spectrum as the random function may contain (in the limit) an infinite number of frequency components.

Sampled time series used with the Discrete Fourier Transform (DFT) give spectra as shown in figure 12 where the component frequencies are only defined within the frequency range $0 - 1/(2\Delta t)$ and for the discrete frequencies $n\Delta f$ where $\Delta f = 1/(N\Delta t)$.

Power Spectra

The mean square value of a time series is given by

$$\psi^2_x = \frac{1}{t_2 - t_1} \int_{t_1}^{t_2} x(t)^2 dt$$

ψ^2_x dimensionally is proportional to the mean square energy per unit time, which is by definition, Power. The Power Spectrum is an extension of this concept in the frequency domain i.e.

$$\psi^2_x(f_1, f_2) = \int_{f_1}^{f_2} G_x(f) df$$

is the power between the two frequencies f_1, f_2 where G_x is defined as the one sided Power Spectrum of the function x .

Thus

$$\psi^2_x = \int_0^{\infty} G_x(f) df$$

The Power Spectrum may be derived directly from the Fourier transform coefficients $X(f)$ of the time series function $x(t)$, by the relation

$$G_X(f) = \frac{2}{T} |X(f)|^2$$

$$G_X(f) = \frac{2}{T} \left| \int_{-T/2}^{T/2} x(t) e^{-j2\pi ft} dt \right|^2$$

Linear Systems and Spectral Analysis

Consider a linear system with one input and one output. If we apply a random signal $x(t)$ to the input we should expect a response $y(t)$ at the output. As the system is linear, by definition power present in the input signal at one frequency cannot be transformed within the system to re-appear at the output at some other frequency. What happens 'inside' the system can then be considered by what the system does to each individual frequency component of the input signal in isolation as the frequency components cannot interact. Referring to figure 13 we can represent the input signal $x(t)$ by the linear superposition of an infinite number of frequency components with complex Fourier coefficients X_i in the frequency domain. If we apply each frequency component X_i to the system it will respond giving the output Y_i . The linear superposition of all the inverse Fourier transformed Y_i will give the output

$y(t)$ as before. The ratio Y_i/X_i at frequency f_i is called the Transfer Function H_i . The spectrum for all the H_i for each frequency gives

$$H_{xy}(f) = Y(f)/X(f)$$

$H_{xy}(f)$ is called the complex Transfer Function Spectrum.

As

$$G_x(f) = \frac{2}{T} |X(f)|^2$$

we can obtain $|H_{xy}(f)|^2$ from the power spectra of the output and input signals by the relation

$$|H_{xy}(f)|^2 = \frac{G_y(f)}{G_x(f)}$$

Note that if we compute the transfer function in this manner we only obtain the $|H_{xy}(f)|$ or 'gain' and the phase relationship between input and output is lost.

We can, however, compute the cross-spectrum

$$G_{xy}(f) = \frac{2}{T} [X(f), Y^*(f)] \quad \text{where } * \text{ denotes the complex conjugate}$$

where the real and imaginary parts of the cross-spectrum, the co-spectrum and the quad-spectrum respectively, can be used to derive the input/output phase difference spectrum $\phi_{xy}(f)$ from the relation

$$G_{xy}(f) = C_{xy}(f) - jQ_{xy}(f) \quad \text{where } C_{xy} \text{ is co-spectrum}$$

$$Q_{xy} \text{ is quad-spectrum.}$$

$$\phi_{xy}(f) = -\frac{180}{\pi} \tan^{-1}(Q_{xy}(f)/C_{xy}(f))$$

where ϕ_{xy} is in degrees

If the output power spectrum G_y contains, in addition to the response to the input G_x , 'noise' from other sources (or internally generated) as is often the case, it can be shown (9) that a more stable estimate for the Transfer Function $H_{xy}(f)$ can be obtained from the relation

$$H_{xy}(f) = \frac{G_{xy}(f)}{G_x(f)}$$

The Coherence function defined as

$$\gamma^2_{xy}(f) = \frac{|G_{xy}(f)|^2}{G_x(f) \cdot G_y(f)}$$

is used to measure the dependence of the output G_y on the input G_x . In a perfect linear single input system the output is entirely dependent on the input and γ^2_{xy} will have a value of 1 for all frequencies. However, if the system is not linear, or the output G_y is dependent upon other inputs than G_x then the value of γ^2_{xy} will be lower, falling to 0 when G_y has no dependence on G_x .

The coherence function can thus be used as an estimator of the linearity of the system under examination, and thus of the confidence that can be placed in the Transfer Function obtained from the measurement of the

input and output power spectra. In multiple input systems the coherence function can be used to determine the dependence of the output upon any given input (16).

Relevance of Spectral Analysis to model tests in waves

For the particular case of model tests in a random seaway the input Power Spectrum G_x would be that due to the seaway, and the system under examination would be a vessel or structure situated on or in the seaway. The output(s) from the system (model) may be one of several parameters of interest e.g. heave or roll motion, acceleration, load etc. from measurements of which we can derive an output Power Spectrum G_y , a cross-spectrum G_{xy} and a Transfer Function H_{xy} .

In many cases the model responses can be shown to obey the Rayleigh probability distribution as did the input seaway. The probability of given motions, accelerations, loads etc. can thus be derived from measurement of the output response Power spectra area m_0 using the same probability formula as in Chapter 4.

For any linear system the ratio G_{xy}/G_x , the Transfer Function, will be independent of the distribution of power within the input Power Spectrum G_x . Many classes of model tested, however, do not respond in a linear manner and thus the Transfer Function is dependent on the input seaway in which the model was tested. Although this departure from

linearity is due to many causes (slamming, catenary mooring load etc.) it is particularly noticeable around the natural frequencies of the model where the viscous damping (dependent upon velocity. $\left| \text{velocity} \right|$ and hence non-linear) plays a dominant role.

Due to this dependence of Transfer Function on the input Power Spectrum we must be able to generate a wide range of different input wave spectra, including scaled versions of those the full size version of the model may encounter in real life, so that the responses in each condition may be determined. The generation of these random wave spectra is dealt with in Chapter 6.

It should be stressed at this point that one cannot test a scale model of a vessel or structure in a scale seaway and hope to obtain the full scale responses by merely directly scaling up the model responses, as the scaling laws governing the different phenomena determining the response are not all simple scalars. The spectral analysis of model motions etc. in random seaways can only be used as a method of validating the analytic solutions, incorporating the appropriate laws, obtained from mathematical models run on Analog or Digital computers. If the computer model predicts the model responses accurately and the computer model incorporates the correct scaling factors for the processes determining the response then the model may be judged to produce results at full scale on which more reliance can be placed than if it had not been

compared against model test results. Scale model testing in scaled seaways can also provide a qualitative 'eyeball' judgement of the gross behaviour of the model or structure.

Analysis of Random time series

Whilst random time series cannot be periodic in the sense that the infinite number of frequencies present are not all harmonic within the sampled record length T , nevertheless the Power Spectra determined from one record is an estimate of the exact Power Spectrum for that period of time. In order to identify processes that are related to longer term phenomena, and to increase our confidence in the Power Spectra estimates obtained from individual records, individual Power Spectra may be averaged in time (ensampled). This process results in the development of an average Power Spectra with an associated probability density function for each frequency component. The average Power Spectrum is defined as:

$$\langle G_x \rangle_K = \frac{1}{K} \sum_{k=1}^K G_{x'}^k$$

where K is the number of frames of length T over which the sample is taken

For time averaging to be truly valid the time series must be 'Ergodic' (the process producing the time series is time invariant) and 'Stationary' (the statistical moments of the time series are time invariant). Note that Ergodic processes are inherently Stationary but not vice-versa.

In order to make reliable conclusions concerning long term variations, K must be large enough to obtain the degree of confidence required. As K becomes infinite so $\langle G_x \rangle$ converges to the true mean value.

It is assumed that the input time series has a Gaussian distribution and thus $\langle G_x \rangle$ has a χ^2 distribution with $2K$ degrees of freedom (16). Hence if an average $\langle G_x \rangle$ is computed collecting N degrees of freedom, the probability is $(1 - \alpha)$ that the true value G_x lies between the limits $B_1 < G_x < B_2$. B_1 and B_2 are given by

$$B_1 = \frac{(N-1)G_x}{\chi^2_{N-1; \alpha/2}} \quad \text{where } \chi^2_{m; \alpha} \text{ is the } \chi^2 \text{ value for } m \text{ degrees of freedom at percentage point } \alpha$$

$$B_2 = \frac{(N-1)G_x}{\chi^2_{N-1; 1-\alpha/2}}$$

In other word we can say with $100(1 - \alpha)\%$ confidence that $B_1 < G_x < B_2$.

Table 3 lists the approximate number of degrees of freedom needed to obtain a particular error band for a given confidence limit.

Confidence limits in Transfer Function estimates

As the Transfer Function is obtained from the ratio of two estimates with χ^2 distributions, the Transfer Function estimate follows an F distribution. It can be shown (16)

that for the single input case the error in Transfer Function estimate is approximately

$$e = \pm 100 \left[\frac{2}{n-2} (F_{n1;n2;\alpha}) (1 - \gamma_{xy}^2) \right] \frac{G_y}{G_x} \%$$

where n is the number of d.f. in each spectral estimate
 $F_{n1;n2;\alpha}$ is the 100α percentage point of an F distribution
 with $n1 = L$ and $n2 = 2_{n-1}$ d.f.

The error is determined to a great extent by the Coherence γ_{xy}^2 between input and output. If the Coherence is good, it is not necessary to ensemble many records to reduce the error to acceptable proportions. In practice one must pass enough power at each frequency for the coherence value at that frequency to rise to its limiting value. The differing velocities of propagation for the different wave frequencies dictate that it may be some time before the power present in the higher frequency wave components have left the wavemaker and moved down the tank through the model test area. This dispersive nature of water waves reduces the coherence between two time series obtained from separate locations within the same seaway. This reduction in 'spatial coherence' is dependant on wavelenth and distance of separation, being more pronounced for short wavelenghts and large separations. If the wave probes are placed too close to the model under test they may not, however, measure the true seaway spectrum but be affected by diffraction and reflection of wave energy from the model. The positioning of the wave probes is thus a

compromise between good coherence and accurate measurement of the incident seaway.

Frequency averaging

In many practical cases it is not possible for enough records of time series to be collected and ensemble averaged to give an adequate number of degrees of freedom to the mean Power Spectrum and hence the resulting values are associated with a large variability.

If the frequency resolution of the mean spectrum is greater than required then additional degrees of freedom can be obtained by averaging adjacent frequency estimates in the Power Spectrum, each estimate averaged supplying a further 2 degrees of freedom.

Total degrees of freedom = 2(no. of records averaged X
no. of frequencies averaged)

or alternately

Degrees of freedom = $2B_e LT$

where B_e = effective bandwidth

L = no. of records averaged

T = record length (seconds)

(B_e the effective bandwidth is explained more fully later)

Convolution

If we know time series $x(t)$ and its Fourier transform $X(f)$, and time series $y(t)$ and its Fourier transform $Y(f)$, it may be shown that (16)

$$\begin{aligned} \mathcal{F} [x(t) y(t)] &= \int_{-\infty}^{\infty} X(f') Y(f-f') df' \\ &= \int_{-\infty}^{\infty} X(f-f') Y(f) df' \end{aligned}$$

where \mathcal{F} denoted the Fourier transform operation

The RHS of the above equations is known as the convolution of X and Y and is denoted by $X * Y$.

Also

$$\begin{aligned} \mathcal{F} [x \cdot y] &= X * Y \\ \mathcal{F} [x * y] &= X \cdot Y \end{aligned}$$

Convolution also obeys the laws of Commutability, Associativity and Distributivity.

Boxcar Function

The Boxcar Function is defined as:

$$u_T(t) = \begin{cases} 0; & t < -T/2 \\ 1; & -T/2 \leq t \leq T/2 \\ 0; & t > T/2 \end{cases}$$

Its Fourier transform is given by

$$\begin{aligned}
 U_T(f) &= \int_{-\infty}^{\infty} u_T(t) e^{-j2\pi ft} dt = \int_{-T/2}^{T/2} e^{-j2\pi ft} dt \\
 &= \left[\frac{1}{-j2\pi f} e^{-j2\pi ft} \right]_{-T/2}^{T/2} \\
 &= -\frac{1}{j2\pi f} \left[\cos\pi ft - j \sin\pi ft - \cos(-\pi ft) + j \sin(-\pi ft) \right] \\
 &= \frac{\sin\pi ft}{\pi f}
 \end{aligned}$$

The time and frequency domain representations of this function are shown in figure 16. It is apparent that the width of the main lobe is $1/(2T)$ and thus if the function in the time domain is broadened the lobe in the frequency domain is made smaller. The amplitude of the side lobes decrease in amplitude proportional to $1/T$.

Finite Record lengths

In practice we cannot record a time series for an infinite time. The effect of using a finite length record instead of an infinite one may be regarded as that of an infinite time series multiplied by a boxcar function representing the length of time over which the record was taken. If we take an infinite time series as before, $x(t)$, and multiply it by the boxcar function

$$u_T(t) = \begin{cases} 1; & -T/2 \leq t \leq T/2 \\ 0; & \text{otherwise} \end{cases}$$

we obtain

$$x'(t) = x(t) u_T(t)$$

Thus the Fourier transform X' of x' is given by

$$X'(f) = \int_{-\infty}^{\infty} x(t) u_T(t) e^{-j2\pi ft} dt$$

Using the concept of convolution discussed above we obtain

$$X'(f) = \int_{-\infty}^{\infty} X(f') U_T(f-f') df'$$

$$X'(f) = \int_{-\infty}^{\infty} X(f') \frac{\sin \pi(f-f')}{\pi(f-f')} T df'$$

As T tends to infinity, $U(f)$ tends to the value 1 as $f = f'$ and zero elsewhere and thus the RHS of the equation reduces to $X(f)$. However, for finite T the convolution of the boxcar transform with the desired transform of the time series will affect the results obtained. This convolution with the boxcar function has important consequences when considering the resolution bandwidth of transformed sampled data, and when working with functions whose frequency components are not harmonics of the record length.

Windowing

As explained above the effect of performing the Fourier transform on time series of finite length is to convolute the Fourier coefficients produced with the $\sin(x)/x$ like function from the transform of the Boxcar window function $u_T(t)$.

If the time series is sampled the Discrete Fourier Transform applies, and if all components in the time series are exactly periodic within the record length T , then the $u_T(t)$ function does not modify the Fourier coefficients produced because the transform of the Boxcar function $U_T(f)$ is zero for all the n/T discrete frequency values except that for which the difference frequency $(f - f') = 0$ in the convolution equation, in which case the value of $U_T(f)$ is 1.

If, however, we sample a time series whose frequency components are not harmonic within the record length T , and perform the DFT, then energy contained at the non-harmonic frequencies cannot be transformed exactly onto the n/T discrete output frequency coefficients and is 'leaked' across adjacent frequency coefficients. An alternative view of this problem in the time domain is gained by noting that all the non-harmonic frequency components in the time series record give rise to discontinuities that do not match at each end of the record. See figure 14. It is the transforms of these discontinuities that give rise to the leakage in the frequency domain.

The most common method of suppressing the leakage in these situations is to modify the 'window' through which the time series is viewed, and instead of the rectangular Boxcar function, use a function that tapers to zero or low value at the ends of the record thus suppressing the discontinuities at these points.

Of the many classes of window function used to taper the time series data (16) (18), the raised-cosine arch class has many advantages, not least of which is that their Fourier transforms are mathematically simple. In the time domain the window is applied multiplying the time series data to 'taper' the series at each end. In the frequency domain the transform of the window is convolved with the Fourier transform coefficients.

The general time domain representation of the raised cosine window is

$$W(t) = A_0 + \sum_{I=1}^n A_I \cos \frac{2\pi I t}{T} \quad \frac{1}{2}T < t < \frac{1}{2}T \quad \begin{array}{l} n \text{ is the number of} \\ \text{terms in filter} \end{array}$$

In the non-dimensional frequency domain $s = fT$ the raised cosine window can be represented by

$$W(s) = \frac{A_0 \sin \pi s}{\pi s} + \sum_{I=1}^n A_I \left(\frac{\sin(\pi s + 1)}{(\pi s + 1)} + \frac{\sin(\pi s - 1)}{(\pi s - 1)} \right)$$

In the frequency domain we can evaluate $W(s)$ for the discrete n/T frequency values resulting from the DFT and apply the window by means of the discrete convolution of the resulting W_k and the transformed time series X_k .

$$W_k * X_k = A_0 X_k + \sum_{I=1}^n A_I (X_{k+1} + X_{k-1}) \quad k = 0, 1, 2 \dots N/2$$

Table 4 lists the most common of these windows

together with their 'A' coefficients and resulting bandwidths. Graphs of the time and frequency domain representations of these windows are given in figures 15 to 21, the frequency domain values being plotted as decibel response relative to the peak value at $(f - f') = 0$.

With all spectral windows there is a trade-off between the increase in width of the main lobe and the reduction in height of the side lobes resulting from the replacement of the convolution of the rectangular Boxcar window with that of the chosen window function.

The Flat-Top Window

Much of the work done on window functions has been done by those working in the fields of electronics and telecommunications. The window functions that have, in the main, resulted have been optimised for as narrow a resolution bandwidth as possible with as low as possible response to 'off-peak' values, to deal with the narrow bandwidths and large dynamic ranges available from electronic and some mechanical devices. In our particular application, however, we are dealing with systems that in general do not exhibit extremely narrow resonance peaks or a large range in dynamic response.

The Power spectra that result from the use of the common window functions do not have a flat response across the measurement bandwidth but dip between adjacent n/T

frequency values caused by the narrow resolution bandwidth due to the window functions used giving a 'scalloped' effect. See figure 32. The dips between adjacent n/T frequency values are as much as -1.5dB (16%) for the Von Hann window. In many cases this degree of error may be tolerable, but for some of the hydrodynamic test work undertaken within the Laboratory, especially the initial response test work done with regular (single frequency) waves, the resulting error was unacceptable. The author therefore developed a flat-topped window function in which the top of the frequency domain response peak is flat to within 0.1% over the range $-1/(2T)$ to $+1/(2T)$ thus giving negligible 'scallop' loss. See figure 33. The sidelobe level (i.e. the response to other frequencies) has been kept to lower than -72dB , i.e. less than the conversion error from a 12 bit Analog-to-Digital converter. Naturally the resulting resolution bandwidth is quite large $3.5/T$. However this wide bandwidth is of little concern as the window function was computed primarily for harmonic analysis in regular waves or in situations where the system under test had wide resonant peaks. The development of this particular window function is discussed more fully in Chapter 11.

One disadvantage of the use of window functions is that due to the 'tapering' of the time series it effectively 'throws away' data. This results in a loss of degrees of freedom in the resulting spectral coefficients when the time series is transformed. For most common

window functions, the windowing process reduces the number of degrees of freedom per record ensembled from 2 to 1. Most (if not all) of the degrees of freedom can be regained if new data records are reconstructed from the ends of the windowed records as shown in figure 22.

The increase in bandwidth due to windowing can be offset by appending zeroes to the end of the record. This has the effect of artificially increasing the record length T and thus reducing the discrete frequency interval between estimates $1/T$. See figure 23.

Effective Resolution Bandwidth

The basic resolution in frequency obtainable from the use of a Discrete Fourier Transform is $1/T$, as the record length T is the period of the fundamental. As the Boxcar Function is convoluted with the time series the response obtained per frequency interval is not flat from $-1/2T$ to $+1/2T$ but is peaked due to the $\sin(x)/x$ like boxcar function. If we take the width of the resulting peak at a level of .7071 of the maximum response (the half-power point), the peak is $0.88/T$ wide. This is our basic resolution bandwidth.

The effect of applying window functions to the time series is to increase the width of the peak, as we are in effect, reducing the effective record length T . The values for the resulting effective resolution bandwidths for

different window functions is given in Table 4.

If in addition to windowing, frequency averaging is employed on the spectrum, the effective resolution bandwidth is again increased. See figure 24.

Thus the final effective resolution bandwidth is given by:

$$B_e = \frac{0.88}{T} + \frac{k-1}{T}$$

where k is the number of estimates frequency averaged.

CHAPTER 6

Synthesis of Irregular Seaway Time Histories

Current methods of simulating irregular seaway properties are based, in the main, on three methods

1. The analog filtering of a broadband random signal with a Gaussian amplitude distribution (White noise).
2. The approximation of the continuous spectra desired by a number of discrete frequencies. The irregular time series being produced by the linear superposition in the time domain of appropriate amplitude sinusoids at these frequencies.
3. By the direct generation of the time series from the inverse Fourier transform of the Fourier coefficients derived from the desired seaway Power spectrum.

A study of these methods was undertaken, their advantages and disadvantages noted, and the most suitable method for the generation of a time series to drive the

Laboratory wavemaker chosen.

The use of filtered white noise as an input for stimulus for response measurement is widespread in the testing of electronic systems. With the advent of integrated circuit logic the most common noise source is the Pseudo-random noise generator constructed from a digital shift register with feedback taps. When such an arrangement is operated on periodic 'clock' pulses the output will change state in coincidence with the clock pulse although not necessarily on every clock pulse. Changes from one logic level to the other occur in a pseudo-random fashion, which gives a frequency spectrum that approximates white noise over the analysis band. A low-pass filter with a corner frequency lower than the clock rate limits the frequency band to the flat part of the output spectrum and shapes the output to an approximation of band limited Gaussian white noise. Such a system is called pseudo-random because although the signal is locally random in character the pattern will repeat, the repeat time being given by

$$T = \frac{2^n}{f}$$

n is number of stages in shift register
f is input clock frequency

The output noise spectrum, as might be expected, is not continuous but consists of components spaced $f = 1/T$ apart and extending to $f_{\max} = n/(2T)$.

The subsequent shaping of the noise signal is carried out using a combination of analog high-pass, low-pass and band-pass filters set to give the desired Power spectrum.

One advantage claimed for a random wave generator based on such a system (19) is that it does not require a digital computer for actual operation. Such an advantage is, however, minimal as one does need a computer to run the program to set up the various filters on such a system for a given seaway condition and to compute the compensation needed to correct for the Transfer function of the wavemaker. The cost of such a system, coupled with the knowledge that we could perform the entire waveform synthesis within the Laboratory computer led to the abandonment of this approach.

It would be possible to perform the digital equivalent of the above analog system on a digital computer. The broadband time series signal could be a series of values created from the summation of several uniformly distributed random numbers produced by one of several modulo arithmetic algorithms (20)(21), the Central Limit Theorem ensuring that the summated values would approximate to the desired Gaussian amplitude distribution. The time series so produced could then be digitally filtered using a combination of high, low and band-pass digital filter algorithms to derive the desired spectrum. This method was again rejected because of the difficulty in representing exactly the desired spectrum by combinations of digital

filter algorithms. Good modelling of the non-linear responses of the models tested depending much on the accurate representation of the seaway.

Discrete frequency combinations in the time domain

The synthesis of a wave spectrum from the linear superposition of a number of discrete frequencies in the time domain could be performed by either digital or electronic analog means. The analog approach was discounted because of the problems associated with the design and construction of a series of electronic sine wave generators each with variable amplitude output, not to mention the problems of repeatability, stability and setting up of such a device.

The digital approach is based in the Discrete Fourier Transform

$$X_i = \frac{1}{T} \sum_{k=1}^M |X_k| \cos(2\pi k i f_0 \Delta t + \phi_k) \quad \text{Where } f_0 = \frac{1}{N\Delta t}$$

ϕ_k is the phase angle of X_k

by noting that we can obtain the sampled time series values x_i from knowledge of the X_k . We can obtain the X_k from the desired discrete seaway Power spectrum by noting

$$G_{xk} = \frac{2}{T} |X_k|^2$$

where G_{xk} is the k^{th} frequency component in the discrete Power Spectrum G_x

and thus

$$|X_k| = \left(\frac{T}{2} G_{xk}\right)^{1/2}$$

As no phase information is contained within the Power spectrum the ϕ_k are chosen as random phases within the interval $[0, 2\pi]$. The time series so generated is not truly random but repeats with period $T = N\Delta t$. By recomputing the time series record of length T using new values of ϕ_k for every record this repeat effect can be eliminated.

The compensation for the Transfer function of the wavemaker for drive signal input to wave generated output can be easily included in this method by deriving a 'drive' spectrum from the wave spectrum

$$G_{x1} = \frac{G_x}{|H_{xx1}|^2}$$

G_x is wave spectrum
 G_{x1} is drive voltage spectrum
 H_{xx1} is 'gain' spectrum of wavemaker

and using the G_{x1} to derive the spectrum of Fourier coefficients X . The direct evaluation of the equation

$$x_i = \frac{1}{T} \sum_{k=1}^M |X_k| \cos(2\pi k f_0 \Delta t + \phi_k) \quad f_0 = \frac{1}{N\Delta t}$$

is computationally inefficient as each time series record will require the evaluation of MN cosine functions. The digital computer algorithms for the evaluation of trigonometric functions are slow. However, this inefficiency can be reduced by rewriting the equation as

$$x_i = \frac{1}{T} \sum_{k=1}^M A_k \cos(2\pi k f_0 \Delta t) + B_k \sin(2\pi k f_0 \Delta t)$$

By calculating

$$A_k = X_k \cos \phi_k \quad B_k = X_k \sin \phi_k$$

and

$$\alpha = \cos(2\pi k f_0 \Delta t) \quad \beta = \sin(2\pi k f_0 \Delta t)$$

the recursion pair

$$\begin{aligned} \cos(2\pi k f_0 \Delta t (i+1)) &= \cos(2\pi k f_0 \Delta t i) \alpha - \sin(2\pi k f_0 \Delta t i) \beta \\ \sin(2\pi k f_0 \Delta t (i+1)) &= \cos(2\pi k f_0 \Delta t i) \beta + \sin(2\pi k f_0 \Delta t i) \alpha \end{aligned}$$

can be used, and the entire time series record can be evaluated using only $2N + 2M$ sine or cosine trigonometric functions.

For the number of coefficients $M=128$ and the number of time series values $N=512$ a reduction in trigonometric computations of the order of 50 could be obtained. Naturally we are replacing every N of these trigonometric evaluations by $4N$ multiplication and addition operations so the decrease in computing time will not be as great as this factor. For the Laboratory PDP 11/40 computer and these values the author obtained a reduction in computing time using the recursion method of 10.

A routine was written, in FORTRAN, with real variables, using this recursion algorithm. The rounding errors due to the use of the recursion were small allowing >1000 iterations before the cumulative error exceeded 1%. For 128 Fourier coefficients and 512 time series values the computer routine took 92 seconds to run with no other concurrent processor activity. For reasons explained in Chapter 7, it had been decided to output the time series values at a rate of 8 per second to the Digital-to-Analog converter to produce the wavemaker drive signal. Thus our 512 point time series would represent a real time record length of 64 seconds. As the routine to produce the record took 92 seconds, it was apparent that we could not run this method for more than one record in 'real time' on the Laboratory computer. Computation of the time series values into a disc file, followed by a replay off disc into the Digital-to-Analog converter was contemplated, but as the author was ⁿconsidering real time run lengths of up to 20 minutes this would require around 30 minutes continuous

processor useage for each spectral form prior to the run, which on the Laboratory multi-user system was unacceptable.

If the number of discrete frequencies used to approximate the wave spectrum are decreased the computation time will be reduced, but because of the now sparse nature of the spectrum there will be areas with no wave energy produced.

If the system has a highly tuned resonance at one of these frequencies it may fail to be exited thus leading to erroneous results. One way of avoiding this effect (22) would be to 'dither' the centre frequency $n\Delta f$ over the band by an amount $-\Delta f/2$ to $+\Delta f/2$ thus smearing the power in each frequency throughout that whole band. The equation for the time series would then become

$$x_i = \frac{1}{T} \sum_{k=1}^n |X_k| \cos(2\pi k i (f_0 + S_f) \Delta t + \phi_k)$$

$$f_0 = \frac{1}{N\Delta t} \quad \begin{array}{l} S_f \text{ is a uniformly distributed value in the} \\ \text{range} \\ (-\frac{1}{2} f_0, \frac{1}{2} f_0) \end{array}$$

If this approach were taken then the recursion algorithm could not be used and thus the computation time would increase. It is, however, a useful method of producing better time series from wave spectra 'off-line'.

An alternative method of acquiring the trigonometrical

sine and cosine values needed for the evaluation of equation (i) would be by the use of a simple look-up table.

If we use the equation

$$x_i = \frac{1}{T} \sum_{k=1}^{N/2} X_k \cos(2\pi k i \Delta t / N + \phi_k)$$

with a look-up table of N equally spaced values over the range 0 to 2π we obtain output frequency components

$$f_k = \frac{k}{N\Delta t}$$

and all values of

$$2\pi k f_i \Delta t$$

can be looked up directly in the table. The values of ϕ_k must also be integer multiples of $2\pi/N$ to enable the full value of the expression

$$\cos(2\pi k f_i \Delta t + \phi_k)$$

to be looked up directly. Thus only one multiplication and add operation is required per wave component per time step. Storage space within the computer for the look-up table can be minimised by storing only values over the $1/4$ range 0 to $\pi/2$ and obtaining the values for the other quadrants by subtraction and/or addition of the value required from π and/or sign reversal as appropriate.

The above is similar to the computational scheme used in the Fast Fourier Transform, but has the advantage that whereas the use of the inverse FFT gives discontinuities in

the time series signal, as explained later, the evaluation of x_i by the above method can be left to run indefinitely with no frame discontinuities being produced. As an efficient FFT algorithm was present on the computer and the discontinuities did not pose a significant problem in this application the look-up approach was not explored further. Given efficient coding in assembly language it would, however, be almost as computationally efficient as the FFT approach which follows.

Direct synthesis of time series via the inverse FFT

This method of synthesis for a time series is a modification of the previous case in which the manipulation of the Fourier coefficients is done in the frequency domain, finally using the inverse FFT to produce the time series directly. The FFT used in the Laboratory is described in Chapter 7. The method can be summarised as follows:

Create the desired wave Power spectrum

Modify as before to correct for the wavemaker Transfer function

$$G_{x1} = \frac{G_x}{|H_{xx1}|^2}$$

Using a random phase ϕ_k create the $N/2$ real and imaginary Fourier coefficients

$$K_x = A_k - j B_k \quad |X_k| = \frac{T}{2} G_{x1k}^{1/2}$$

$$A_k = |X_k| \cos \phi_k \quad B_k = |X_k| \sin \phi_k$$

Apply the inverse FFT defined as:

$$x_i = \frac{1}{T} \sum_{k=0}^{N-1} x_k e^{-j2\pi i k / N}$$

The resulting time series values are complex, but if we express the above equation in terms of sine and cosine and expand we obtain

$$x_i = \frac{1}{T} \sum_{k=0}^{N-1} (A_k + j B_k) (\cos 2\pi i k / N - j \sin (2\pi i k / N))$$

$$x_i = \frac{1}{T} \sum_{k=0}^{N-1} (A_k \cos 2\pi i k / N + B_k \sin (2\pi i k / N) + j (A_k \sin (2\pi i k / N) - B_k \cos (2\pi i k / N)))$$

The real part of the expression is the desired time series because

$$\begin{aligned} \text{real part of } x_i &= \frac{1}{T} \sum_{k=0}^{N-1} A_k \cos(2\pi i k / N) + B_k \sin(2\pi i k / N) \\ &= \frac{1}{T} \sum_{k=0}^{N-1} (A_k^2 + B_k^2)^{1/2} \cos(2\pi i k / N + \phi_k) \end{aligned}$$

$$\text{where } \phi_k = \tan^{-1} B_k / A_k$$

$$= \frac{1}{T} \sum_{k=0}^{N-1} |X_k| \cos(2\pi i k / N + \phi_k)$$

the desired Fourier expression.

The integer FFT routine on the Laboratory PDP 11/40 computer for $N=512$ points takes 186 milliseconds processor time, and the entire computation including the evaluation of the ϕ_k , A_k and B_k , scaling and limiting of the final time series 2.3 seconds processor time. With this method we can therefore operate in real time with sufficient spare processor time for the other users of the system.

This was the method finally chosen for the generation of the random seaway time series for the Laboratory. The program WAVGEN was written using this procedure and incorporating the selection of the desired wave spectral formulation and various output options. The program is described in Chapter 7.

CHAPTER 7

Wave generation programs.

This chapter describes the programs WAVGEN and WAVEM written to generate the analog time series signals used as input to the wavemaker system generating random seaways in the Laboratory tank. The program WAVGEN produces the time series signal based on an estimate of the wavemaker Transfer function, whilst WAVEM is used to measure the seaway spectrum produced and compare it with the desired spectrum. On the basis of this comparison WAVEM can correct the estimate of the wavemaker Transfer function, so that when WAVGEN is run again the time series produced should give a better approximation to the desired wave spectrum. This iterative process can thus be used to 'tune' the wave generation system to the generation of a particular spectrum. The iterative tuning process was introduced because it was found that, when preliminary tests were carried out on the wavemaker system using a sinusoidal drive signal, for any given frequency the wave amplitude was not a linear function of drive voltage. See figure 37a. No one Transfer function could thus be used to describe the wavemaker system exactly. Iterative tuning allows the Transfer function estimate to be modified so as to give, for a particular wave spectrum, a seaway spectrum

closely approaching that desired by repeated modification of the Transfer function of the wavemaker based on the seaway spectrum desired and the seaway actually produced, until the two are sufficiently similar for the tests to be done. See figure 25. If a time series is produced, derived from a wave spectral formula, that uses an estimate of the wavemaker Transfer function obtained from a wave spectrum of markedly different characteristics, one or two iterations of the Transfer function correction procedure may be necessary before the seaway spectrum produced matches the desired spectrum. However, if the difference between the spectrum desired and that used to derive the Transfer function estimate is not too large, in many cases no modification of the Transfer function estimate is needed and the wavemaker drive signal may be produced without any iterative tuning process. See figure 25.

One drawback of the present wave generation and data acquisition system should be noted at this time. The AR11 analog sub-system contains only one 'real-time' clock to control the analog-to-digital or digital-to-analog conversion process. If both are to proceed at the same sample interval timing then it would be possible to synchronise both events to the clock. However the RSX11-M AR11 device handler software supplied by Digital Equipment does not allow the clock to synchronise to more than one input or output process so that the PDP 11/40 is limited, at present, to either acquiring analog data through the analog-to-digital converter at precisely timed intervals, or

producing an analog time series from the digital-to-analog converters. This problem has been circumvented, for the moment, by recording the wavemaker drive signal from the digital-to-analog converter on an F.M. recorder which is subsequently used to replay the signal. The computer can then use the AR11 to sample the wave and model data. If full computer control over both analog data input and output is desired in the future then another clock system will have to be purchased or the AR11 device handler software modified.

Wave Generation Program

The random wave generation program WAVGEN was written primarily to provide the time series drive signal for the Laboratory wavemaker, although, as an option it can produce the time series as a set of FORTRAN Direct-access records of REAL values on disc for further processing or for use as input into digital computer based models of the vessel or structure under test.

In the first section, figure 26, the program prompts for the desired total run length in seconds, and the scale ratio. The program time series output is a series of digital-to-analog conversions with an interval of 125 milliseconds between conversions, the values supplied to the digital-to-analog converter being from 512 point frames. The program calculates the number of time series frames it needs to compute to give, at least, the length of

run desired. The scale ratio is defined as

$$\text{Scale ratio} = \text{Model size} / \text{Full size}$$

Input scale ratio values of up to 1 are valid. This enables full scale testing of small buoys etc. in addition to the generation of full scale time series output to disc files.

The basic frequency spectrum used for output to the wavemaker covers the range 0 - 2 Hertz using 128 discrete frequency values, although as an option we can reduce the range of frequencies actually produced (irrespective of the spectrum type) by means of bandwidth variables within the program. Currently the largest bandwidth that can be used is 0.3 to 1.7 Hertz, as outside this band the wavemaker efficiency is so low that when the wavemaker Transfer function correction is applied the digital-to-analog converter output voltage signal quickly runs into saturation.

As

$$\text{Full scale frequency} = \text{model scale frequency} \times (\text{scale ratio})^{1/2}$$

the corresponding frequency range for full scale can be easily computed.

The second part of the program offers a 'menu' of eight spectral formula from which the desired option is chosen. The formula are

1. Pierson-Moskowitz
2. Pierson-Moskowitz-Silvester
3. JONSWAP
4. Darbyshire
5. ISSC
6. Bretschneider
7. BTTP
8. $1/f$ 'noise'

the routines used to compute the spectrums being those in SPECLIB. See Chapter 10. The $1/f$ noise, although not a true seaway spectrum, was included as it gives a reasonably similar power level to all the transform wave frequencies within the output band. This allows the capability of computing the Transfer function of linear or near linear systems using short run lengths. With some seaway spectra the power contained falls off rapidly at the low and high ends of the frequency spectrum, leading to low coherence values for the derived Transfer function of the system

under test. The coherence can only be improved by extending the run length. By applying sufficient power at all frequencies in the measurement band the coherence over the band for most systems under test can reach acceptable levels more rapidly than for tests where the input power at some frequencies is low.

An equal power per unit bandwidth drive spectrum was tried initially, but led to extreme wavemaker excursions and loosening of the wavemaker assembly mountings due to the large amplitude high frequency components. For this reason the $1/f$ form with reducing power at high frequency was chosen.

When the appropriate parameters have been entered for the chosen spectral formula the resulting full scale spectrum is displayed on the storage terminal along with the spectrum significant wave height. If for any reason the spectrum produced is not satisfactory this stage can be repeated with a new choice from the menu.

The third part of the program converts the full scale spectrum to model scale using the relations

$$\text{Model frequency} = \text{full scale frequency} \times (\text{scale ratio})^{\frac{1}{2}}$$

and as

$$\text{Model } H_s = \text{Full scale } H_s \times (\text{scale factor})$$

where H_s is the significant wave height

the areas under the spectra must scale as

$$\text{Model spectrum area} = \text{Full scale spectrum area} \times (\text{scale ratio})^2$$

but as the frequency base is scaled

$$\text{Model power spectrum values} = \text{full scale power spectrum values} \times (\text{scale ratio})^{2.5}$$

If the option to correct for the wavemaker function has been made the model power spectrum values are now multiplied by the latest values of $1/|H_k|^2$ produced by WAVEM to give the drive voltage Power Spectrum.

$$G_{dk} = \frac{G_{wk}}{|H_k|^2}$$

G_d is drive voltage spectrum
 G_w is wave spectrum
 $|H_k|$ is wavemaker gain function

This stage can, however, be ignored if the water surface elevation time series values are required for the option of disc storage.

Finally the modulus of the Fourier coefficients for each frequency increment are evaluated using the relation

$$|X_k| = \frac{T}{2} G_{xk}^{1/2}$$

At this point 128 Fourier Coefficient modulii which when given random phases and inverse Fourier transformed would give a 256 point time series are available. The relationship between the frequency and time increments being given by

$$\Delta t = \frac{1}{2fn} \quad \begin{array}{l} fn = \text{folding frequency} \\ = 2 \text{ Hertz} \end{array}$$

$$\therefore \Delta t = 0.25 \text{ sec}$$

The Fourier coefficient array has 128 zeroes appended at this point before the inverse FFT is applied. The reason for this procedure is explained in the section 'Selection of output conversion rate and analog filtering'. The Fourier coefficient modulii plus appended zeroes are now scaled to integer values in preparation for the inverse FFT.

Depending on whether a disc file or real time analog output is desired the program takes one of two routes.

If a disc file is chosen, a set of random phases are computed and the real and imaginary parts of the complex integer Fourier coefficients at each frequency computed.

$$X_k = A_k + jB_k \quad \begin{array}{l} \text{where } A_k = |X_k| \cos\phi_k \\ B_k = |X_k| \sin\phi_k \end{array}$$

The A_k , B_k are inverse Fourier transformed, and the real part of the time series (see Chapter 6) scaled into REAL

values and the resulting time series record stored on disc. This process is repeated with new phases until the desired number of records have been output. The file is then closed and control returns to the start of the program for another run. If a real-time time series is desired the rest of the program operates in real time with the output time series 'double-buffered' and the program priority raised so that as one time series is being output the next is being calculated from the Fourier coefficient moduli with a new set of random phase values. The computation of the time series is similar to the storage on disc case but in addition a check is made to ensure that the output conversion values do not exceed the upper or lower limits of the digital-to-analog converter. Values exceeding the conversion limits are set to equal the appropriate limit to prevent 'wrap around' phenomena occurring. The number of times that the digital-to-analog converter saturates is counted and the total is output at the end of the run so that the experimenter can check if he is trying to produce a spectrum exceeding the limits of the system. The low-pass filtered output can be fed directly to the wavemaker, or as is more often the case, to an FM analog tape recorder for subsequent replay into the wavemaker. When the output time series has run for the appropriate time the terminal bell rings, the D/A saturation count message is output to the terminal and program control returns to the start of the WAVGEN program.

Selection of output conversion rate and analog filtering

An analog time series produced from 4 conversions per second would resolve all the frequency components up to 2 Hertz, but it will also contain frequency components at the conversion frequency and odd harmonics viz. 4, 12, 20, 28 Hertz etc. due to the discrete level nature of the output. The subsequent low-pass filtering needed to remove these components presents a problem as the unwanted fundamental is but one octave removed from the wanted passband extending up to 2 Hertz. The analog output filtering can be simplified if 128 zeroes are appended to the end of the Fourier coefficient array signifying no frequency components in the time series from 2 to 4 Hertz when transformed into the 512 point time series. As the time interval is now halved Δt is now 0.125 seconds and the output conversion rate must be 8 samples per second. Thus the unwanted fundamental is now 2 octaves removed from the wanted passband signal and the analog filter circuit easier to design to give good rejection at 8 Hertz whilst leaving the 0 to 2 Hertz passband relatively untouched.

The analog filter used is a 4 section device comprising 2 LC notch filters at 8 and 24 Hertz followed by a 2 section low-pass filter with a corner frequency at 8 Hertz. The inductive elements in the notch filters are realised using an operational amplifier based 'gyrator' circuit. The complete low-pass circuit gives greater than

40dB rejection of the fundamental and third conversion frequency harmonics and greater than 48dB rejection of the fifth and subsequent harmonics.

Wavemaker Transfer Function program

The purpose of the program WAVEM (see figure 27) is to modify the existing estimate of the Wavemaker Transfer function based on knowledge of the desired input spectra and the actual wave spectra obtained, so that when the WAVGEN program is run again using the modified values the spectrum obtained is a better approximation to the spectrum desired.

The first part of the program is identical to that of WAVGEN, allowing the selection of the spectrum actually used to run the test, and the correct model scale to allow the model spectrum to be calculated.

The second part prompts the experimenter for the name of the file containing the sampled records of the seaway produced. Flexibility is built into the program to allow the definition of the wave probe records, number of frames etc. so that the file may be of any FORTRAN Direct-access format. In practice the file format for the subsequent model tests is normally used removing the need for a separate set-up and calibration procedure for each transducer configuration. The only restriction is that the records must be of 512 samples and the sample rate must be

8 samples per second. The selected records in the selected frames are then Fast Fourier Transformed and ensemble averaged to produce an estimate of the model sea spectra produced. Initially no spectral window was employed at this stage as the time series records for the wavemaker signal were of the same length as those required for WAVEM and thus all the wave generated frequencies should fall on the WAVEM spectrum frequencies and no spectral leakage should result. However, non-linear effects are evident as the windowed and non-windowed spectra can be different, though not markedly so, and so Blackman windowing is now routinely employed in the computation of the generated wave spectrum estimate. One effect causing this problem is the variation in tape speed between record and replay of the drive signal on the FM tape recorder used. If the drive signal was obtained directly from the AR11 digital-to-analog converter using the same crystal controlled timebase for both input data sampling and output conversion this effect would not occur.

After optional frequency smoothing the two spectra are displayed on the storage terminal screen or on the plotter. If the difference between the two is significant the experimenter can instruct the program to open the file containing the current values of $1/|H_{xx}^1|^2$ for the wavemaker and correct the values using

$$\frac{1}{\langle |H_{xx}^{-1}|^2 \rangle} = \frac{1}{\frac{|H_{xx}^{-1}|^2 + G_{wk}}{2}}$$

where G_s is the drive spectrum
 G_w is the measured spectrum
 $|H_{xx}^{-1}|^2$ is the previous 'gain' estimate
 $\langle |H_{xx}^{-1}|^2 \rangle$ is the new 'gain' estimate

the new values being written into a new version of the wavemaker correction file before the program exits. Note that this form of 'exponential' averaging of the data places equal weight on the current estimate and the average of all the previous estimates. This has the advantage of biasing the estimate of the Inverse Transfer function toward the latest and hopefully most accurate estimate. If further caution in the estimation procedure is deemed necessary only a fraction of the new estimate may be averaged with the old, however, this results in more iterations needing to be run before an estimated Inverse Transfer function of sufficient accuracy is achieved.

If, on the other hand, the difference between the two spectra is not significant, that is the spectrum generated is a good representation of that desired, the experimenter may choose to exit without updating the wavemaker Transfer function correction file.

CHAPTER 8

Data acquisition hardware and programs.

Hardware

The general availability of inexpensive mini and microcomputers during the last decade has brought a new dimension in power and flexibility to Data Acquisition systems. The ability to reprogram systems designed around a digital computer enables the various parameters associated with the acquisition process (e.g. sample rate, number of input channels, output format) to be easily changed to meet different demands. In the main this was not true of the older 'hard-wired' data logger systems.

The Laboratory data-acquisition system is based on a PDP 11/40 computer using 2.4 Mbyte removable disc cartridges as the main mass storage medium. The analog data are interfaced to the digital computer by an AR11 Analog-to-Digital converter sub-system contained within the main computer chassis. See figure 28.

The AR11 sub-system is composed of 4 main components, the 16 channel analog multiplexer, the 10 bit analog-to-digital converter, the 'real-time' clock timer

and the two 10 bit digital-to-analog converters. A brief specification of these items is contained in Table 5. The 16 channel analog multiplexer allows the connection of any one of the 16 analog channels to the analog-to-digital converter under program control. The analog-to-digital converter converts the analog level present on its input into 1 of 1024 digital values in 30 microseconds. The clock timer circuit can be set under program control with a clock rate and sample interval so that once started will initiate a branch to a specified memory address (an 'interrupt') every time a sample interval completes. The interrupt code then acquires a sample from every desired input channel, or outputs a value to be converted in the digital-to-analog converters. The two digital-to-analog converters were designed as part of the X/Y control of a storage oscilloscope, but in the Laboratory are used as general output drive voltages. In particular one digital-to-analog converter is used to output the analog time series to drive the Laboratory wavemaker.

On each analog input to the system a voltage attenuator was built so that the basic input voltage range of +2.5 to -2.5 volts or 0 to 5 Volts could be increased to +5 to -5 Volts, +10 to -10 Volts, 0 to 10 Volts or 0 to 20 Volts, all with a common input impedance of $10 \Omega k$ in parallel with 200 pF. The +10 to -10 Volt input range is the most commonly used as all the Laboratory signal conditioning equipment, where possible, has been bought or modified to produce a +10 to -10 Volt peak to peak output.

The input to the attenuator is connected to a set of twisted pair cables running the length of the Laboratory tank area running inside a one inch diameter steel conduit. The twisted pair cables are brought out to multiway sockets at several points within the tank area to which a multicore umbilical cable can be attached.

Thus electronic signals from an experiment anywhere within the tank area can be simply routed to the computer system for acquisition. A 20 milliamp. current-loop computer terminal link is also routed along the tank area with sockets at various points allowing the operation of a computer terminal at the experiment test area.

The careful attention to screening of the analog input cables plus the use of a quasi-differential input circuit has kept the R.M.S. input noise level (10 Volt attenuator setting, inputs terminated by $10 \Omega k$) to less than 2 converted values at the analog-to-digital converter output.

Programs

The present data sampling programs, written in FORTRAN, are designed to run under the Digital Equipment Corporation's RSX11-M operating system on any PDP 11 series computer with an AR11 converter sub-system. The programs were, however, initially developed using the simpler DEC RT11 single-user operating system, the main change being that the RT11 programs contained their own code for driving

the AR11 and handling the interrupts it generated, whereas the RSX11-M version uses the AR11 device handler supplied by DEC. This change has meant that some of the features available under RT11 are not available under RSX11-M. The most important of these is the loss in potential sample rate. Under RT11 one could run the analog-to-digital converter at a sample rate limited only by the conversion interval of the converter; under RSX11-M the maximum sample rate is limited to around 50 samples per second on all channels by the very much higher software 'overhead' associated with the multi-user, multi-processing system and the queued nature of the system input and output. This low sample rate is not a problem for model response real-time data acquisition, but becomes a limitation to the amount which we can increase the speed of replay of some FM recorder tapes, to decrease the time taken to sample them onto magnetic disc. The RSX11-M handler, when sampling several channels simultaneously, converts each 'set' of samples at the maximum conversion rate, thus minimising the 'time skew' across channels.

The data sampling software consists of two programs, CALIBR is used to determine the particular input configuration, desired output, sample rate and calibration information. The output of CALIBR is a file containing the channel numbers to use, sample rate, calibration and other factors. This parameter file is then read by the second program RUNDAT which uses these values to run the AR11 system, storing the converted and scaled data in a disc

file when the run is complete.

Output file format

The output data format was chosen as FORTRAN direct-access as opposed to sequential files for 3 main reasons. The first was the ability to read the records in a random order which simplifies subsequent analysis. The second was that direct-access files because of their fixed length records, occupy less space than a sequential file containing the same data, as sequential files assume variable length records and thus have an associated record header for each record. Finally the RSX11-M file system handles direct-access files more efficiently, especially so if the records have lengths in words that are integer powers of 2, as then records will not cross disc blocks and can thus be retrieved in a single read operation. Unformatted binary rather than formatted ASCII code records were chosen on the grounds of a 3 fold reduction in disc storage space for integer values. Storage of unformatted FORTRAN INTEGER values instead of REAL values was chosen for a halving of the storage space used on disc, and also because the FFT algorithm used in later spectral analysis operates only on INTEGER arrays of time series values. Storage of REAL values would necessitate a time consuming scaling and 'FIX'ing operation on all records before they could be used with the FFT routine. The storage of integer values has the disadvantage that for every record of time series values from each analog input data channel there

must be an associated zero value and calibration constant to be applied to the integer time series values to obtain the true 'physical' quantity values. The zero value is stored in the calibration parameter file, and (if desired) is subtracted from the converted values before storage in the output disc file. The calibration constant is also contained in the calibration parameter file in two parts, the calibration factor and the scale factor. Before storage all the converted values from RUNDAT (with the zero value removed) are multiplied by the calibration factor resulting in another integer number the value of which is stored. This value plus the scale factor can be likened to the mantissa and exponent of a number expressed in exponential notation, except that the mantissa (i.e. the value in the stored array) is an integer and the scale factor (always calculated to be a power of 10) corresponds to the exponent and is the same for all record values stored from one channel. As the conversion is only to 10 binary bits of accuracy and the integer value stored can be up to 16 bits, one can choose suitable values for the calibration factor and a scale factor can be chosen that will retain all the accuracy of the analog-to-digital conversion.

The analysis program must therefore have access to both data file and calibration parameter file in order to express the analysed data results in 'physical' values. In general this is no hardship as the parameter file may have to be consulted to extract the sample rate and other

details of the channel arrangement before further processing. The routine GETPF in TSALIB (see Chapter 9) has been written to simplify the extraction of values from the parameter file for this purpose.

The analysis of random time series often involves the use of extended lengths of data record. To make the handling and subsequent analysis of this type of record easier the sampling program can be set to sample the long record as a series of smaller records, contiguous in time. The data storage method is illustrated in figure 29.

The total number of samples that can at present be acquired at one time into one file is 1.2×10^6 , limited by the capacity of one removable disc. The largest file created to date has been 1.2×10^5 samples.

Calibration program

The calibration program consists of 4 phases. See figure 30.

In the first phase an attempt is made to read an existing calibration file parameter file, so that the values may be used as defaults for the updated version. If no file is found a 'dummy' file with zero entries is written. In the second phase the experimenter defines the format of the output file (number of samples per record, frames per file etc.), the sample interval (in integer

milliseconds, seconds, minutes) and whether long term drift may be eliminated by taking a zero run before the start of every run.

The third phase is ^{the} channel calibration part in which a channel (or group of channels) is selected and two known signal levels are applied in turn to the analog-to-digital converter from the associated transducer(s). Two mean converted values are obtained by sampling the channel(s) for 1 second at 50 samples per second and the mean value calculated. The values obtained, in conjunction with the physical value they represent entered from the computer terminal are used to compute a suitable calibration factor and scale factor pair for each channel, or channels, in the group. This phase may be repeated if the values obtained are, for any reason, not satisfactory. The input analog channels may be calibrated in any desired order. An option allows a channel, or group of channels, to be left in a condition where no zero removal or calibration occurs and in which just the 'raw' converted values are stored. Note that default values for the calibration factor and scale factor are obtained from the previous calibration parameter file. It is thus not necessary to recalibrate all channels every time the calibration program is run, merely those analog channels whose gain or function has been changed.

The final phase is to write the updated parameter file back to disc as a new version, with new time and creation date. The new contents of the calibration parameter file

can be printed on the terminal, as an option, before the program finally exits.

Data acquisition program

The data acquisition program consists of 3 phases. See figure 31. In the first phase the most recent calibration parameter file is read into the program and the values stored. If no file exists an error message is generated and the program exits.

In the second phase the program issues a request to the operating system monitor to run the program at a high software priority so that it will receive processor time in preference to other programs running at the same time. If selected in the calibration routine zero values are taken on the selected channels when the experimenter is ready, then the program waits for the selected start signal. When activated the incoming converted data from the analog-to-digital converters is 'double-buffered' in memory and when a buffer is full, transferred to a temporary file on disc, no scaling or zero removal being done at this stage. This section of FORTRAN code is written to execute as quickly and efficiently as possible, allowing a fast sample rate, or alternatively, extra processor time for other users when the sample rate is slow. If, for any reason, the data-acquisition has to be stopped before the collection of all the records requested in the calibration process, this can be achieved via the switches on the

processor front panel. Completed records acquired before this abnormal termination of the data-acquisition phase continue to be processed as normal in the last phase.

When the data records have all been acquired, the third phase begins. Firstly the software priority of the program is dropped so that subsequent operations compete on level terms with other user programs for system resources. An output file is opened and the data in the temporary file 'demultiplexed', zero removed, scaled, blocked into records and written to the output file. When complete the output file is closed and the program optionally loops to the start of phase 2 in preparation for the collection of another file of data.

Although relatively complex internally, much effort was expended in making the programs easy to use by an experimenter with little computer experience. This was achieved by extensive use of error and diagnostic messages, informative prompts on the terminal and the opportunity of allowing the experimenter to re-try the operation if an error was detected. In addition a comprehensive explanatory booklet on the programs complete with examples was produced (23).

There have been no problems encountered with the use of either program, as far as the author is aware, by any experimenter within the Laboratory. The flexibility of the programs to meet differing needs and general reliability

have been so good that no modification or further 'debugging' of the code has been required for the last 2 years of heavy use.

CHAPTER 9

Spectral Analysis Routines

The routines to carry out the computer spectral analysis were written, for several reasons, as a collection of short FORTRAN subroutines. The first was to allow each component operation of the full spectral analysis procedure to be examined and 'debugged' in isolation, and only when found to operate correctly to be added to the library of user routines. The second reason was that due to the memory and speed limitations of our present minicomputer it was not possible, or indeed desirable, to write a large all purpose analysis program. The author took the view that rather than attempt to keep one large analysis program fully maintained, and continually modified to cater for different and new procedures as they were developed, a better approach would be for the experimenter himself to write his own analysis program incorporating some of the subroutine library 'building blocks'. The benefit of this approach was that it would lead to smaller, simpler, faster programs, and also enable the experimenter to understand the processes involved to arrive at the results. This approach would hopefully reduce the errors that arise from the use of a 'black box' program in which the experimenter has little or no knowledge of the internal operation of the

program and hence the limitations of the analysis techniques used.

The subroutines available in the library are all written in FORTRAN with the exception of the Fast Fourier Transform part of the FASTFT subroutine which is written in PDP11 machine code. The subroutines fall into 5 types: the utility routines, the preprocessing (window) routines, the FFT routine, the spectral function routines and the post processing (frequency smoothing) routines.

The scaling of the time series data is handled by the scale value variable, originally obtained from the calibration parameter file by the utility routine GETPF, and subsequently modified by the windowing and Fast Fourier Transform routines, until it is used in one of the spectral function routines whose output is a REAL array. The user has thus no need to concern himself with the problems of scaling data values at any time during the program as the output spectrum estimates will be scaled to the correct values the accuracy of which, if we neglect computational rounding and truncation error, depends solely on the experimental calibration procedure and the linearity of the transducer systems employed. The resolution in the estimates produced is limited to 0.1 per cent by the 10 bit (1 part in 1024) resolution of the analog-to-digital converter used.

The effective bandwidth of the spectral estimates is

handled in a similar manner. The output run time T is extracted from the calibration parameter file by the utility GETPF, passed to BW3DB to compute the base resolution bandwidth which is subsequently modified by the windowing and frequency smoothing routines to reflect the increases in effective resolution bandwidth that both these operations imply.

Ensemble averaging is simply handled by the spectral output routines as they all add the new estimate into the output array. An argument flag is available on these routines to zero the elements of the output array prior to output if this is desired.

The preprocessing (window) subroutines

Five basic window formula are catered for by the library. Each window has 3 different methods of application to the data. The window routines are:

1. HANNn -- the 2 term Von Hann window.
2. HAMMn -- the 2 term Hamming window.
3. BLACKn -- the 3 term Blackman window.
4. BH4Tn -- the 4 term Blackman-Harris window.
5. FLATTn -- the 4 term 'Flat-top' window developed

by the author.

Routines where $n=1$ (e.g. HANN1, BLACK1 etc.) are used to compute the time domain weights of the selected window and store them in a REAL array of the same length as the time series to be windowed. The $n=4$ routine is then used to multiply the time series by the window weights array.

Routines of the $n=2$ type are used to compute the time series weights and apply them direct to the data in the one subroutine.

Routines of the $n=3$ type are used to apply the window to the raw complex Fourier coefficients by means of the discrete convolution detailed in Chapter 5.

The decision on what method to use to apply the window depends on a speed/storage tradeoff. For all window functions the $n=4$ routines run quickest, indeed once the companion $n=1$ routine has been run to create the time series window weights all the $n=4$ routines execute at the same speed irrespective of the number of cosine terms in the window. Thus for medium to large amounts of data one can choose the better 3 or 4 term windows with little increased computation time penalty over the simpler 2 term window forms. The $n=1$ routines, however, require the allocation of a REAL array of length equivalent to the input time series records. This array area can be reused at a later stage in the program when the window function

weight values are no longer needed.

The n=3 routines, operating in the frequency domain, execute at virtually the the same speed as the n=1, n=4 routines for the 2 term windows, but get progressively slower for the 3 and 4 term window formulas.

The n=2 routines are the slowest of all methods and should only be used when memory space is at a premium.

Relative speeds can be estimated from the number of trigonometric computations, REAL multiplies and adds, FIXEs and FLOATs that are performed in each routine as shown in the table:

n is the number of samples in the time series record.

T is the number of coefficient terms in the window.

...1 -- N × T cosine lookups.

+ N × T-1 Real additions.

...2 -- N × T cosine lookups

+ N × T-1 Real additions + N floats

+ N real multiplications + N fixes.

...3 -- N × T float, real multiplication, add

and fixes.

...4 -- N float, real multiplication and fixes.

The window function coefficients and bandwidths are listed in Table 4, whilst the window forms, in both time and frequency domains, are shown in Figures 16 to 21.

Fast Fourier Transform routine

The Fast Fourier Transform subroutine is a modified version of a routine written by Day and Pearson of the Digital Equipment Corporation Special Systems division.

The subroutine uses the Sande-Tukey FFT algorithm for ordered data with the coefficient re-ordering by the bit-reversal technique^{as} the last stage in the subroutine. The subroutine is written in assembler code for data arrays of INTEGER values, the maximum length of time series being 1024 points, limited by the interval of the quarter wave sine-cosine lookup table used. An overflow routine divides all values by 2 if an arithmetic overflow occurs during computation of the two-point inner transform loop values, a count being kept of the number of times this occurs. A software 'flag' can be set to negate the sine part of inner transform loop thus allowing the inverse FFT to be evaluated using the same subroutine code.

The main modification to the subroutine was to rewrite the code for passing the input parameters and error returns, making the code obey the same conventions (24) as that used for FORTRAN subroutine calls produced by the DEC FORTRAN IV compiler. The subroutine was also modified in

two areas to allow the use of the integer multiply instruction available on the PDP 11/40 instead of the software multiply routine previously used, and in the overflow routine to reduce execution time.

The present routine executes a 512 point transform, on average, in 186 milliseconds and a 1024 transform in 376 milliseconds on a PDP 11/40.

The assembler subroutine replaces the real and imaginary parts of the time series contained in integer arrays, with the double-sided (i.e. positive and negative frequency) complex Fourier coefficients. For time series data consisting only of the real values, the negative frequency part of the Fourier coefficients is merely a sign reversed version of the positive frequency part, and so only the positive part of the complex Fourier coefficient spectrum is subsequently used. The FORTRAN subroutine FASFT which calls the assembler FFT subroutine recomputes the input scale factor to correct for any FFT overflow scaling and the double to single sided spectrum conversion.

An increase in computing speed for 'real only' time series can be achieved by constructing a complex time series composed of two real time series x and y.

$$z_i = x_i + jy_i \quad i = 0, 1, 2 \dots N-1$$

The transforms of x and y can be obtained from the single transform of z (16) by

$$X_k = \frac{Z_k + Z^*(n-k)}{2}$$

$$Y_k = \frac{Z_k - Z^*(n-k)}{2}$$

$$k = 0.1.2 \dots N/2$$

The above procedure has not been programmed as at present the computation times achieved for analysis have been sufficiently fast. The majority of the computation time is taken up with the preprocessing of data, and the computation of Cross spectra, Coherence etc. rather than with the FFT itself. In future as analysis computation times increase, or analysis in 'real time' is considered, the increase in speed afforded by this method may be useful and it will be incorporated in the library.

Spectral functions

Six subroutines are incorporated into the library to further process the Fourier coefficients from FASTFT into useful frequency spectra. These routines are:

1. AMP
2. PSD
3. CROSS
4. TFUNCT

5. PHASE

6. COHERE

AMP

This routine computes the magnitude of the integer Fourier transform coefficients from FASTFT to produce the discrete Amplitude spectrum A_{xk} .

$$\begin{aligned} A_{xk} &= |X_k| \\ &= \sqrt{X_k \cdot X_k^*} \end{aligned} \quad k = 0, 1, 2 \dots N/2$$

The output estimates are scaled then added into a REAL array.

PSD

This routine computes the discrete Power Spectral Density function G_x using the integer Fourier transform coefficients from FASTFT using the relation

$$G_{xk} = 1/\Delta F |X_k|^2 \quad k = 0, 1, 2 \dots N/2$$

The output estimates are scaled then added into the REAL output array.

CROSS

This routine computes the Cross-spectrum magnitude

spectral function between an output and input of a system using the integer Fourier transform values of the output Y, and input X, time series.

$$G_{xyk} = 1/\Delta F |X_k^* Y_k| \quad k = 0, 1, 2 \dots N/2$$

$$= C_{xyk} - jQ_{xyk}$$

C_{xy} is the co-spectrum
 Q_{xy} is the quad-spectrum

and if

$$X_k = A_k - j B_k$$

$$Y_k = C_k - j D_k$$

then

$$C_{xyk} = A_k C_k + B_k D_k$$

$$Q_{xyk} = A_k D_k - B_k C_k$$

The cross-spectrum magnitude estimate is scaled and added into a REAL array.

TFUNCT

This subroutine computes the Transfer function magnitude or 'gain' spectrum from previously computed estimates of the Cross-spectrum G_{xy} and the output Power spectrum G_y of the system. The Transfer function uses the relation

$$|H_k| = \frac{|G_{xyk}|}{G_{xk}} \quad k = 0, 1, 2 \dots N/2$$

The gain estimate so computed is added into a REAL array.

PHASE

The subroutine computes the phase angle spectrum for a system from the integer Fourier transforms X and Y of its input and output respectively using the relation

$$\phi_{xyk} = \frac{-180}{\pi} \tan^{-1} Q_{xyk}/C_{xyk} \quad k = 0, 1, 2 \dots N/2$$

and if

$$X_k = A_k - jB_k$$

$$Y_k = C_k - jD_k$$

then

$$C_{xyk} = A_k C_k + B_k D_k$$

$$Q_{xyk} = A_k D_k - B_k C_k$$

The phase estimates calculated lie in the range -180 to +180 degrees and are added into a REAL array.

COHERE

This routine computes the Coherence spectrum function γ_{xy}^2 for an input and output pair of a system, from previously calculated values of its Cross spectrum G_{xy} , input Power spectrum G_x and output Power spectrum G_y . The

relation used is

$$\gamma_{xyk}^2 = \frac{G_{xyk}}{G_{xk}G_{yk}} \quad k = 0, 1, 2 \dots N/2$$

The computed Coherence estimate being added into a REAL output array.

Frequency averaging routine

The subroutine SMTHB is used to apply frequency averaging to spectral estimates to improve the statistical reliability of the spectrum produced by giving more Degrees of Freedom to each spectral estimate. This increase in Degrees of Freedom is gained at the expense of an increase in resolution bandwidth of the spectrum concerned. The increase in resolution bandwidth is given by

$$B_e' = B_e + \frac{p-1}{T}$$

B_e' is bandwidth after averaging
 B_e is bandwidth before averaging
 p is no. of adjacent estimates averaged
 T is length of time series record in seconds

The algorithm used replaces the estimate at the current frequency value by the mean of the current value and the $(p-1)/2$ values on either side viz.

$$G'_k = \frac{1}{p} \sum_{i=(p-1)/2}^{-(p-1)/2} G_{k+i} \quad k = 0, 1, 2 \dots N/2$$

For end values where $k-i$ would be <0 or $>N/2$ the spectrum is 'folded over' so that if $0 > k-i > N/2$ then $G_{k-i} = G_{k+i}$.

The routine cannot overwrite G_k with G'_k as the old value of G_k is required for later averaging. The input and output arrays containing G_k and G'_k must therefore occupy different areas of computer memory. It is possible to write the algorithm with $(p-1)/2$ temporary storage locations to hold the values of G'_k until they can be replaced in the array, but this complicates the averaging procedure, especially if we are to allow for different values of p . The use of the separate input and output arrays was considered preferable, especially as some smoothing is often applied on a 'trial and error' basis in programs, and thus cannot be allowed to overwrite the existing values as then subsequent averaging with a new value of p would require the recomputation of the spectral estimate.

Utility routines

The utility routines are a set of 6 subroutines that, whilst not performing any major computation, make the use of the spectral analysis subroutines simpler.

GETPF is used to open and retrieve values from the calibration parameter file for subsequent use in the program. Values returned from the routine give information on the organisation and contents of the data file, the scale values associated with the integer records, the sample interval and data acquisition mode. If the argument array containing the name of the desired calibration parameter file is full of 'null' characters the routine will prompt for the name of the file to be entered on the users terminal.

BW3DB is a simple subroutine to calculate the base resolution bandwidth from the length of the sample record i.e.

$$B_e = 0.88/T$$

SET and ISET are also simple subroutines used to fill a REAL or INTEGER array with a constant value.

FBASE is used to fill an array with corresponding frequency values to the spectra being produced so that the corresponding elements of the array filled by FBASE and the array containing the spectral function value constitute an X Y pair for subsequent plotting of the spectrum on the storage screen or plotter. This routine was primarily written to allow a simple interface between the TSALIB subroutines and plotting of the spectra using the SIMPLEPLOT graphics package.

The routine WNOISE adds 'white noise' to the input power spectrum estimate G_x before calculation of the Transfer function gain by use of the relations

$$|H_{xyk}|^2 = \frac{G_{yk}}{G_{xk}} \qquad H_{xyk} = \frac{G_{xyk}}{G_{xk}}$$

The addition of the noise signal tends to stabilise the calculated values of H_{xy} especially where there is little or no input power present. The amount of noise added is an input parameter and is expressed as a fraction of the total power present in the input signal.

CHAPTER 10

The Wave Spectrum Routines.

The need for a set of subroutines to evaluate the more common wave spectra formulations was apparent at an early stage in the development of the wave generation program. It was also realised, however, that subroutines of this type, if sufficiently general, could have a much wider use in response prediction and downtime study programs. An initial study of the formulations for wave spectra convinced the author of the need for rationalisation of the input units used, in addition to a standard output spectrum form. The formula used were modified to use S.I. derived input units for all input values and give a $1/2$ amplitude² spectrum for output. The input values are in metres for significant wave height, kilometres for fetch, metres per second for wind velocity, seconds for zero-crossing and significant wave period and frequencies in Hertz. The output spectrum values are all in metres² seconds (metres² per Hertz).

All subroutines are written in standard ANSI FORTRAN IV, and on the laboratory system contained as a library of 'object code' routines which can be selectively linked to the user program before the program is run.

Single Parameter Spectrums

The form of the subroutine call for single parameter spectra types was chosen as

```
CALL SUB(LUN, ISIZ, ARRAY, DELTF, U10, FM, HSIG[ , FETCH])
```

where

1. SUB is the subroutine name.

PM for Pierson-Moskowitz.

PMS for Pierson-Moskowitz-Silvester.

JONSWP for the 'JONSWAP' spectrum.

DARBY for the Darbyshire coastal spectrum.

2. LUN is the logical unit number of the device to which the prompt message (if any) will be directed, and also the logical unit number from which the spectrum parameter values will be received.
3. ISIZ is the number of spectral values to be evaluated.
4. ARRAY is a REAL array of length at least ISIZ to

contain the output spectrum values.

5. DELTF is the frequency increment between the spectra values. On output ARRAY(I) will contain the spectra value at frequency (I-1)DELTF. ARRAY(1) contains the zero frequency spectrum value, set to zero for all routines.
6. U10 is the wind velocity at 10 metres above sea level.
7. FM is the frequency corresponding to the maximum value in the spectrum.
8. HSIG is the significant wave height of the spectrum.
9. FETCH is the effective distance over which the wind can act upon the water surface to produce waves. This argument is not used in the PM routine as the Pierson-Moskowitz is a 'fully aroused sea' spectrum.

As the quantities u_{10} , f_m and H_s are all interdependent, for all the spectra formulations used (see Chapter 4) we need only input a value for one of these arguments and the corresponding values for the other two will be set within the subroutine. Some of the relationships between these quantities are not simple

(especially so for the JONSWAP spectral formulation) and iterative or repeated bisection methods are used to solve them. In all cases the parameter used to calculate the spectrum values is f , i.e. the f_m/f form of the spectrum formula is used, so that for maximum accuracy this is the desired input parameter.

If all three spectrum parameter inputs are set zero on entry to the subroutine, and a legal value for LUN is supplied, then the subroutine will prompt for input with the following message on the terminal associated with the logical unit number LUN.

ENTER A SPECTRUM PARAMETER VALUE

APPEND A ",U" IF WINDSPEED AT 10M. A.S.L. IN METRES/SEC

" ,F" IF PEAK FREQUENCY IN HERTZ

" ,H" IF SIG. WAVE HEIGHT IN METRES

The desired input parameter and code is then entered from the terminal keyboard.

In a similar manner, if the FETCH argument is zero for the fetch limited formula and a legal LUN is supplied, the prompt

ENTER FETCH IN KILOMETRES ?

is sent to the associated terminal and the routine waits for a fetch length to be entered from the keyboard.

At this point the array ARRAY is filled with the calculated values of the wave spectrum, and HSIG is recalculated by numerical integration of the spectral values using Simpson's 1-4-1 rule. On exit the subroutine arguments U10, FM and HSIG all contain values related to the values in ARRAY. The value of HSIG derived by numerical integration can be checked against the true value and can indicate if the spectrum 'tail' has been truncated or the value chosen for DELTF was too large.

Two Parameter Spectrums

The form of the subroutine call for the two parameter spectra types was chosen as

```
CALL SUB(LUN,ISIZ,ARRAY,DELTF,HSIG[,TSIG or ,TZ])
```

where

1. LUN is the logical unit number of the device to which the prompt message (if any) will be directed, and from which the input parameter values will be received.
2. ISIZ is the number of spectral values to evaluate.
3. ARRAY is a REAL array of length at least ISIZ, to contain the output spectral values.

4. DELTF is the frequency increment between spectral values as detailed under single parameter spectrums.
5. HSIK is the significant wave height.
6. TSIK is the significant wave period (for ITTC and BRET).
7. TZ is the input mean wave zero-crossing period (for BTTP).

As the output spectrum depends on both HSIK and TSIK (or TZ) if either or both of the arguments are zero the following prompt(s) will appear on the terminal associated with LUN

WHAT IS SIGNIFICANT WAVE HEIGHT IN METRES ?

WHAT IS SIGNIFICANT WAVE PERIOD IN SECONDS ?

WHAT IS ZERO CROSSING PERIOD IN SECONDS ?

and the subroutine will pause to allow the relevant legal value to be entered. The spectral values are then computed and placed in ARRAY. The value of HSIK, the significant wave height, is recomputed from a numerical integration of the wave spectral values to allow a check to be performed on the values produced as in the single parameter spectrum case.

CHAPTER 11

Derivation of the Flat-Top Window coefficients

In Chapter 5 reference was made to the use of window functions applied to the sampled time series data in either the time domain or as a convolution in the frequency domain to reduce the smearing of the resultant discrete spectrum due to components in the time series which are not harmonically related to the basic period T , the sample record length.

This smearing occurs because the finite length record, when Fourier transformed, results in a frequency spectrum where the time series values are convoluted with the continuous Boxcar function $U_T(s)$

$$U_T(s) = \frac{\sin \pi s}{\pi s} \quad \text{where } s \text{ is the non-dimensional frequency}$$

$$s = fT$$

T is the length of the time series in seconds

Note: As the transformed frequency values from a D.F.T. are at frequencies n/T apart starting at a frequency of zero, the corresponding s values are at $s = 0, 1, 2, 3, 4, \dots (N-1)/2$

This function has non zero values for all points except

$s = 1, 2, 3, 4, \dots (N-1)/2$

and thus due to the convolution of this function with the discrete Fourier transform coefficients, any Power in these areas appears in the main lobes of the U_T function.

One method of windowing consists of applying a tapering function to the time series values so that they approach zero at each end of the record, hence making all the components of the time series appear to be harmonic within the record length T . The Fourier transform of such a window function will be found to be similar in form to the Boxcar function but with the 'sidelobes' reduced in amplitude thus causing less smearing. The width of the peak of the function will have increased with respect to the Boxcar function reflecting the greater resolution bandwidth due to the shortening of the effective record length by tapering.

If the transformed window function is shown centred on each transformed frequency value (as it is by convolution) we can obtain a representation of the 'response' of the discrete transform to all frequencies below the folding frequency limit. A section of such a diagram is shown in Figure 32. The effect of the discrete transform can be likened to passing the continuous time series signal through a set of tuned bandpass filters of centre frequencies n/T where $n = 0, 1, 2, 3, 4, \dots, (N-1)/2$, the response function of each filter corresponding to the window function in the frequency domain. The response at

all frequencies is not the same as the 'filters' have a narrow bandwidth and the response curves fall before they overlap adjacent 'filter' response curves. This 'scalloping' or 'picket-fencing' of the response is of concern when attempting to accurately measure the amplitudes of frequency components that are not harmonically related to the record length as they will fall on areas of reduced response of the spectrum.

It occurred to the author and others (25) that if a window function could be found corresponding to a Flat-Top bandpass filter using the electrical filter analogy, the 'scalloping loss' could be reduced if the 'bandpass filters' curves could be made to overlap before their response fell off. The decision was made to base the search for such a window function on the raised cosine arch class of window functions as they are simple to operate on in either the time or frequency domains. Another possible alternative would have been the window functions based on Bessel functions (18). However these Kaiser-Bessel windows do not give rise to simple functions in the frequency domain.

Reference (25) implied that such a raised cosine arch window function could be made with 4 or at the most 5 coefficients.

The 'Least Squares' approach

In the non-dimensional frequency (s) domain the raised cosine arch class of window functions can be represented by

$$W(s) = \frac{A_0 \sin \pi s}{\pi s} + \sum_{I=1}^{n-1} A_I \left(\frac{\sin(\pi s + I)}{(\pi s + I)} + \frac{\sin(\pi s - I)}{(\pi s - I)} \right)$$

if we substitute $F(\pi s)$ for $\sin \pi s / \pi s$ we obtain

$$W(s) = A_0 F(\pi s) + \sum_{I=1}^{n-1} A_I (F(\pi s + I) + F(\pi s - I))$$

This expression can be expanded as

$$W(s) = A_0 F(\pi s) + A_1 (F(\pi s + 1) + F(\pi s - 1)) \dots A_{n-1} (F(\pi s + (n-1)) + F(\pi s - (n-1)))$$

At this stage we can note that for $s=0$

$$W(0) = A_0 + A_1 + A_2 + A_3 \dots \dots \dots A_n$$

and that at $n = 1, 2, 3, 4, \dots$

$$W(n) = A_n$$

If a graph of the window function is available one can easily obtain the coefficients from the above two relationships. In many cases one does not have an exact representation of the window response desired, but we can sketch a graph of the response required and pick, say, m critical values for $W(s)$ at

$$s_1, s_2, s_3, s_4, \dots, s_m$$

and calculate the corresponding

$$F(\pi s_m), F(\pi s_m+1), F(\pi s_m-1), F(\pi s_m+2), F(\pi s_m-2), \dots$$

we can obtain the set of linear equations

$$W(s) = A_0 F(\pi s_1) + A_1 (F(\pi s_1+1) + F(\pi s_1-1)) + A_{n-1} (F(\pi s_1+n-1) + F(\pi s_1-n-1))$$

$$W(s_2) = A_0 F(\pi s_2) + A_1 (F(\pi s_2+1) + F(\pi s_2-1)) + A_{n-1} (F(\pi s_2+n-1) + F(\pi s_2-n-1))$$

$$W(s_m) = A_0 F(\pi s_m) + A_1 (F(\pi s_m+1) + F(\pi s_m-1)) + A_{n-1} (F(\pi s_m+n-1) + F(\pi s_m-n-1))$$

If $m=n$ one has n equations in n unknowns and one can solve directly for $A_0, A_1, A_2, \dots, A_{n-1}$. In cases where exact values of the window response function can not be defined it is preferable to make $m \gg n$ yielding m equations in n unknowns. This overdetermined set of equations can then be decomposed into n equations using least squares procedures and the n equations solved, as before, for A_0, A_1, \dots, A_{n-1} . The values obtained will be the 'best fit' to the desired window response in a 'least squares' sense.

This method was written as a computer program SOLVEL and gave some insight into the operation of the raised

cosine window function. The method, however, is sensitive to the exact values of 's' chosen to define the function, and a great deal of adjustment is needed to obtain useful functions. In any event none of the coefficient 'sets' created by this method had a sufficiently flat-top over the range $+s/2$ to $-s/2$ to give a flat response over the measurement range.

Linear Programming method

Normally the two parameters determining the 'shape' of the window function that are of most interest are the peak width and the sidelobe level. In addition for the Flat-Top window we would require that the window response function be flat to within some tolerance over the range $+s/2$ to $-s/2$. Thus the author defined his desired window function response by the following limits

$$\begin{array}{ll}
 0.999 \leq W(s) \leq 1.0 & \text{for } -0.5 \leq s \leq 0.5 \\
 W(s) > 0.0 & \text{for } -4.0 \leq s \leq 4.0 \\
 -2.44 \times 10^{-4} \leq W(s) \leq 2.44 \times 10^{-4} & \text{for } 4.0 < s < -4.0
 \end{array}$$

The first limit ensures that the top will be flat to within 0.1%, the resolution attainable from the Laboratory 10 bit Analog-to-Digital converter. The second limit ensures that the peak extends not further than $+4s$ to $-4s$ from before $W(s)=0$ (and by implication that a 4 term series will result). The third limit ensures that the sidelobe

level is at least -72dB down with respect to the peak value. The value -72dB was chosen as it corresponds to 1 converted value in the range of a 12 bit Analog-to-Digital converter (a 12 bit converter was being considered at that time for another project) and thus the sidelobe level would be much less than 1 converted value for the 10 bit converter used.

This set of limits, or constraints, are directly compatible with those used in Linear programming methods (26)(27) as constraints in the problem of minimising (or maximising) a function. In this case the function would be the expression for $W(s)$ in terms of $A_0, A_1, A_2, \dots, A_{n-1}$. A suitable value of the function to minimise would be that at the end of the window, in the time domain, so that the window weights fall as near to zero as possible at each end of the time series record. As the raised cosine arch class of window can be defined in the time domain as

$$W(t) = A_0 + \sum_{I=1}^{n-1} A_I \frac{\cos 2\pi I t}{T} \quad \text{where } -\frac{1}{2}T < t < \frac{1}{2}T$$

In our case for $n=4$

$$W(-\frac{1}{2}T) = A_0 + \sum_{I=1}^3 A_I \cos (-\pi I)$$

$$W(\frac{1}{2}T) = A_0 + \sum_{I=1}^3 A_I \cos (\pi I)$$

but as

$$\cos(-\pi I) = \cos(\pi I)$$

$$\text{and } \cos(\pi I) = \begin{matrix} 1 \text{ for } I \text{ even} \\ -1 \text{ for } I \text{ odd} \end{matrix}$$

and we want to minimise

$$A_0 + \sum_{I=1}^3 A_I \cos(\pi I)$$

which infers that we want to minimise the value

$$A_0 - A_1 + A_2 - A_3 \dots$$

A program was written to set up the linear constraint equations of the form

$$A_0 F(\pi s) + A_1 (F(\pi s+1) + F(\pi s-1)) + A_2 (F(\pi s+2) + F(\pi s-2)) + A_3 (F(\pi s+3) + F(\pi s-3)) \begin{matrix} (\geq) \\ (\quad) \\ (=) \\ (\quad) \\ (\leq) \end{matrix} W(s)$$

for the following values of W(s) and s

$$W(0) = 1.0$$

$$0.999 \leq W(0.5) \leq 1.0$$

$$W(1.0) \leq 1.0$$

$$W(2.0) \leq 1.0$$

$$W(3.0) \leq 1.0$$

$$W(4.0) \leq 1.0$$

and for selected s values > 4.0

$$-2.44 \times 10^{-4} \leq W(s) \leq 2.44 \times 10^{-4}$$

In practice this gave a total of 27 constraint equations. The constraint equations plus the function to be minimised were passed via data file to the program SOLVE2. SOLVE2 is a linear programming program written around the Numerical Algorithms Group (NAG) FORTRAN routine H01ADF which solves the linear programming problem by the Revised Simplex method (27). The routine automatically sets up the 'slack' variables and finds the solution at the 'extreme feasible point' by means of exchange and edge following. Solution values found were

$$A_0 = 0.5$$

$$A_1 = 0.9571529$$

$$A_2 = 0.54618353$$

$$A_3 = 0.09658094$$

and $A_0 - A_1 + A_2 - A_3 = -0.0076$

The time and frequency domain representations of this window are shown in Figure 21 and in comparison with other

popular window functions, in the frequency domain, in Figure 15. The flat frequency response obtained from the use of the Flat-Top window is evident from Figure 33. Figures 34 and 35 show the improvement in measurement of a unit amplitude sinusoid at frequencies on and off transformed 's' values.

Using Linear Programming methods in which the desired window response is defined by constraints is thus a useful design tool for the construction of raised cosine window functions. The Flat-Top window is only one such window and by simple manipulation of the constraint equations a whole family of window functions may be obtained, each one being tailored to a specific user requirement.

CHAPTER 12

Test of Random Wave Generation and Analysis System

Three series of tests were conducted in the Laboratory tank using using the modified hydraulic powered wavemaker system. The first series of tests were to conduct an evaluation of the new wavemaker system to find its capabilities for the generation of regular waves and to compare it with the previous system. The second set of tests were to find the problems associated with running the random wave time series generated from the wave generation programs, to generate the wave spectra needed for the subsequent model tests, and to determine qualitatively the efficiency of the new sub-beach system. The third set of tests were to find if we could obtain accurate, repeatable, spectral results from a model test conducted in a seaway. Each test series is now described in detail.

First test series

The aims of the first tests were to perform the following:

1. Optimise the open-loop gain of the servo-hydraulic system.

2. To determine the range in frequency and height of waves that could be generated with the new system.
3. To provide a regular wave calibration chart for the wavemaker.
4. To investigate the linearity of the amplitude response of the system.
5. To determine an initial approximate value of $1/|H(f)|^2$ for the wavemaker system as a starting point for the WAVGEN-WAVEM iterative process.
6. To measure the efficiency of the original beach system.

To begin the hydraulic system was carefully 'bled' of all air, and then driven with a 1 Hertz square wave of small amplitude from a signal generator. The open-loop gain of the system was increased by the feedback potentiometer in the drive electronics until the onset of self-oscillation. The feedback open-loop gain was then reduced until the output from the feedback transducer, when viewed on an oscilloscope, showed no overshoot on the leading edge of the square wave trace. The closed-loop gain was adjusted so that 1 Volt input gave a 1.5 centimetre deflection of the plunger. The +10 to -10 Volt input range allowable before saturation of the drive electronics amplifiers thus gave a total plunger deflection

of +15 to -15 centimetres.

The experimental arrangement shown in Figure 36 was then set up with the signal generator set to give sine waves of known frequency and amplitude. The procedure was to connect the signal generator output to the wavemaker for 10 to 15 cycles and then disconnect. The 'wave packet' so produced passed the calibrated wave probe in the otherwise clear tank, travelled down to the beach, the reflected wave travelling back up the tank to again pass the wave probe. The output of the signal generator and the wave probe amplifier were plotted on two channels of a 4 channel pen recorder of adequate frequency response. The process was repeated at different drive voltages and frequencies, allowing time between runs for the tank to settle. The results were plotted and are presented as Figures 37, 38 and 39.

It was apparent from Figure 39 that there would be no wave output from the system for drive frequencies of less than 0.2 Hertz, and that the wave amplitude was not a linear function of drive voltage. Figure 38, showing the calibration of the wavemaker against a wavelength base shows the onset of wavebreaking occurs at a wave steepness h/λ of approximately 1/10. This figure is a large improvement over the results from the previous drive system (28) where values of 1/20 or less were obtained. Some of this improvement can be explained by the smoother and more regular motion of the hydraulic ram driven plunger, the

speed of the motor powered system increasing as the plunger descended and decreasing as the load on the motor increased when the plunger was raised. The vibration of the motor gearbox drive also superimposed small amplitude ripples on the surface of the generated waves which tended to precipitate any incipient wavebreaking. Regrettably there was not further time available to study the wavebreaking phenomena more closely to see if any further improvement could be made.

The values of $1/|H(f)|^2$ were computed from Figure 39 and stored in a disc file as a starting point for the WAVGEN-WAVEM programs.

The graph of beach attenuation, Figure 40, shows the poor wave absorbing capacity of the short steep beach for both long, low frequency waves and also, for large, higher frequency short waves. At this time a removable 'transparent' sub-beach was designed by Mr. D. Sinclair of the department, to be fitted in front of the existing beach as shown in Figure 41. The purpose of this beach was to increase the effective length of the beach arrangement and thus improve the absorption of the long, low frequency waves.

Second test series

The main aims and objectives of the second set of tests were:

1. To investigate the operation of the random seaway generation system, and modify it, if necessary, for satisfactory operation.
2. To investigate the use of the WAVGEN-WAVEM iterative process for the production of reproducible sea spectra.
3. To produce the F.M. magnetic tapes of wave spectra drive signals for the subsequent (third series) tests.
4. Investigate qualitatively the efficiency of the new sub-beach. Instrumentation was not available to measure the wave attenuation in the same manner as was used in the measurements of wave attenuation in the first series of tests.

The experimental arrangement for the second series of tests is shown in Figure 42. Initial tests involved running the program WAVGEN to create a time series corresponding to a spectrum with constant power density per unit bandwidth from 0.2 to 2.0 Hertz. The total run length was set at 18 records of 64 seconds for a total time of 1152 seconds. When replayed via the filter described in Chapter 7 an extremely confused seaway resulted, showing excessive wavebraking, and the wavemaker system itself showing signs of distress as the system attempted to follow the large amplitude higher frequency excursions. The

spectrum actually produced when analysed using WAVEM over a time of 1280 seconds (20 records) showed a rapid fall off in wavemaker response below 0.3 Hertz and above 1.7 Hertz. The author decided to reduce the range of frequencies produced to between these two limits, in order to reduce the excessive drive voltage amplitudes that would result from attempting to produce waves outside this region. The constant power density time series was recomputed using WAVGEN with these new frequency limits and the test re-run. The seaway produced when analysed using WAVGEN was much improved but still showed a gradual fall off in wave power toward the high frequency end of the spectrum. As there was still excessive wavebreaking in the spectrum the author decided to replace the constant power per unit bandwidth spectrum used with one in which the power per unit bandwidth reduced at a rate proportional to $1/f$. The time series for this type of spectrum was created using WAVEM for the frequency band 0.3 to 1.7 Hertz, using the modified version of the wavemaker Transfer function correction file produced^{by} the two previous runs of WAVEM. In retrospect it should have been obvious that a constant energy per unit bandwidth spectrum would have been too violent a drive signal but thankfully no damage was done. The seaway produced from this time series was analysed and found to be a reasonable representation of the spectrum desired. At this stage, due to shortage of tank time, it was decided to proceed to attempt to produce the seaway spectra needed for the subsequent tests of a 1/100 scale model, the spectra chosen being open-sea Pierson-Moskowitz spectrum for sea

conditions corresponding to significant waveheights of 5, 10 and 15 metres full scale.

The H = 10 metres case was generated first and after two iterations of the WAVGEN-WAVEM programs, starting from the wavemaker correction file for the 1/f spectrum test, the spectrum shown in Figure 43 was produced. The second iteration of the process produced only a marginal improvement. The H = 5 metres spectrum, Figure 44, was produced after one iteration of the WAVGEN-WAVEM program using the wavemaker correction file values for the H = 10 metres case. The 'hump' in the response at 1.5 Hertz was found not to be substantially reduced by the iterative correction process.

Several possible sources of wave generation at this 'hump' frequency were investigated, including vibration of the new sub-beach due to its temporary mountings and possible transverse wave modes generated across the tank. The most likely cause found was, however, in the wavemaker itself. It was found that due to wear in the guide rod bearing sleeves for the plunger, the plunger could rock transversely, the natural period of vibration being around 1.5 Hertz. As the feedback displacement transducer was offset to one side of the wavemaker centreline (and also the hydraulic ram) any 'rocking' of the plunger appeared as an error signal in the feedback loop. As a test the plunger was raised 10 centimetres from the still water position to reduce the damping of the system due to the

immersion of the plunger in the water, and 'rocking' induced by manually shaking one end of the plunger. The plunger then proceeded to 'rock' continuously at a frequency of 1.5 Hertz being driven by the hydraulic ram and associated feedback system. Raising the wavemaker plunger would also reduce the added virtual mass of the plunger system and so alter the resonant frequency in 'rocking' to a frequency less than 1.5 Hz. As the actual frequency was only measured to within 0.1 Hz. and the effect of resiting the feedback transducer was could not be carried out within the time available, 'rocking' motion being the cause of the hump on the spectrum produced can only be regarded as a tentative conclusion.

A note was made to re-site the feedback transducer on the plunger centreline and to re-line the bearings as soon as time became available.

As tank time available for further tests was now extremely short the $H = 15$ metres spectrum, Figure 45, was obtained directly using the wavemaker correction file for the $H = 10$ metres case. It was noticed that 2% of the time series values produced were logged as exceeding the Digital-to-Analog conversion limits and were thus truncated. This may account, in part, for the spectrum produced not attaining the desired peak value.

In all the above cases the time series produced had lengths of 1152 seconds, but the actual seaway time series

record from the wave probes was recorded for 1280 seconds to ensure that all the seaway produced by the wavemaker was recorded, thus removing any bias in the results due to wave energy being 'lost' in transit between wavemaker and the wave probes sited some distance down the tank.

A qualitative look at the effect of the new sub-beach convinced the author, and others, that although reducing wave height, it was not retarding waves sufficiently to cause them to break. It was decided that the areas between the slats should be filled with a filter material to further reduce the 'transparency' of the sub-beach.

Third test series

The aims of the third series of tests were:

1. To test the Spectral Analysis routines.
2. To check the repeatability of results using the system.
3. To compare the motion responses obtained with the use of the LDVT displacement transducers to that obtained with the 'Selspot' system.
4. To obtain the Response Amplitude Operator (R.A.O.) in pitch and heave for a 1/100 scale model of a 'Scotbuoy' oil tanker loading and storage buoy for

3 significant wave height conditions.

The test arrangement is shown in Figure 46 and Plate 4. Five runs were made with the LVDT transducers disconnected from the model, and model motion recorded only through the Selspot system. Six further runs were then made with the LVDT displacement transducers reconnected to the model. Table 6 gives a list of the runs made and the corresponding experimental conditions.

Two programs were written to analyse the data and display the results. The program RWAP (Random Wave Analysis Program) used the spectral analysis routines in the time series analysis library TSALIB to produce raw, ensembled, spectral values. The program RWDP (Random Wave Display Program) optionally frequency smooths these raw values and plots the results. For each run the following spectra could be plotted:

1. Power Spectral Density of mean signal from 3 forward wave probes.
2. Power Spectral Density of model heave.
3. Power Spectral Density of model pitch.
4. Heave Response Amplitude Operator = Heave Transfer Function.

5. Pitch Response Amplitude Operator = Pitch Transfer Function.
6. Heave Coherence Function.
7. Pitch Coherence Function.
8. Phase angle between heave signal and 'on beam' wave probe signal.
9. Phase angle between pitch signal and 'on beam' wave probe signal.

Complete sets of plotted output for runs TEST06, TEST09, and TEST10 are presented in Figures 47-55, 56-64, and 65-73 respectively. The wave spectra, pitch and heave R.A.O. spectra obtained from TEST08 are also displayed in Figures 74, 75 and 76. Figures 77 and 78 give the R.A.O. computed via the Selspot system during TEST06.

Regrettably the 'Scotbuoy' model used in these tests had natural frequencies in heave and pitch of 0.191 and 0.326 Hertz, the natural heave period thus lying outside the the generated wave band of the system. The natural pitch period also lies close to the lower end of the generated wave band and thus the peak in pitch R.A.O. associated with the natural period is not well defined. The results obtained, however, show the potential of the wave generation and analysis method.

The R.A.O. and phase angle spectrum values obtained from the model tests agree well with similar values derived from a mathematical model of the same structure run on the Laboratory PDP11/40 computer(29)(30).

Comparisons of the R.A.O. obtained from the 3 different wave conditions show the non-linear dependence of the Response Amplitude Operator on input wave power around the heave and pitch natural frequencies (Figures 50-51, 59-60 and 68-69).

Comparison of the R.A.O. and wave spectra obtained from TEST06 with those obtained from the 'repeat' run TEST08 show that excellent repeatability can be obtained with this system (Figures 47, 50, 51 and 74, 75, 76).

The R.A.O. spectra obtained from motion measurement using using the Selspot system are identical to those obtained from LVDT signals when both systems are run at the same time (figures 50-51 and 77-78). In future it will be recommended that the Selspot system is used for this type of work as it has the advantage of non-contact measurement and should thus give more realistic results especially with small test models, there being little or no need to apply corrections to the mass and inertia of the model because of the effect of the diodes' mass on the deck. This is not the case when LDVT displacement transducers with heavy iron cores are used with the smaller scale models.

Some degradation of the generated wave spectra was noted when the model was placed in the tank due to the absorption and regeneration of wave energy from the model. The coherence values obtained between heave and pitch signals and the mean incident wave are good, especially so as the wave probes were physically separated from the model by a distance of 10 metres. These values could be improved by siting the wave probes somewhat nearer the model in future tests of this type (Figures 52-53, 61-63, and 70-71).

CHAPTER 13

Conclusions and Possible Future Improvements

The main aim of this work was to construct a workable system for the measurement of the spectral responses of models in a predefined, statistically reproducible irregular seaway. The procedures detailed in this thesis have been tested and achieve the above aim.

The present system has, at present, several limitations which narrow its field of use and ease of operation. The main limitations are:

1. Restricted generated frequency bandwidth.
2. Restricted wave height.
3. Inefficient wave absorbing beach degrading the statistical stationarity of the seaway spectrum.
4. Time consuming iterative process to achieve desired spectrum.
5. Inability of present computer system to operate two 'real-time' processes simultaneously.

Improvements to the present system can be achieved by modification in 3 areas.

The frequency and wave height range of the wavemaker could be improved by the use of a longer stroke ram to give increased plunger displacement, with either an increase in hydraulic pressure or ram diameter to give the extra force required to drive the plunger over greater displacements. Reinforcement of the wavemaker foundations and guide rod assemblies would allow the upper generated frequency limit to be raised to around 2.0 Hertz. The lower frequency generation limit is a function of the plunger dimensions and so any useful improvement to the lower end of the generated frequency range can only be made by the substitution of a plunger of increased cross-sectional area.

Improvements to the wave absorbing beach design will have to be made to reduce the reflected wave energy at both extremes of generated frequencies. This is especially important should any of the above modifications be contemplated.

The modification of the AR11 Analog-to-Digital converter sub-system driver software to allow the operation of two 'Real time' processes or, preferably, the purchase of another AR11 type sub-system plus additional software driver code. The second option is preferable because the

modification of the existing software would, at best, only allow both processes to run at the same sample rate, reducing the flexibility available in the choice of wave time series output and data sampling intervals. This limitation of sample rates would entail modification of both the wave generation and data sampling programs. The addition of a second AR11 would give the computer system two 'real time' clocks and thus the ability to generate or sample data at two independent rates.

Longer term modifications

Improvements in the speed of setting-up and ease of operation could be obtained by running the computer controlled wave generation as a closed-loop process. In such a system the generated output wave would be sampled, records constructed and the Power spectrum for the record generated via the FFT. The spectrum so computed would be compared with the desired wave power spectrum, and the difference or error spectrum computed. Before the next wavemaker time series was generated from the inverse FFT of the desired spectrum, the desired spectrum would be corrected by the error spectrum, and so each time series record would give a seaway spectrum in the tank more closely approaching the desired spectrum.

In operation, one would start the wave generation program and allow it to run for two or three time series records until the seaway process became reasonably

stationary, in a statistical sense, before starting to sample and store the necessary data from the model under test.

As the wave generation software would be more complex, and moreover be required to run in real-time, the program would best be run on a small dedicated computer system, leaving the Laboratory PDP11/40 system to handle the data analysis and program development load.

As experience with spectral analysis grows within the Laboratory and 'standard' transducer arrangements for model tests are identified, an attempt could be made to write a generalised analysis program to cover these 'standard' test situations.

Ultimately the existing wavemaker and beach assemblies could be replaced with more suitable and efficient designs after a suitable study of available types. The beach could be of an 'active absorber' type similar in design to the wavemaker (31).

There is a limit to the possible improvement of the Laboratory test tank as a random wave test system as the tank itself is primarily a ship model towing tank and the narrow width and long length are far from suitable dimensions for a random wave test tank. The present system is, however, a valuable addition to the test capability of the Laboratory.

References

1. "A linear twin-wire probe for measuring water waves." D.K. Fryer and M.W.S. Thomas. Journal of Physics E: Scientific Instruments, 1975, Volume 8.
2. "Mathematical Elements for Computer Graphics." D.F. Rogers and J.A. Adams, McGraw-Hill, 1976. ISBN 0-07-053527-2.
3. "SSLIB and XYLIB Plotting Libraries." M.C.R. Sharp. NAOE-HL-78-01.
4. "FORTRAN subroutine package for the VT55." M.C.R. Sharp. NAOE-HL-78-03.
5. "Marine Hydrodynamics." J.N. Newman. M.I.T. Press 1977. ISBN 0-262-14026-8.
6. "Rules for the Design, Construction and Inspection of Fixed Offshore Structures," Det Norske Veritas, 1974.
7. "A Proposed spectral form for fully developed wind

- seas based on the similarity theory of S.A. Kitaigorodskii." Journal Geographical Research, Vol. 69, No.24, December 1964.
8. "Coastal Engineering." R. Silvester, Elsvier, 1974.
 9. "Measurements of Wind-Wave Growth and Small Decay during the Joint North Sea Wave Project," Hasselmann, K. et al. Ergonzingsheft zur Deutschen Hydrographischen Zeitschrift, Rihe A(8), November 12, 1973.
 10. "The One-dimensionalised Wave Spectrum in the Atlantic and in Coastal Waters." J. Derbyshire. Proceedings of the Conference on Ocean Wave Spectra.
 11. "Wave Variability and Wave Spectra for Wind generated Gravity Waves." C.L. Bretschneider. Beach Erosion Board, Corps. of Engineers Technical Memo 118 (1959).
 12. "Environmental Conditions". Report of Committee 1. Proceedings International Ship Structures Congress (1970).
 13. "The influence on ship motions of different wave spectra and of ship length." Ewing, J.A. and

Goodrich, G.J. Transaction Royal Institute of Naval Architects, 1967.

14. "Measurement of Power Spectra". Blackman and Tukey. Dover Publications, 1958.
15. "Random Data, Analysis and Measurement Procedures." Bendat and Piersol, Wiley Interscience 1971.
16. "Digital Time Series Analysis." Otnes and Enochson, Wiley Interscience, 1972.
17. "Digital Filters". R.W. Hamming, Prentice-Hall, 1977.
18. "On the use of Windows for Harmonic Analysis with the Discrete Fourier Transform". Harris, F.J. Proc. IEEE Vol.66, No.1, January 1978.
19. "Wave Spectrum Synthesizer." Application Note SP3179. Experiments and Electronic Laboratories, British Hovercraft Corporation.
20. "A Technique for Computer Simulation of Ocean Waves." L. Borgman, Probabalistic Mechanics .
21. Notes on the PDP-11 Fortran callable Pseudo-Random

- Number Generator Routines RAN and RANDU." Martin H. Ackroyd. DECUS RT-11 SIG Newsletter, February 1980.
22. "Digital Synthesis of Modelled Irregular Seaway". J. Brooks Peters, Time Histories, Proc ATTC, Vol.2, August 1977.
23. "RUNDAT and CALIBR Data Sampling Programs." M.C.R. Sharp, NAOE-HL-80-04.
24. "IAS/RSX Fortran II Users Guide Digital Equipment Company." Order Code PA-19360-TC.
25. "Window functions for Spectrum Analysis". R.G. Cox. Hewlett Packard Journal, September 1978.
26. "Numerical Analysis". Francis Scheid. Schaum's Outline Series, McGraw Hill, 1968, ISBN 07-055197-9. Chapter 27.
27. "Numerical Algorithms Group Fortran Library Manual." Mk 5. Section H, Operations Research.
28. "Investigation into characteristics of Wavemaker of Glasgow University Tank." T. Fuwa. G.U. Report, 1977.
29. "A Computer Program for the Dynamic Response

Analysis of a Spar Buoy". S.G. Tsinipizoglou.
NAOE-HL-79-08.

30. "Dynamic Response Analysis of 'Scot-buoy'". S.G.
Tsinipizoglou. NAOE- HL-80-15. .

31. "Active Wave Absorbers". J. Fluid Mech. Vol.42,
part 4, September 20,1970.

Table 1

CONVERSION TABLE FOR DIFFERENT SPECTRA DEFINITIONS

<u>Spectra Type</u>	<u>Area</u>	<u>H_{1/3}</u>	<u>H_{av}</u>	<u>H_{1/10}</u>	
(Ampl.) ²	m ₀	4√m ₀	2.5√m ₀	5.1√m ₀	m ₀ = Area = ∫ ₀ [∞] S(ω) dω
(Ampl.) ²	2m ₀	2.828√Area	1.767√Area	3.6√Area	Area = ∫ ₀ [∞] S(ω) dω
(Height) ²	8m ₀	1.414√Area	0.886√Area	1.80√Area	Area = ∫ ₀ [∞] S(ω) dω
(Height) ²	16m ₀	√Area	0.625√Area	1.275√Area	Area = ∫ ₀ [∞] S(ω) dω

Statistical Parameters and Approximate Sea State for Pierson-Moskowitz Spectrum

<u>Wind Speed, U_{10} (knots)</u>	<u>Wind Speed, U_{10} (metres/sec)</u>	<u>Approximate Sea State</u>	<u>Significant Wave Height</u>	<u>Peak Period (T_p) (Secs)</u>
10	5.15	2	0.58	3.88
20	10.29	4	2.33	7.76
30	15.44	6	5.25	11.64
40	20.59	7	9.32	15.52
50	25.74	8	14.57	19.40

Table 2

TABLE 4

Window Function Coefficients and Resolution Bandwidths

<u>Name</u>	<u>No. of Terms</u>	<u>Coefficients A_0, A_1, \dots, A_n</u>	<u>'Half Power' Bandwidth</u>
Boxcar	1	1.0	0.88Δf
Von Hann	2	0.5, -0.5	1.44Δf
Hamming	2	0.54, -0.46	1.25Δf
Blackman	3	0.42, -0.5, 0.08	1.64Δf
Blackman-Harris	4	0.35875, -0.48829, 0.14128, -0.01168	2.0 Δf
Flat-top	4	0.5, -0.95715285, 0.54618353, -0.096580939	3.5 Δf

TABLE 5

AR11 Analog-to-Digital
Converter Specifications

Characteristics	Specifications
Input Voltage Range	0 to +5 V } Program Selectable -2.5 to +2.5V }
Resolution	10 bits (1 part in 1024)
Accuracy at 25° C	0.1% of full scale
Number of Channels	16 (single-ended)
Linearity	1/2 LSB (0.05% of full scale)
Conversion time	30-32 μ S
Throughput Rate	PDP-11/10 with optimal coding:
Programmed Start	30 kHz
Overflow or External Start	35 kHz
Input Impedance	10M Ω min., -5V \leq V _{in} \leq +5V
Input Bias Current	100 nA max., unselected channel } -2 μ A max., selected channel } -5V \leq V _{in} \leq +5
Sample-and-Hold Tracking	Small signal bandwidth: 700 kHz Large signal slew rate limit: 1 V/ μ s
Sample-and-Hold Aperture	100 ns max. delay 1 ns jitter
Repeatability	rms noise 1/4 LSB maximum 1/15 LSB typical
Crosstalk	80 dB at 1 kHz, rolling off at 20 dB per decade
Warmup Time	5 minutes
Control	Controlled by programmed instructions, clock counter overflow, or external input
Output Format	Parallel, 10-bits, right-justified, offset binary, double buffered

TABLE 6

Scotbuoy Model Tests Run 27/5/80 to 29/5/80

<u>Data filename</u>	<u>Wave Spectrum</u>	Wave probes + Selspot
Test 01	P.M. spectrum Hs = 15.0 m	
Test 02	1/f white noise 'Hs' = 10.8 m	" " + "
Test 03	P.M. spectrum Hs = 10.0 m	" " + "
Test 04	P.M. spectrum Hs = 5.0 m	" " + "
Test 05	1/f white noise 'Hs' = 10.8 m	
Test 06	P.M. spectrum Hs = 10.0 m	Wave probes + Selspot + LVDT transducers
Test 07	1/f white noise 'Hs' = 10.8 m	" " + " + "
Test 08	P.M. spectrum Hs = 10.0 m	" " + " + "
Test 09	P.M. spectrum Hs = 15.0 m	" " + " + "
Test 10	P.M. spectrum Hs = 5.0 m	" " + " + "
Test 11	1/f white noise 'Hs' = 10.8 m	" " + " + "

TEST TANK EXPERIMENT AREA

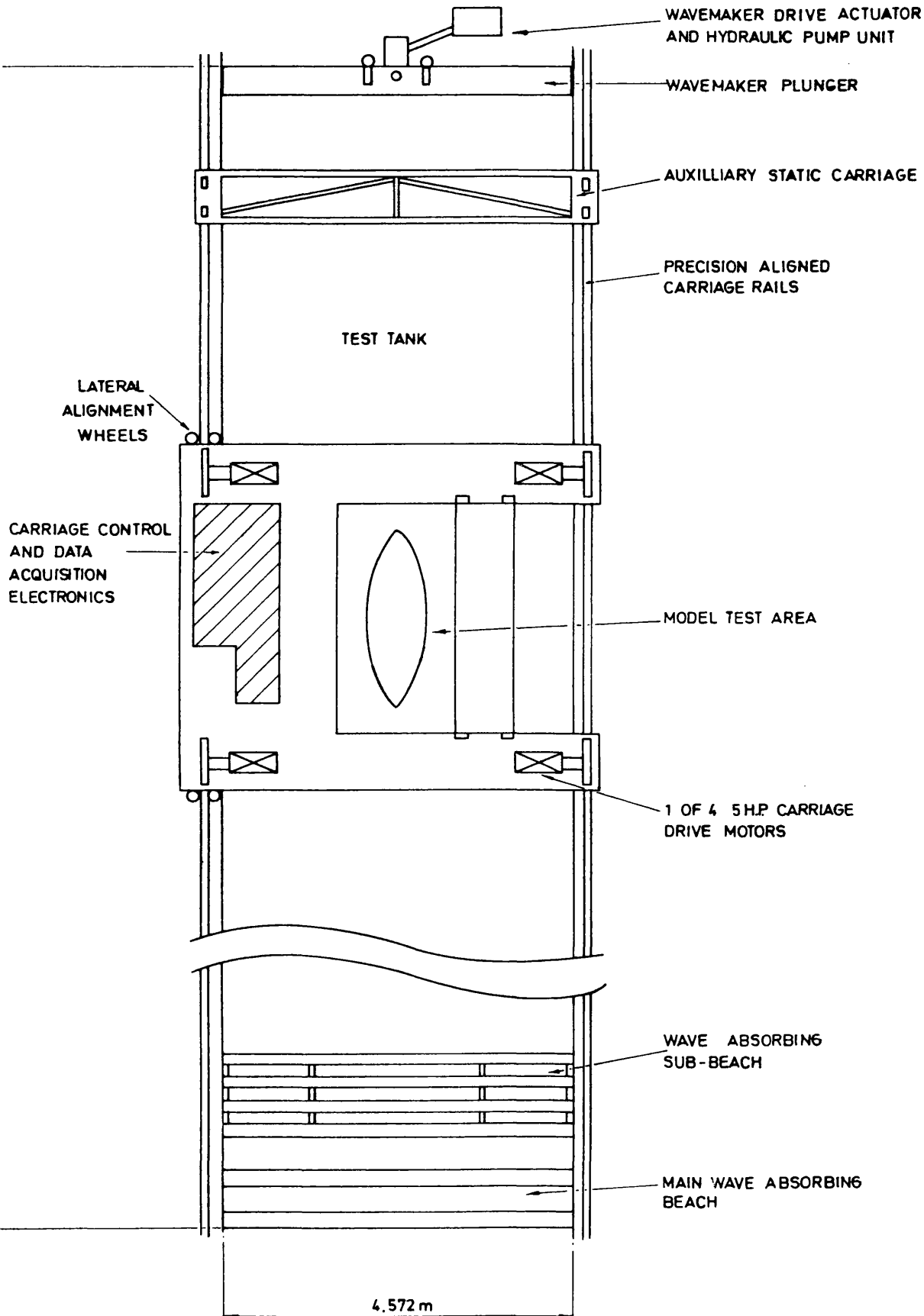


Figure 1

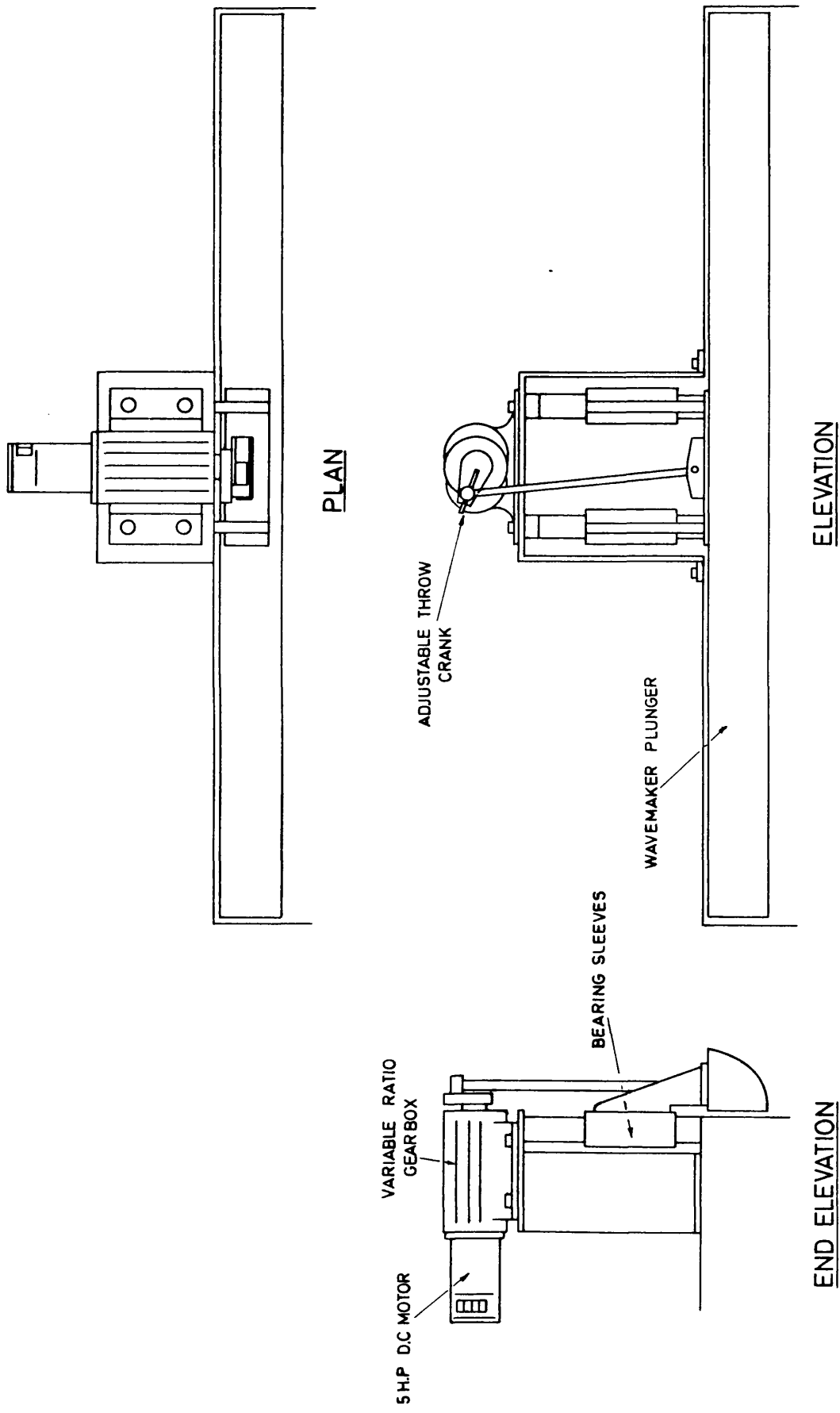


Figure 2.

'OLD' WAVEMAKER SYSTEM

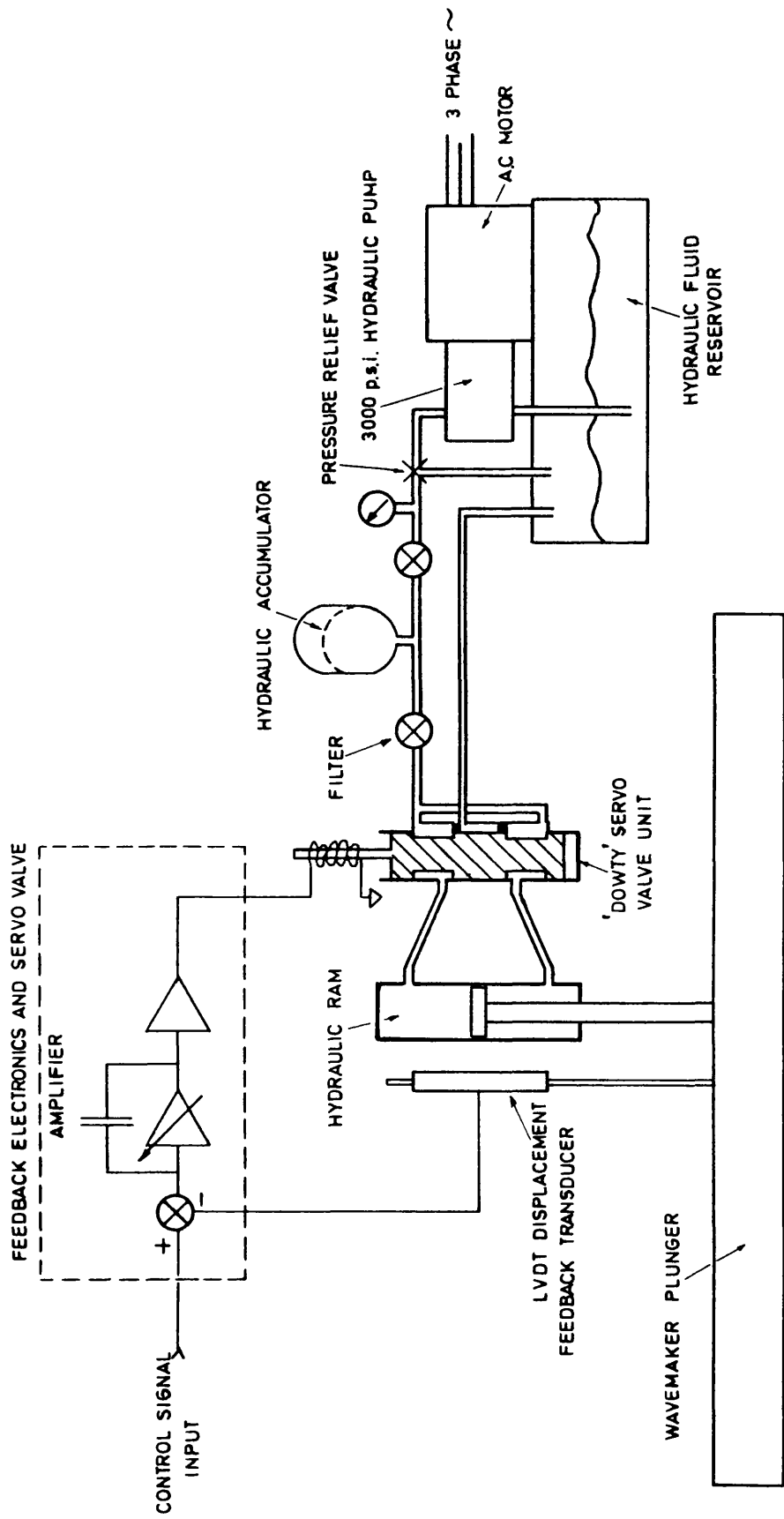


Figure 3

SERVO-HYDRAULIC WAVEMAKER SCHEMATIC

Distribution Of Energy In A Seaway

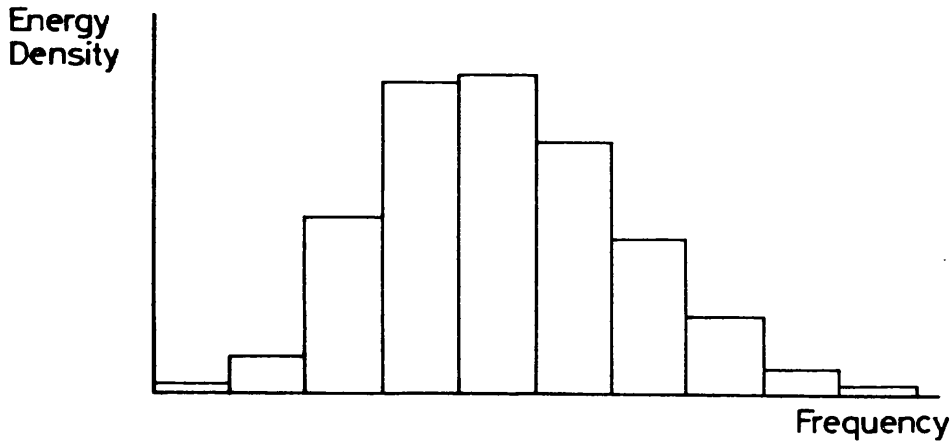


Figure. 4

Note: Energy density usually scaled in units of
 $0,5 \times \text{amplitude}^2 \cdot \text{sec}^{-1}$

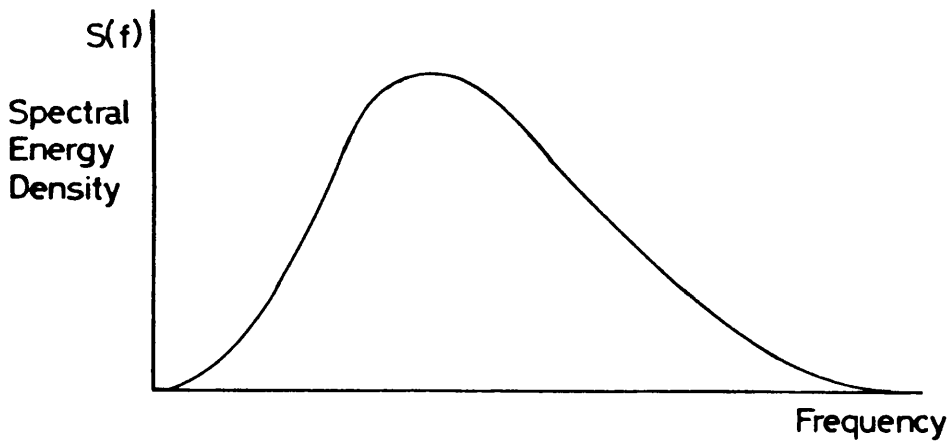


Figure. 5

Calculation Of m_0 From Time Series Records

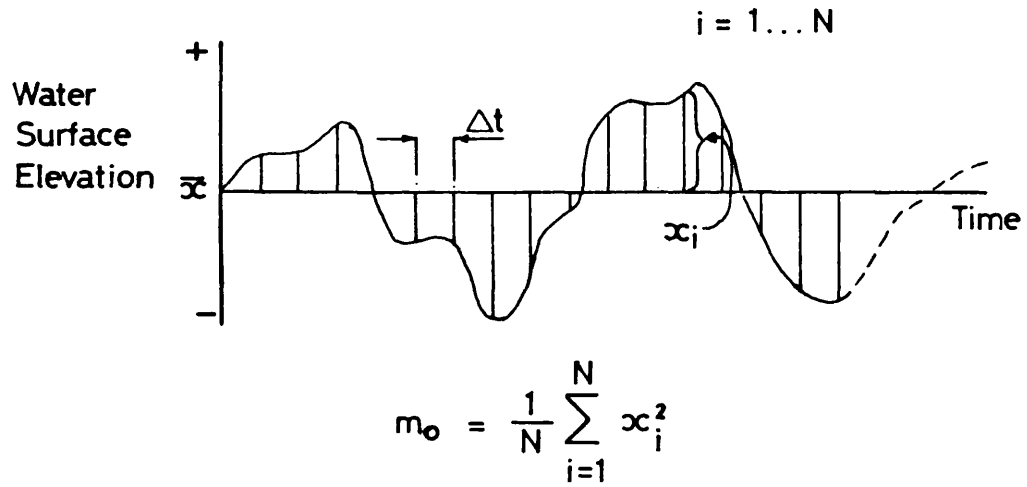


Figure. 6

Effect Of Windspeed On Spectrum

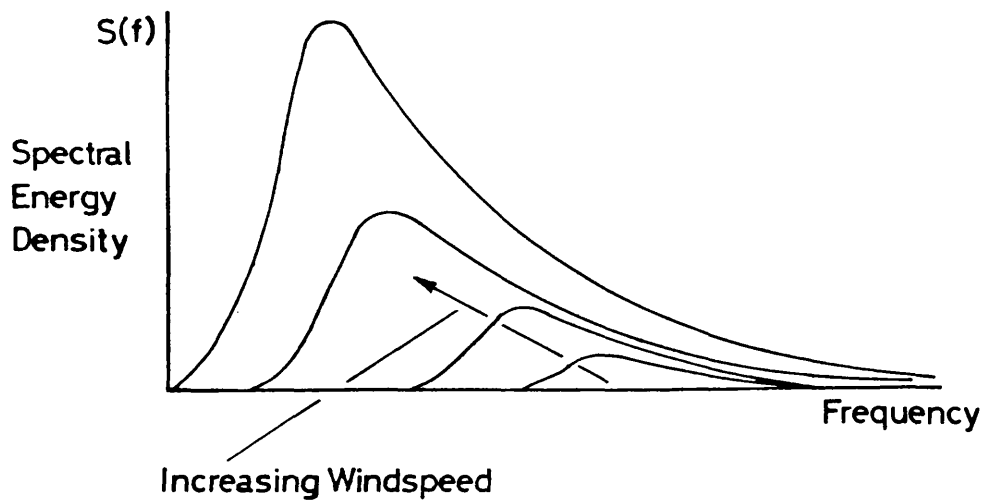
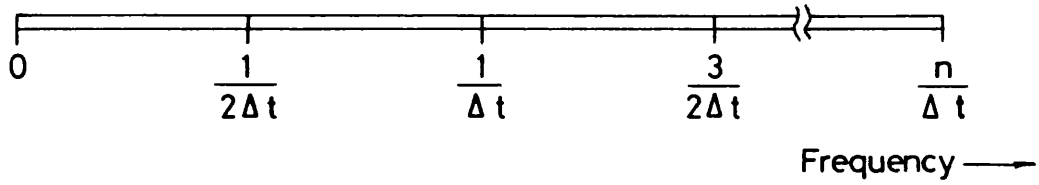
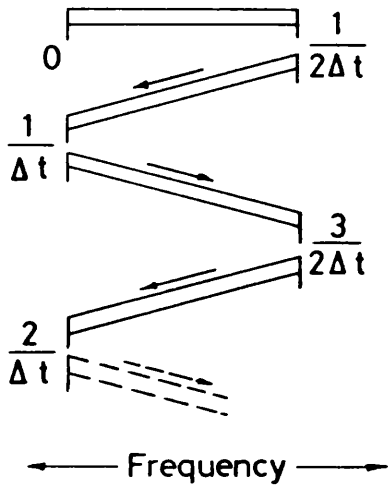


Figure. 7



Unsampled Time Series Gives Continuous Infinite Frequency Spectra



Sampled Time Series Gives Finite Frequency Spectra $0 - \frac{1}{2\Delta t}$ And Exhibits 'Aliasing'

Aliasing Of Frequency Values Due To Sampling

Figure 8.

Sampled Function For D.F. T

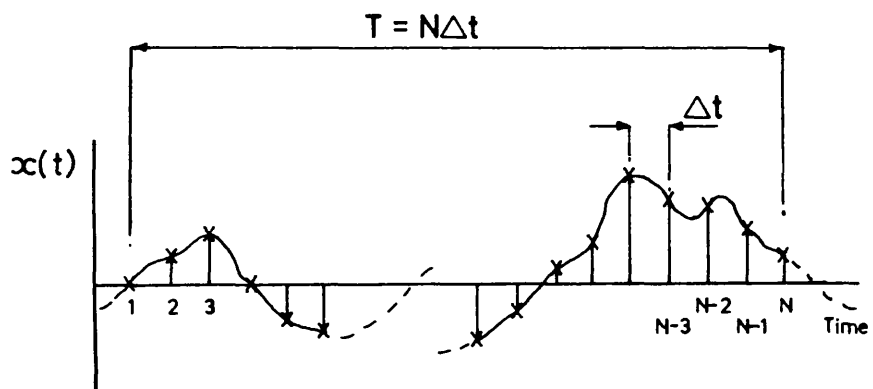
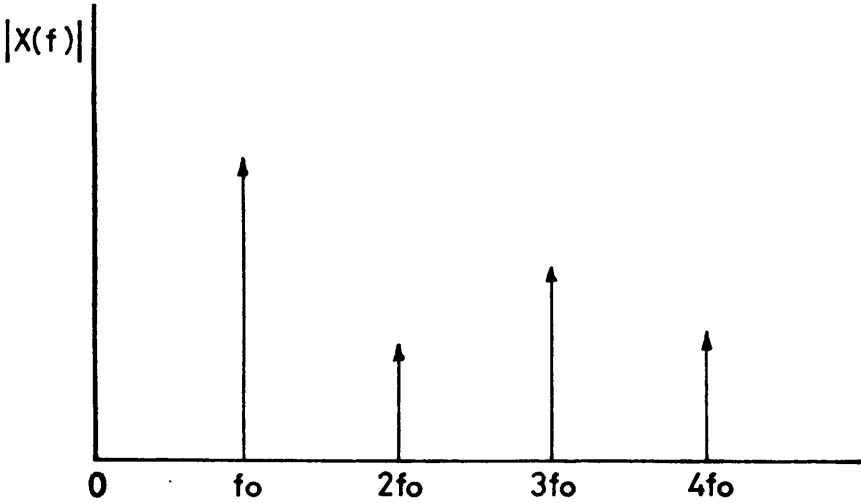
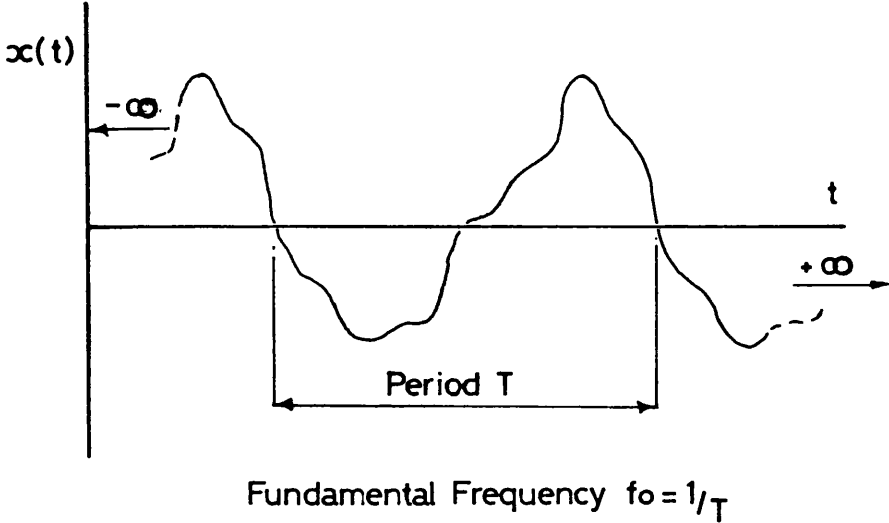


Figure. 9

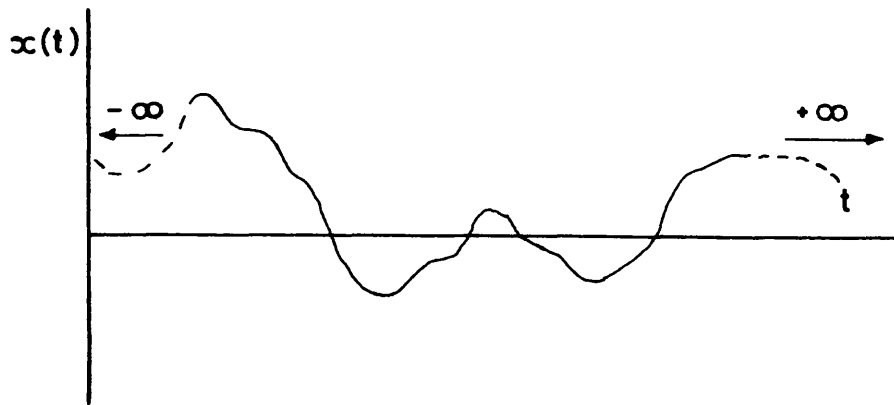
Infinite Periodic Continuous Time Series And
Corresponding Continuous Frequency Spectrum



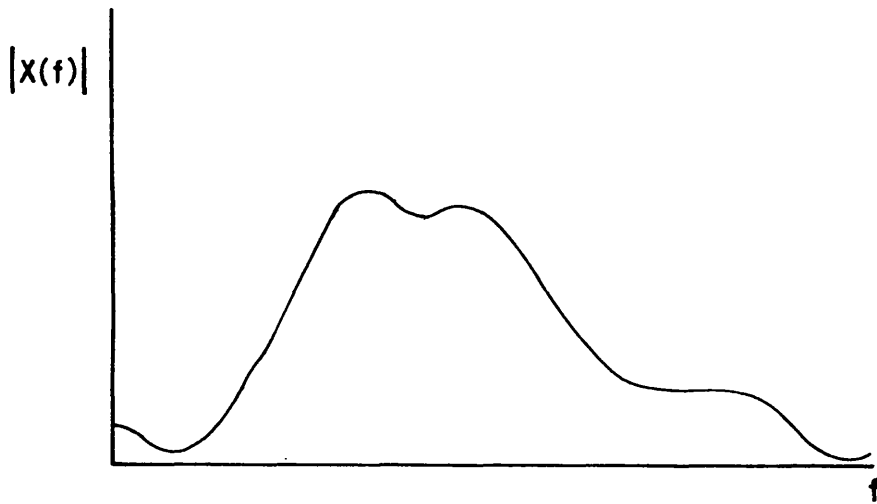
Note: Frequency Components At Fundamental And Harmonics Only

Figure.10

Infinite Random Time Series And Corresponding
Continuous Frequency Spectrum



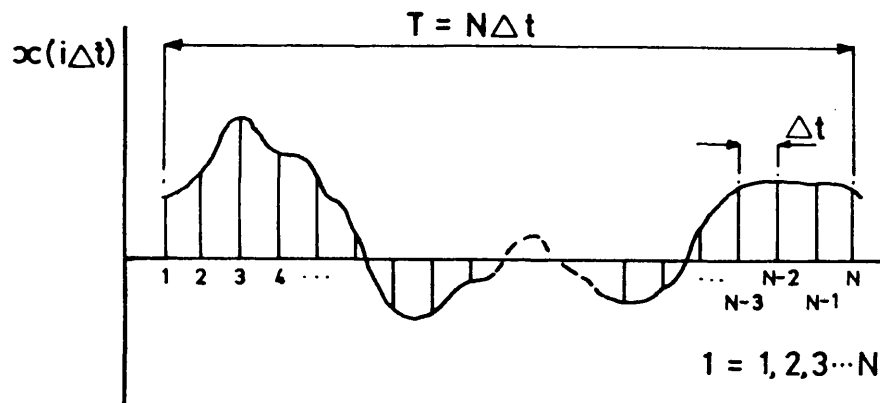
Infinite Random Time Series



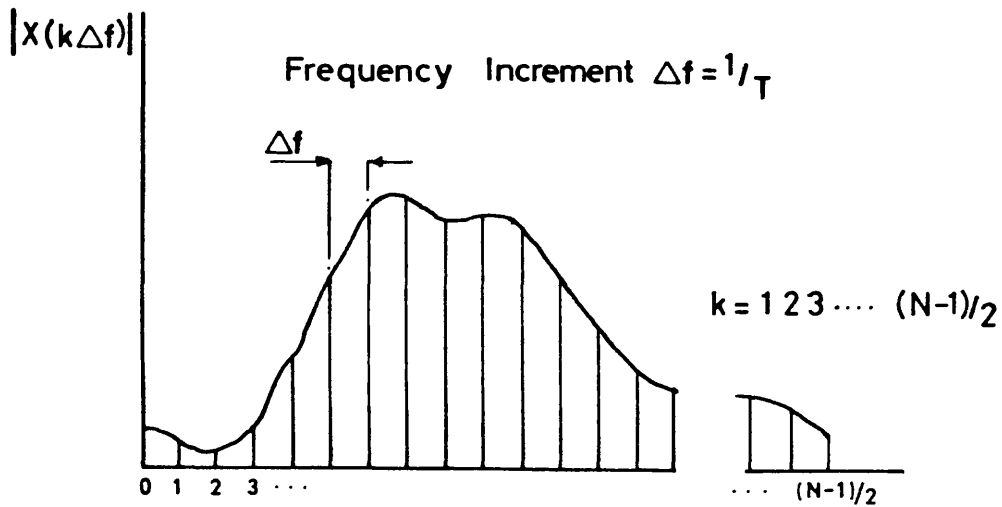
Continuous Frequency Spectrum

Figure 11

Sampled Random Time Series And Corresponding
Discrete Frequency Spectrum

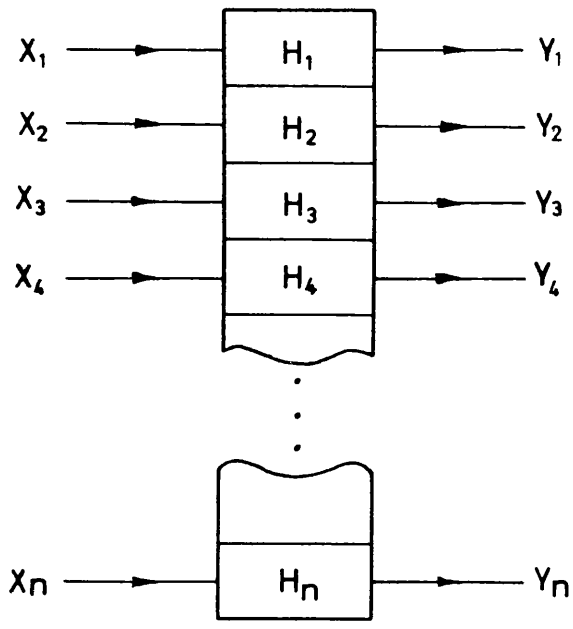


Sampled Random Time Series



Discrete Frequency Spectrum

Figure. 12



Input $X = \sum_{i=1}^n X_i$

Output $Y = \sum_{i=1}^n Y_i$

System $H = \sum_{i=1}^n H_i$

Figure 13.

Discontinuities In Non Periodic Components
Within Frame

Periodic Signal, Natural Period = r

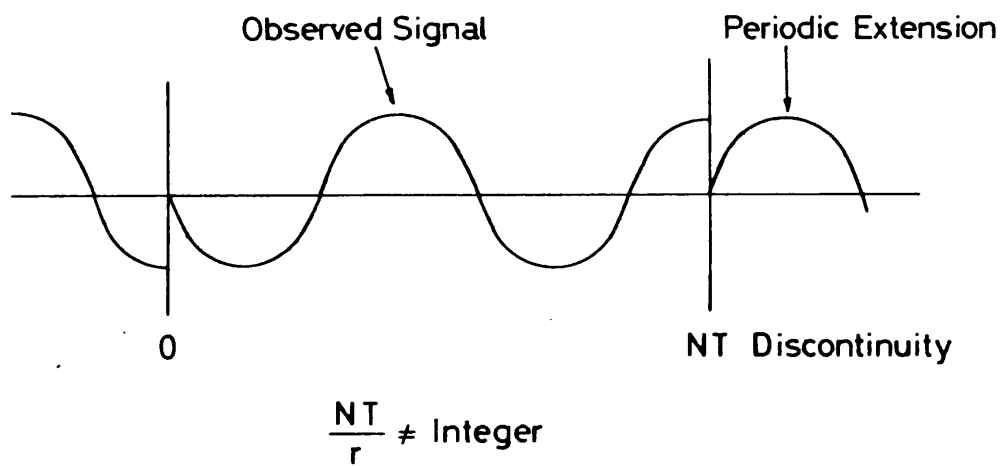
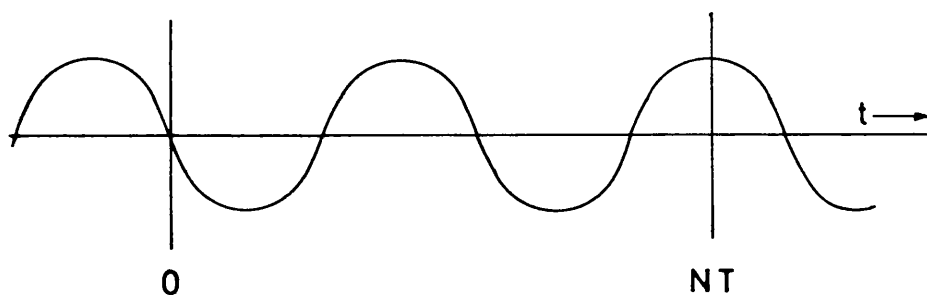


Figure 14

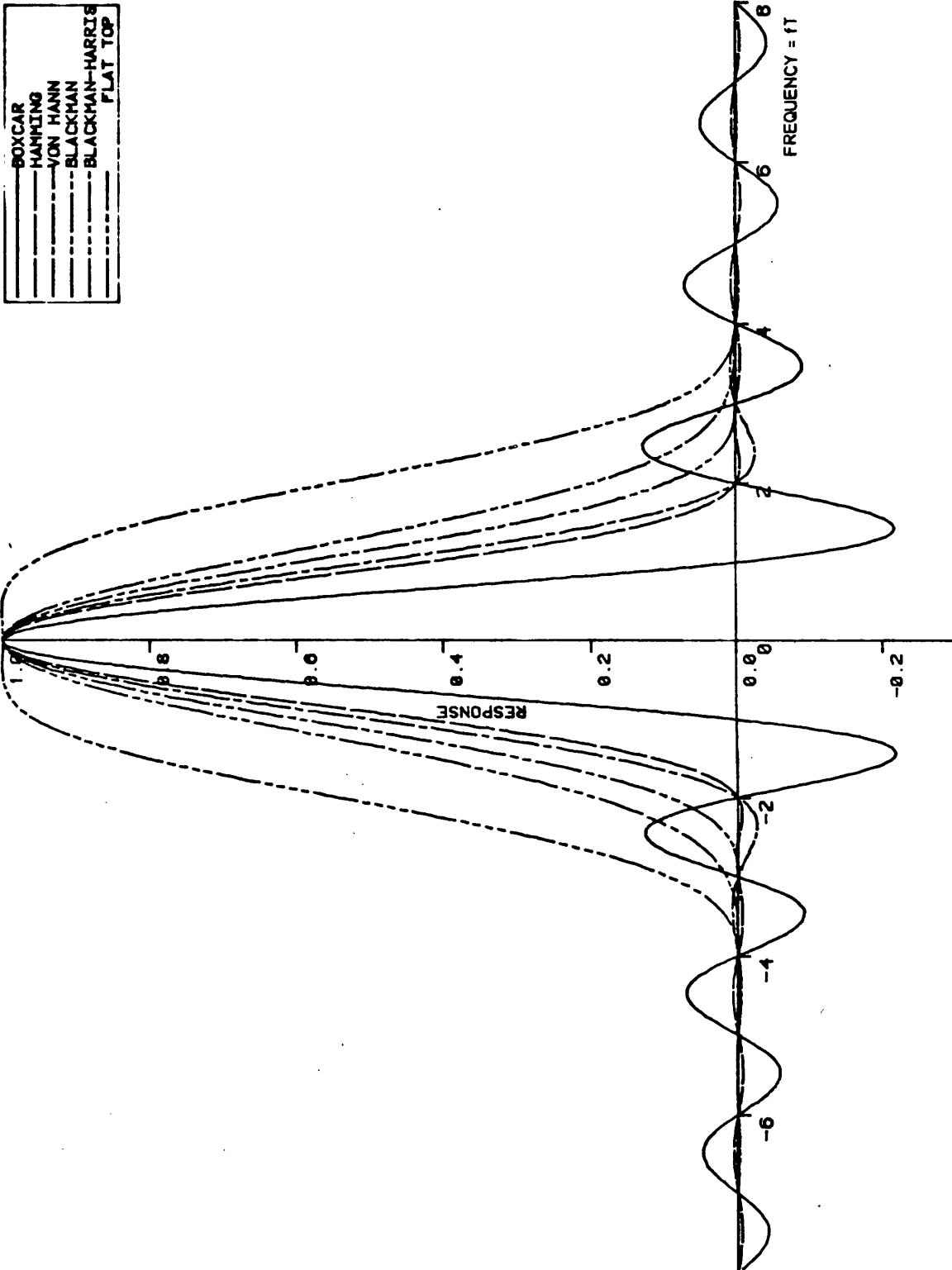
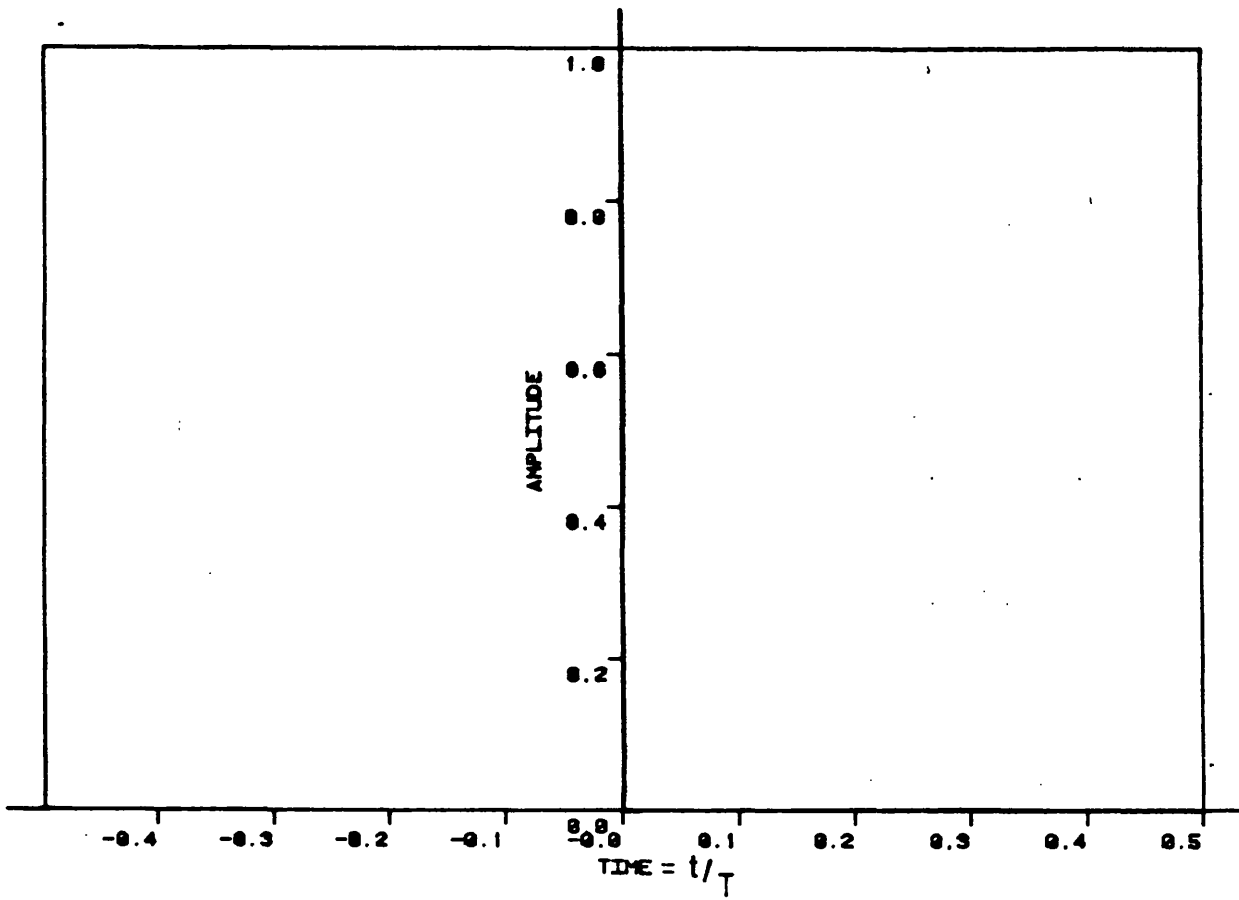


Figure 15



BOXCAR

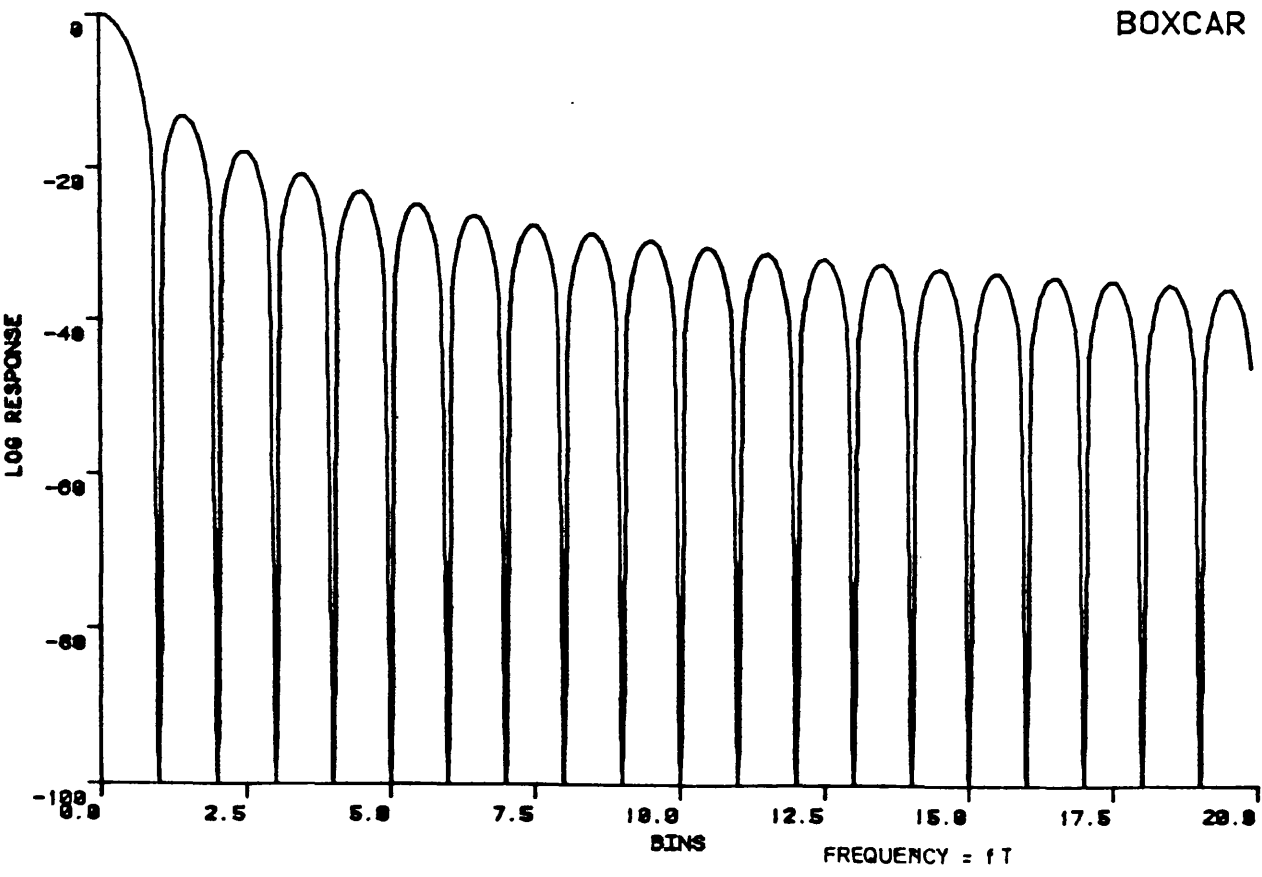
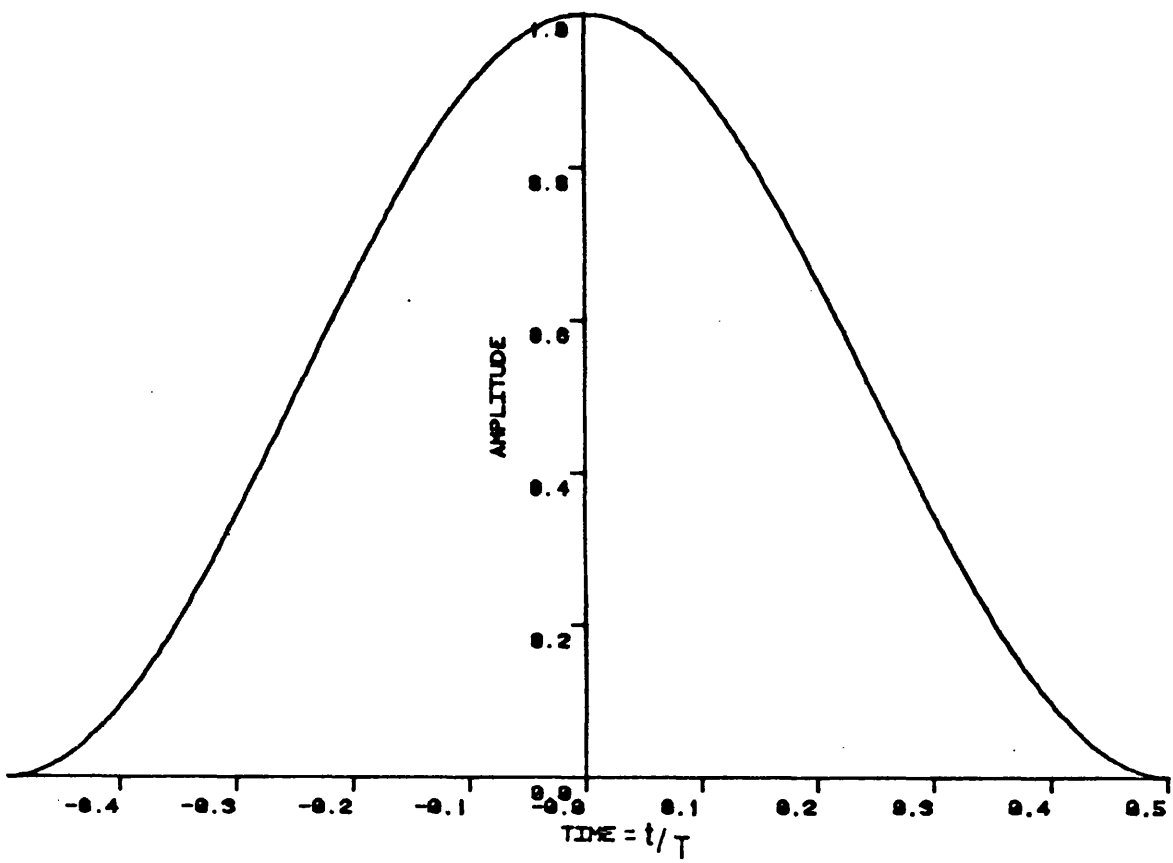


Figure 16



VON HANN

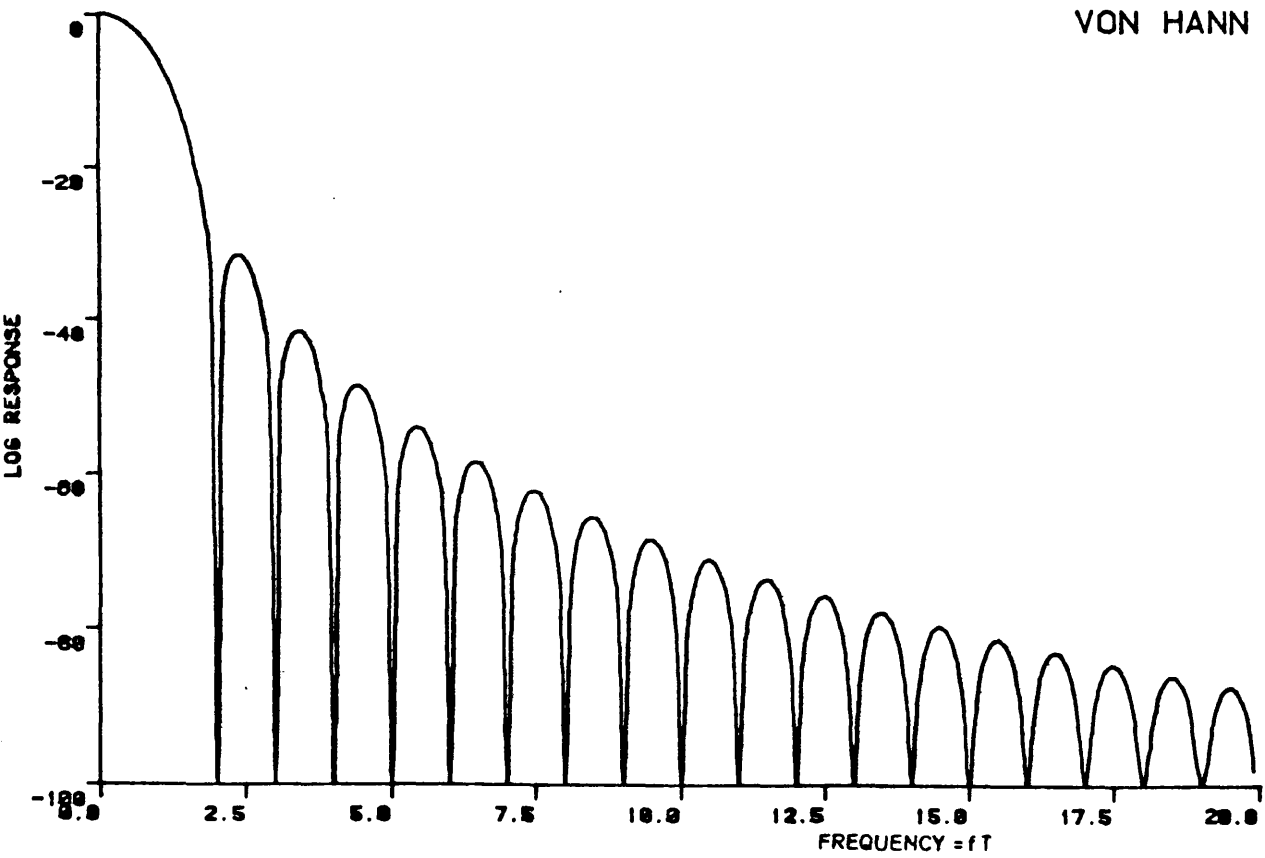
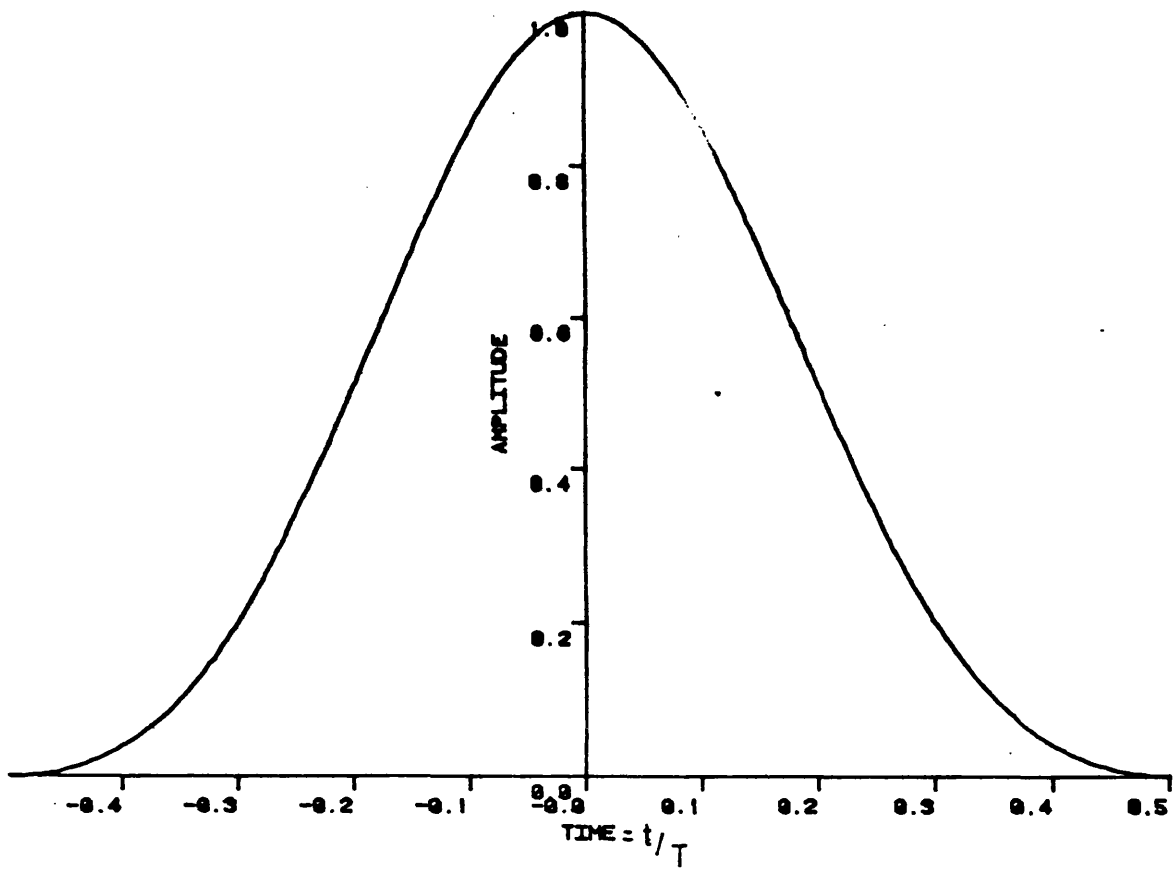


Figure 17



BLACKMAN

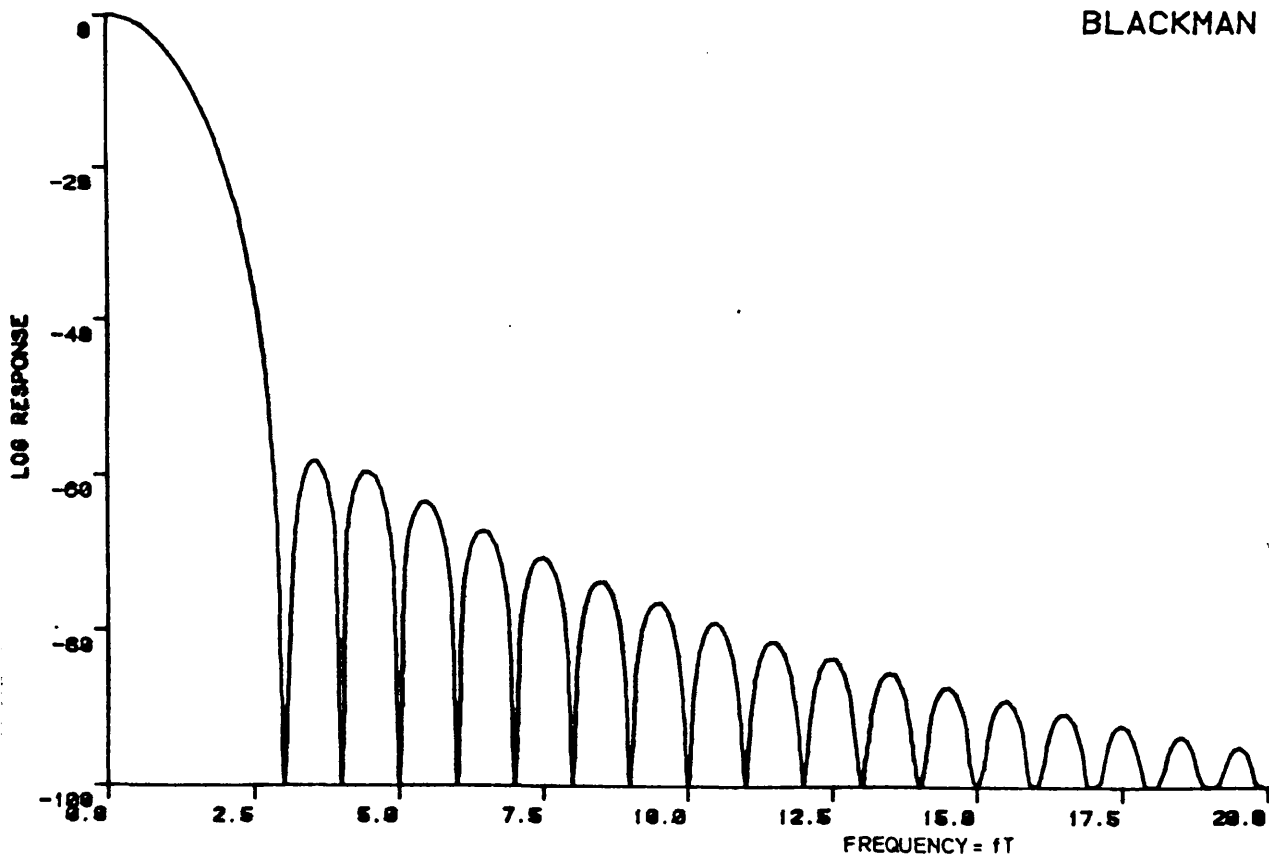
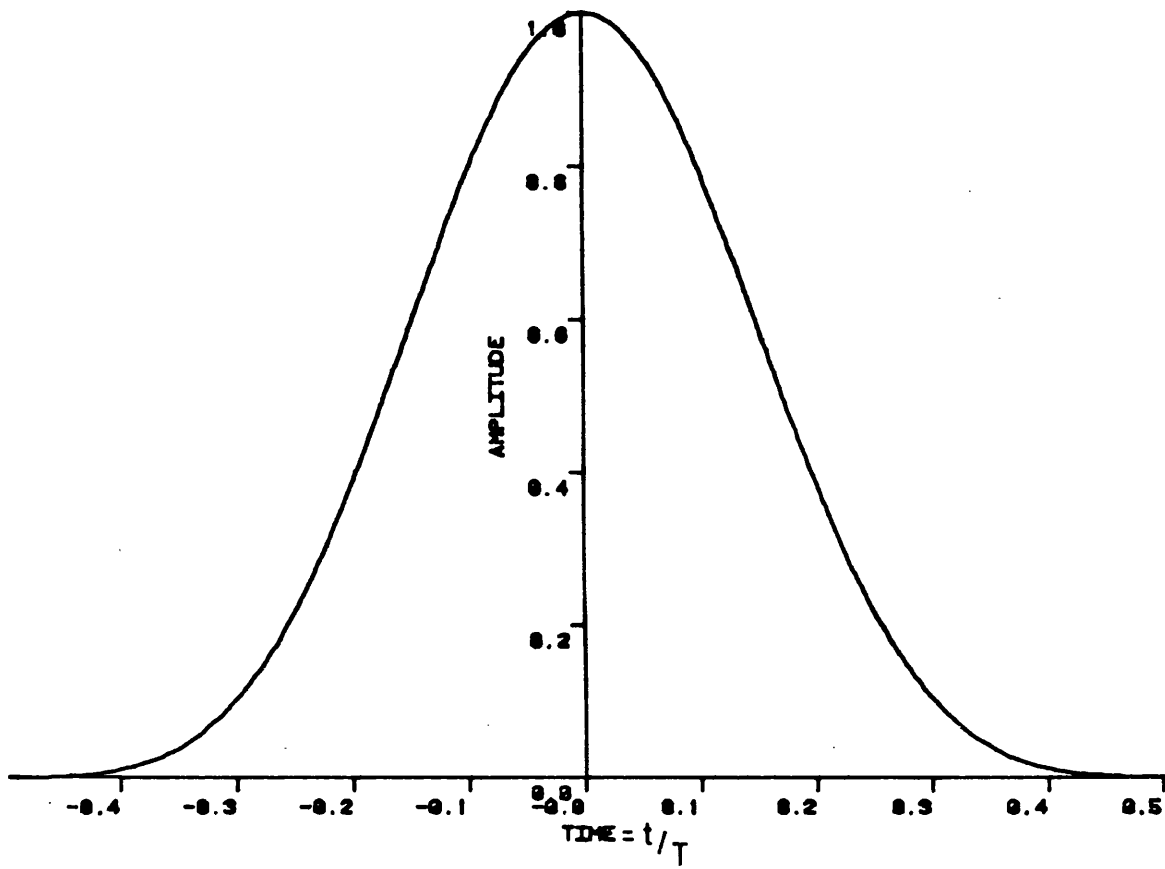


Figure 19



BLACKMAN-HARRIS

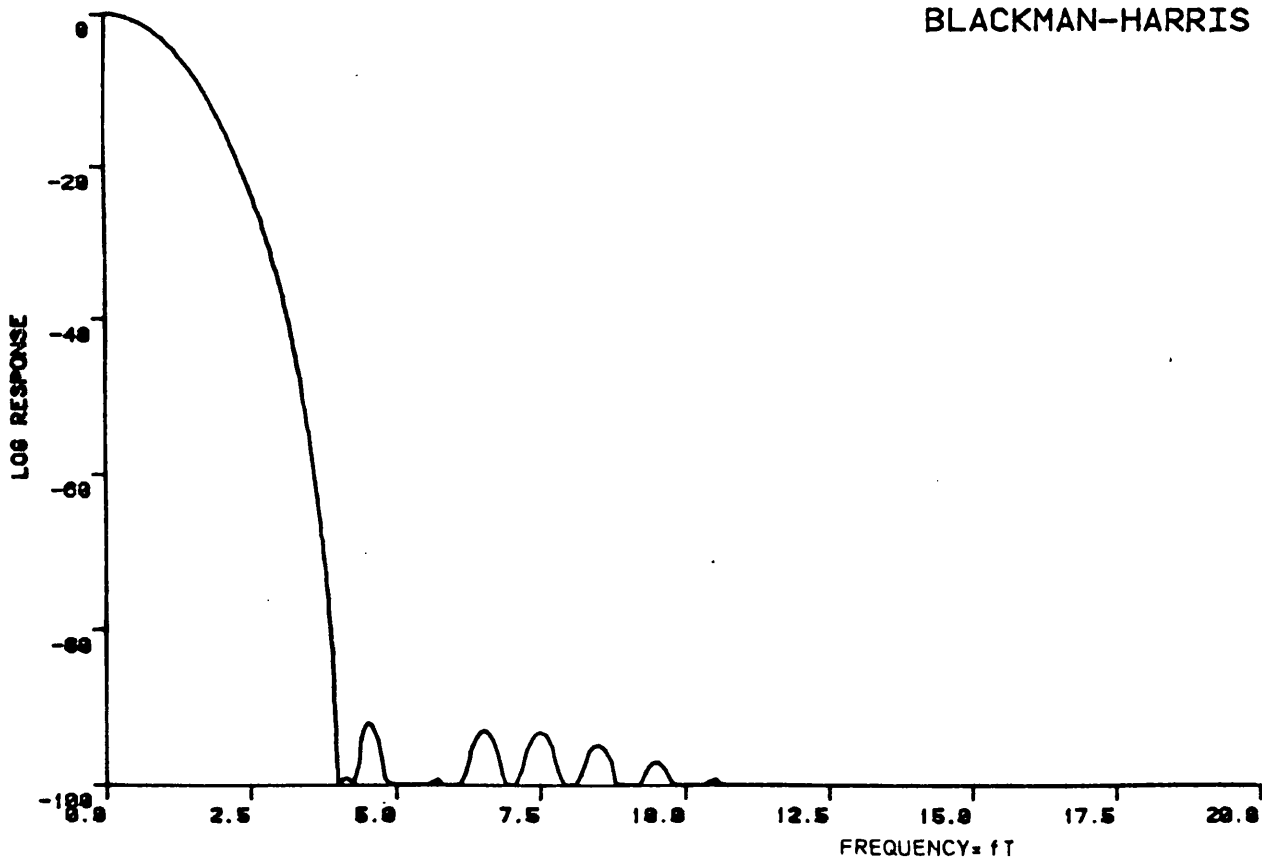
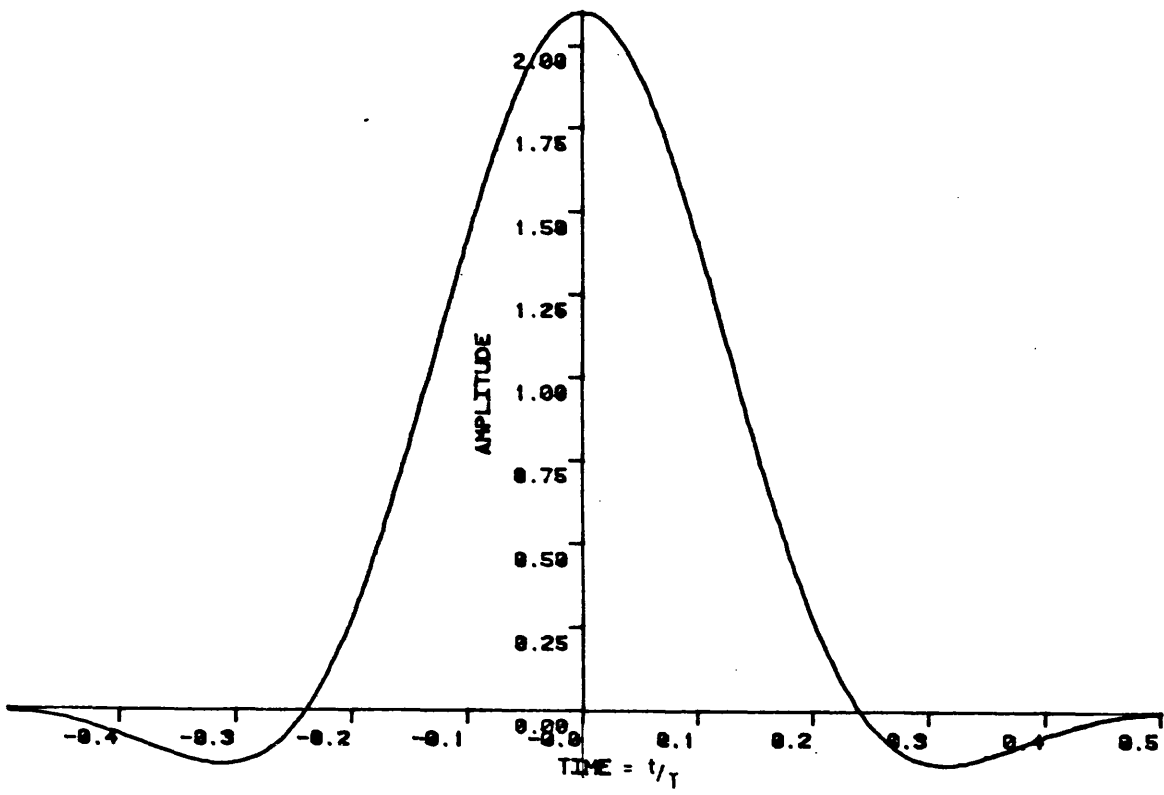


Figure 20



Flat Top

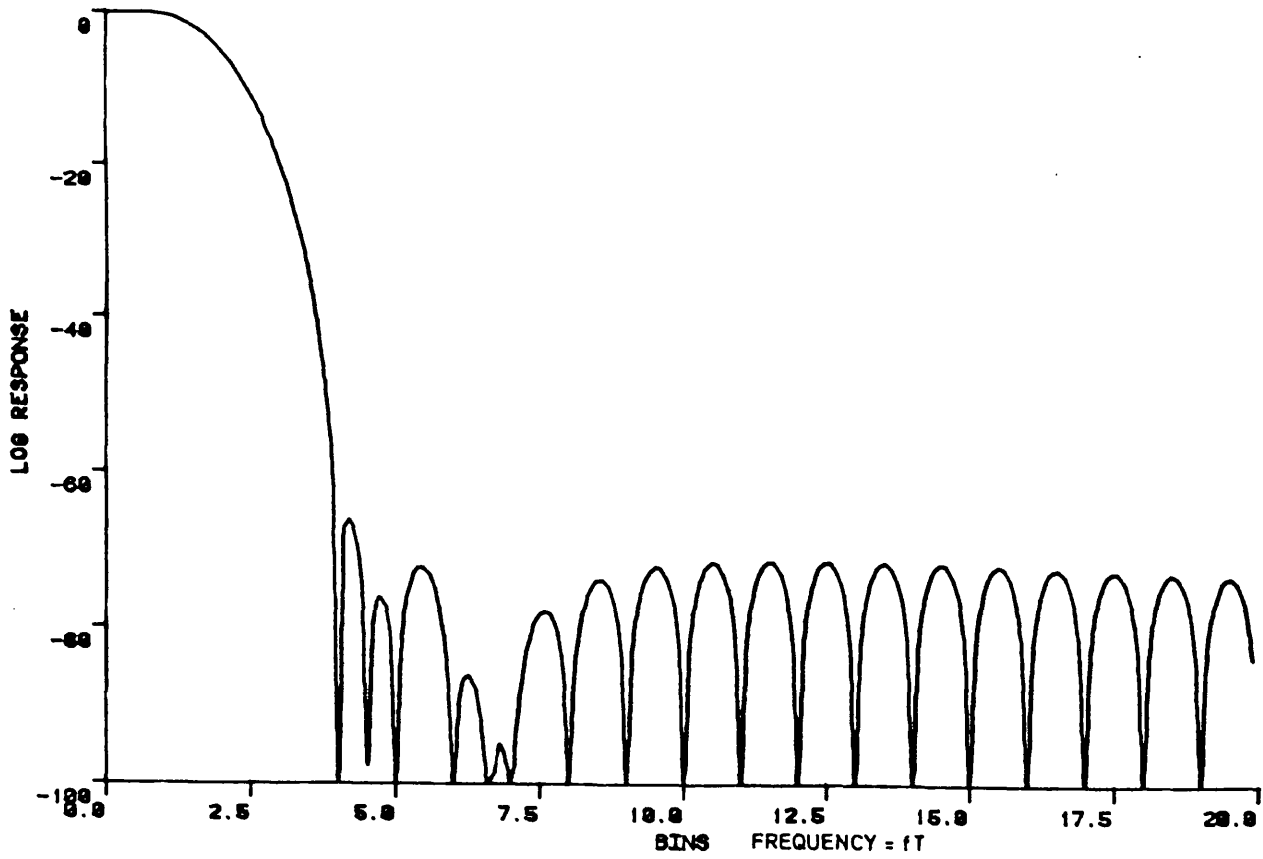


Figure 21

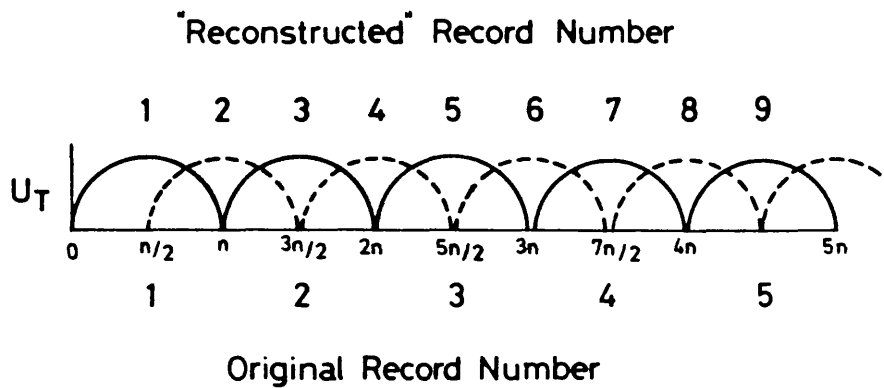
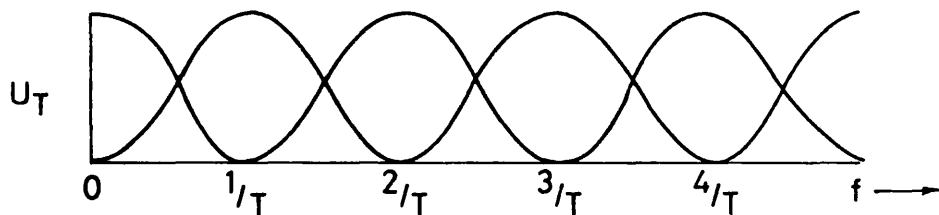
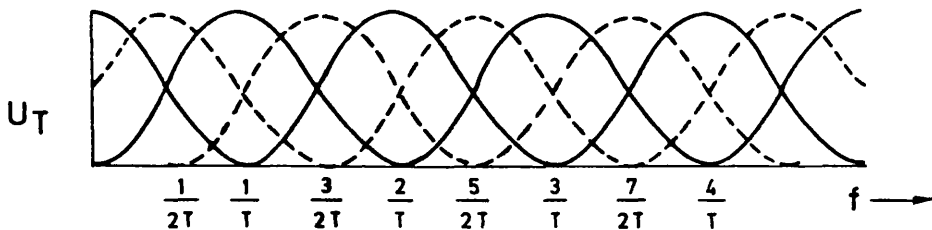


Figure 22.



N Point Record - No Zeroes Added

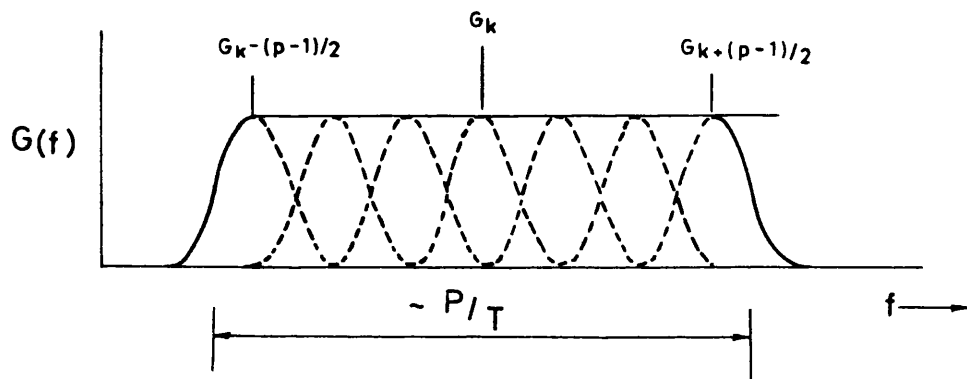
$$\Delta f = \frac{1}{N\Delta t} = \frac{1}{T}$$



N Point Record - N Zeroes Added

$$\Delta f = \frac{1}{(N + N_z)\Delta t}$$

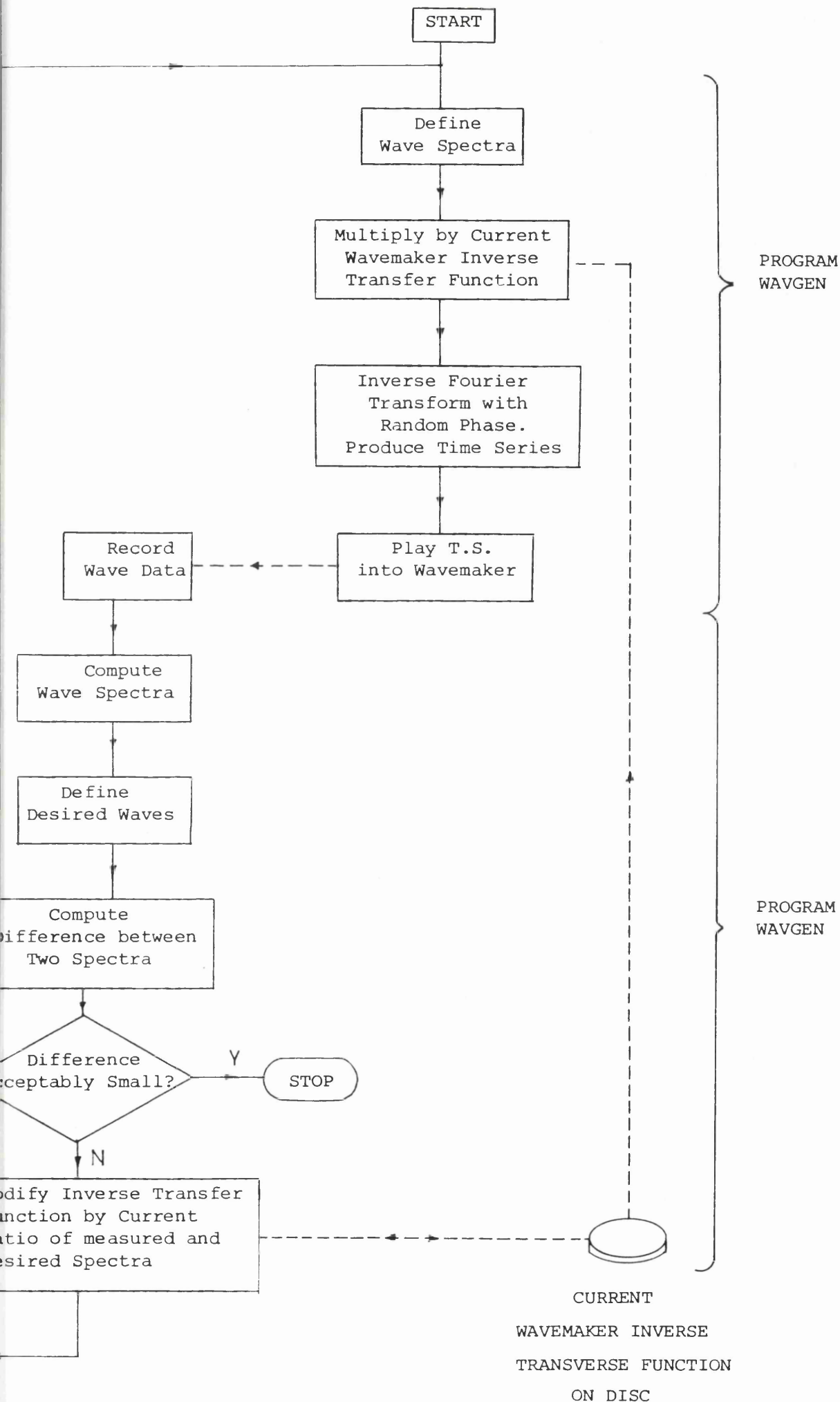
Figure 23



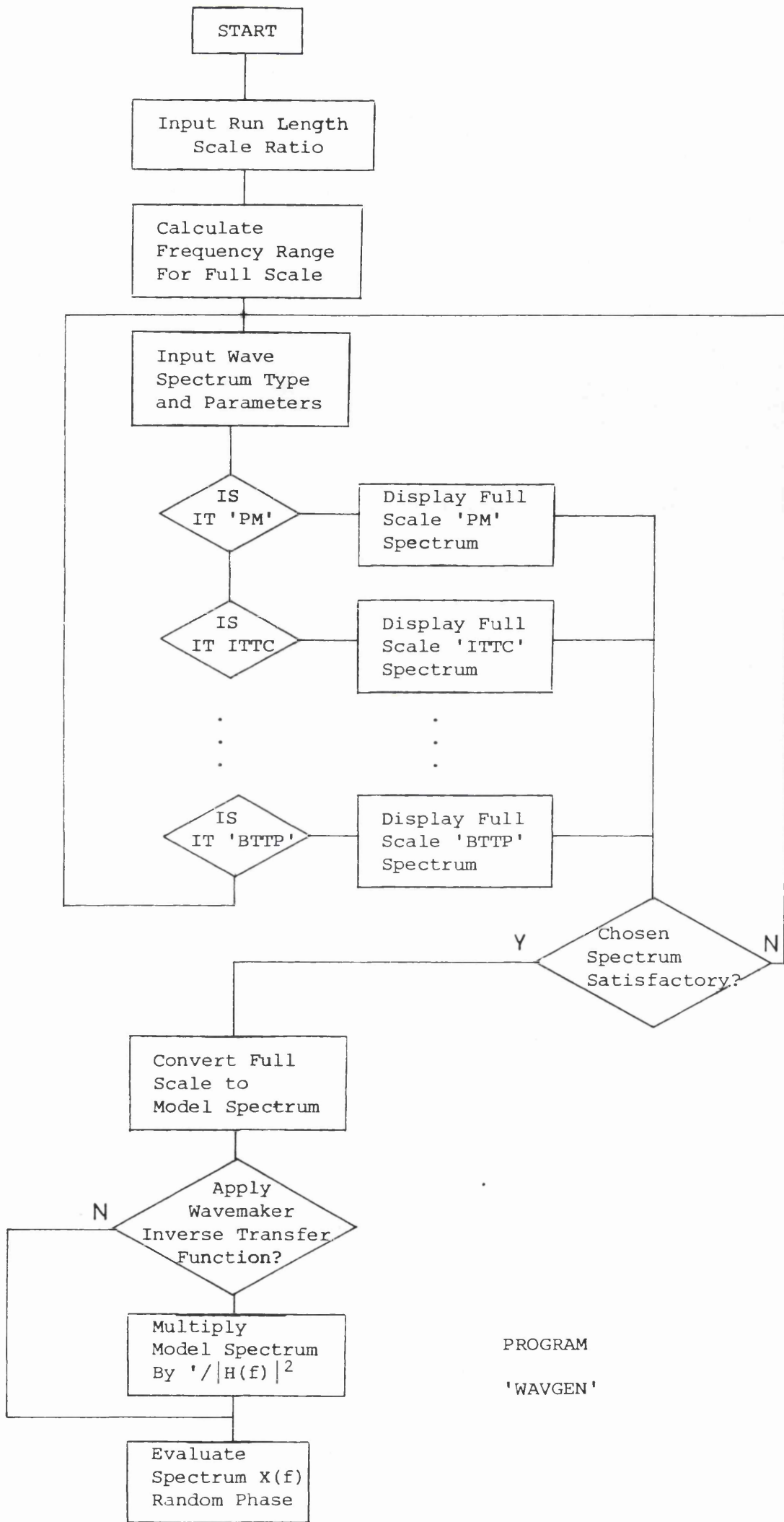
$$\hat{G}_k = \frac{1}{p} \sum_{i=-p}^p G_{k+i} \quad \text{where } p=(P-1)/2 \text{ and } P \text{ is odd}$$

Resolution Bandwidth $\approx P/T$

Figure 24



Iterative Loop Flow Diagram



PROGRAM
'WAVGEN'

Figure 26

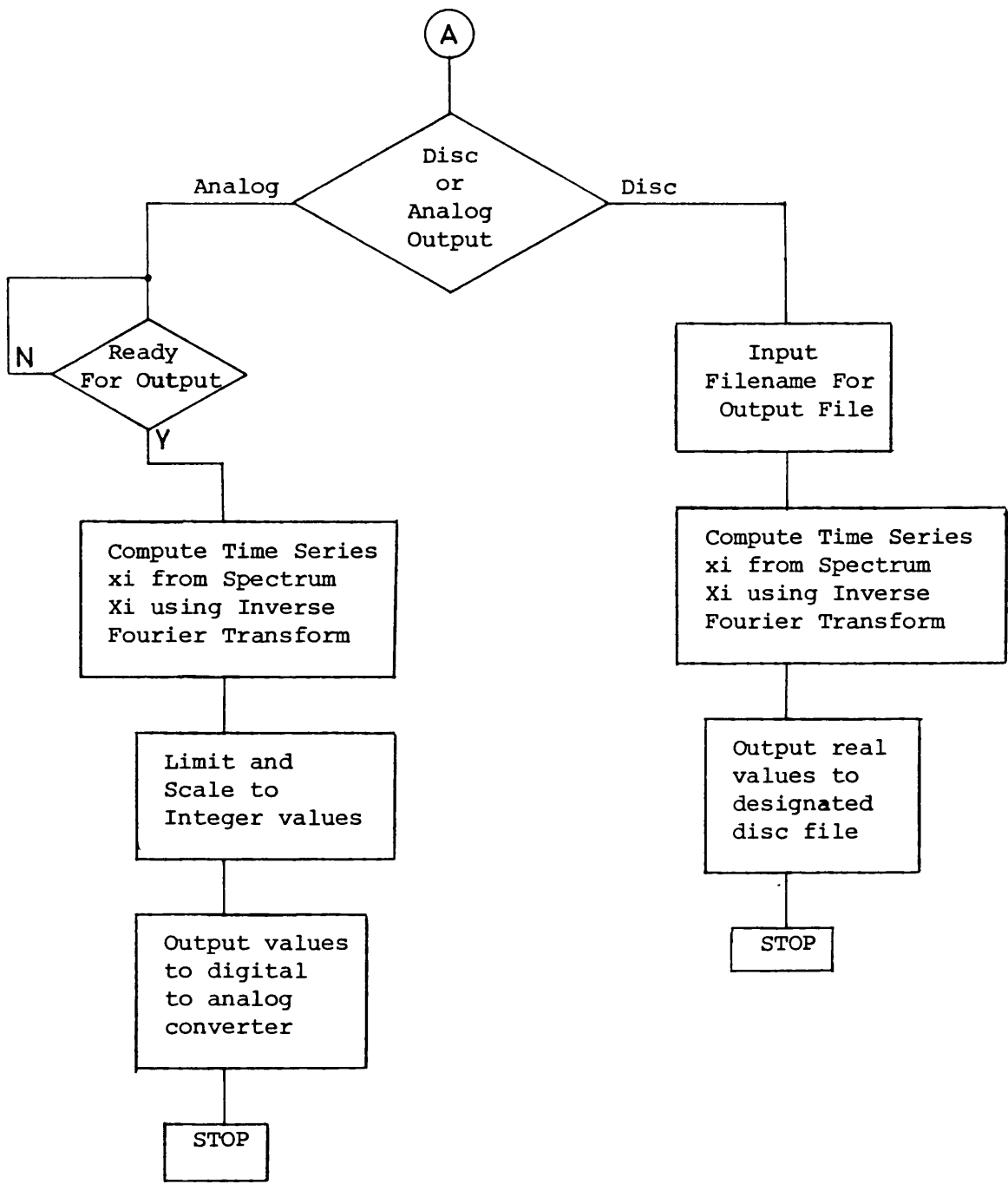
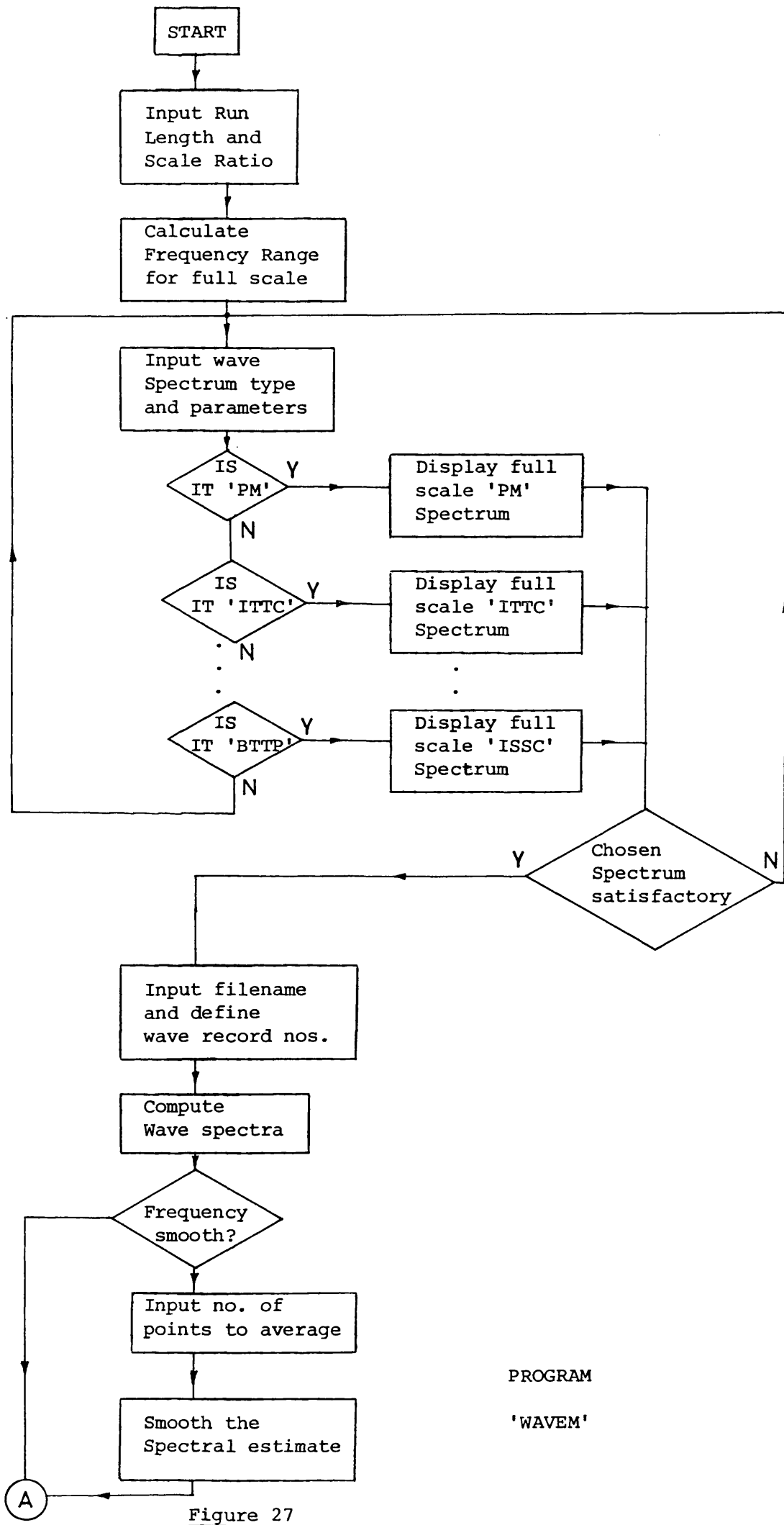


Figure 26 (Continued)



PROGRAM
'WAVEM'

Figure 27

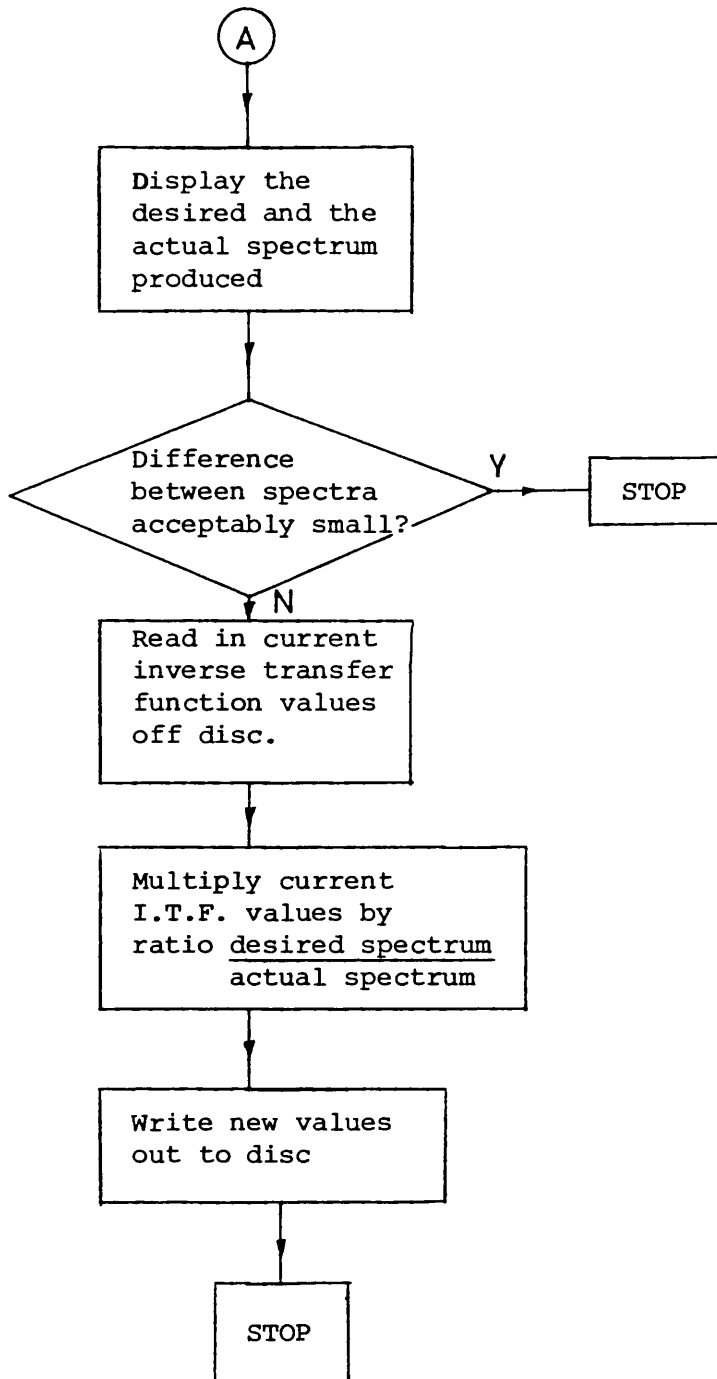
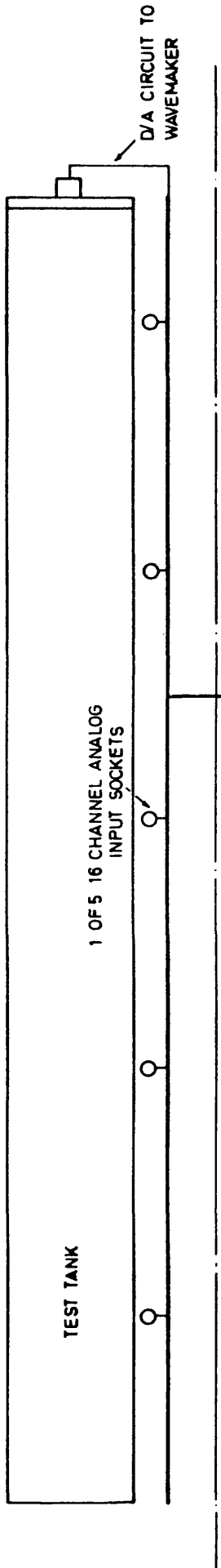
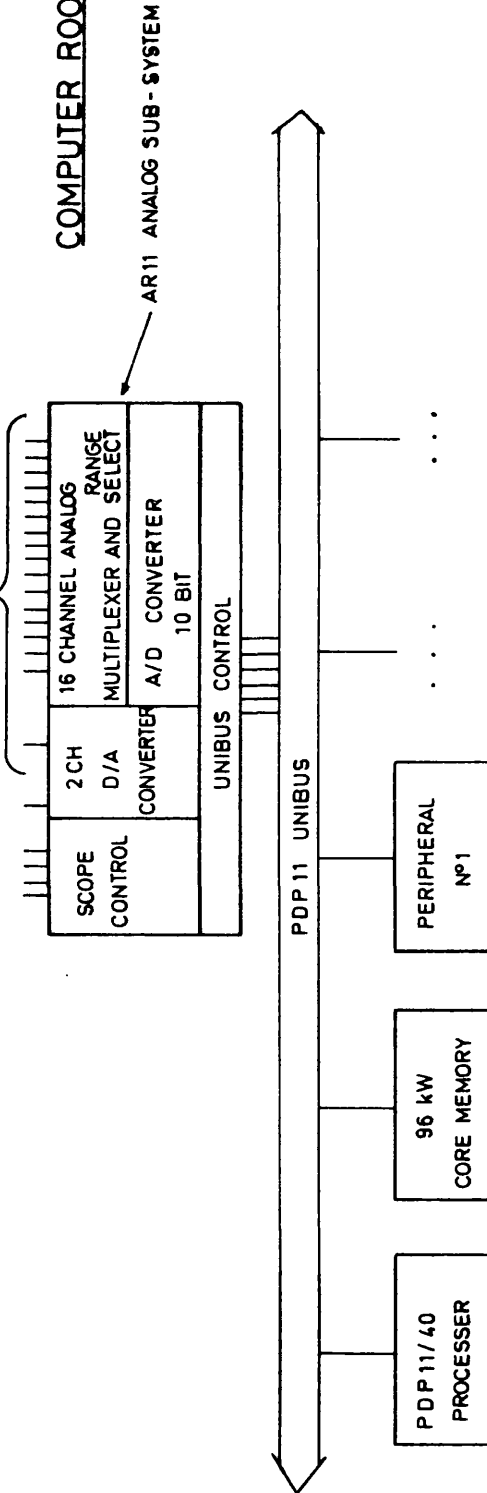


Figure 27 (Continued)

TANK TEST AREA

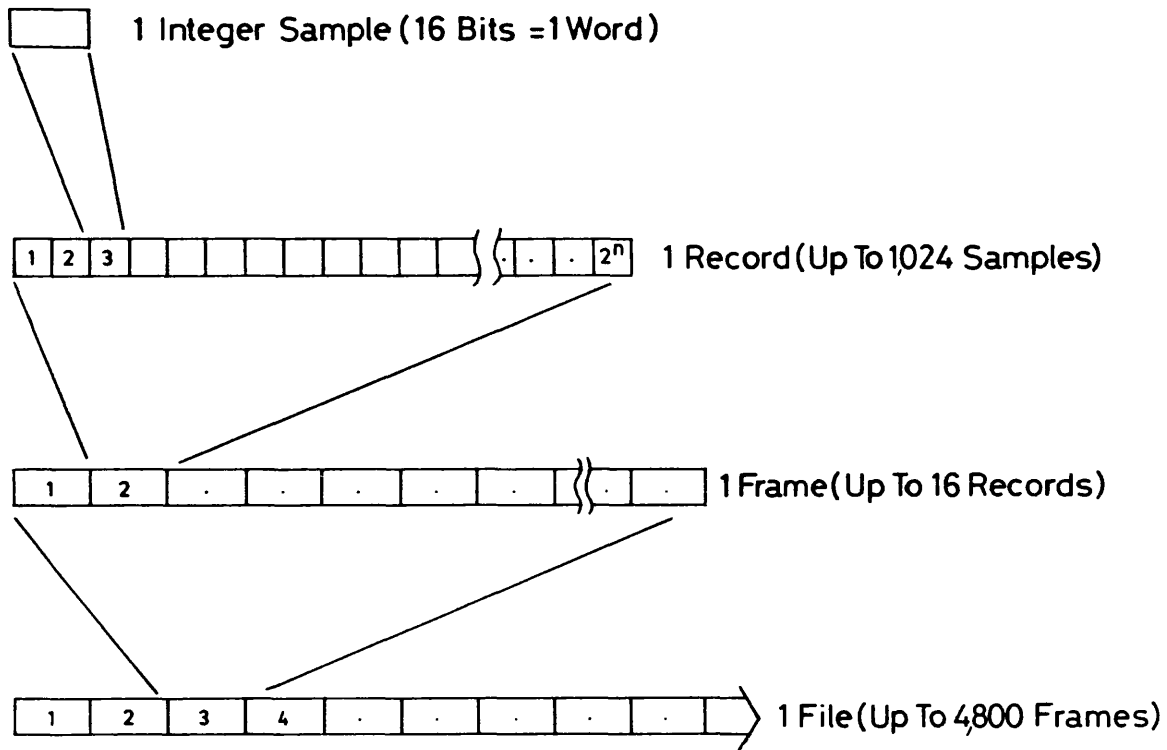


COMPUTER ROOM



AR11 ANALOG SUB SYSTEM AND TEST TANK WIRING LAYOUT

Figure 28



Data Storage Format

Figure 29

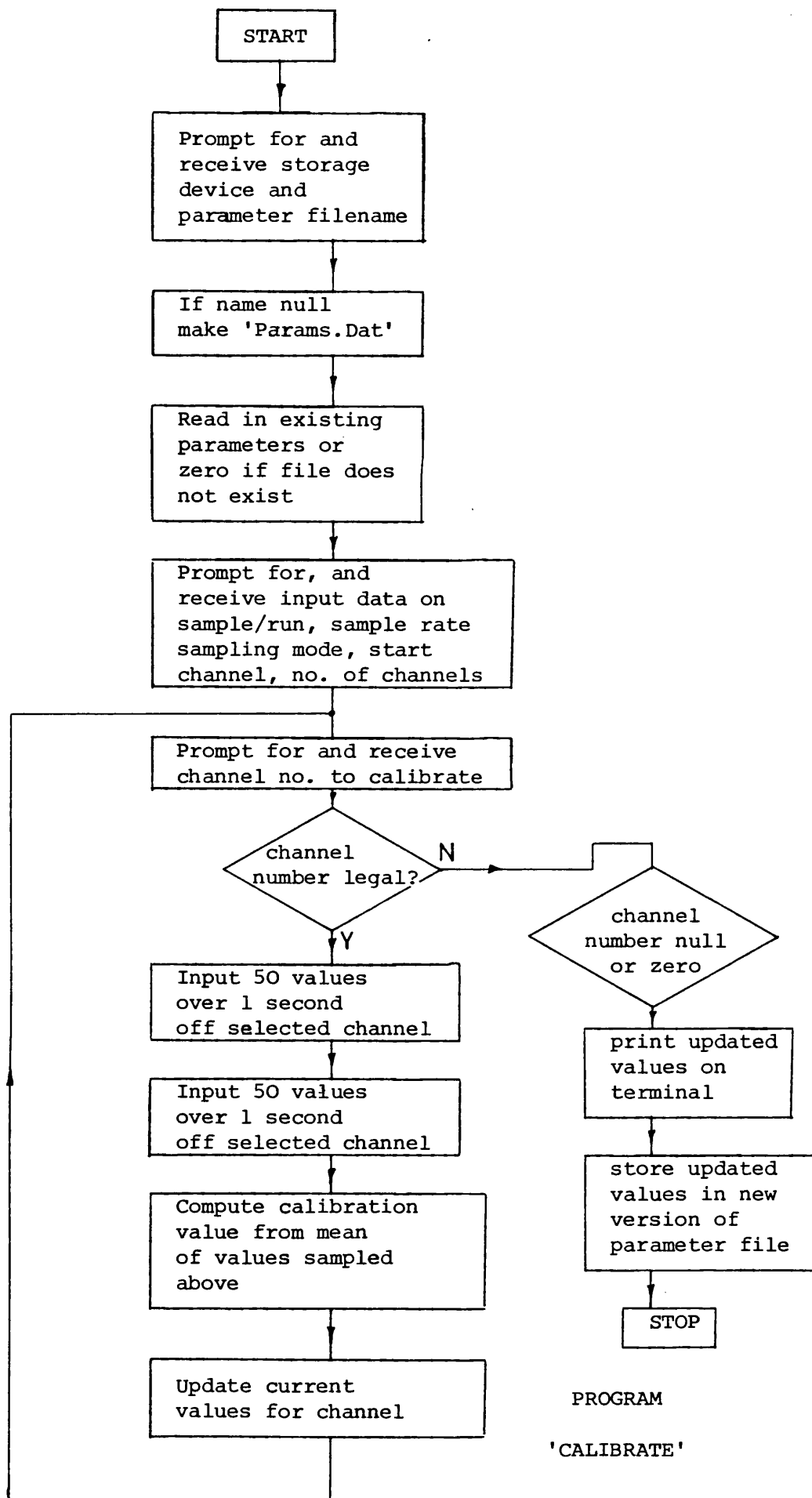
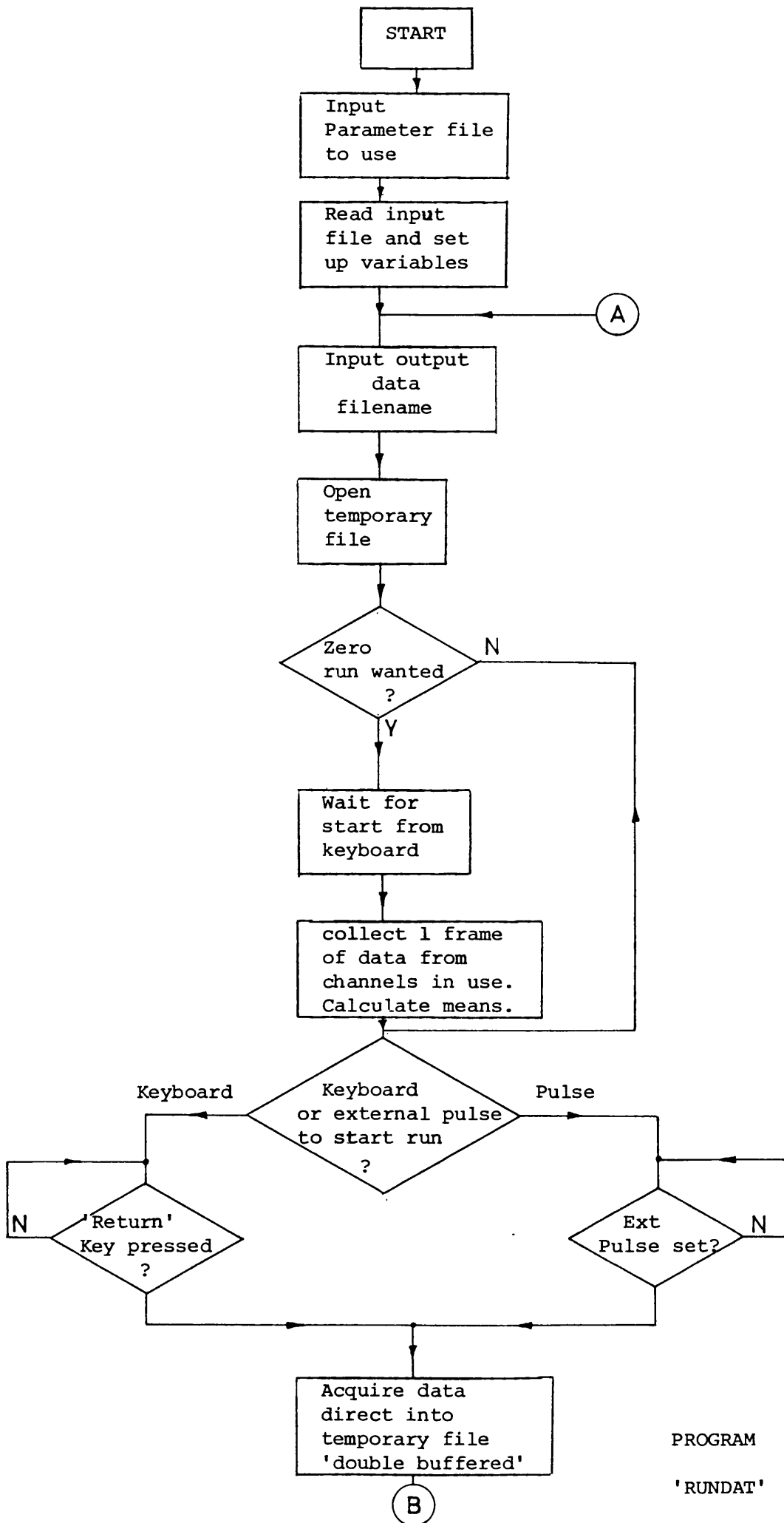


Figure 30



PROGRAM
'RUNDAT'

Figure 31

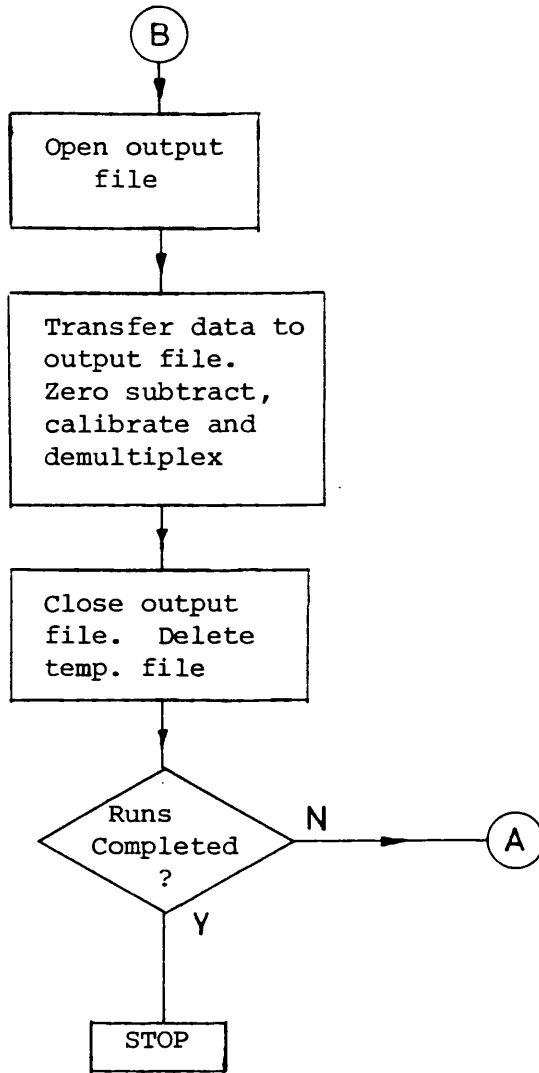
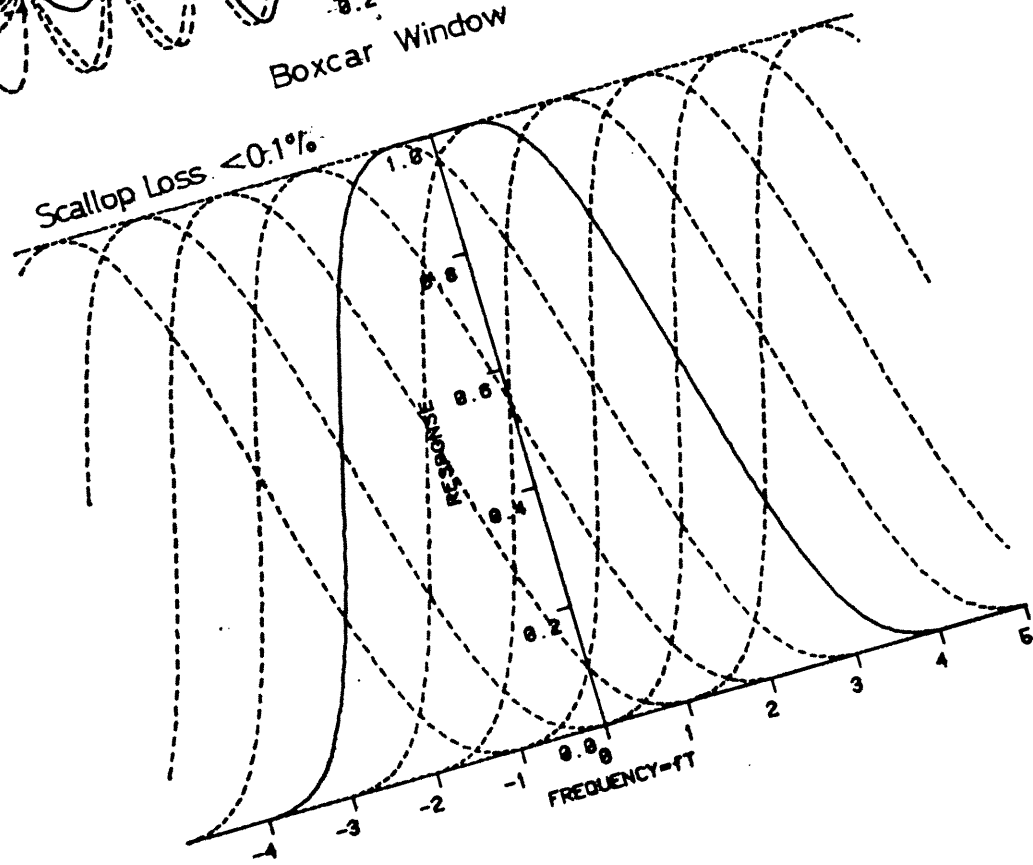
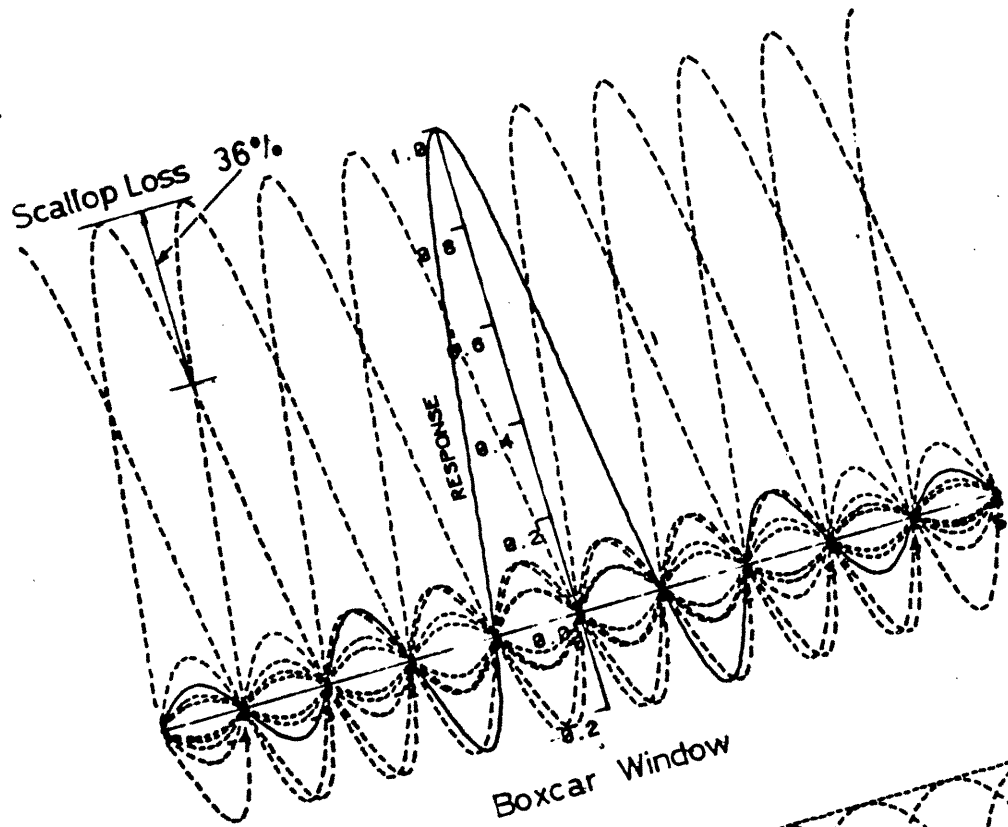
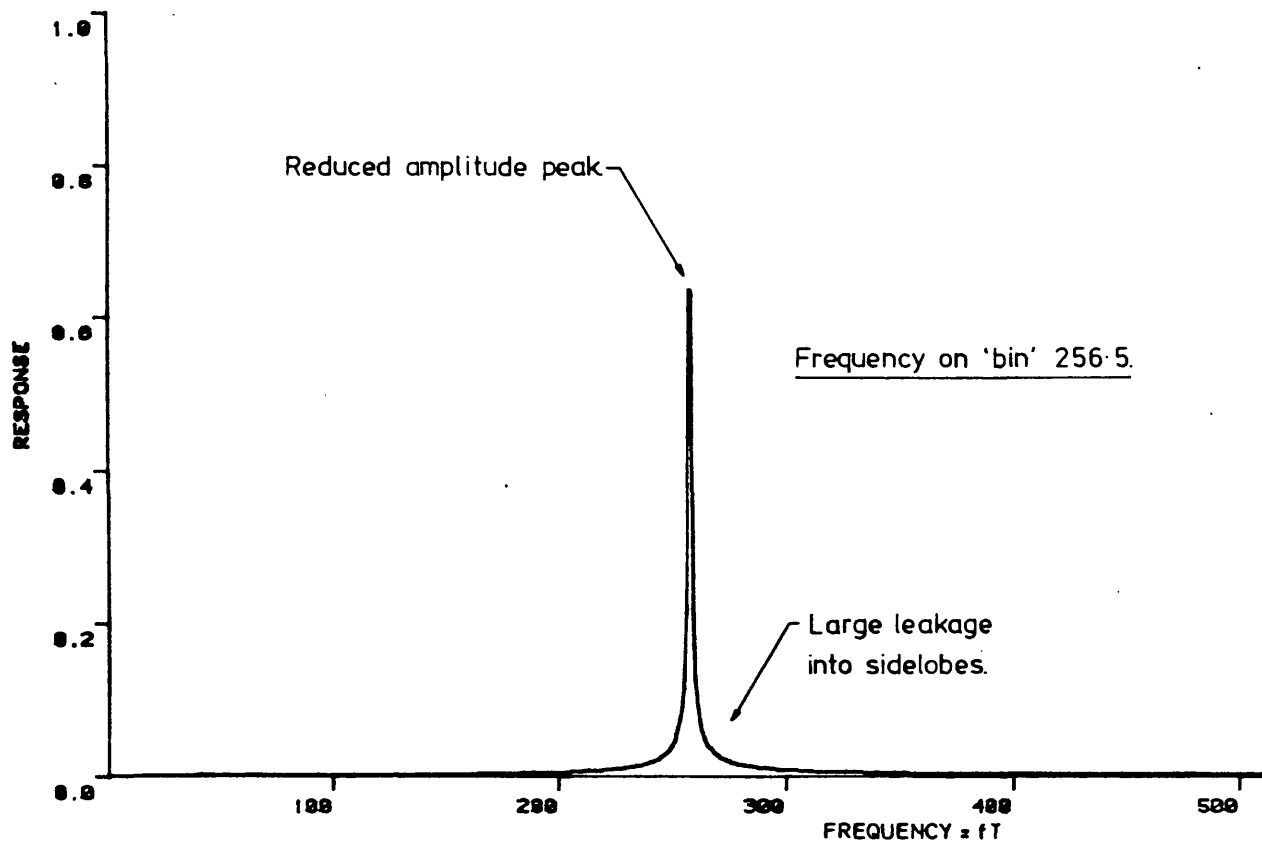
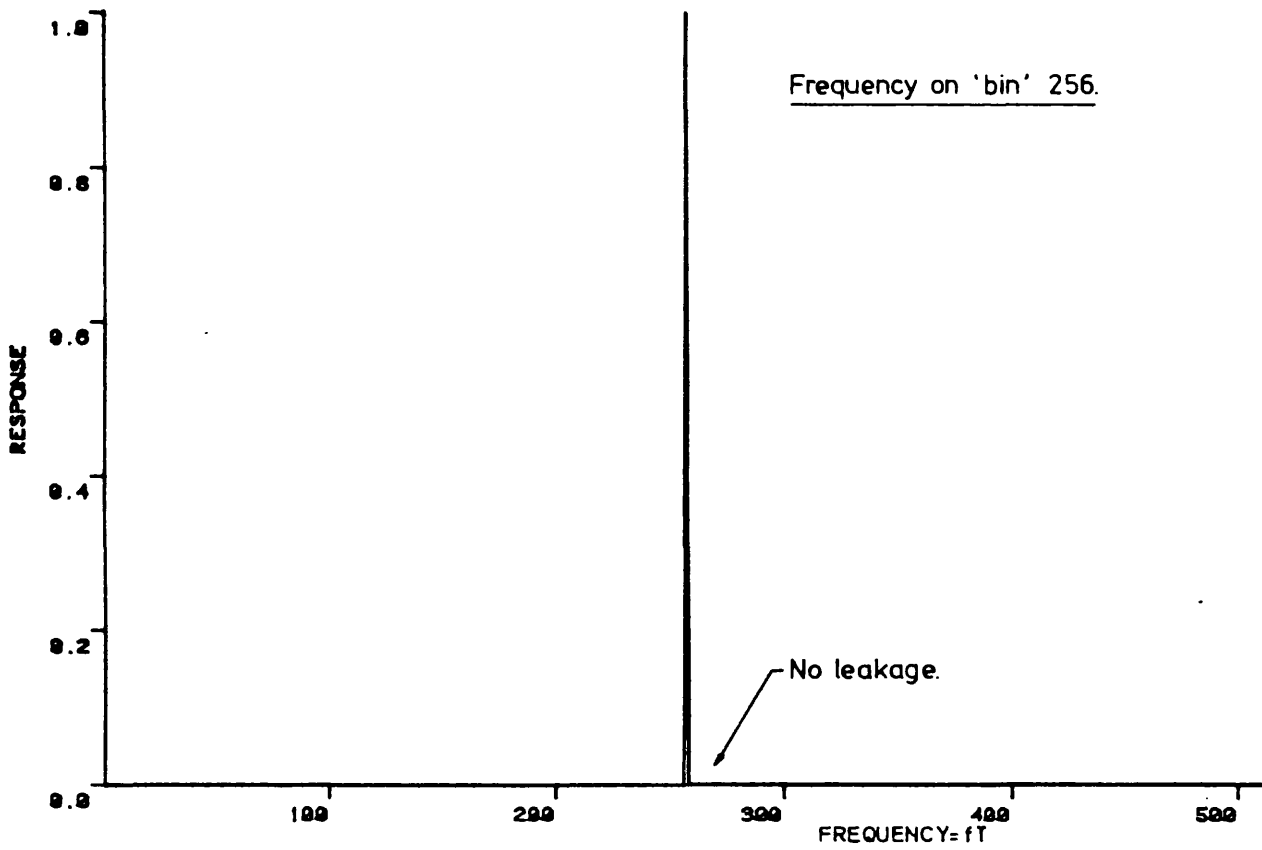


Figure 31 (Continued)



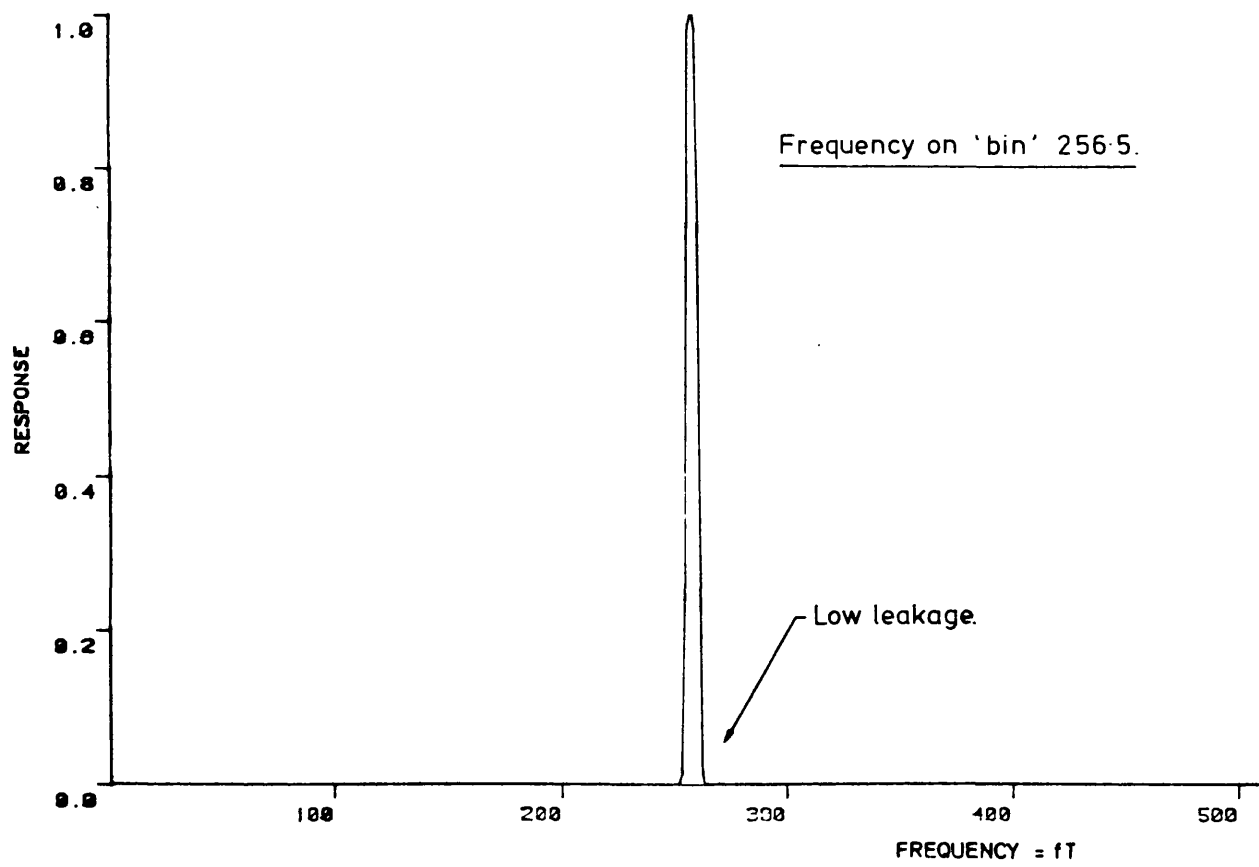
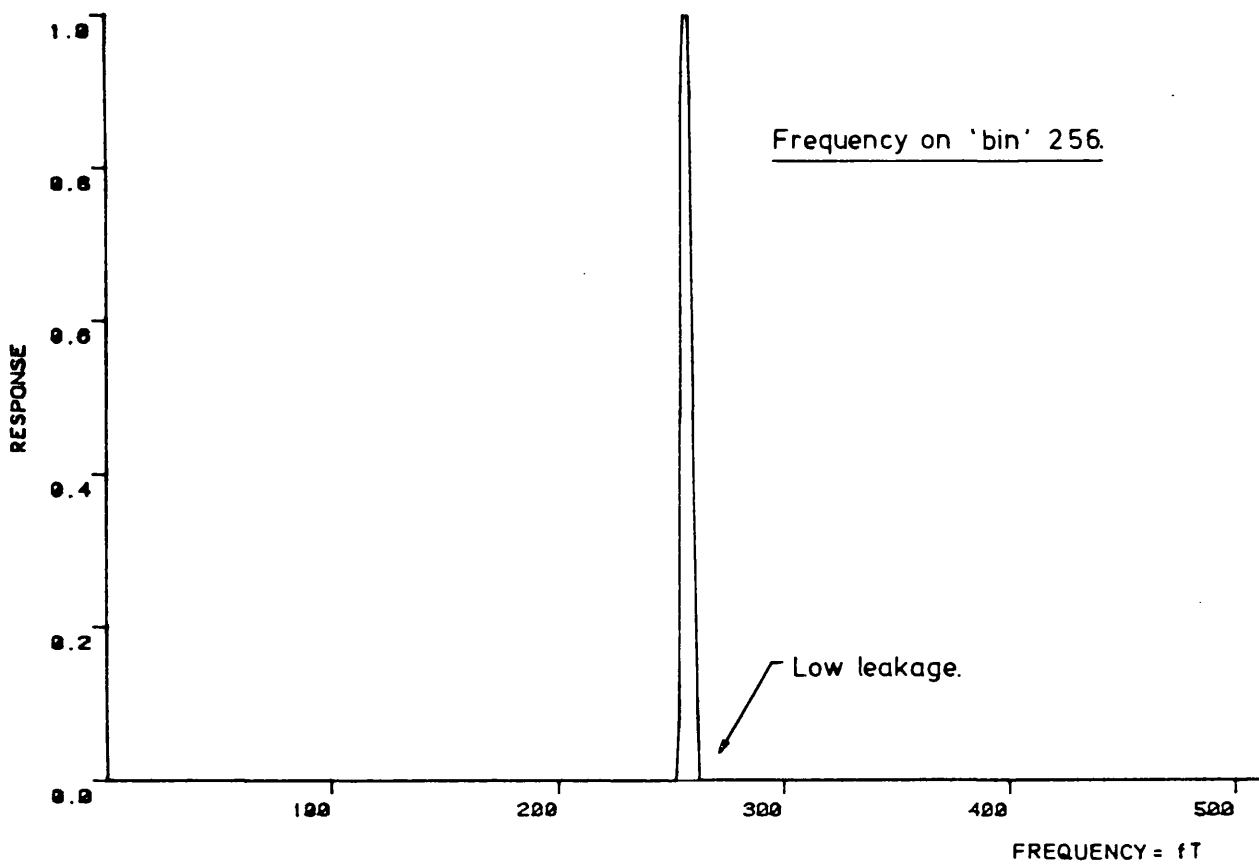
Flat Top Window

Figures 32 & 33



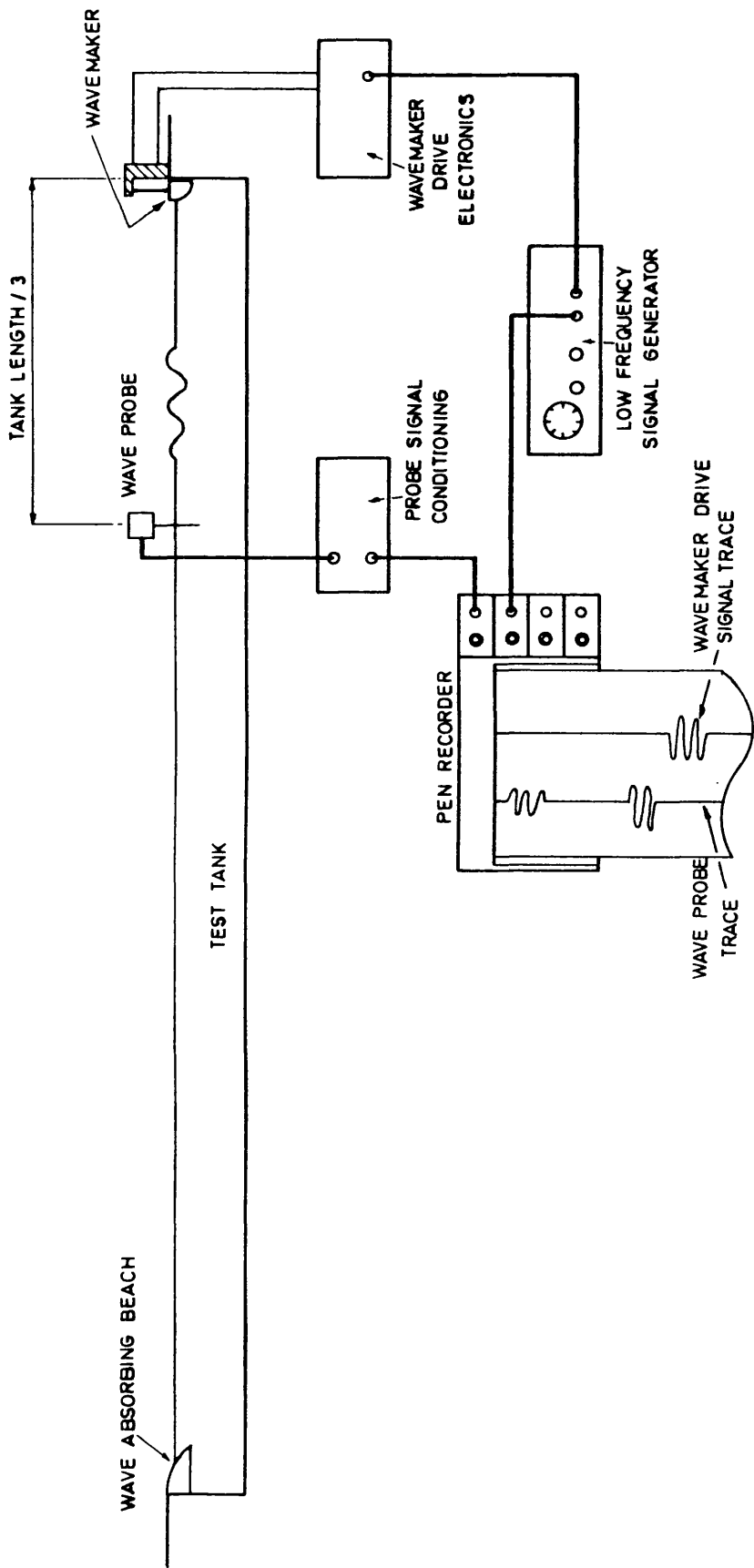
AMPLITUDE SPECTRA OF UNIT AMPLITUDE SINGLE FREQUENCY
TIME SERIES VIA FFT AND USING 'BOXCAR' WINDOW.

FIGURE 34



AMPLITUDE SPECTRA OF UNIT AMPLITUDE SINGLE FREQUENCY
TIME SERIES VIA FFT AND USING FLAT TOP WINDOW.

FIGURE 35



FIRST TEST SERIES EXPERIMENT LAYOUT

Figure 36

WAVEMAKER CALIBRATION - FREQUENCY BASE

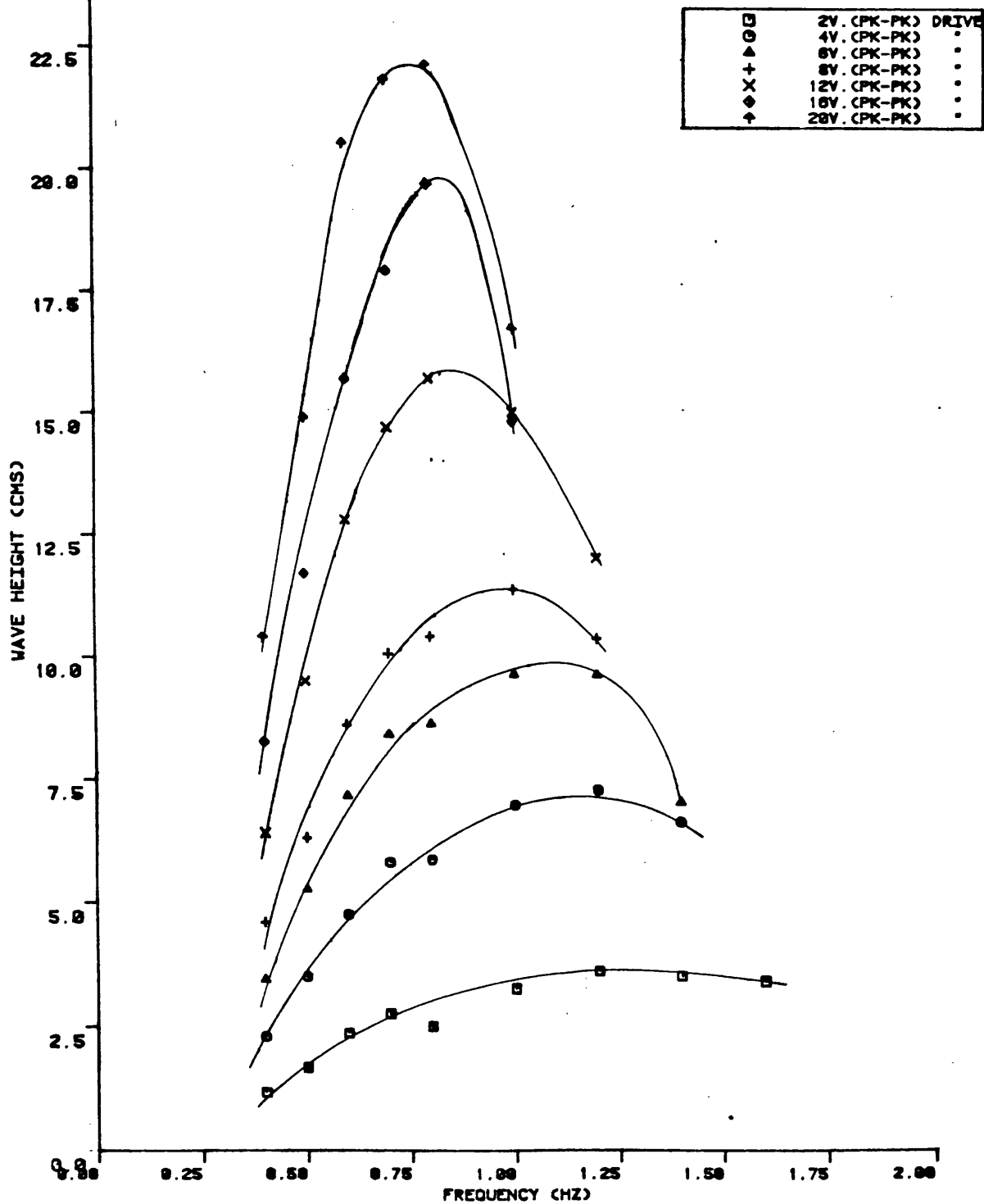


Figure 37

WAVEMAKER CALIBRATION - WAVEPERIOD BASE

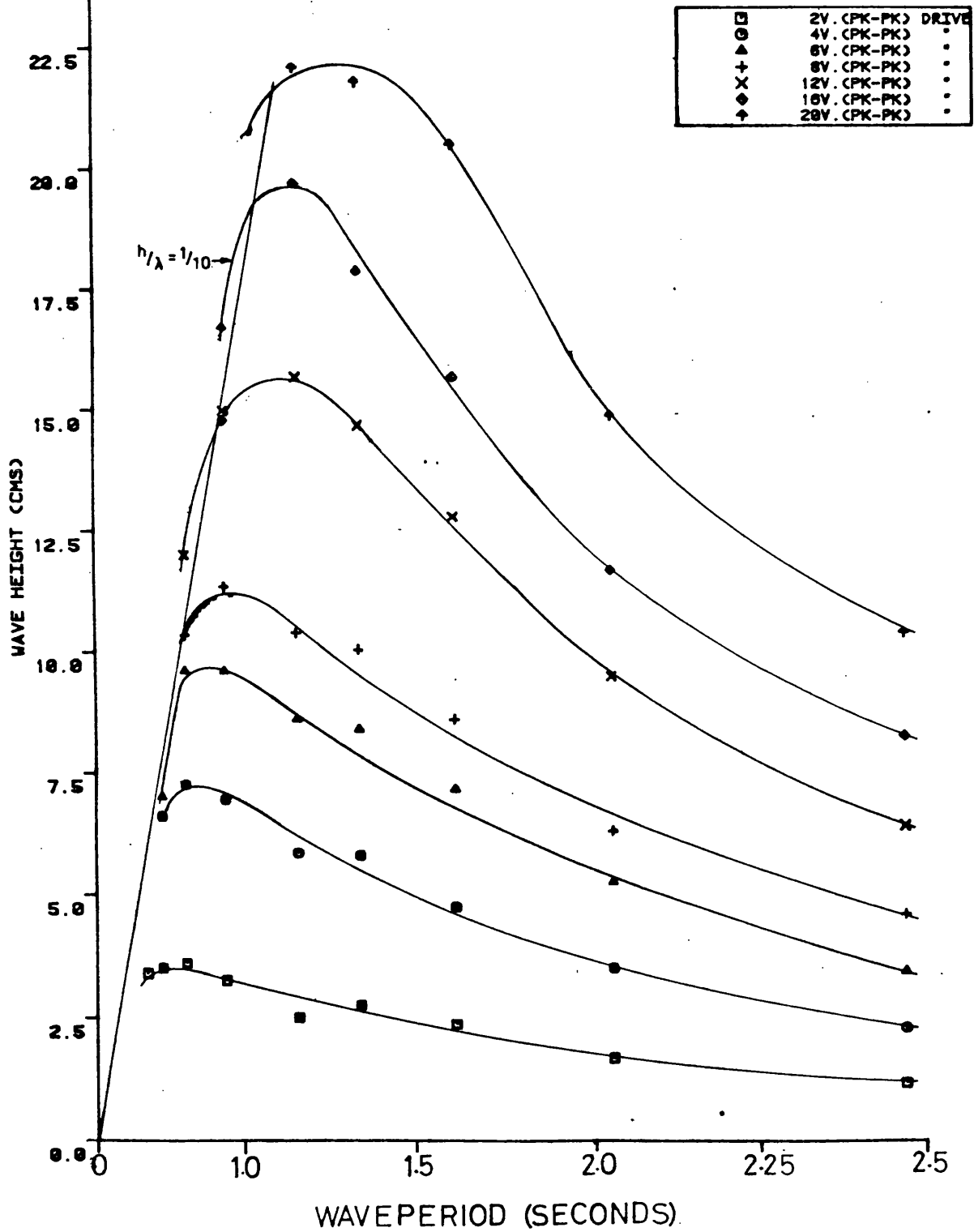


Figure 38

WAVEMAKER TRANSFER FUNCTION

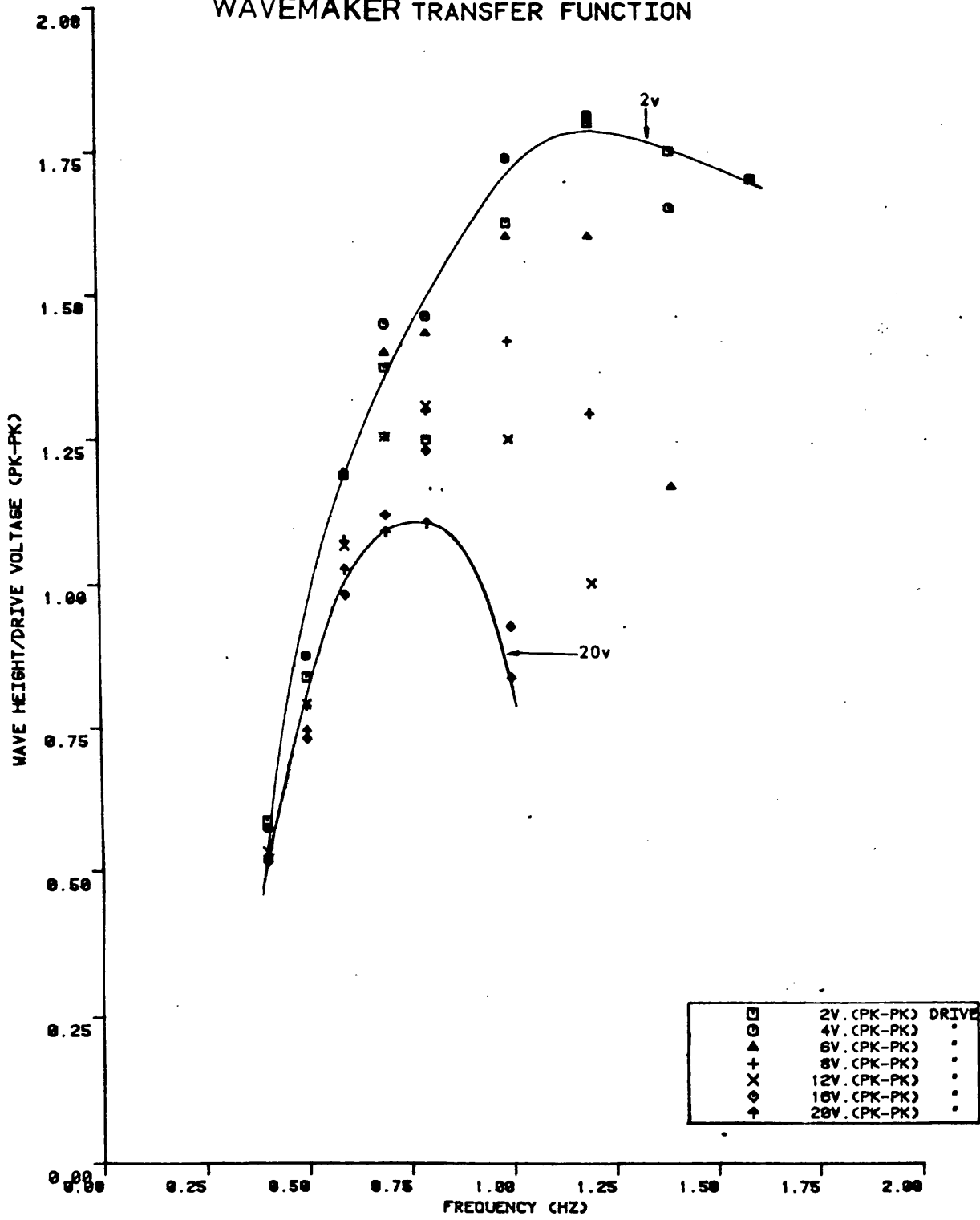


Figure 39

BEACH WAVE ATTENUATION

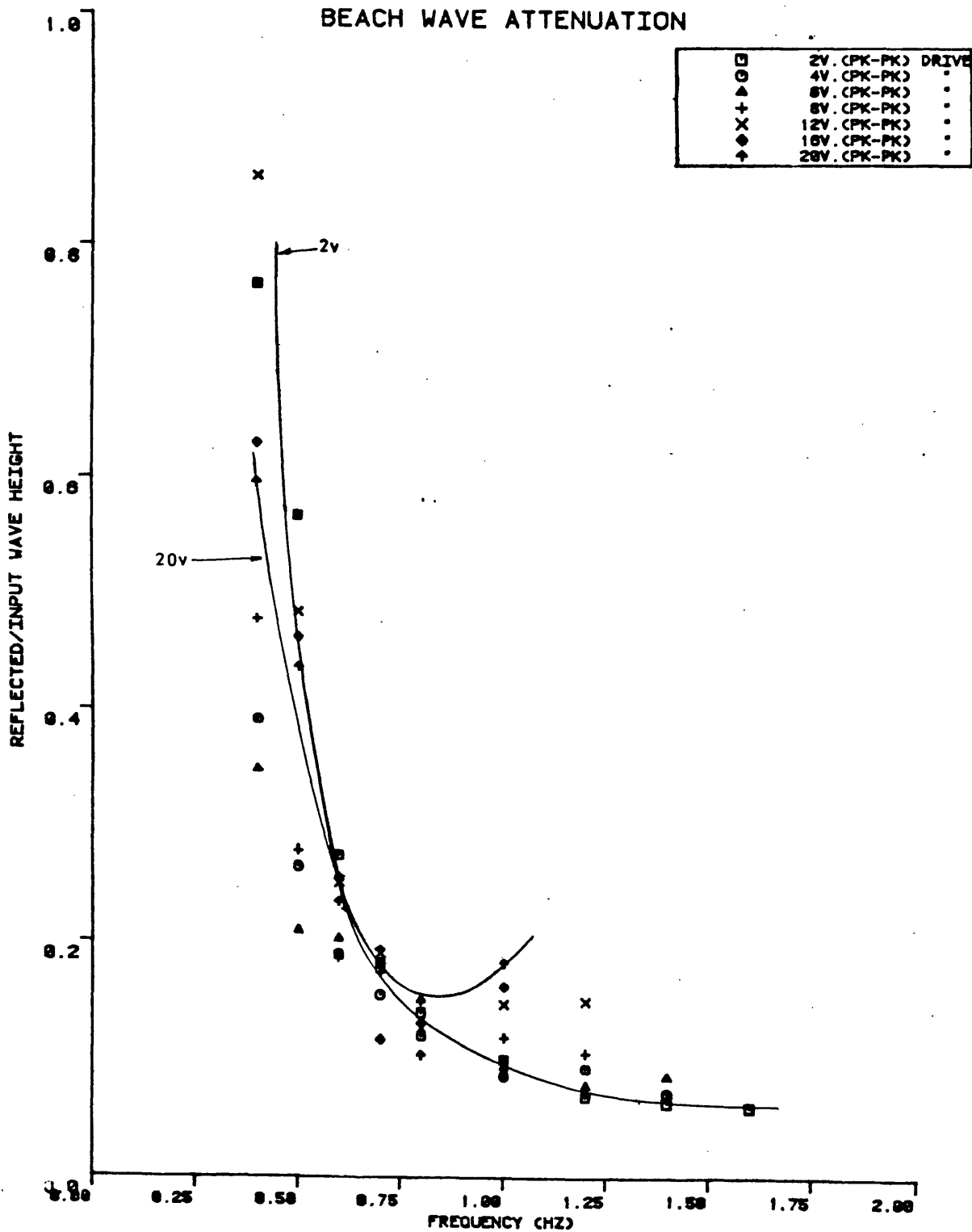


Figure 40

TANK SUB-BEACH

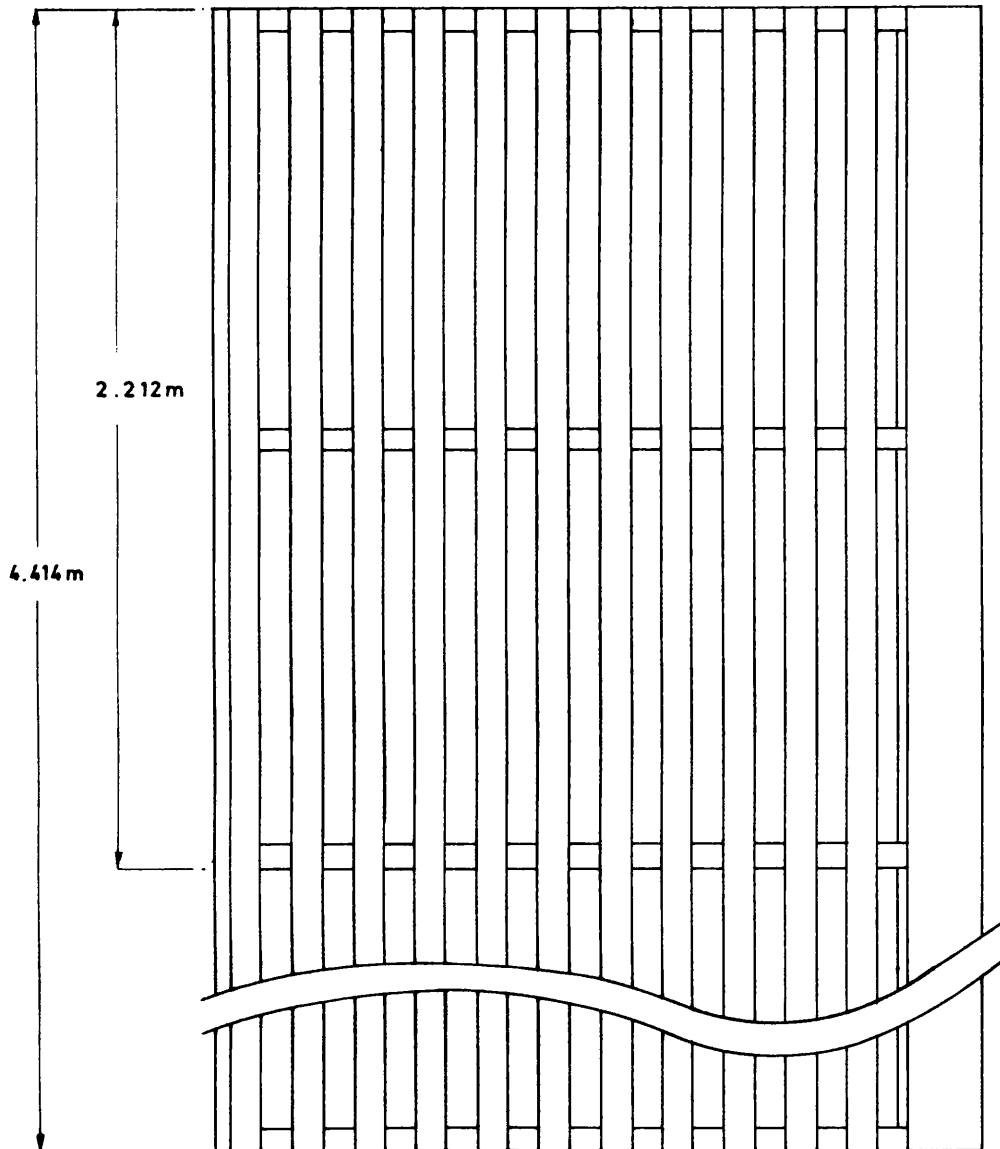
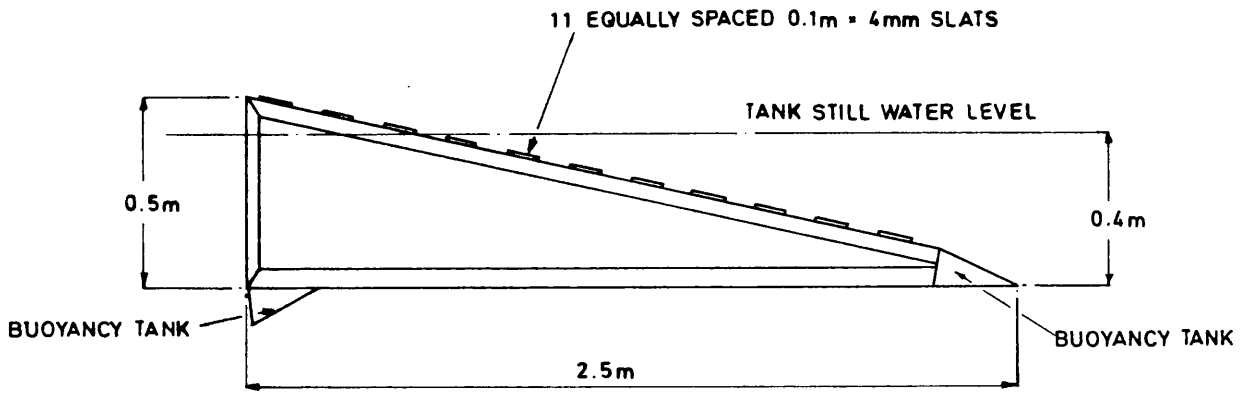


Figure 41

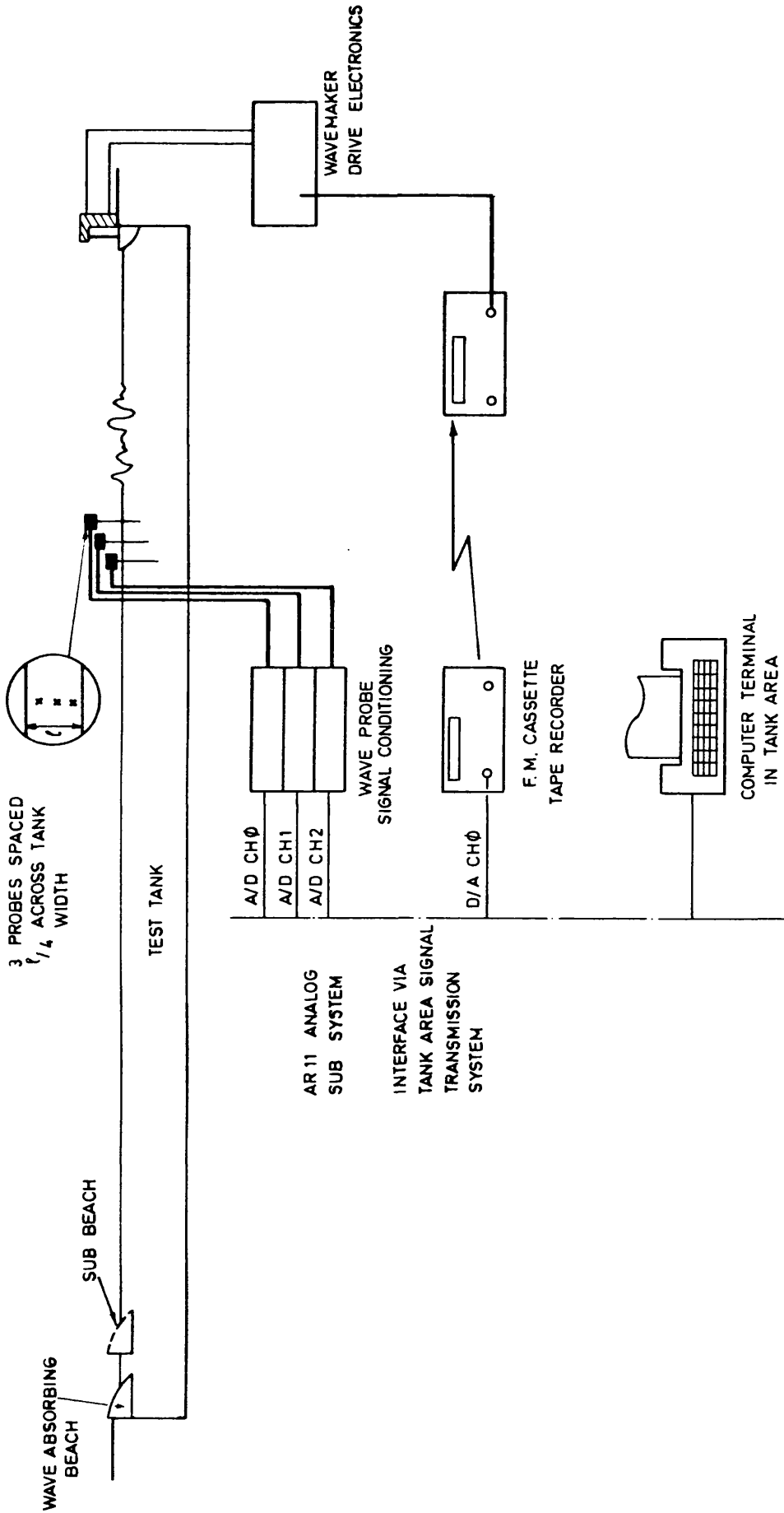


Figure 42

SECOND TEST SERIES EXPERIMENT LAYOUT

Spectrum $m_{1/3} = 10m$ Full Scale

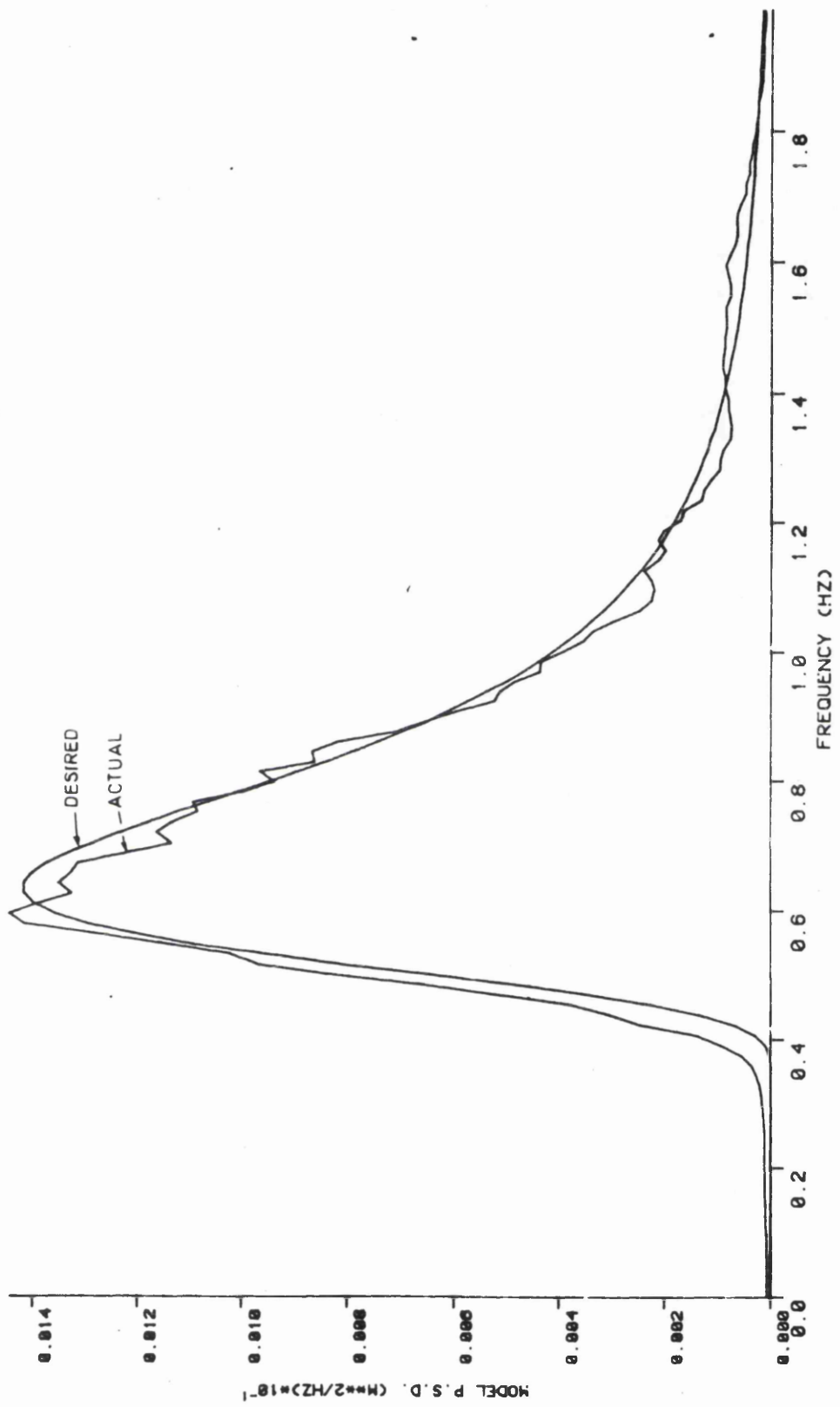


FIGURE 43

Spectrum $H_{1/3} = 5\text{m Full Scale}$

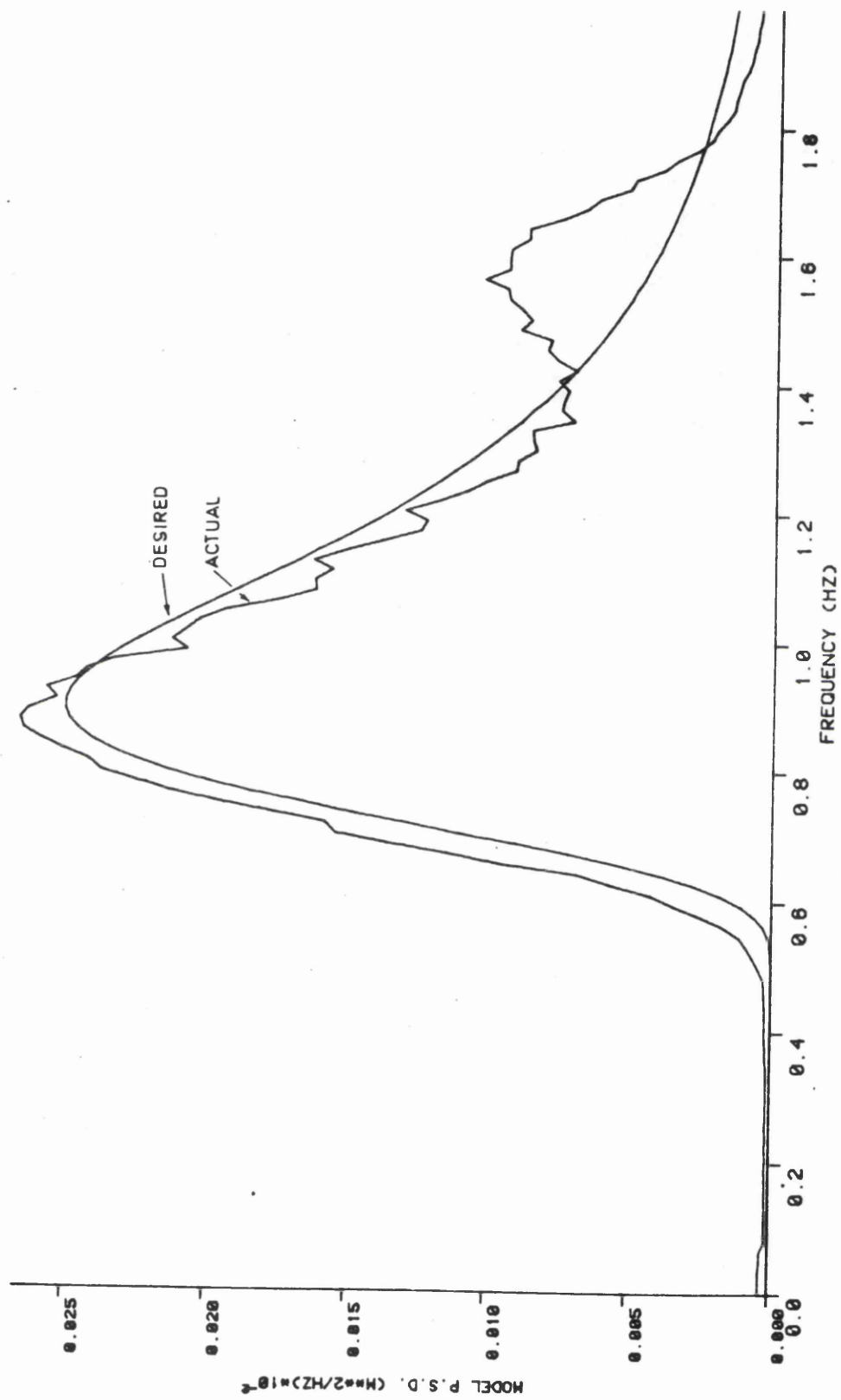


FIGURE 44

Spectrum $\eta^{1/3} = 13M$ FULL SCALE

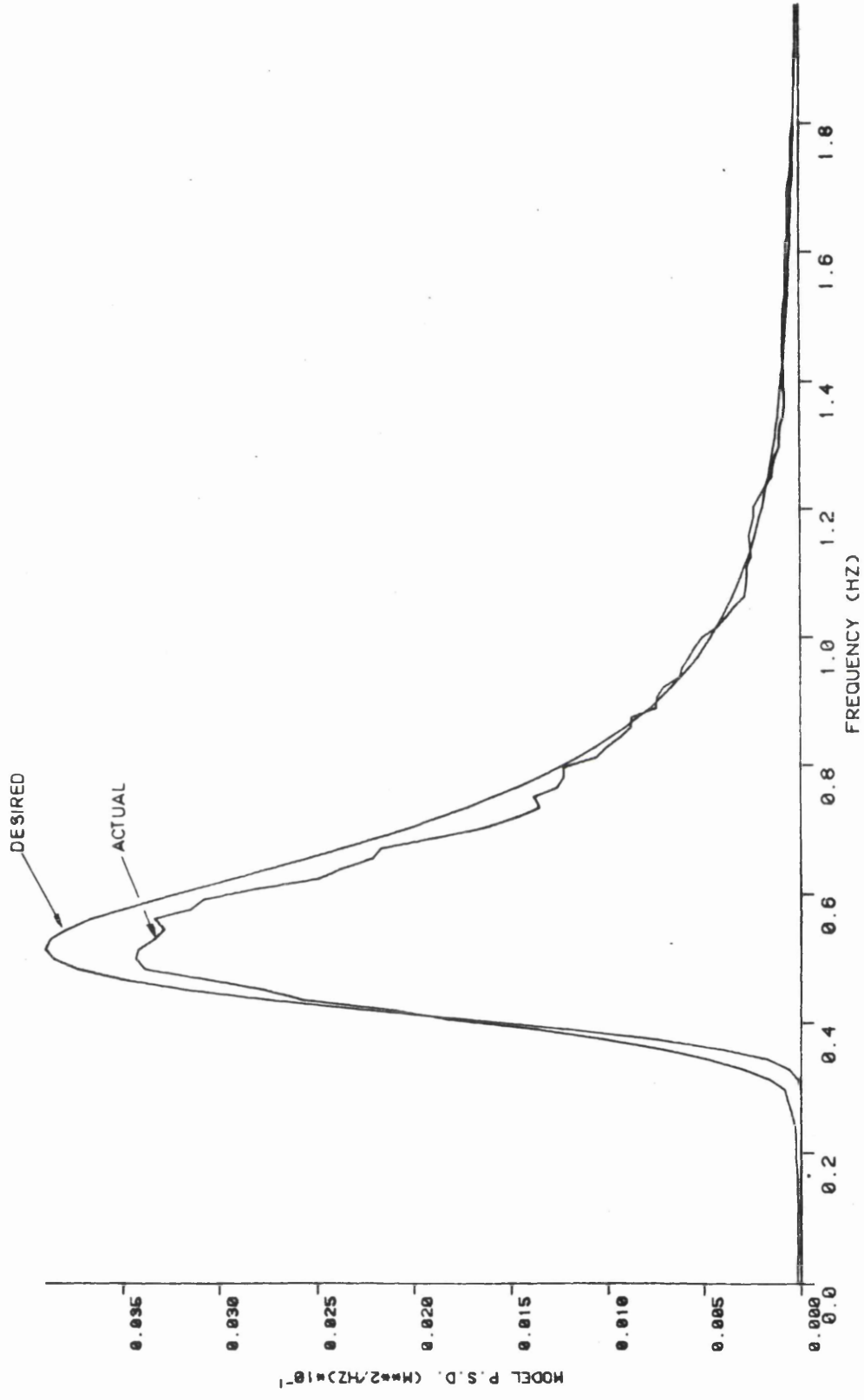


FIGURE 45

SCOTBUOY TEST ARRANGEMENT

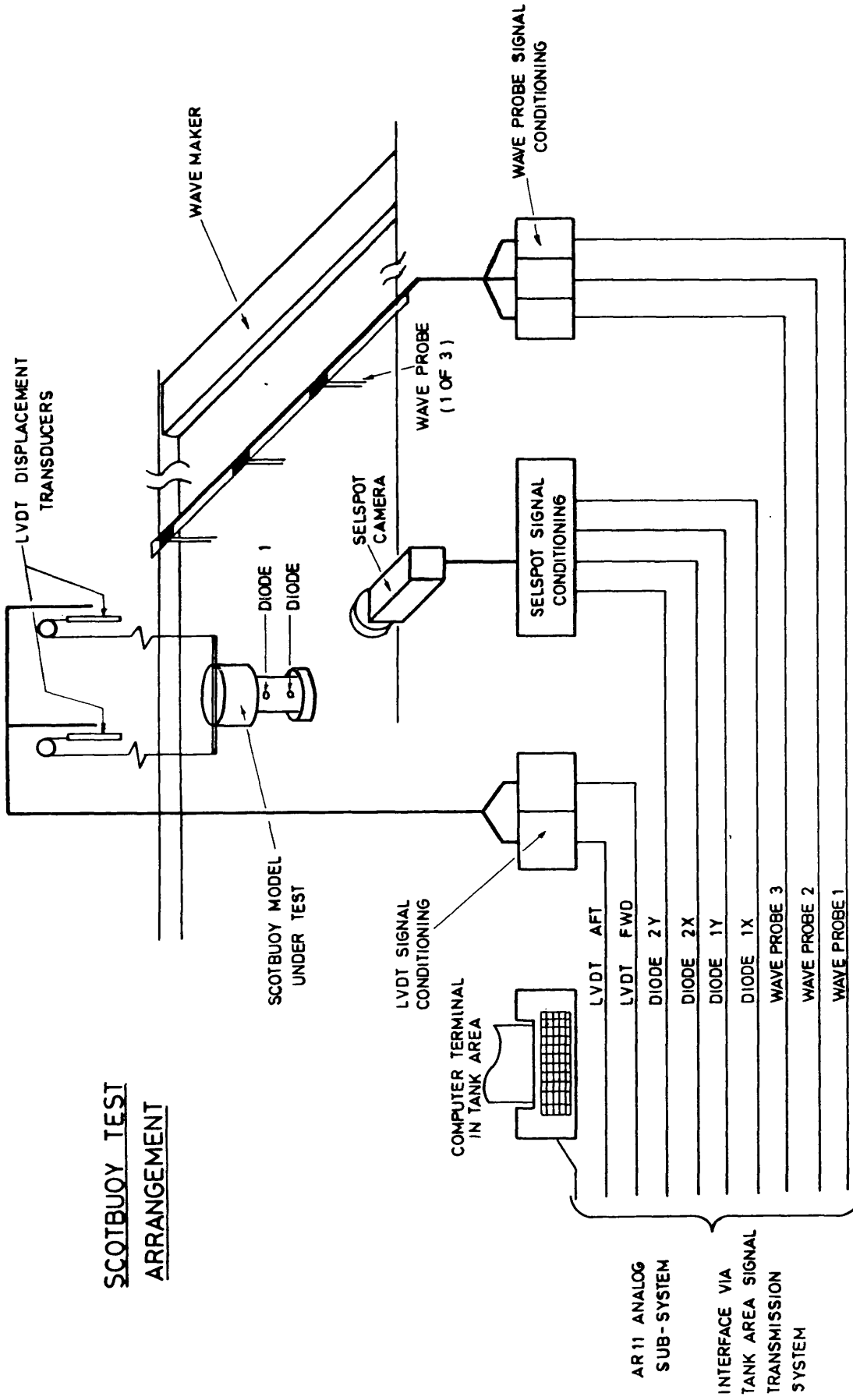


Figure 46

FILE=TEST06 ENSEMBLES= 20 F. AVERAGES= 3 RESOLUTION= 0.06 HZ

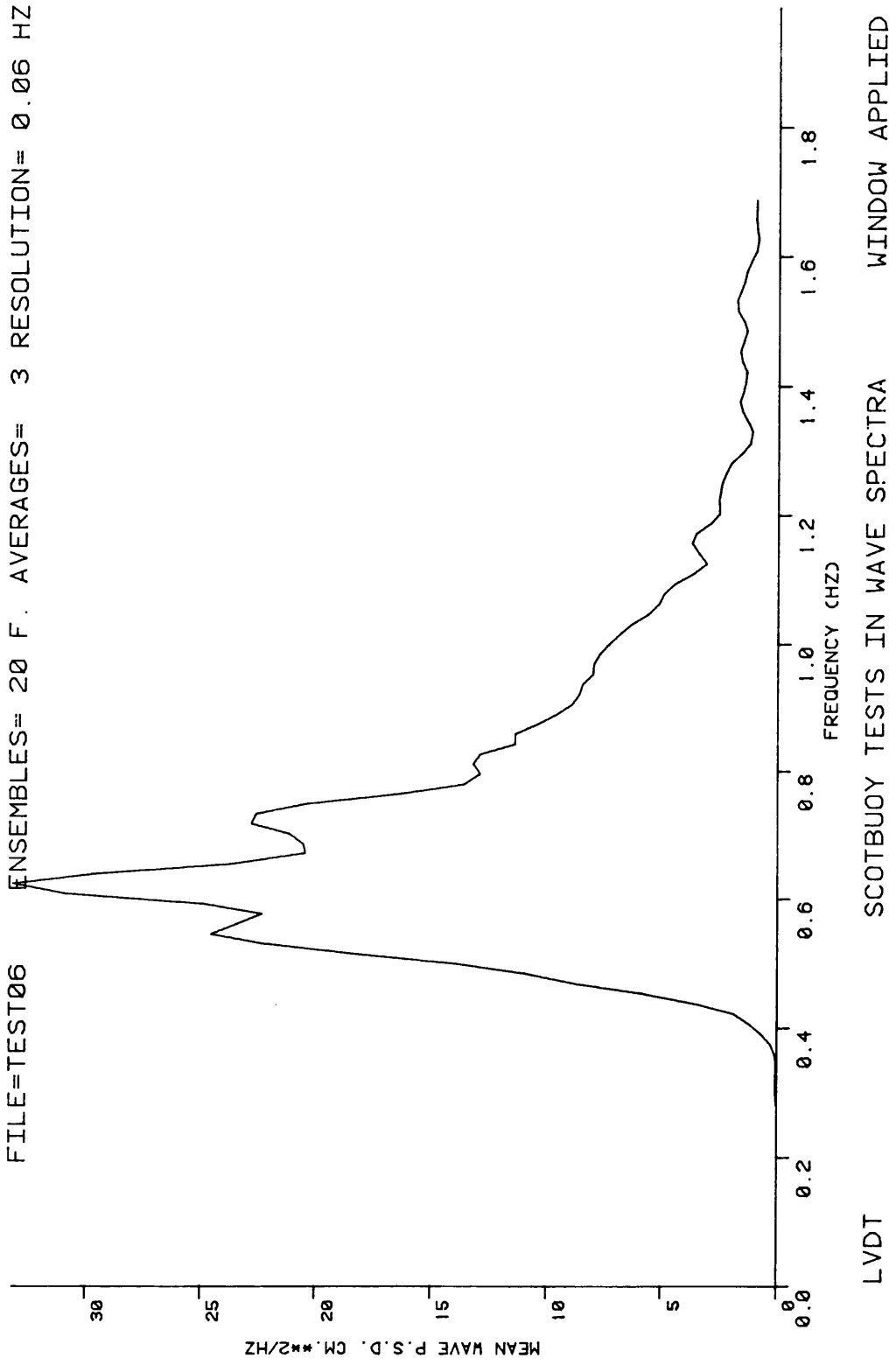


FIGURE 47

FILE=TEST06 ENSEMBLES= 20 F. AVERAGES= 3 RESOLUTION= 0.06 HZ

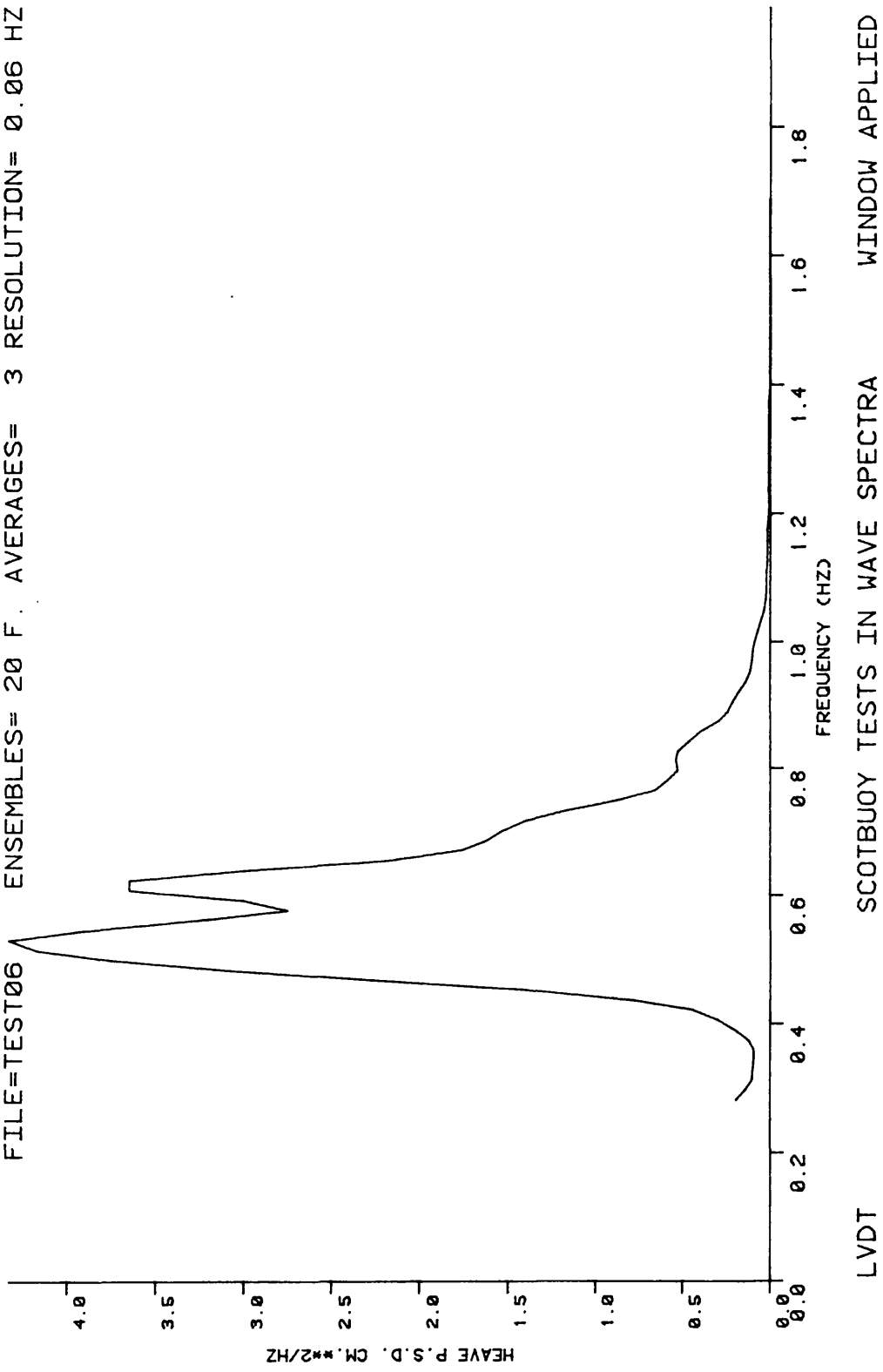
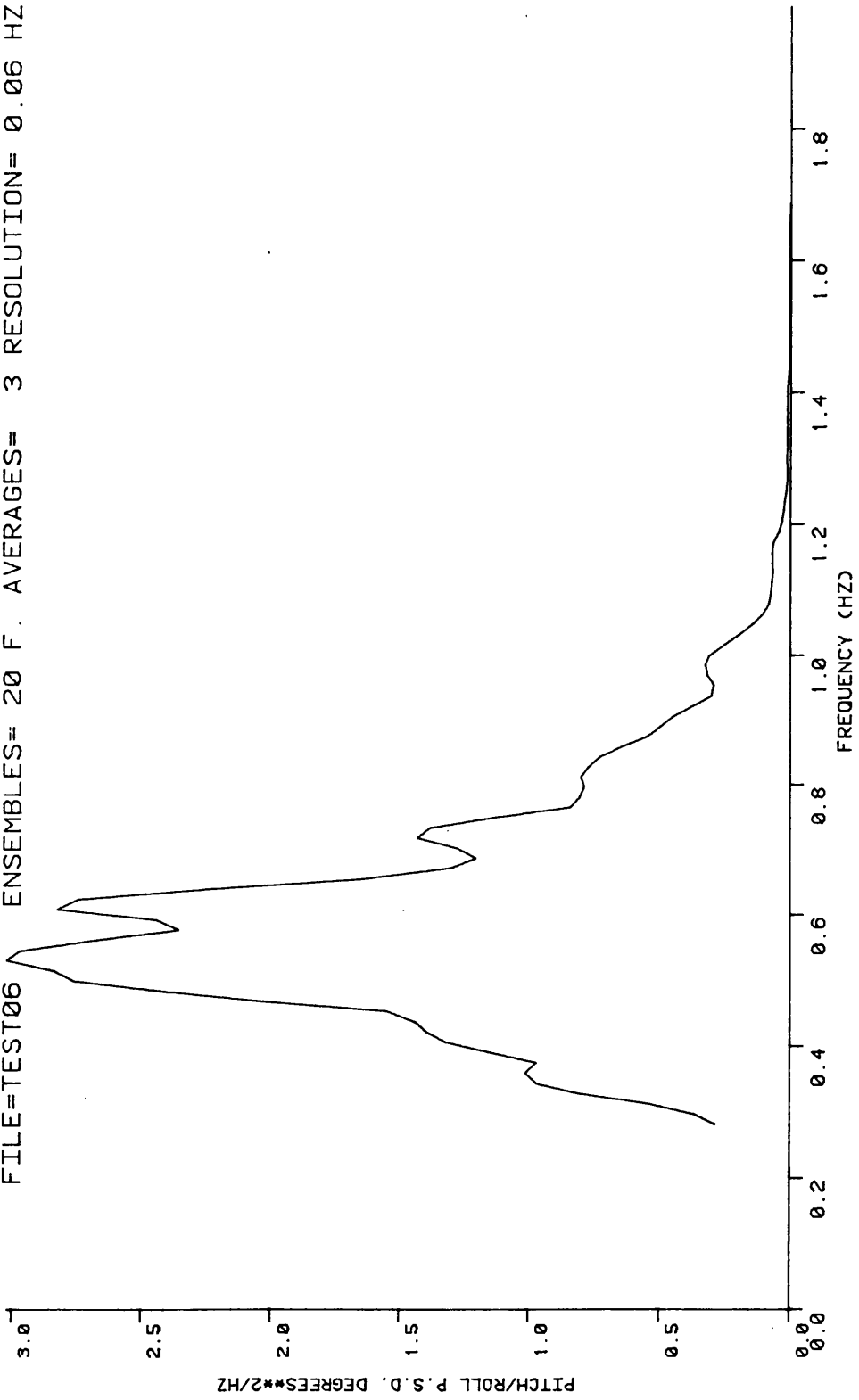


FIGURE 48

FILE=TEST06 ENSEMBLES= 20 F. AVERAGES= 3 RESOLUTION= 0.06 HZ



LVDT SCOTBUOY TESTS IN WAVE SPECTRA WINDOW APPLIED

FIGURE 49

FILE=TEST06 ENSEMBLES= 20 F. AVERAGES= 3 RESOLUTION= 0.06 HZ

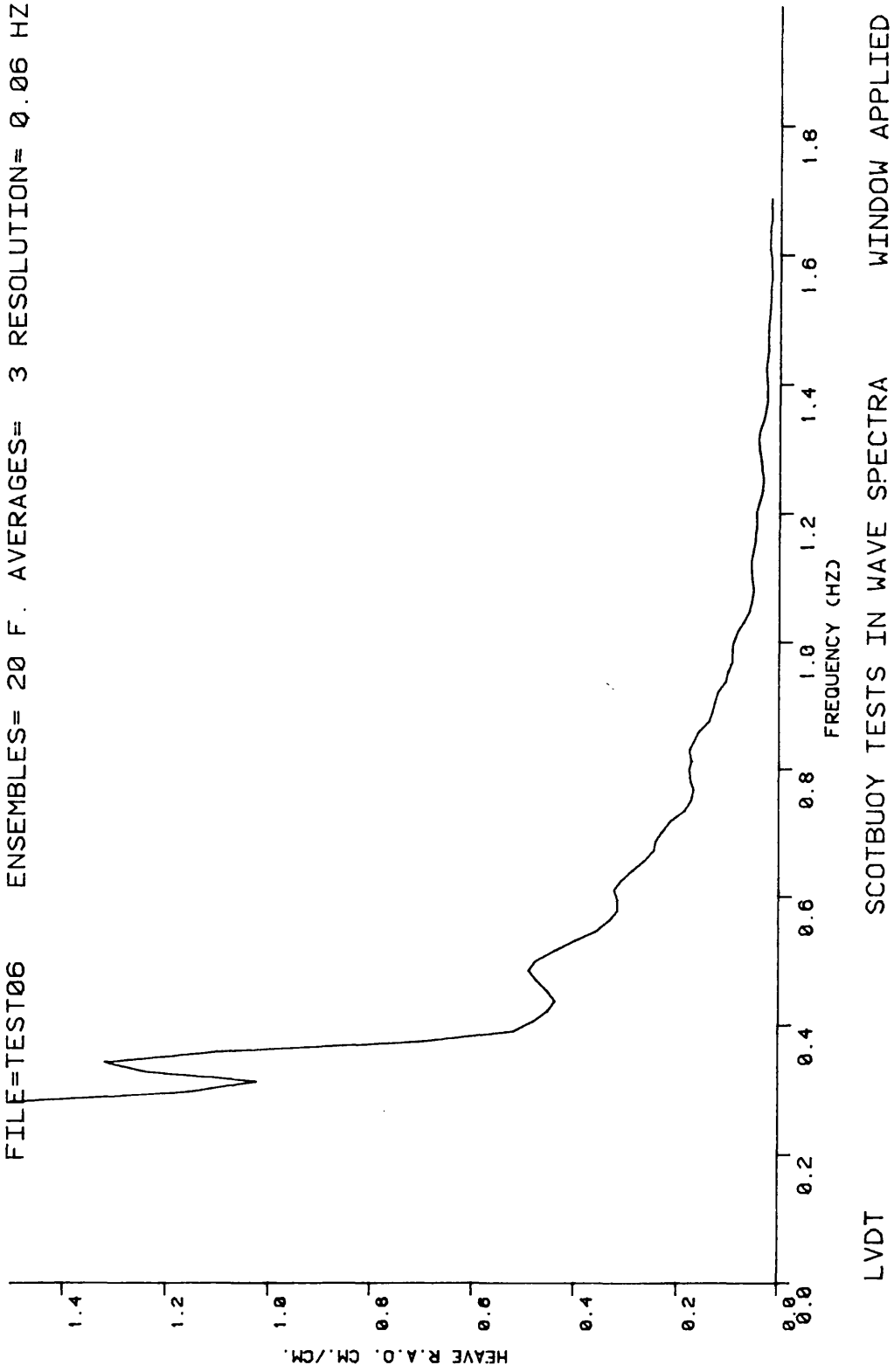


FIGURE 50

FILE=TEST06 ENSEMBLES= 20 F. AVERAGES= 3 RESOLUTION= 0.06 HZ

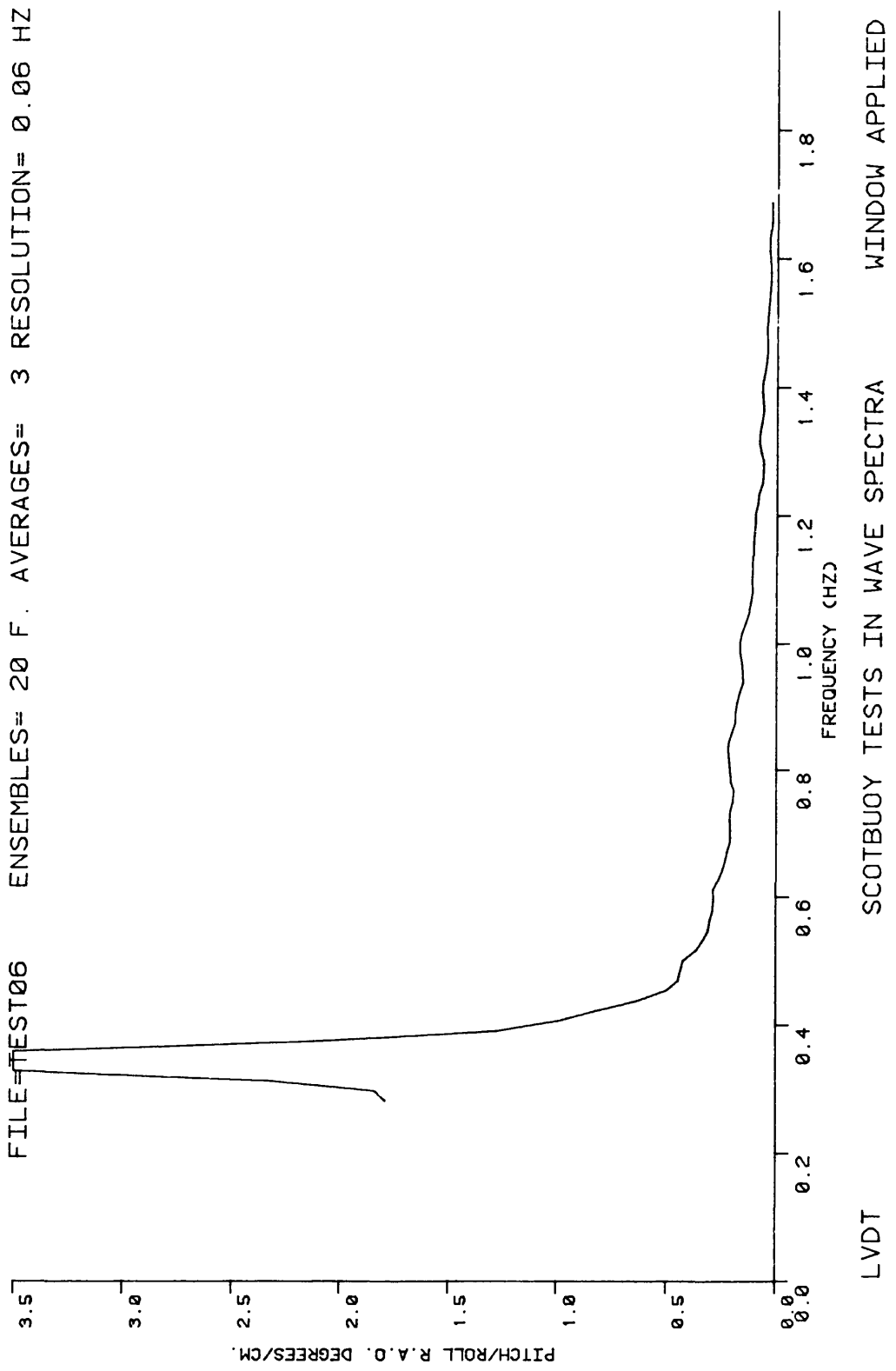


FIGURE 51

FILE=TEST06 ENSEMBLES= 20 F. AVERAGES= 3 RESOLUTION= 0.06 HZ

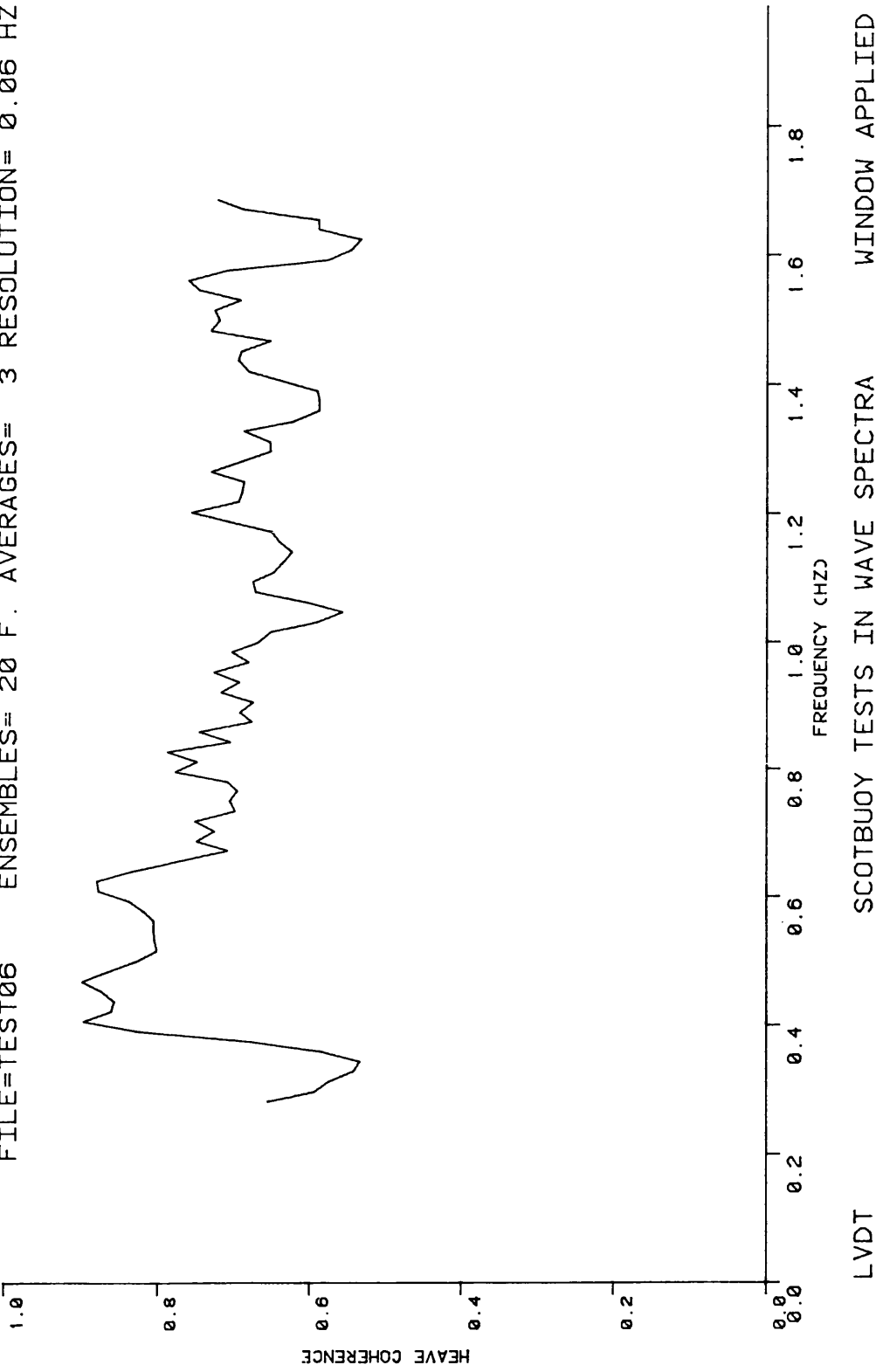


FIGURE 52

FILE=TEST06 ENSEMBLES= 20 F. AVERAGES= 3 RESOLUTION= 0.06 HZ

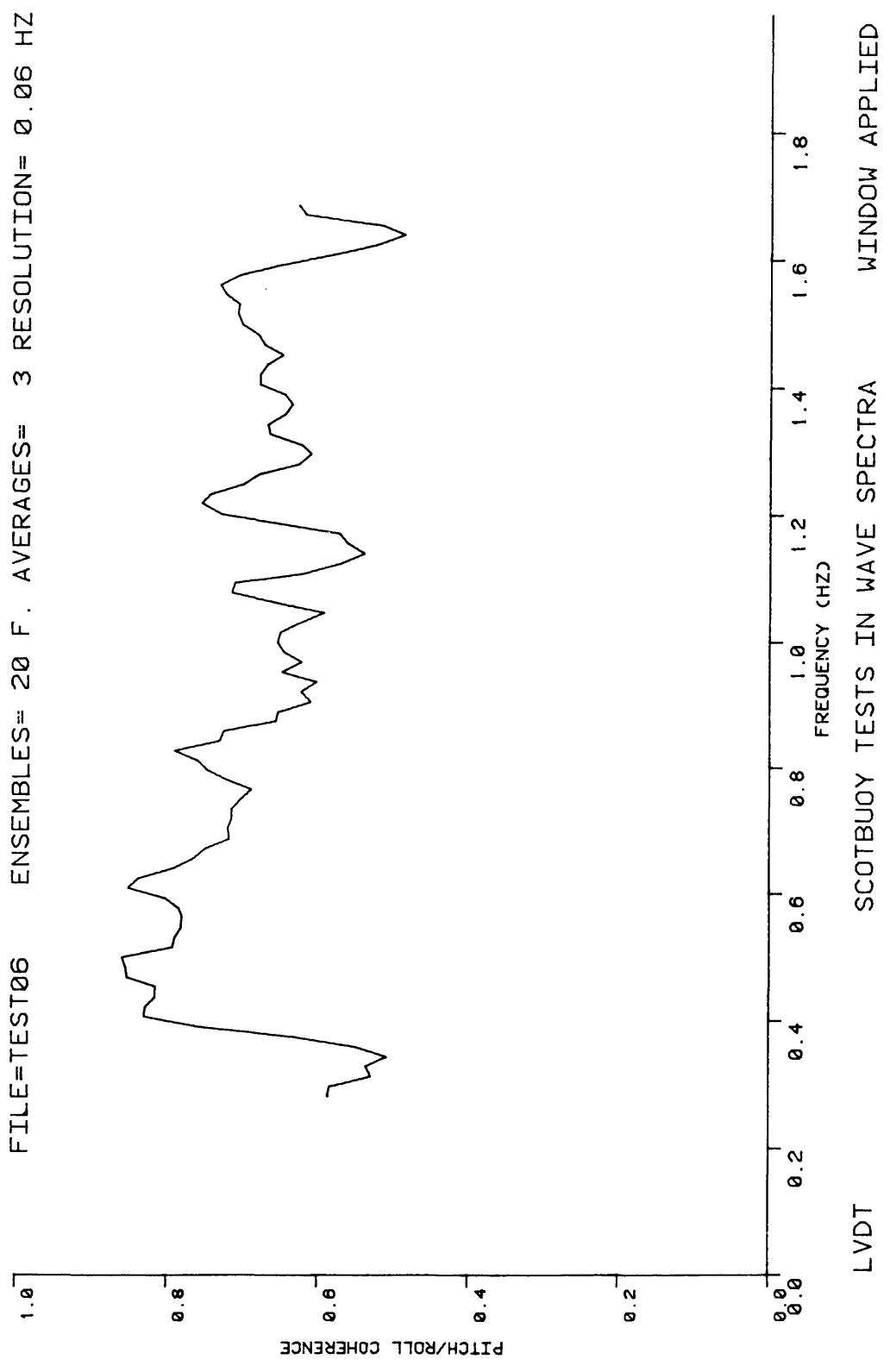


FIGURE 53

FILE=TEST06 ENSEMBLES= 20 F. AVERAGES= 3 RESOLUTION= 0.06 HZ

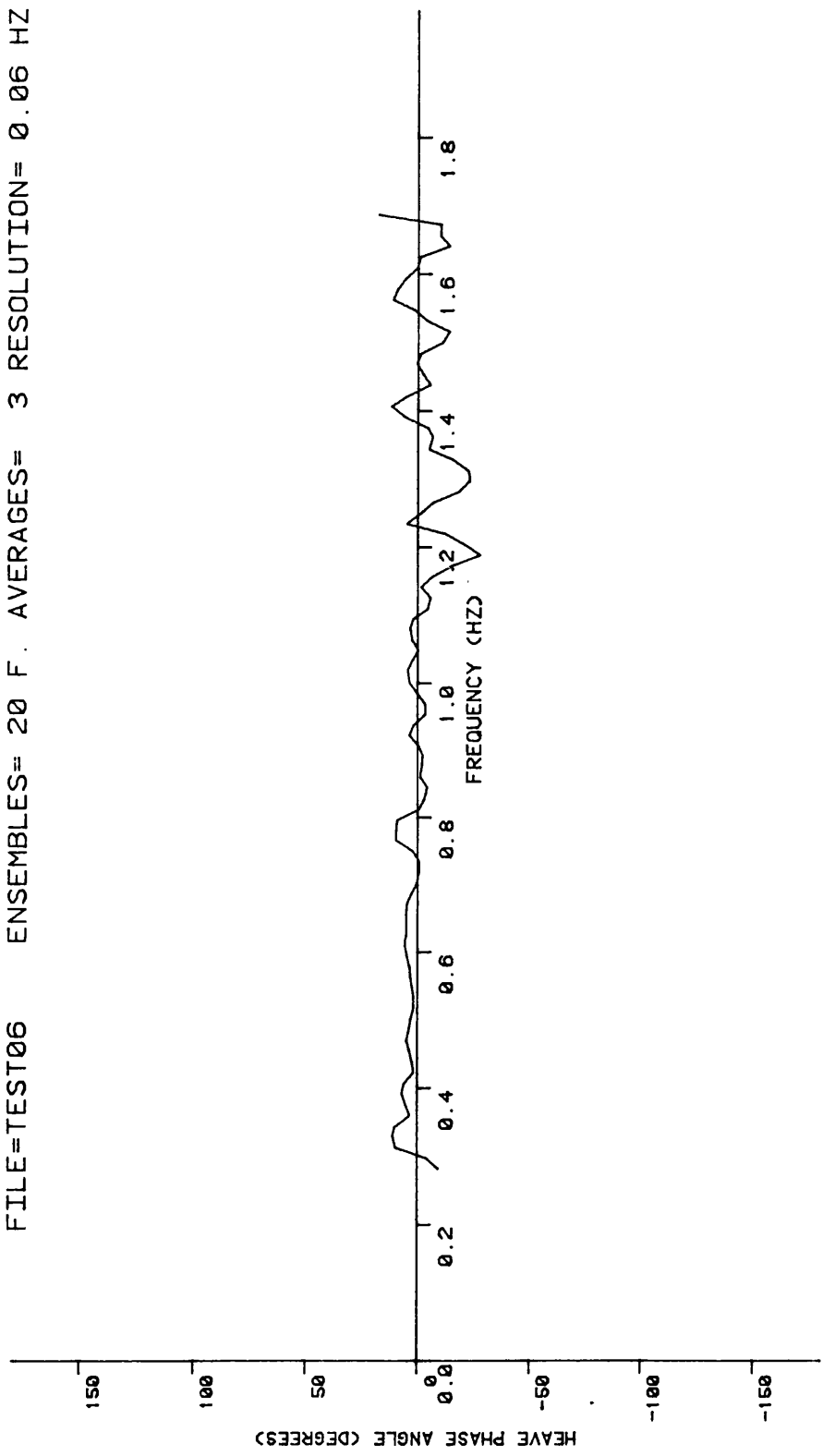


FIGURE 54

LVDT SCOTBUOY TESTS IN WAVE SPECTRA WINDOW APPLIED

FILE=TEST06 ENSEMBLES= 20 F. AVERAGES= 3 RESOLUTION= 0.06 HZ

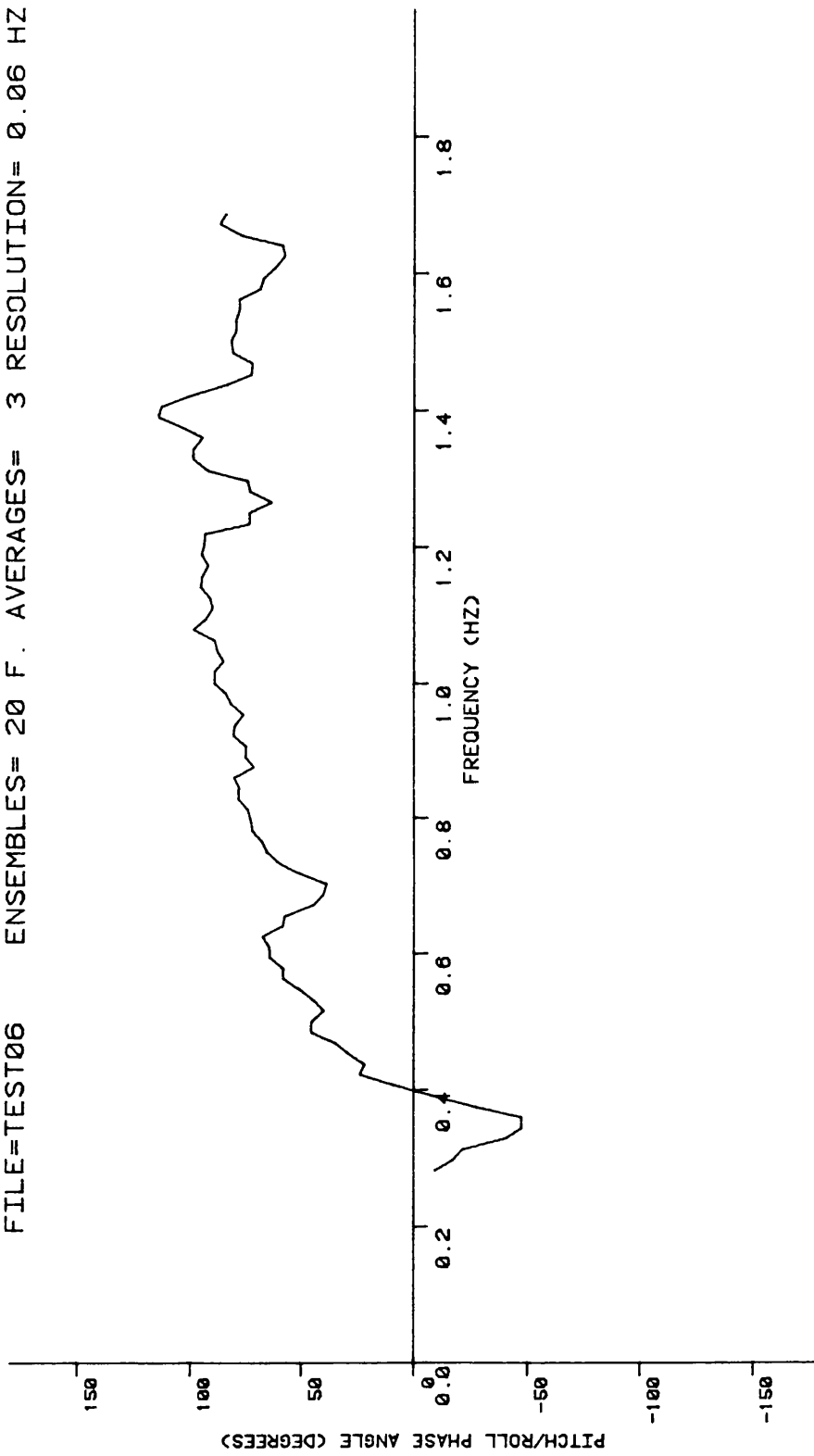


FIGURE 55

LVDT SCOTBUOY TESTS IN WAVE SPECTRA WINDOW APPLIED

FILE=TEST09 ENSEMBLES= 20 F. AVERAGES= 3 RESOLUTION= 0.06 HZ

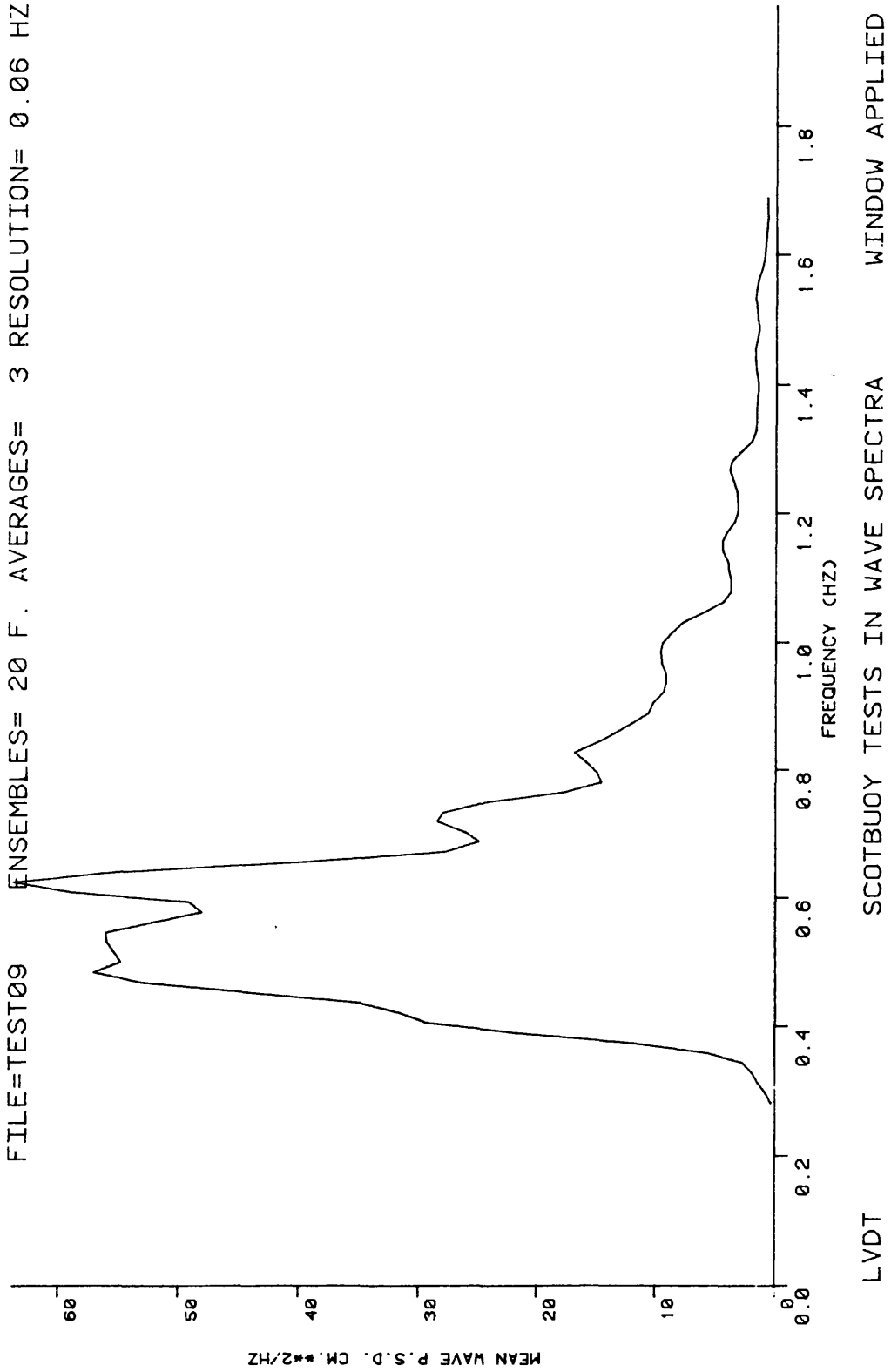


FIGURE 56

FILE=TEST08 ENSEMBLES= 20 F. AVERAGES= 3 RESOLUTION= 0.06 HZ

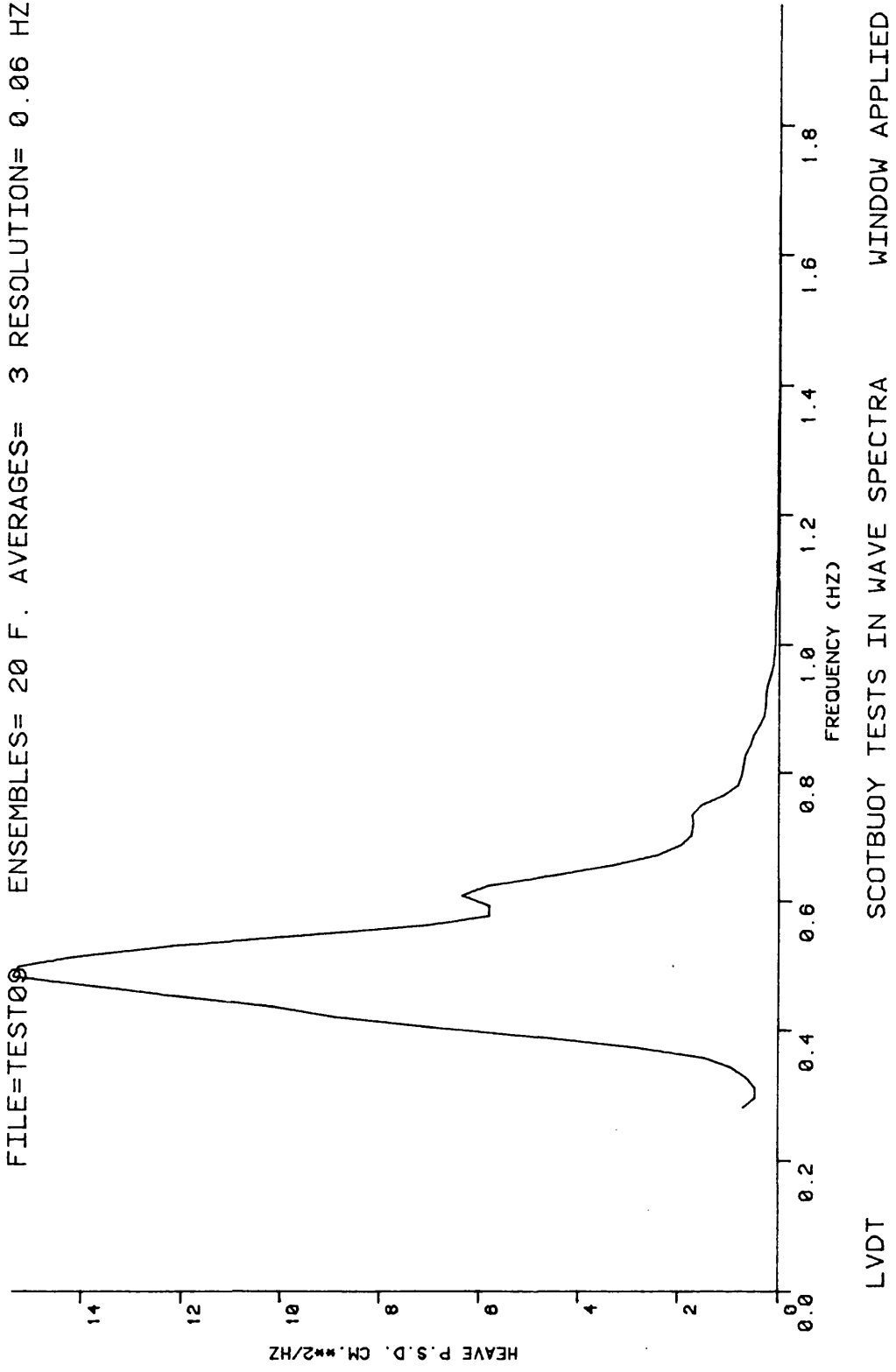


FIGURE 57

FILE=TEST09 ENSEMBLES= 20 F. AVERAGES= 3 RESOLUTION= 0.06 HZ

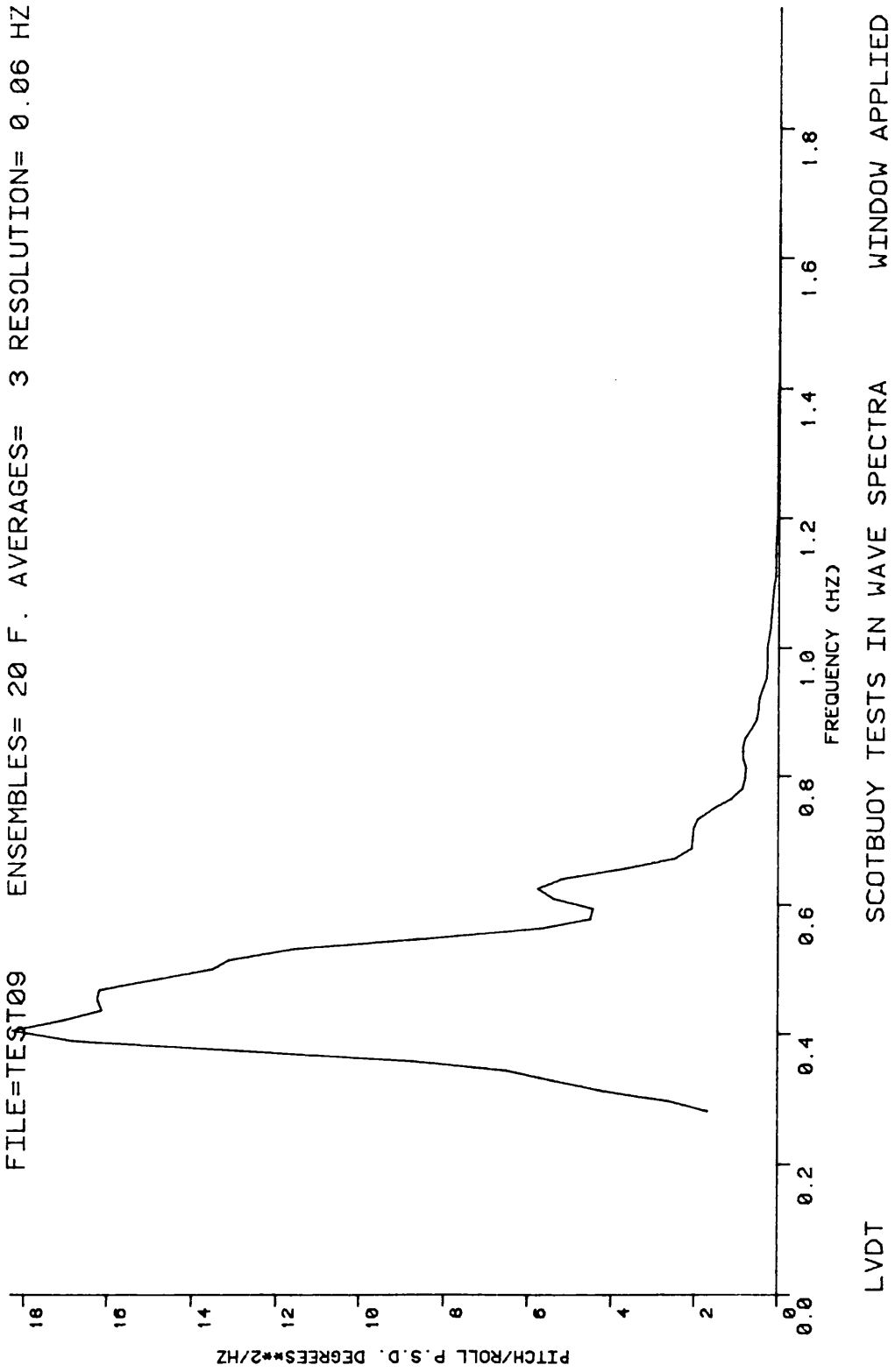


FIGURE 58

FILE=TEST09 ENSEMBLES= 20 F. AVERAGES= 3 RESOLUTION= 0.06 HZ

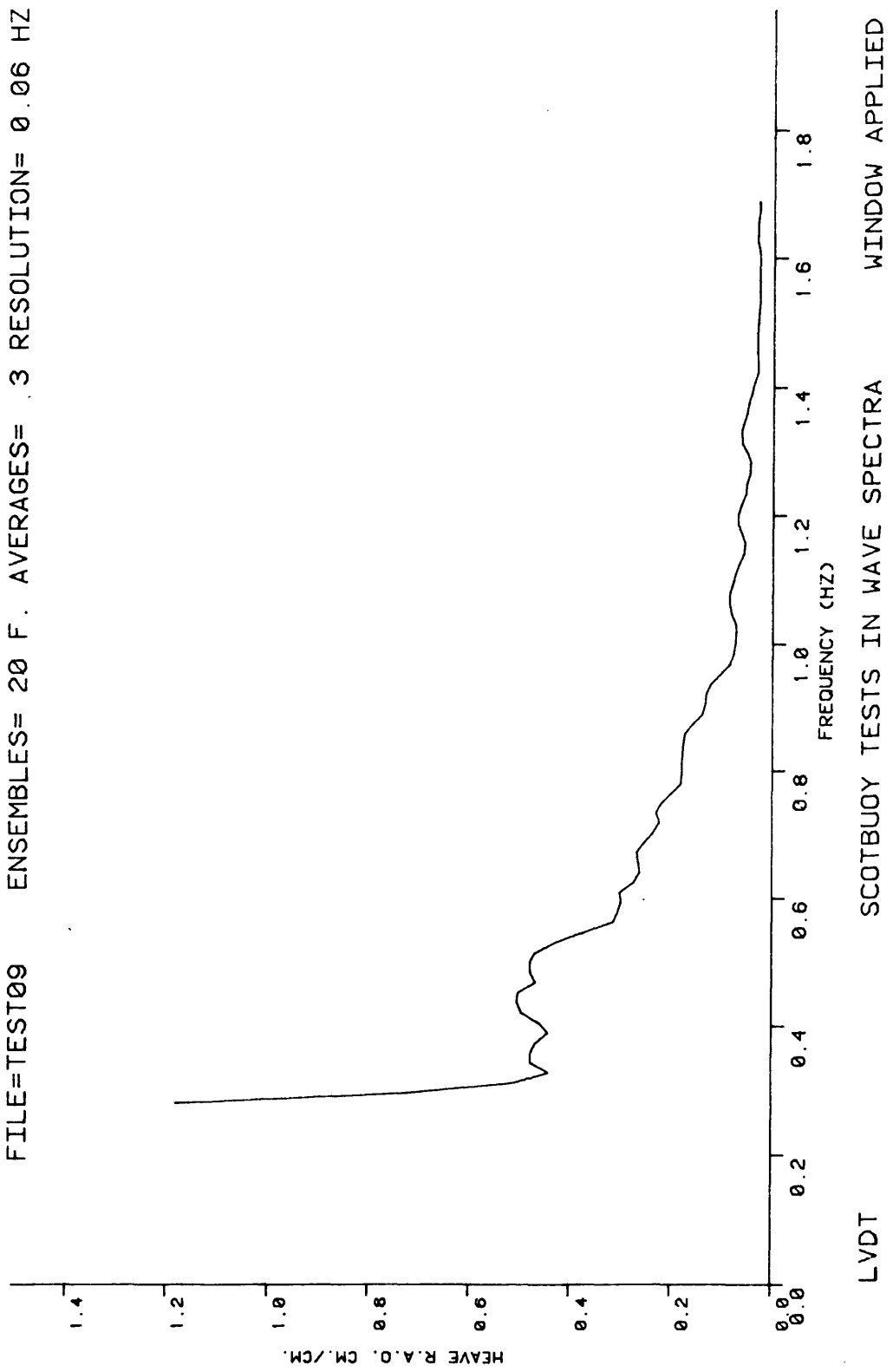
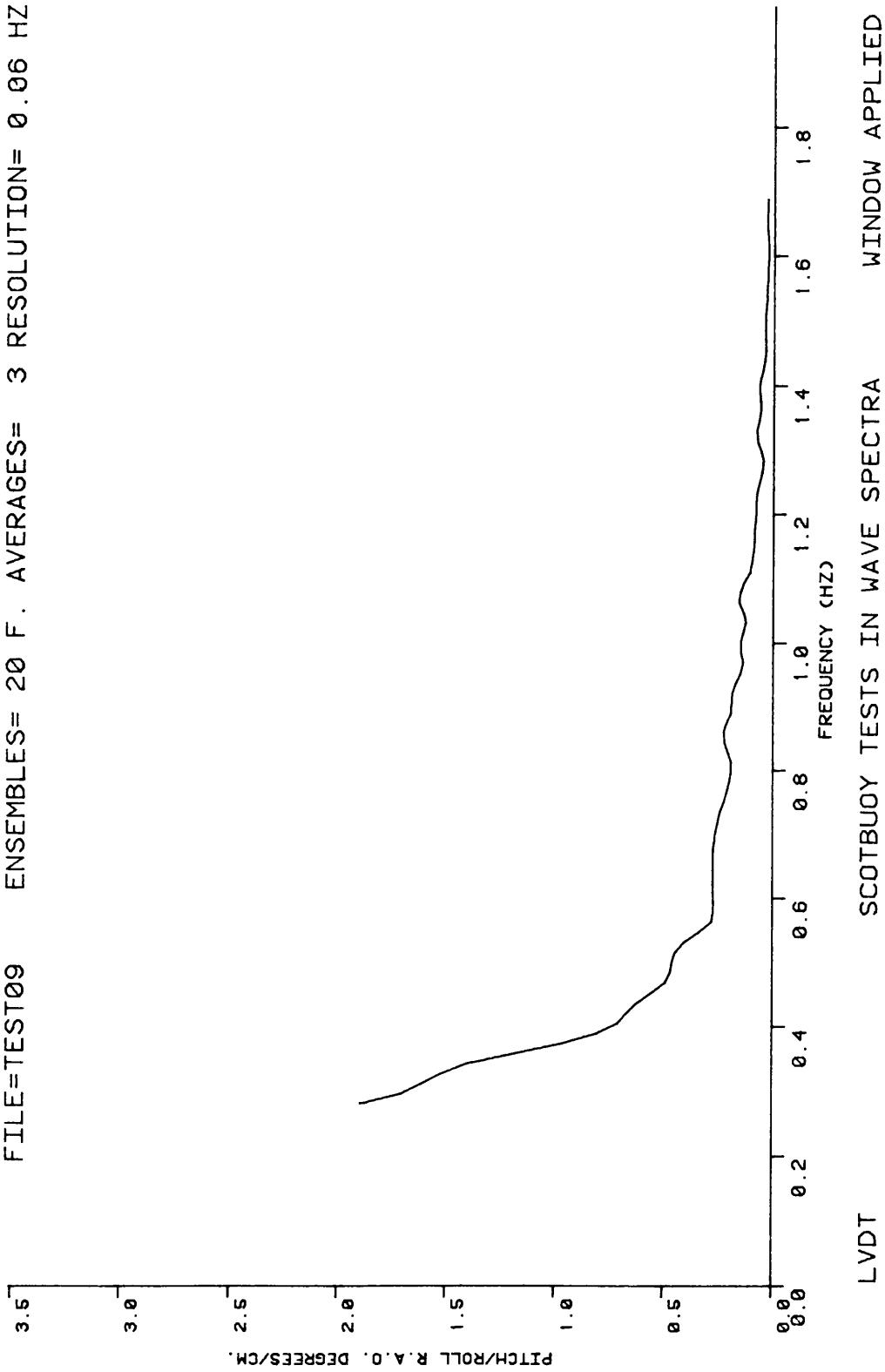


FIGURE 59

FILE=TEST09 ENSEMBLES= 20 F. AVERAGES= 3 RESOLUTION= 0.06 HZ



LVDT SCOTBUOY TESTS IN WAVE SPECTRA WINDOW APPLIED

FIGURE 60

FILE=TEST09 ENSEMBLES= 20 F. AVERAGES= 3 RESOLUTION= 0.06 HZ

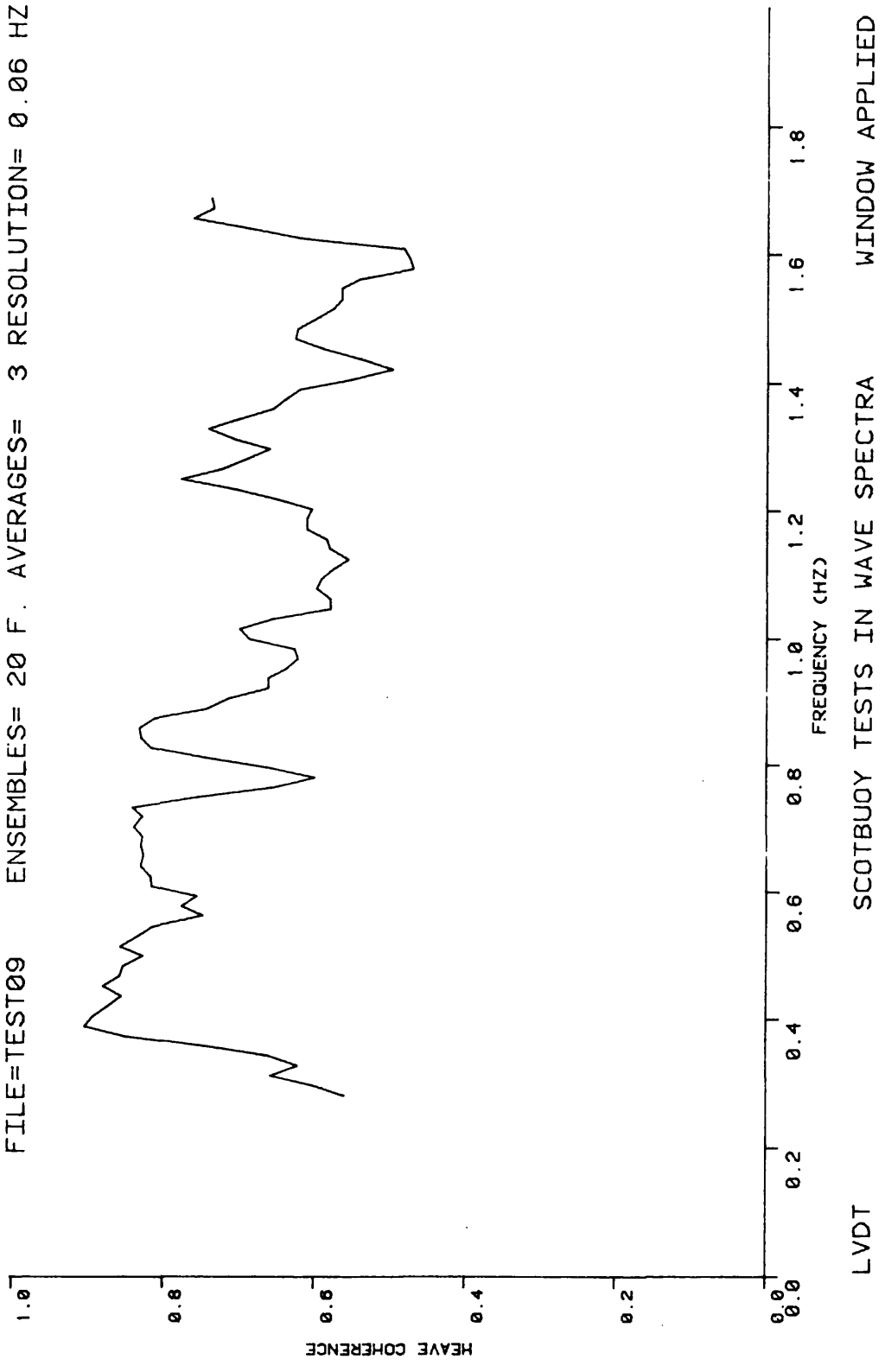


FIGURE 61

FILE=TEST09 ENSEMBLES= 20 F. AVERAGES= 3 RESOLUTION= 0.06 HZ

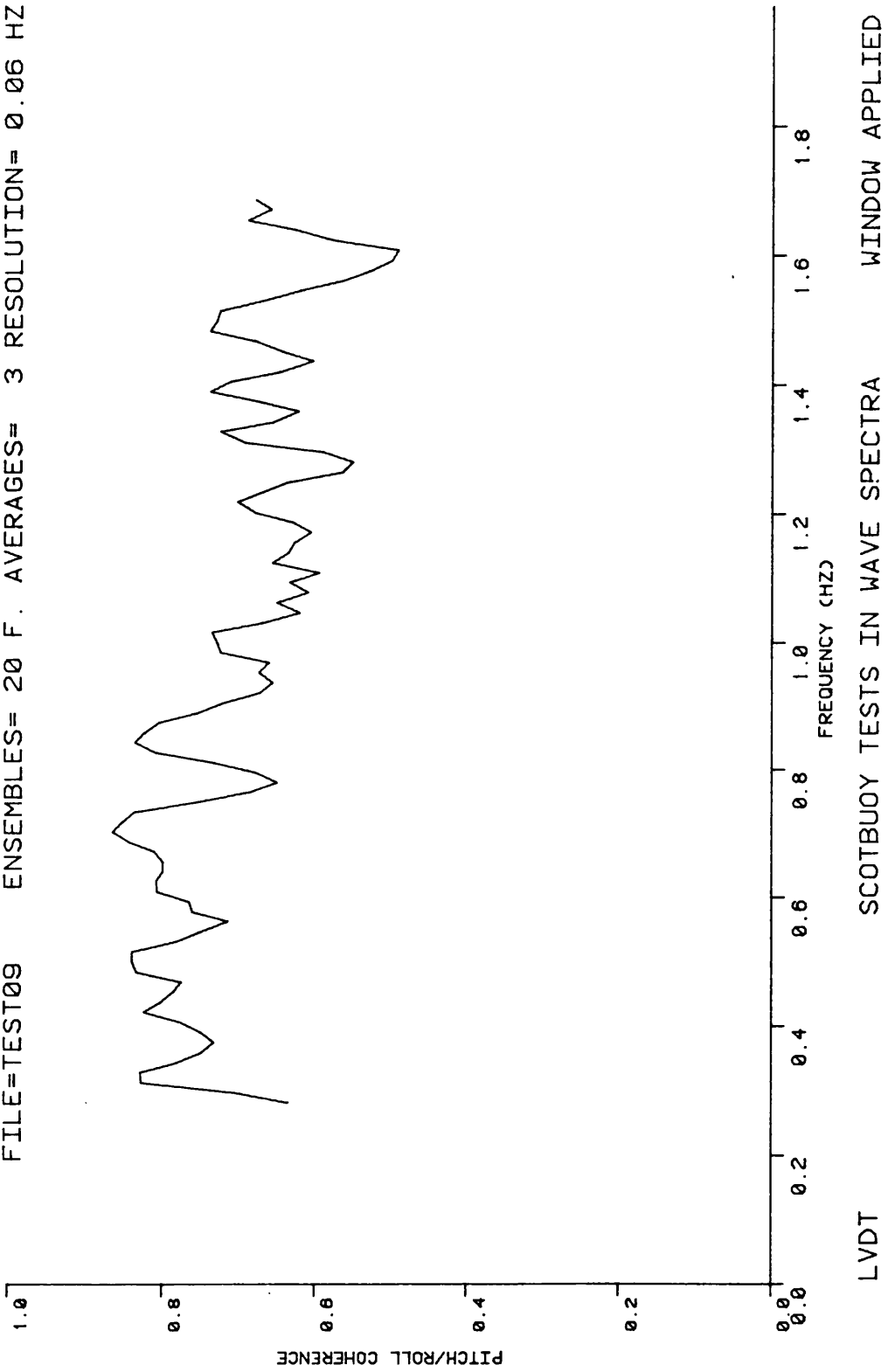


FIGURE 62

FILE=TEST09 ENSEMBLES= 20 F. AVERAGES= 3 RESOLUTION= 0.06 HZ

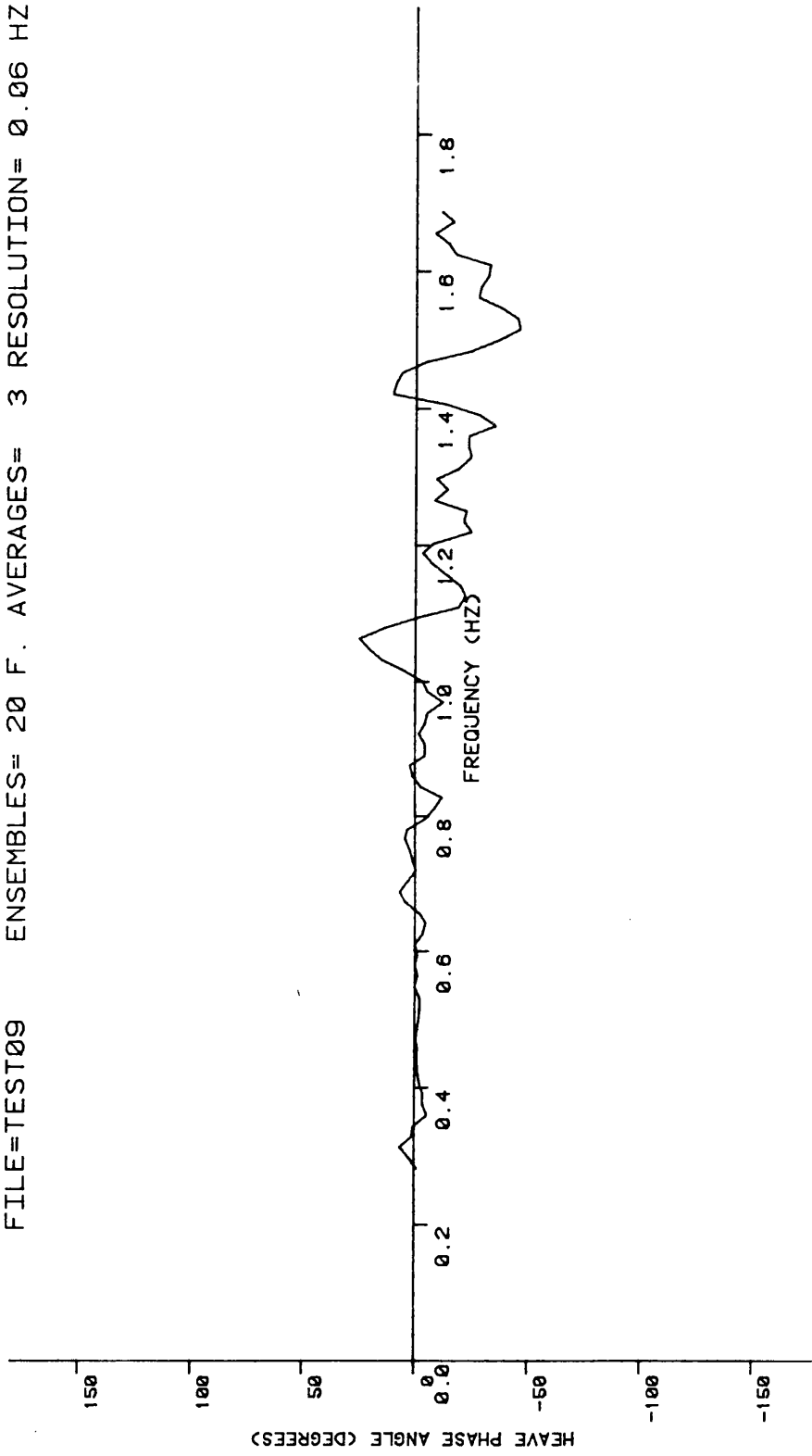


FIGURE 63

LVDT SCOTBUOY TESTS IN WAVE SPECTRA WINDOW APPLIED

FILE=TEST09 ENSEMBLES= 20 F. AVERAGES= 3 RESOLUTION= 0.06 HZ

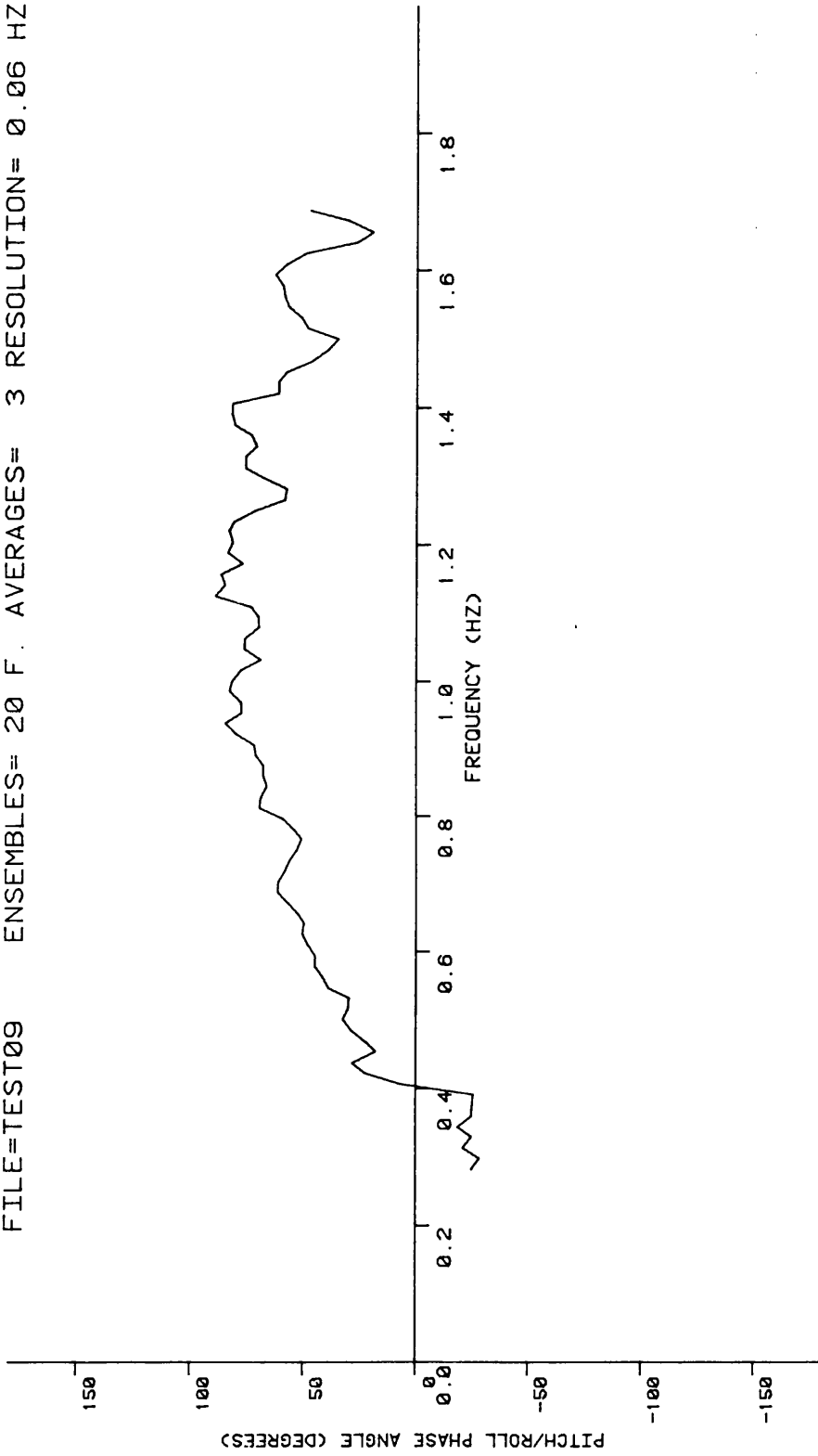


FIGURE 64

LVDT

SCOTBUOY TESTS IN WAVE SPECTRA

WINDOW APPLIED

FILE=TEST10 ENSEMBLES= 20 F. AVERAGES= 3 RESOLUTION= 0.06 HZ

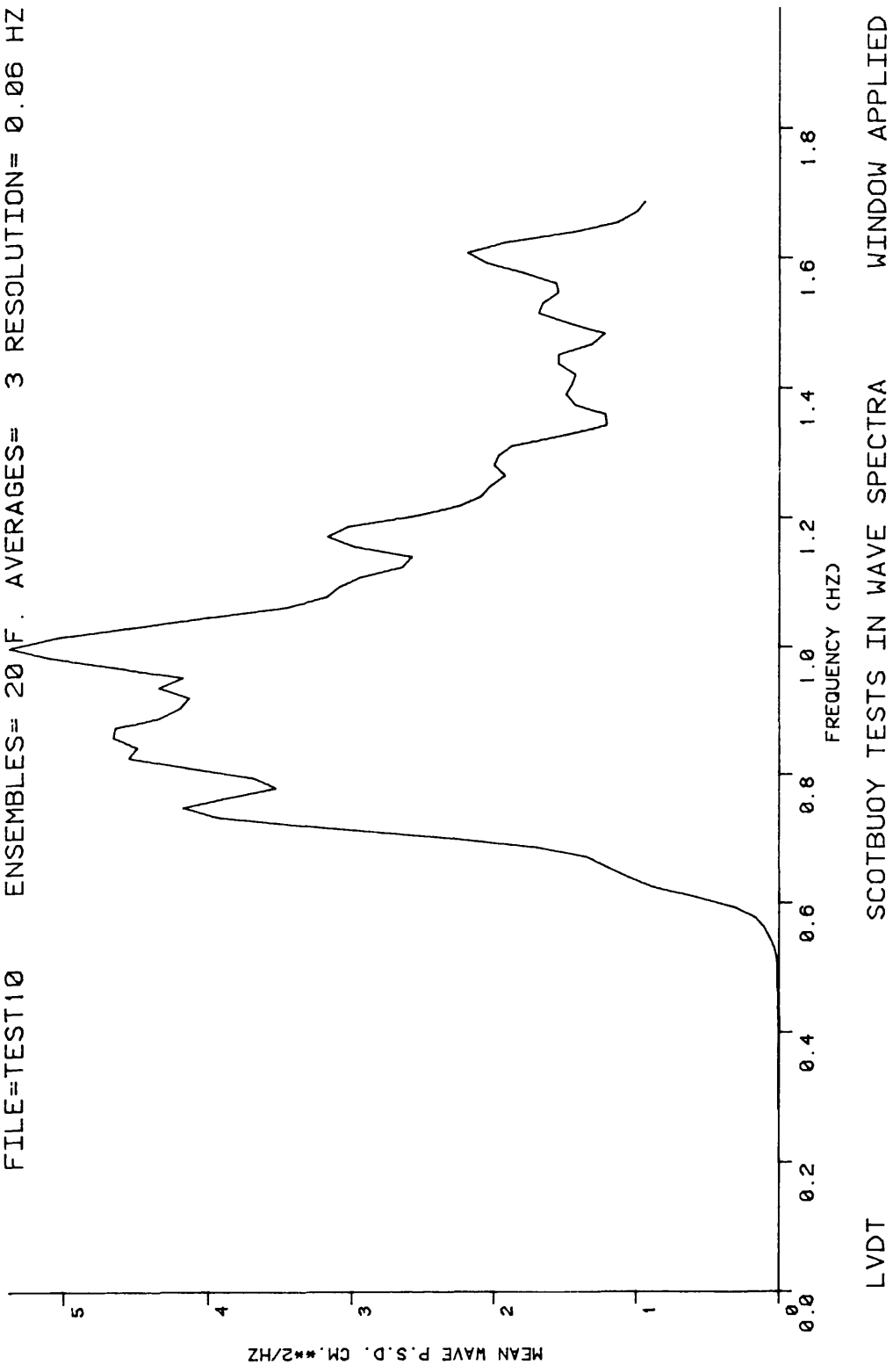
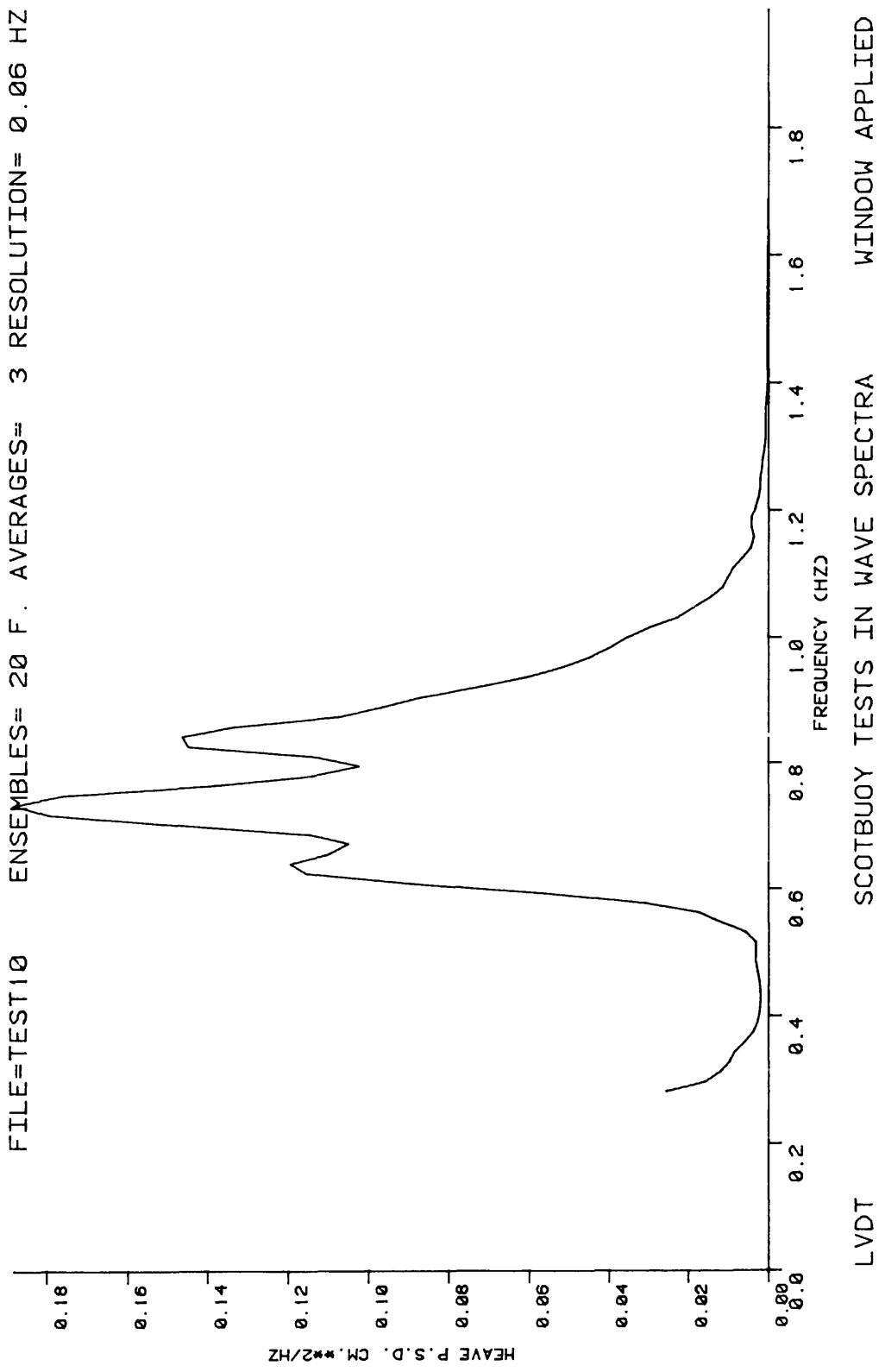


FIGURE 65

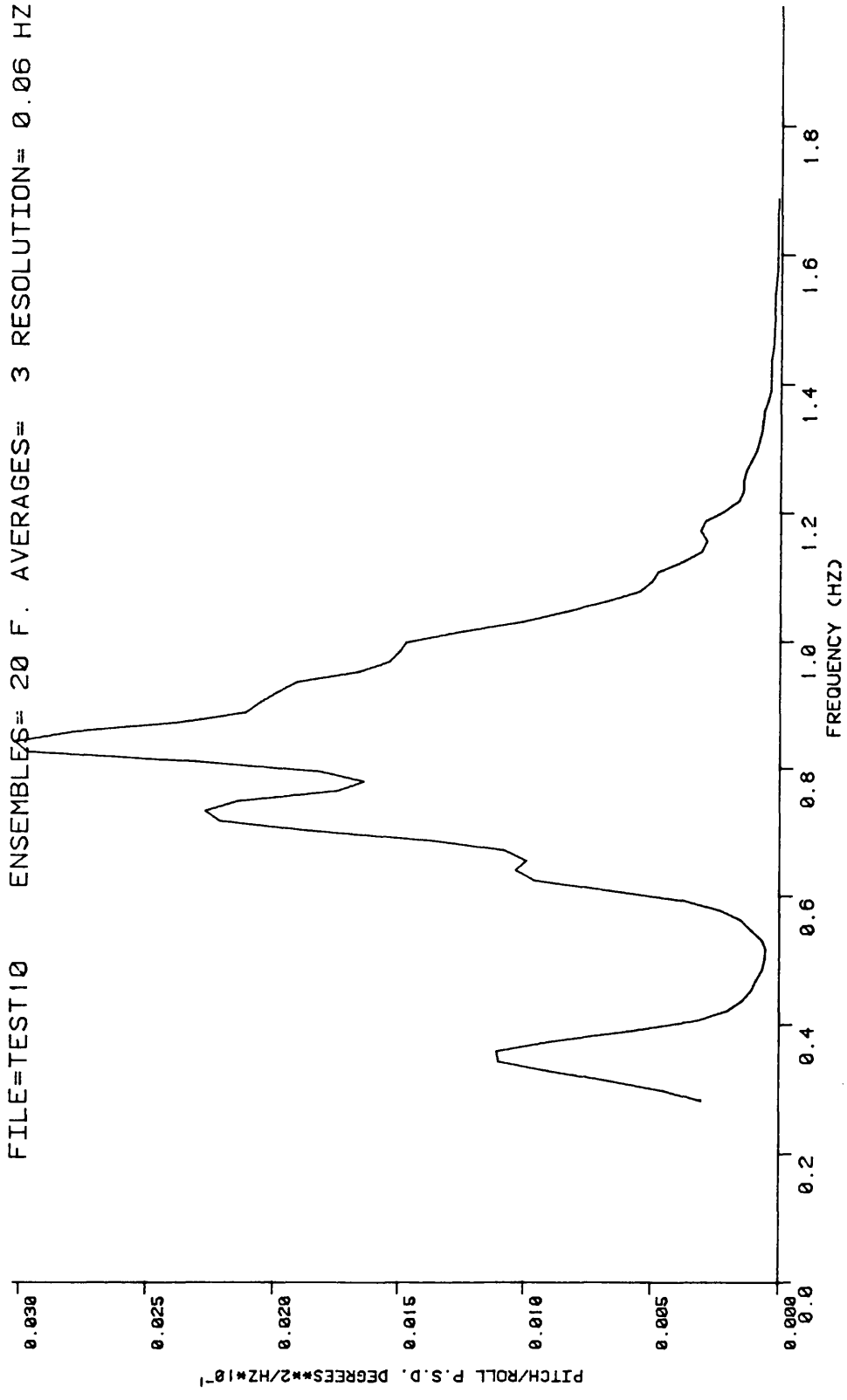
FILE=TEST10 ENSEMBLES= 20 F. AVERAGES= 3 RESOLUTION= 0.06 HZ



LVDT SCOTBUOY TESTS IN WAVE SPECTRA WINDOW APPLIED

FIGURE 66

FILE=TEST10 ENSEMBLES= 20 F. AVERAGES= 3 RESOLUTION= 0.06 HZ



LVDT SCOTBUOY TESTS IN WAVE SPECTRA WINDOW APPLIED

FIGURE 67

FILE=TEST10 ENSEMBLES= 20 F. AVERAGES= 3 RESOLUTION= 0.06 HZ

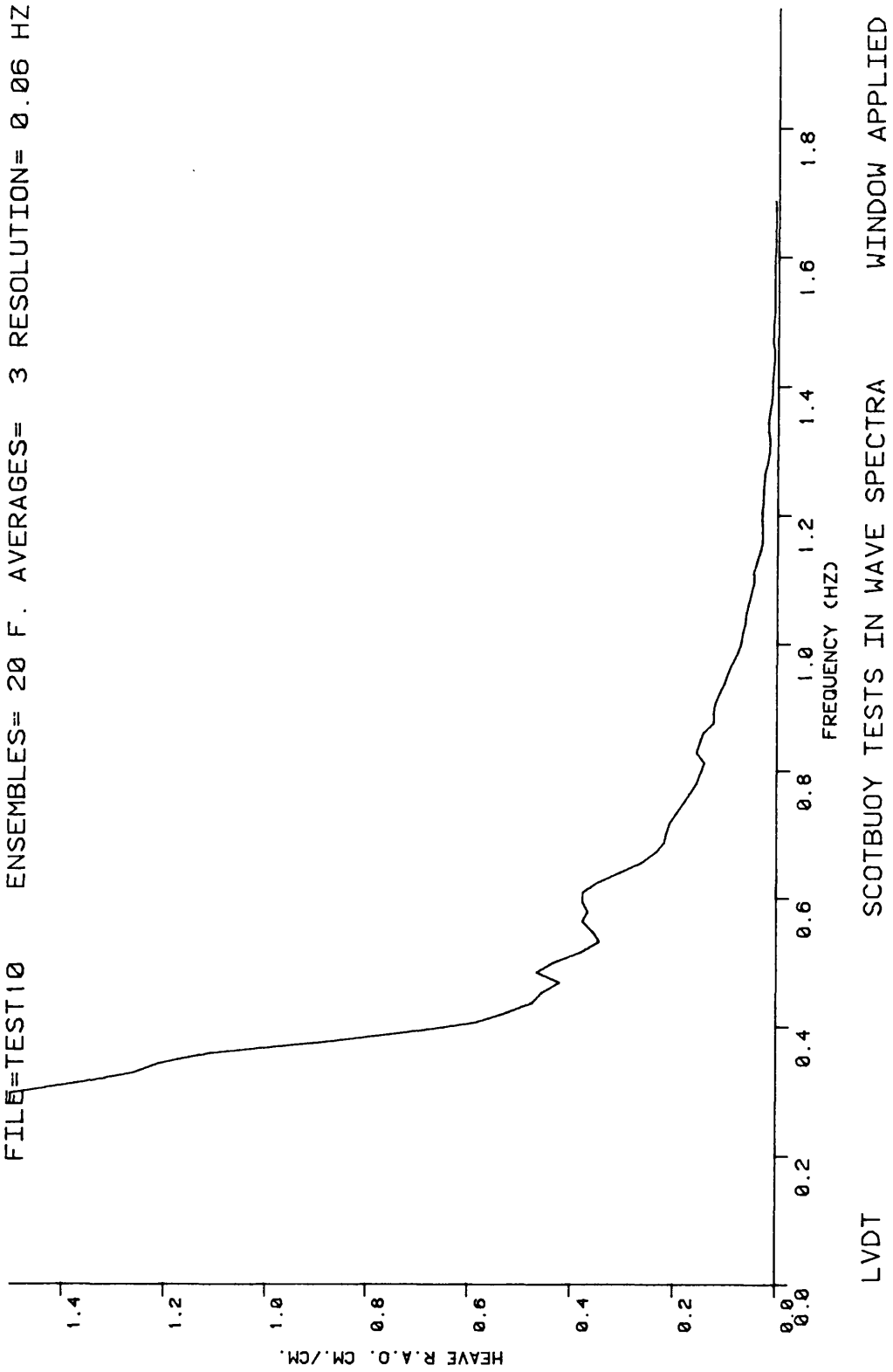


FIGURE 68

FILE=TEST10 ENSEMBLES= 20 F. AVERAGES= 3 RESOLUTION= 0.06 HZ

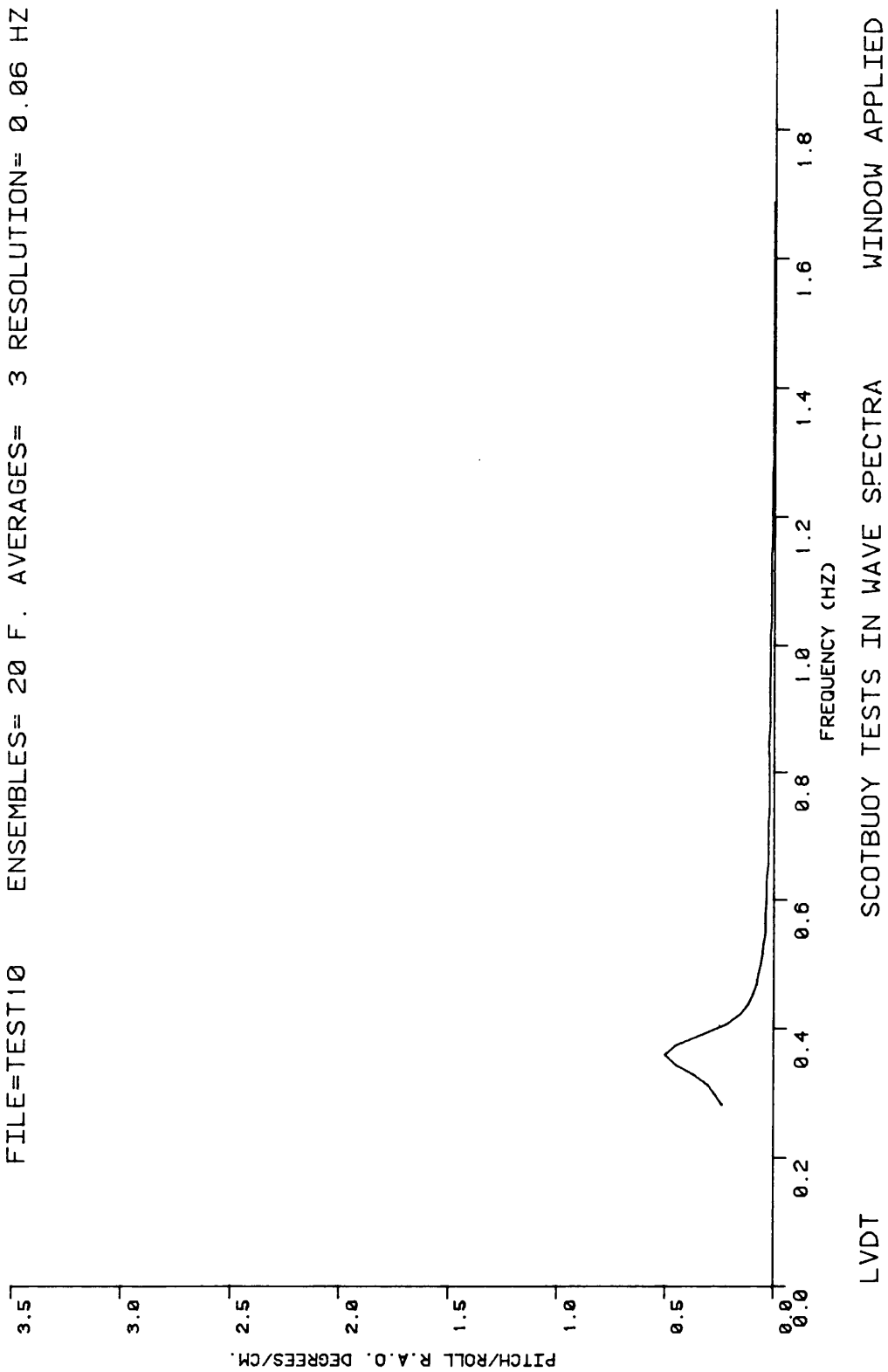


FIGURE 69

FILE=TEST10 ENSEMBLES= 20 F. AVERAGES= 3 RESOLUTION= 0.06 HZ

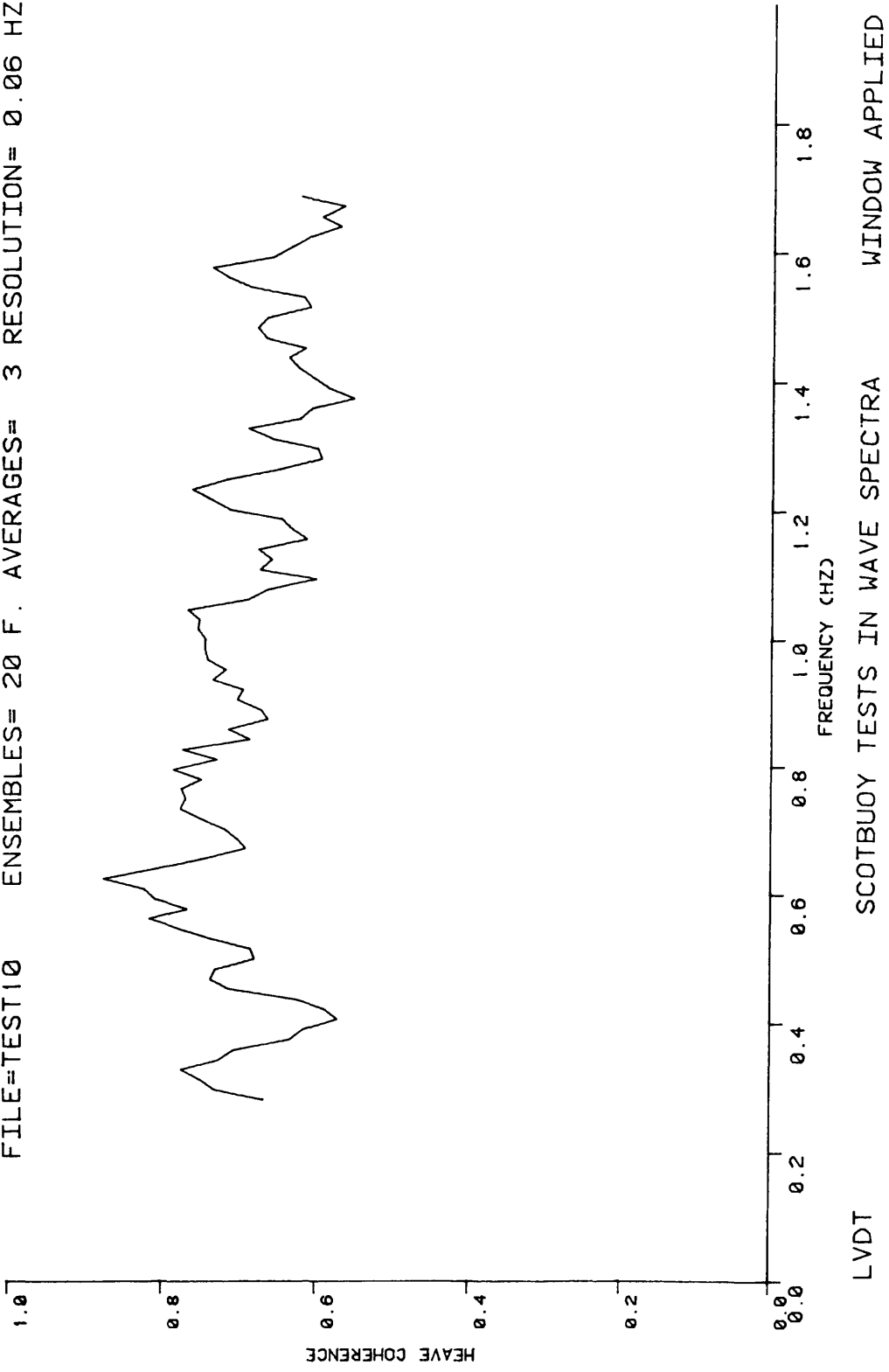


FIGURE 70

FILE=TEST10 ENSEMBLES= 20 F. AVERAGES= 3 RESOLUTION= 0.06 HZ

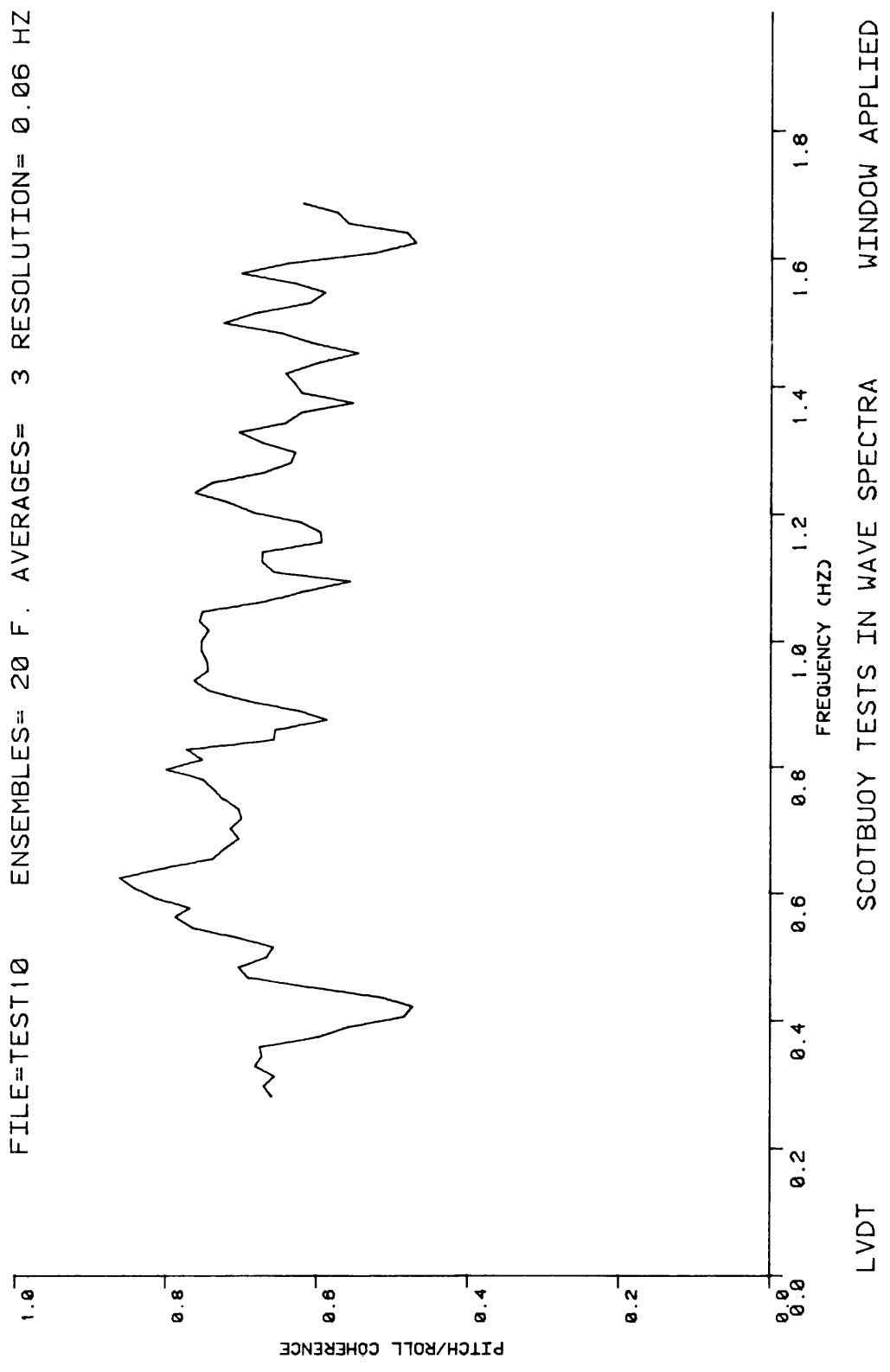


FIGURE 71

FILE=TEST10 ENSEMBLES= 20 F. AVERAGES= 3 RESOLUTION= 0.06 HZ

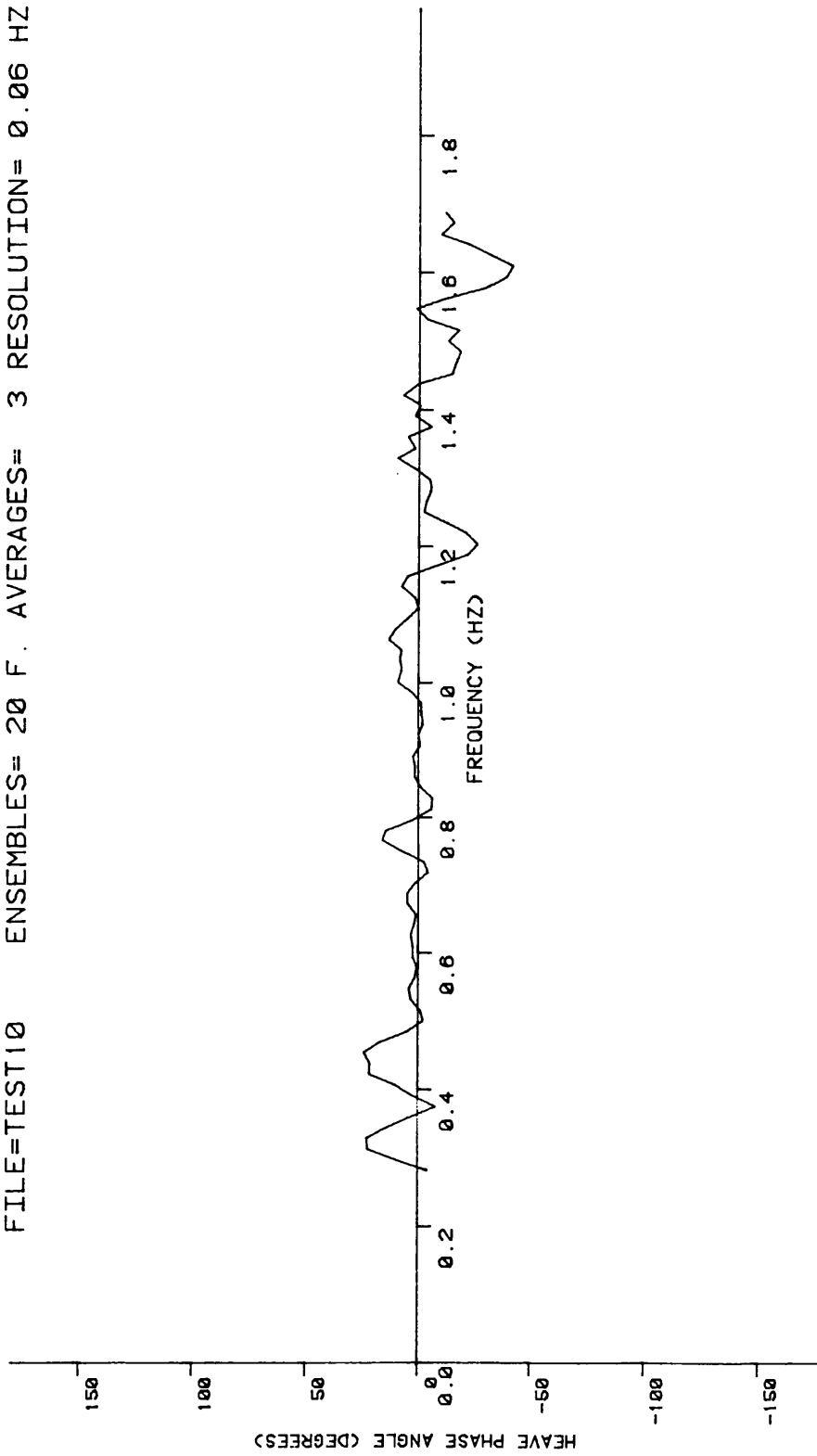


FIGURE 72

LVDT

SCOTBUOY TESTS IN WAVE SPECTRA

WINDOW APPLIED

FILE=TEST10 ENSEMBLES= 20 F. AVERAGES= 3 RESOLUTION= 0.06 HZ

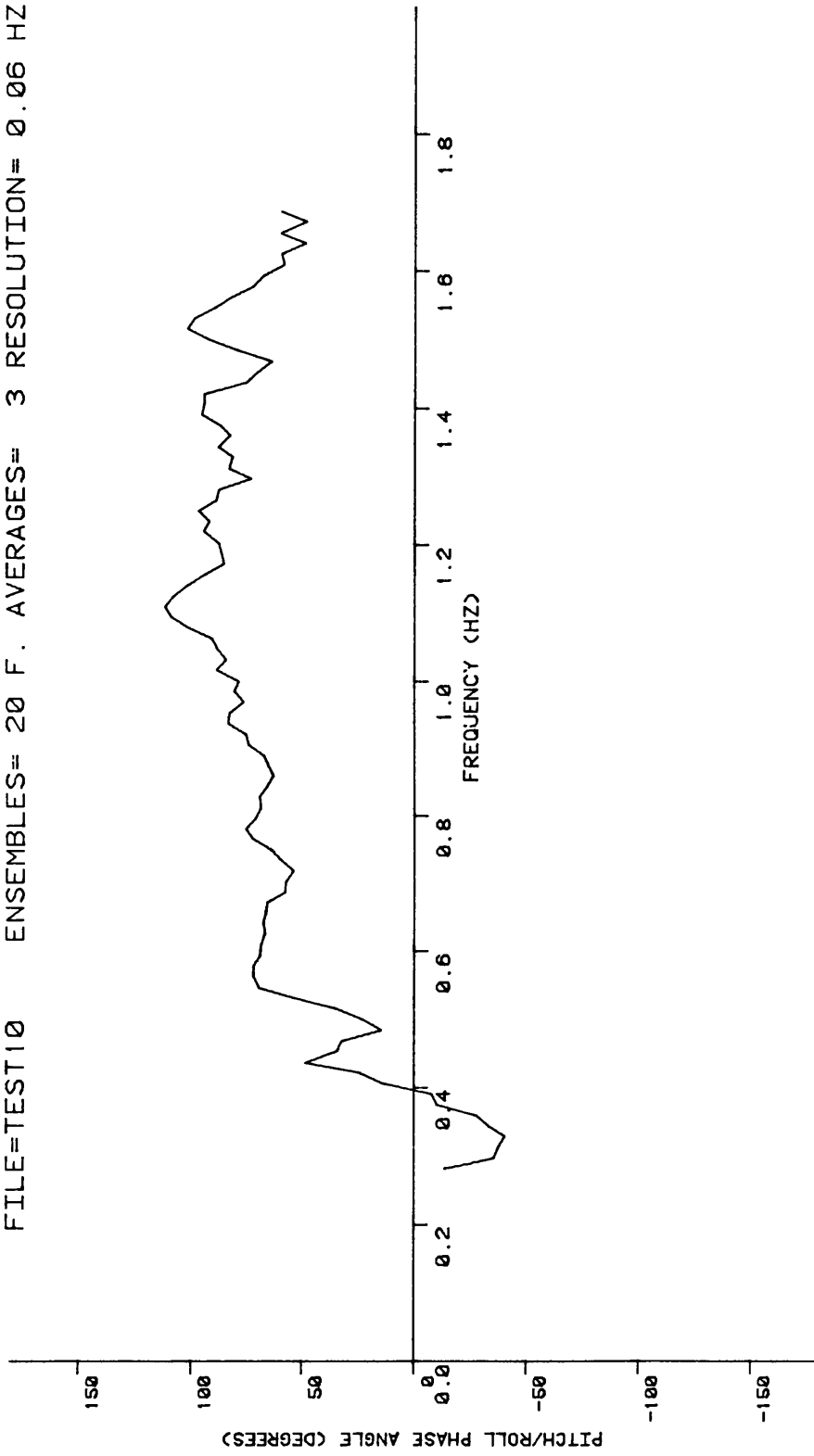


FIGURE 73

LVDT

SCOTBUOY TESTS IN WAVE SPECTRA

WINDOW APPLIED

FILE=TEST08 ENSEMBLES= 20 F. AVERAGES= 3 RESOLUTION= 0.06 HZ

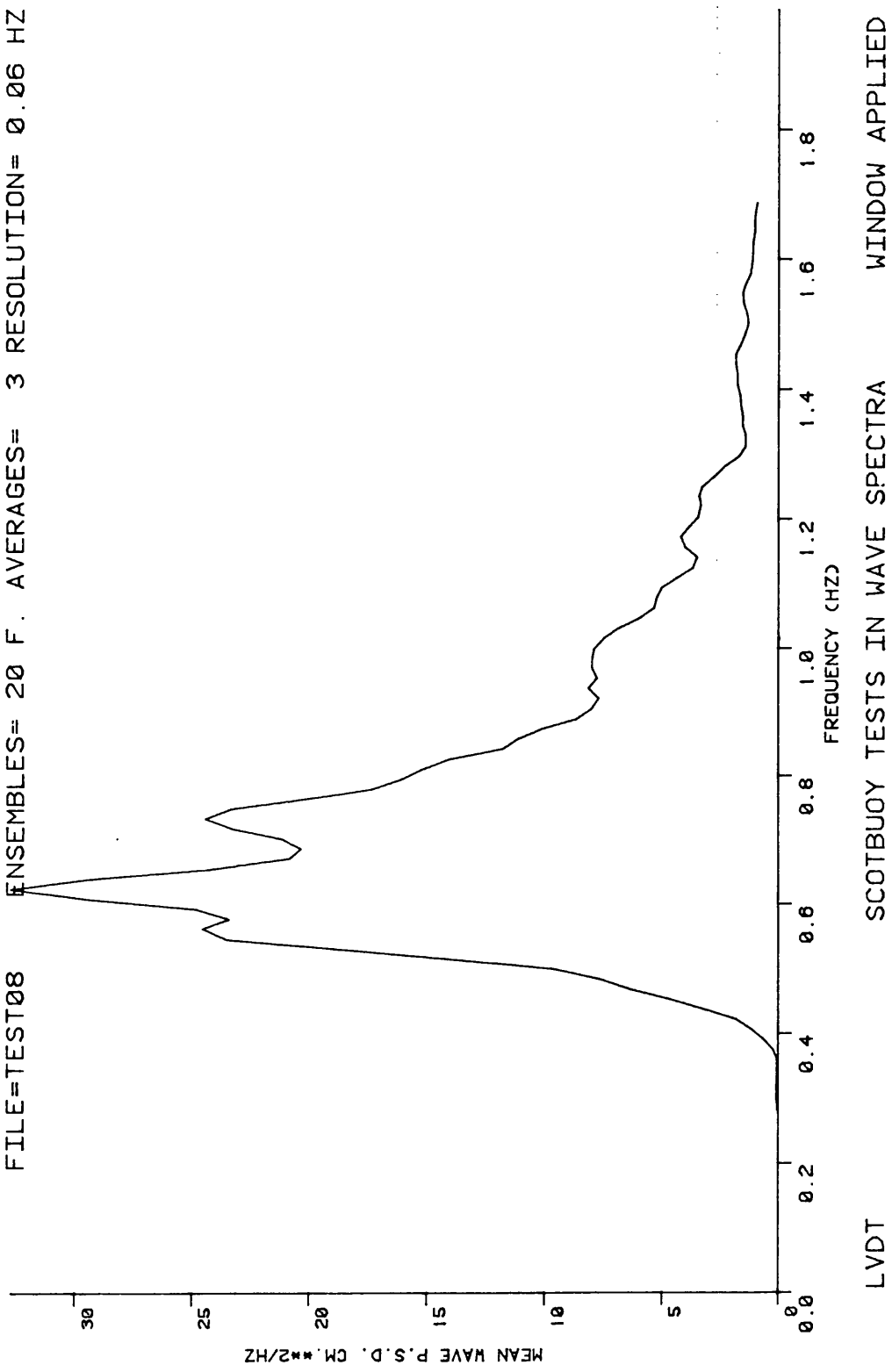


FIGURE 74

FILE=TEST08 ENSEMBLES= 20 F. AVERAGES= 3 RESOLUTION= 0.06 HZ

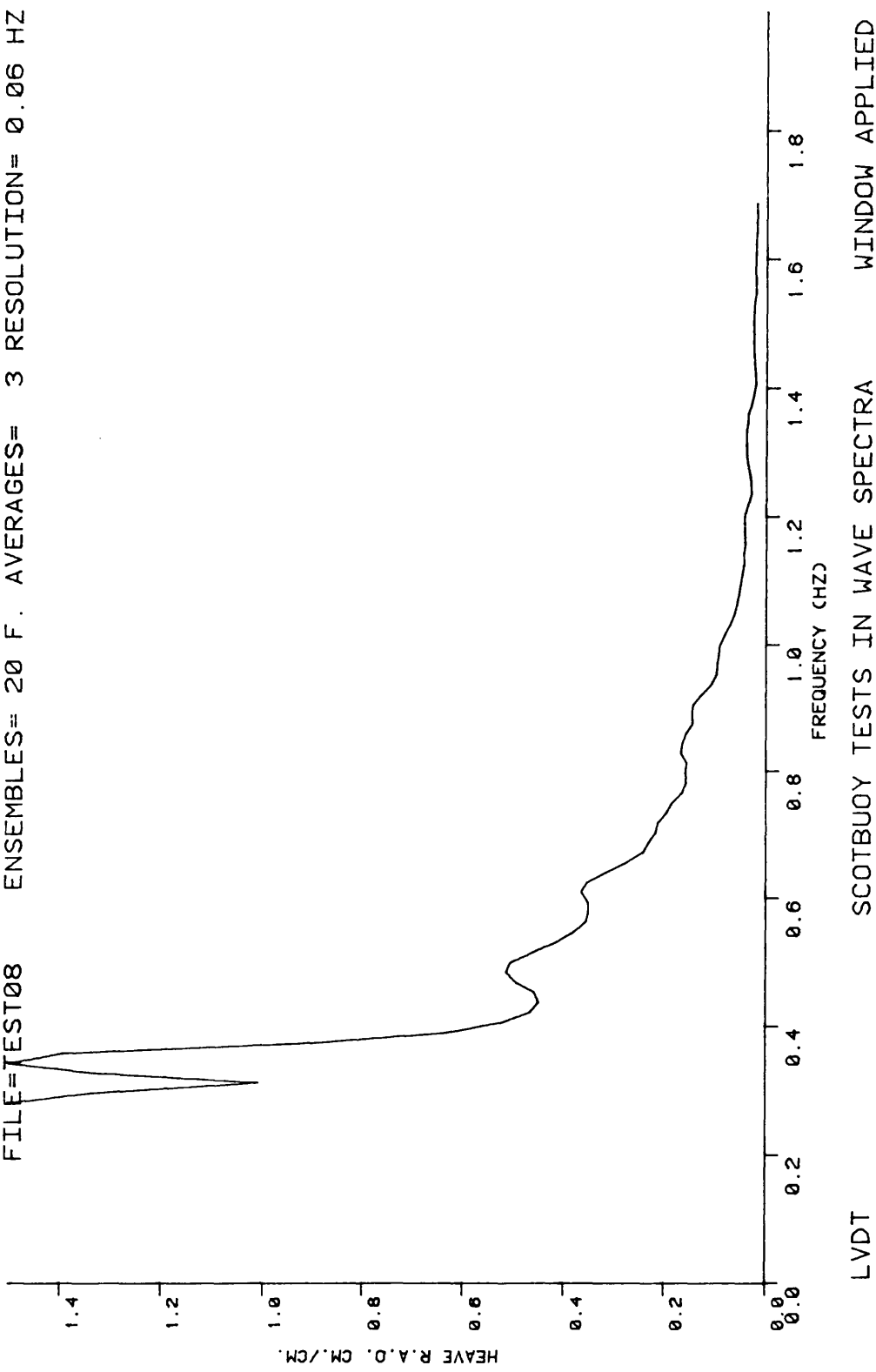
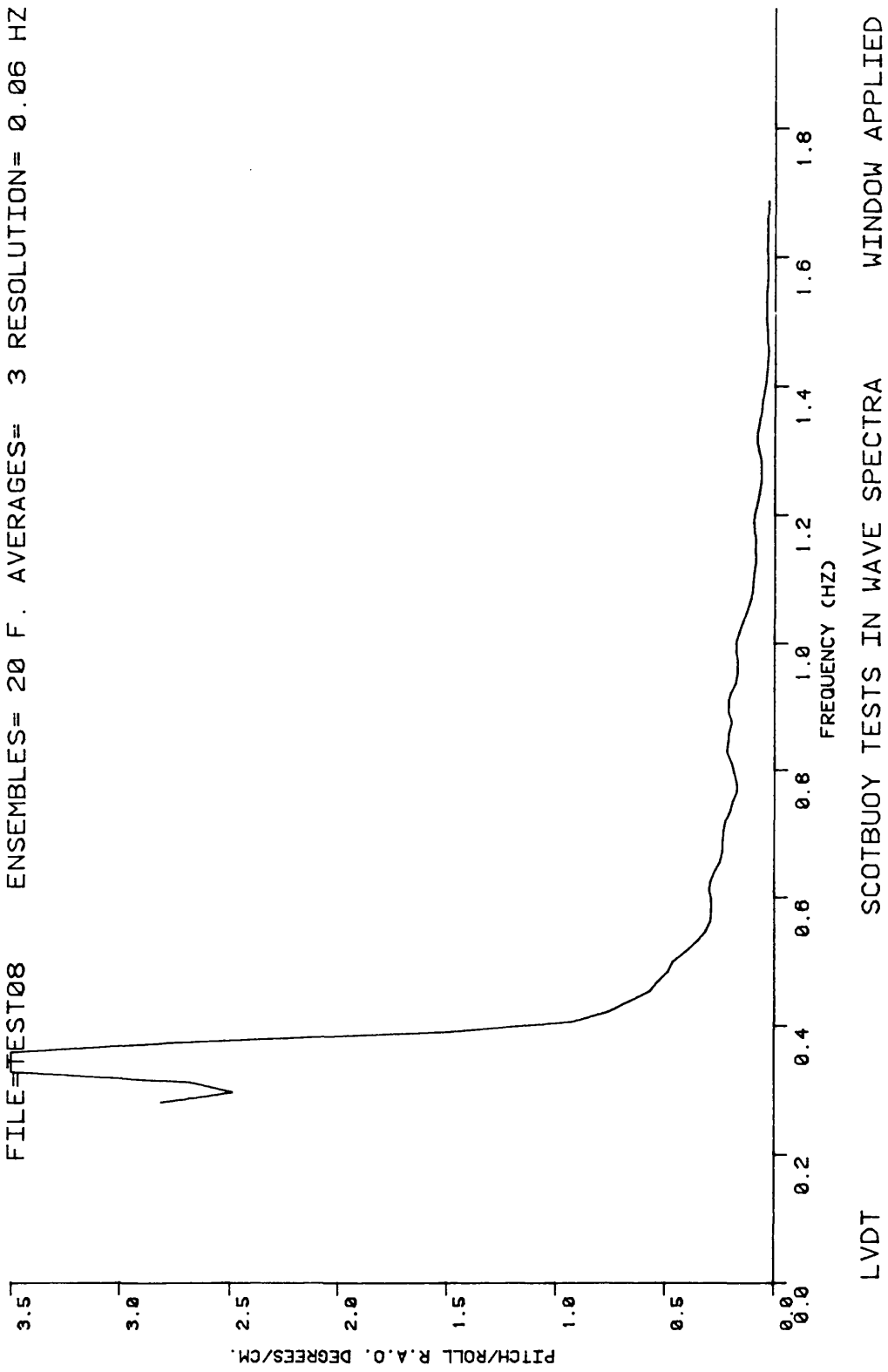


FIGURE 75

FILE=TEST08 ENSEMBLES= 20 F. AVERAGES= 3 RESOLUTION= 0.06 HZ



LVDT SCOTBUOY TESTS IN WAVE SPECTRA WINDOW APPLIED

FIGURE 76

FILE=TEST06 ENSEMBLES= 20 F. AVERAGES= 3 RESOLUTION= 0.06 HZ

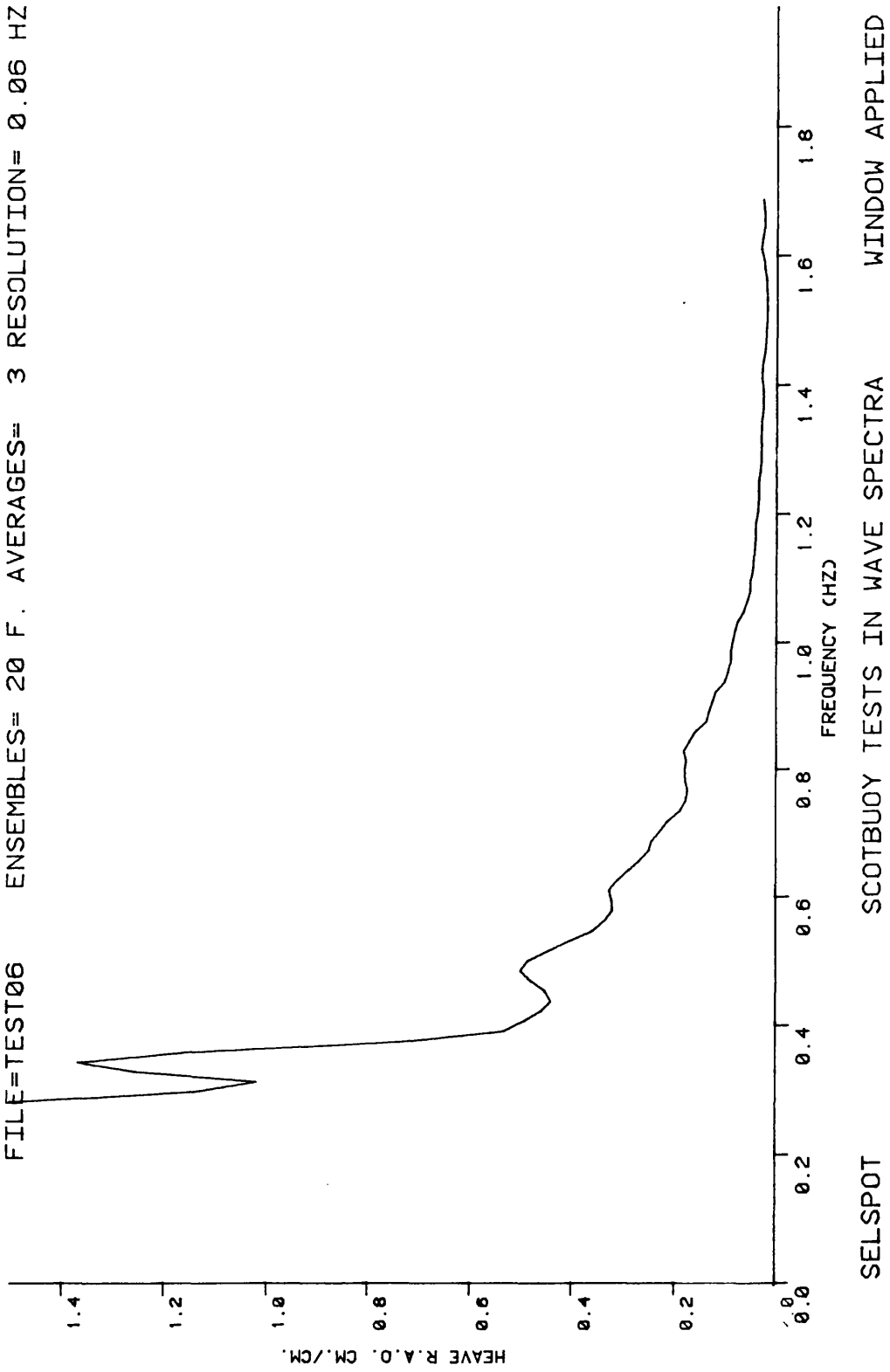
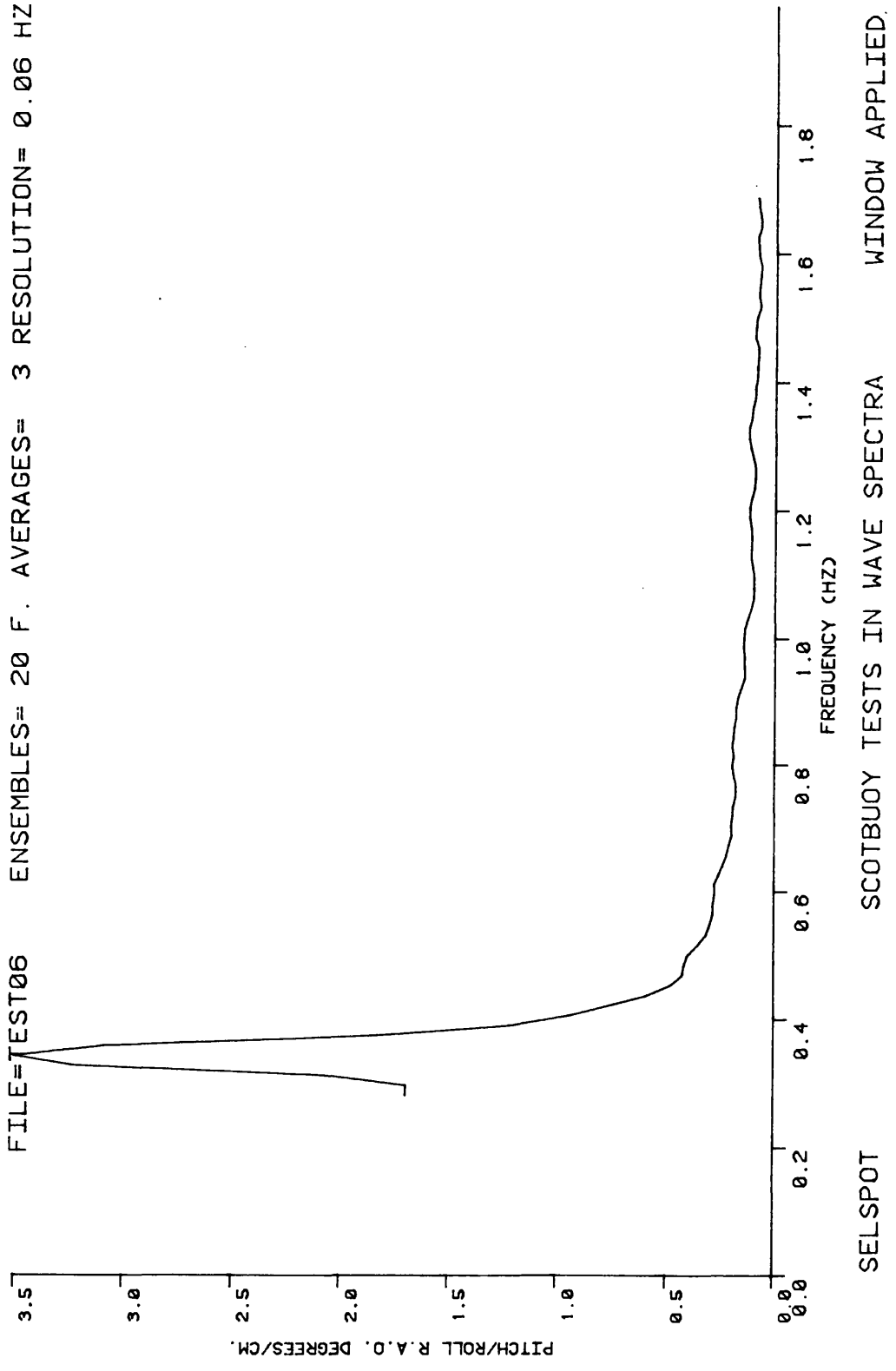


FIGURE 77

FILE=TEST06 ENSEMBLES= 20 F. AVERAGES= 3 RESOLUTION= 0.06 HZ



SELSPOT SCOTBUOY TESTS IN WAVE SPECTRA WINDOW APPLIED.

FIGURE 78

